TISSUE ENGINEERING THE MENISCUS FOR CLINICAL TRANSLATION: STEM CELLS, FIBERS, AND ATTACHMENTS

A Dissertation

Presented to the Faculty of the Graduate School

of Cornell University

In Partial Fulfillment of the Requirements for the Degree of

Doctor of Philosophy

by

Mary Clare McCorry

August 2017

TISSUE ENGINEERING THE MENISCUS FOR CLINICAL TRANSLATION: STEM CELLS, FIBERS, AND ATTACHMENTS

Mary Clare McCorry, Ph. D.

Cornell University 2017

In the United States, there are over 1 million meniscus related surgeries per year. Meniscus injury is often caused by trauma or overuse. The best treatment option for extensive meniscal degeneration or loss is allograft replacement, however, allograft availability is limited by immunological and anatomical constraints. This work aims to develop a tissue-engineered meniscus that eliminates these constraints by using the patient's own cells and the exact anatomical shape.

In order for tissue engineered menisci to become a viable treatment alternative, several pre-clinical challenges must be addressed (Chapter 1). Mesenchymal stem cells (MSCs) are a promising clinically available cell source. Co-culture with the native cell type was evaluated as a technique to guide fibrochondrogenic differentiation (Chapter 3). The development of large diameter and organized collagen fibers is essential to mechanical stability of a tissue engineered meniscus. The ability of MSCs to form fibers in mono and co-culture was evaluated (Chapter 4) as well as addition of glucose as a technique to improve fiber formation was explored (Chapter 5). Engineering soft tissue to bone interfaces with appropriate mechanical, chemical, and cellular gradients is essential for the long term stability of an implant, however this presents unique tissue engineering design challenges (Chapter 2). A model system was developed to run high throughput experiments targeted at designing meniscal entheses for surgical fixation of tissue engineered constructs (Chapter 6).

BIOGRAPHICAL SKETCH

Mary Clare McCorry received her Bachelor of Science degree from Worcester Polytechnic University (WPI), majoring in Biomedical Engineering. As an undergraduate at WPI, Mary Clare worked on a diverse range of research topics related to cell biology, material science and engineering, and tissue engineering. During her sophomore year at WPI, she joined Dr. Jane Lian's lab at the University of Massachusetts Medical School. As a student researcher, she studied the effect of canonical Wnt signaling on bone formation and repair. As a junior she took part in a National Science Foundation (NSF) Material Science and Engineering Research Experience for Undergraduates (REU) at Carnegie Mellon University. She worked with Dr. Kris Dahl to develop bioactive dispersions of single wall carbon nanotubes (SWCNTs) for cellular targeting. For her senior thesis project at WPI, she worked with a team of three in Dr. Raymond Page's lab on skeletal muscle regeneration. This project focused on developing tissue-engineered muscle for patients who experience volumetric muscle loss due to trauma or disease. In conjunction with her senior thesis, she completed an independent research project with Dr. George Pins and Dr. Raymond Page. The project involved evaluating the effects of different extracellular matrix proteins absorbed into fibrin gels on human skeletal muscle cells.

In fall of 2012, Mary Clare started her Ph.D. at Cornell University and joined Dr. Bonassar's lab working on the meniscus project. During the summer of 2013, she took part in two different clinical immersion experiences. In May, she traveled to Bugando Hospital in Tanzania in order to investigate biomedical engineering projects and potential collaborations for senior design or Masters of Engineering projects. Her second clinical experience was a two-month clinical immersion at the Hospital for Special Surgery (HSS) as a part of Biomedical Engineering Clinical Immersion

Program. She shadowed Dr. Scott Rodeo, an orthopaedic surgeon specializing in the knee and shoulder. In addition to the clinical immersion, she worked with a postdoctoral fellow, Dr. Tony Chen, at the Laboratory for Soft Tissue Research under the direction of Dr. Suzanne Maher. The project she conducted examined how dynamic compression affects fibrochondrocyte expression in different zones of skeletally immature and mature meniscus. During her time as a Ph.D. student, Mary Clare has worked on independent training fellowships from Howard Hughes Medical Center and the NIH. In 2015-2016, she worked on a collaborative NYSTAR grant with GE Global Research, developing a real-time monitoring meniscal bioreactor.

Mary Clare is excited to begin the next chapter as an AIMBE fellow at the U.S. Food and Drug Administration.

Dedicated to my parents, Carole and Jim, who have always fostered my love for science and my husband, Jeff, who has always been my biggest cheerleader.

ACKNOWLEDGEMENTS

I would first like to thank my advisor, Dr. Larry Bonassar, for his patient and ever positive mentorship. I would also like to thank my special committee, Drs. Suzanne Maher, Lisa Fortier, and Lara Estroff for their guidance and expertise throughout this project.

The work presented in this dissertation involved the collaboration of many of my colleges. Meniscus meeting and lab meeting have been fantastic groups to get feedback on my work. I would like to specifically thank members of Team Meniscus that I have worked with: Jennifer Puetzer, Alex Boys, Jongkil Kim, Edward Bonnevie, Jon Lee, Dan Cappola, Kahini Vaid, Melissa Mansfield, Richard Sha, and Leanne Iannucci. I would also like to thank other members of the lab that make up Team MSC: Jorge Mojica Santiago, Katherine Hudson, and Ben Cohen. MSCs often have minds of their own, so I've always appreciated the help of Team MSC in experimental planning, data analysis, or simply coverage of media changes. Brandon Gold, Esther Koo, Logan Northcutt, Tyler Khilnani, and Marc-Anthony Rodriguez were all talented undergraduates who helped contribute to this work. Nora Springer, deserves a special thanks as my go to person for all questions on westerns blots and protocols to analyze bone and fat. A special thanks to Michelle Delco, who veterinary surgery background has been invaluable in the lab. I would also like to thank all the members of the Bonassar lab, who have helped make these past five years an enjoyable experience.

Last year I had the privilege to work with a team of scientists from GE Global Research, Dr. Vandana Keskar, Dr. Weston Griffin, and Dr. Xiaohua Zhang. This collaboration was a wonderful mutual sharing of skills and knowledge. Additionally, this relationship helped provide insight and training on high level research at a large company.

Every good scientist needs a good editor, organizer, and motivator to help them along the way. I would like to thank Eileen Wrabel and Hiral Dutia for spending weeknights after work proof reading various grants, journal articles, and thesis chapters I've written over the years. Special thanks to Belinda Floyd for keeping everything afloat and on course. Last, but not certainly not least, I would like to thanks my loving husband Jeff Rosen. Jeff has made countless sacrifices to support me and my goals throughout the Ph.D process. I knew I found someone special when he spent hours converting .czi's to .tiff's, so I could spend an afternoon hiking with him. Without him, this would not have been possible.

Funding for this work was provided by Howard Hughes Medical Institute's Med into Grad Fellowship, NIH TL1 through Clinical and Translational Science Center at Weill Cornell, and NYSTAR in collaboration with GE Global Research.

TABLE OF CONTENTS

LIST OF ABBREVIATIONS

AI: alignment index

AR: aspect ratio

BG: biglycan

DC: decorin

DW: dry weight;

DMEM: Dulbecco's modified Eagle's medium

DMMB: dimethylmethylene blue

DNA: deoxyribonucleic acid

E: Young's modulus

FBS: fetal bovine serum

FCC: fibrochondrocyte

FD: fiber diameter

FM: fibromodulin

GAG: glycosaminoglycan

HA: aggregate modulus

Hypro: hydroxyproline

k: hydraulic permeability

MSC: mesenchymal stem cell

PBS: phosphate buffered saline

SLRP: small-leucine rich proteoglycan

TE: Tissue Engineered

UTS: ultimate tensile strength

WW: wet weight

CHAPTER 1

INTRODUCTION

The meniscus is a crescent shaped cartilaginous structure acting as the articulating surface between the femur and the tibia in the knee joint. Within the joint, the meniscus acts as a shock absorber which transmits and diffuses loads in the knee, as well as lubricating and protecting the articular cartilage.[1] The outer portion of the meniscus is vascularized tissue, with capillaries extending 10-25% into the peripheral adult human meniscus.[2–4] However, the inner portion of the meniscus is avascular and makes up the majority (~2/3) of the meniscus composition in an adult human.[2–4] Several ligaments including the anterior and posterior horn attach the meniscus to the tibial plateau**,** which is essential to meniscus stability.[5] Within the meniscus exists a unique cellular population, termed meniscal fibrochondrocytes (FCCs).[4],[6] The meniscus is predominantly type I collagen and proteoglycans with some elastin and types II, III, V, VI collagen.[7] Fibers are circumferentially aligned with radial tie fibers in the deep zone and an anisotropic orientation near the surface. These fibers and proteoglycans contribute to the unique mechanical properties of the meniscus.[8]

Meniscus injury is one of the most common knee injuries with reported incidences of 61/100,000 people and over 1 million meniscus repair procedures performed annually in the United States.[1],[9] The meniscus is essential to the mechanical stability of the knee and therefore must be repaired if possible in order to prevent long-term joint degeneration.[10] Since the meniscus is primarily avascular, healing is often slow or non-existent; therefore, avascular zone tears must be repaired

by surgical intervention.[11] Depending on the severity of the tear, partial meniscectomy is a potential treatment option, however, in severe cases, such as failed repair or extensive complex tears, meniscus allograft is the best option for short-term pain relief and long-term functional improvement.[12],[13] Since the shape of the meniscus is critical for biomechanical stability, the patient must wait several months for an allograft that is both immunologically compatible and a comparable size to the recipient.[11] Using tissue engineering approaches, it is possible to develop an immunological and geometrically correct meniscus using the patient's own cells and x-ray microtomography generated 3D images of the patient's meniscus. By creating a tissue engineered (TE) meniscus, we can offer a solution that negates the allograft limitation of availability and improves the patient's quality of life.

Tissue Engineering Approaches

A major initiative of meniscus replacement research is partial repair. There are some commercially available constructs on the market in Europe: Collagen Meniscal Implant (CMI) also known as Menaflex (Ivy Sports Medicine, Germany), NUsurface (Active Implants, Memphis, Tennesse), and Actifit (Orteq Bioengineering, UK).[14] As of 2010, the Food and Drug Administration (FDA) rescinded its approval of CMI because it failed to promote tissue ingrowth. However, in 2015 Ivy Sports won an appeal and the product was reintroduced to US markets.[15] Polymer scaffolds, such as Actifit, have yet to match native compression modulus and show similar ingrowth of fibrovascular cells and cartilage degeneration.[16] NUsurface is a free-floating Kevlar-reinforced polycarbonate urethane meniscus replacement that received IDE approval to conduct clinical trials in the US. Although these approaches relieve patient reported

pain, partial repair techniques are not applicable for extensive meniscus injury. Furthermore, mixed results in clinical trials, have cast doubt on the medical impact of these treatments.

Previous efforts to TE the whole meniscus utilized synthetic polymers, hydrogels, and tissue-derived scaffolds.[17],[18],[19],[20],[21] However, none of these are currently in clinical practice because they lack the anatomical, mechanical or biochemical properties necessary for native meniscal function.[1] Natural scaffolds, such as collagen, silk, and alginate, are appropriately biocompatible but lack the mechanical strength of native tissue.[11] Synthetic scaffolds can better match mechanical properties of the native meniscus but can incite an immune response and may contain harmful degradation products.[11] Scaffolds seeded with FCCs have shown comparative properties to native menisci in histological appearance and mechanical properties, however they have yet to be tested in large animal models.[22],[23] The cellular component of TE menisci provides essential mediators that develop and modify constructs to better match native properties. Recently, a growth factor releasing scaffold encouraged endogenous progenitors cells to populate the scaffold and synthesize location-specific matrix in a sheep model.[24] A cellular component in TE meniscus is essential to the clinical relevance of the product, yet further research needs to be conducted in this field in order to make total meniscus replacement clinically successful.

Dr. Bonassar's lab has developed an image-based anatomically accurate TE meniscus construct.[25] Using a collagen scaffold seeded with FCCs we have shown that mechanical boundary conditions result in anisotropic fiber formation.[26] Currently, *in vitro* studies use bovine FCCs, but obtaining the sufficient number of cells for TE

meniscus is challenging because FCCs proliferate slowly and often lose their phenotype in two-dimensional (2D) culture.[27] In order to begin *in vivo* studies there is a need for a larger and more readily available cell source. Mesenchymal stem cells (MSCs) can be easily obtained and expanded in culture, secrete a variety of immunoregulatory molecules and provide paracrine trophic mediators, which contribute to the healing process.[28] *In vivo* studies in both animals and humans have shown that MSCs delivered through intraarticular injection, mobilize to the site of injury and contribute to tissue regeneration.[29–32] Additionally, MSCs are multipotent and have been observed to differentiate down a chondrogenic pathway; however, this pathway, specifically fibrochondrogenesis, is not well characterized.[33] A pellet co-culture study using FCCs and MSCs showed an increased expression of fibrochondrogenic genes, reduced hypertrophy, and increased matrix production.[34],[35] Most studies examining MSC fibrochondrogenic differentiation are in a 2D culture environment, which limits the study of extracellular matrix interactions and cell-cell contact.[1] Co-culture techniques applied to a 3D collagen matrix with homogeneous mixing of FCC to MSC ratio have yet to be examined. In order for cell based tissue engineered menisci to progress toward the clinic there needs to be an increased understanding of how MSCs behave and what techniques can be used to drive differentiation, co-culture is one technique that needs further exploration.

Mechanical Influences on Meniscus Development

To better understand fibrochondrogenic differentiation we can look to *in vivo* development. In native meniscus development, formation of the meniscus can be identified in a seven-week-old embryo. Fibrous and fibrocartilaginous tissues start out

as unorganized mesenchymal condensations.[36] Fibrocartilaginous development occurs after the formation of meniscus ligament attachments including anterior and posterior tibial attachments at the horn. Throughout early development the meniscus is vascularized which helps provide chemical signals that direct mesenchymal differentiation into fibrochondrocytes.[37] However the inner portion of the meniscus becomes progressively avascular during post-natal development.[2] Biomechanical signals play an essential role in directing meniscus maturation and formation, however this has yet to be fully explored in the literature.

The primary function of the meniscus is to act as a shock absorber and assist with load bearing transmission. The anisotropic fiber alignment in the meniscus enables the meniscus to manage tensile, compressive, and shear loads.[38] Immobilization studies in the meniscus have shown that mechanical stimulation is essential for the maintenance and healing of the meniscus.[39] It has been well established in the literature that mechanical stimulation provides critical cues for tissue development, both formation and maturation, prenatal and postnatal. Fibroblast studies in collagen gels have shown that applying a partial mechanical boundary condition results in collagen alignment.[40] Mimicking the loads experienced by the meniscus *in vivo* may help direct anisotropic fiber alignment *in vitro.* Previously, the Bonassar lab tested the effects of mechanical boundary conditions on FCCs in a collagen gel,[26] however we do not know how MSCs or MSC:FCC co-cultures will behave to this system, specifically MSCs ability to form large organized fibers on the meniscal fiber scale is relatively unknown.

The Meniscal Enthesis

Several ligaments act as attachment points to the knee joint. The anterior and posterior horn attaches the meniscus to the tibial plateau, see left panel of Figure 1.1. Other attachment points include the medial collateral ligament, the meniscofemoral ligament, and the transverse ligament, which all contribute to the meniscus stability.[5] The anterior and posterior horn entheses are essential to mechanical function of the meniscus in the knee. The meniscus withstands compressive, tensile, and shear stresses.[38] As seen in the middle panel of Figure 1.1, the meniscus contains horn attachments to the underlying bone that help to appropriately distribute forces in the meniscus.[38] Without these attachment sites, the meniscus is unable to perform its normal function and degeneration of the tissue will occur.[7,41] The anterior and posterior insertion sites are comprised of a fibrocartilaginous transition zone that includes uncalcified fibrocartilage, calcified fibrocartilage, and bone.[42] The fibrocartilage to bone gradient, Figure 1.1 right, consists of type I collagen throughout, with more type II collagen seen in the fibrocartilaginous zone and type X collagen seen in the calcified fibrocartilage zone.[43] The fibrocartilage to bone gradient of content and structure contributes to its unique function. The native menisci enthesis structure and function are described in greater detail in Chapter 2.

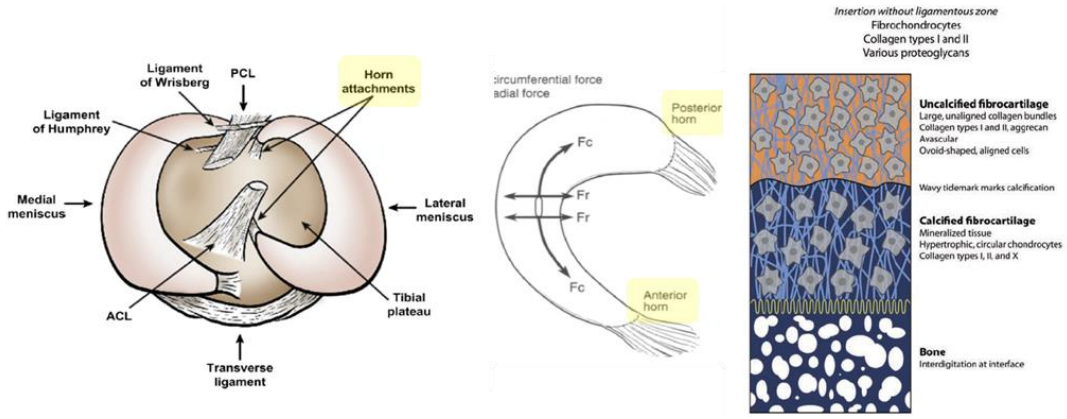

Figure 1.1 Top down view of the meniscus with insertion sites highlighted (left).[1] The force distribution in the meniscus depends on mechanical fixation at the horns (middle).[11] The meniscus to bone transition zone from ligament to bone.[43]

Much progress has been made in creating a TE meniscus, however little to no research has been conducted on how to mimic the meniscus to bone interface and attach the TE meniscus to the patient. The most common and successful allograft fixation techniques are soft tissue fixation and the double bone plug, or hard tissue fixation. Soft tissue fixation removes the patient's meniscus with the bony insertion and then an all-inside suture fixation technique is used to attach the allograft to the bone. The meniscus can also be affixed to the bone using a screw or pin.[44] In the double plug technique, the graft is excised from the patient leaving the meniscus horn attachment sites intact with a section of bone. In the receiving patient, 10 mm holes are prepared at the horn insertion site and the graft bone plugs are secured into the hole using a cancellous screw.[45] The double bone plug technique better restores native load distribution in the knee compared to soft tissue fixation.[46]

Current TE meniscus efforts have not developed a soft tissue-to-bone interface for bone plug fixation and soft tissue may not have the mechanical strength to survive a

soft tissue fixation procedure or restore the native enthesis structure. Currently, a bone plug technique is simply not feasible due to the absence of a TE meniscus interface to bone. Some TE meniscus studies have been conducted *in vivo*, however the fixation techniques do not restore the native physiological structure and function of the meniscus enthesis. Many total meniscal replacements are reduced to partial meniscal replacements due to fixation difficulties and resulting meniscal extrusion.[47,48] The overall success of a graft is dependent on graft fixation and the absence of the interface can compromise the stability of the graft.[49] In order for TE meniscus to become a long-term solution for meniscus replacement, an appropriate technique for TE meniscus fixation must be established.

Currently little research has been conducted on tissue engineering of the meniscus interface.[43] However, the meniscus interface is analogous to the ligament-bone interface, which has a larger body of research. Heterogeneous composite or multiphasic scaffolds are a popular approach in which material properties are fine tuned to mimic the material gradient of the native interface.[50] Other approaches use a homogenous or heterozygous material and seed a cellular gradient of fibroblasts to osteoblasts.[43,51] Cellular interactions have been shown to be essential to the development and maintenance of the ligament to bone interface.[52] As a result, heavy emphasize for interface tissue engineering is placed on cell phenotype gradient. Interface tissue engineering efforts have had some success but have yet to reach native properties and often these approaches involve complex manufacturing and limited integration between phases of the graft. Tissue engineering soft tissue-to-bone interface for orthopedic application is reviewed in Chapter 2.

Previous Research

Anatomically Accurate Collagen Meniscus Constructs

Tissue engineering the meniscus is a major research aim of Dr. Bonassar's lab. Previous research in the lab established a method using microcomputed tomography (μCT) and magnetic resonance imaging (MRI) to create anatomically accurate meniscus implants (Figure 1.2 left).[25] Tissue injection molding techniques were used to create a construct integrated with living cells. These molds can be customized to a specific patient or subject, which facilitates personalized treatment in clinical application. These constructs were viable throughout 8 weeks of culture with enhanced tissue formation and improved mechanical properties.[53],[54]

Initial TE menisci developed in the lab were generated using alginate and FCCs.[55] To better mimic native meniscus composition, recent TE meniscus studies have investigated the use of high-density collagen type I as the main construct material (Figure 1.2 right).[56] Studies of high density collagen demonstrated that samples contracted uniformly with 20 mg/mL and 10 mg/mL collagen constructs. Biochemical analysis showed that collagen menisci had significantly higher percent retention of DNA, GAGs, and collagen over time, compared to the alginate constructs. At 4 weeks, collagen constructs at 10 and 20 mg/mL had 3 and 6 fold increases in tensile modulus compared to alginate constructs and improved formation of organized collagen fibers compared to alginate. However fibers did not show anisotropic native fiber alignment. Anisotropic fiber formation will be a primary focus in this dissertation.

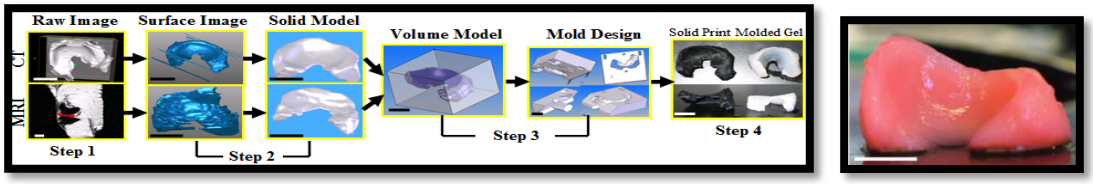

Figure 1.2: (left) Image processing steps.[25] (right) Anatomically accurate alginate menisci (bar=5mm).

Mechanical Boundary Conditions

Development of meniscus attachments to the tibia at the horns is a pivotal point in meniscus maturation into fibrocartilage.[37] Since fixation as a mechanical boundary condition helps direct fiber alignment and formation,[40] we have developed a system to fix our construct at the anterior and posterior meniscus extensions (Figure 1.3 top). The clamping technique encourages FCC matrix reorganization with circumferential fibers and radial tie fibers comparable to native anisotropic fiber alignment (Figure 1.3 bottom).[26] The formation of anisotropic fiber alignment comparable to native tissue has yet to be shown in other TE meniscus constructs. In this dissertation, we will extend this study to examine the behavior of co-cultured MSCs and FCCs under mechanical constraint.

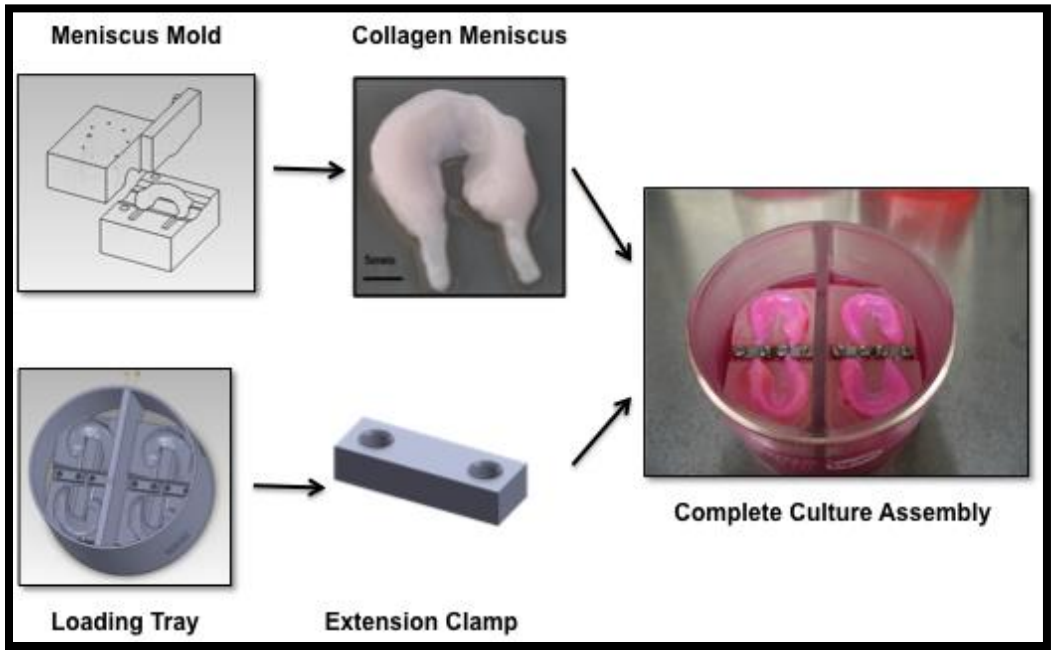

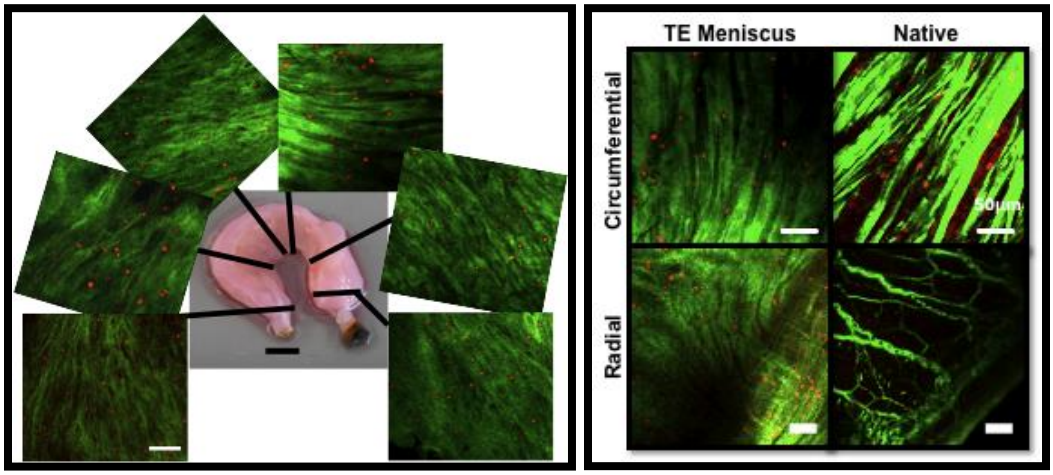

Figure 1.3: (top) Meniscus clamping process. (bottom left) Circumferential fiber formation in clamped meniscus. (bottom right) fiber alignment in clamped TE meniscus. (bar=50 μm)

Research Objectives

Producing functional TE menisci is challenging, requiring constructs that are anatomically accurate with anisotropic mechanics and biochemical properties equivalent to native menisci. Cellular approaches for TE menisci development do not translate into clinical practice because they lack a feasible cell source as well as critical anatomical, mechanical, or biochemical properties.[17,38,57,58] Mesenchymal stem cells (MSCs) are easily obtained and expanded in culture.[28] During native meniscus development, fibrocartilaginous tissue originates as unorganized mesenchymal condensations that become fibrocartilaginous after the formation of meniscus ligament attachments.[37] MSC fibrochondrogenic differentiation is not well understood *in vitro*, however previous research indicates improved differentiation through co-culture and mimicking biochemical and mechanical signals present during development.[34],[35] We have developed a novel anchoring technique to generate anatomically accurate TE menisci which has not been tested using MSCs.[26] The anchoring technique models the enthesis fixation to bone, however is not a true enthesis. Recreating the meniscal enthesis and establishing appropriate fixation techniques must be developed for a tissue engineered meniscus. The **long-term goal** of this project is to develop a clinically relevant, implantable, and anatomically accurate meniscal replacement with anisotropic and biochemical properties that mimic native menisci. The **goal of this dissertation** is to address key pre-clinical challenges: directing stem cell behavior to produce and appropriately organize matrix molecules and developing a tissue engineered meniscal enthesis for implant fixation.

Specifically we will address the following research questions: (a) does FCC and MSC co-culture improve MSC fibrochondrogenic behavior in anatomically shaped TE meniscus constructs, (b) how will mechanical boundary conditions affect co-cultured cells and matrix re-organization, (c) what is the role of proteoglycans in directing fiber formation, and (d) does mechanical fixation direct integrated collagen fiber formation at a bone-collagen gel interface?

Specific Aim 1 (Chapter 3)

Rationale 1: Current TE menisci utilize meniscal FCCs. However, FCCs proliferate slowly and lose their phenotype in 2D culture.[27] MSCs are easily obtained and in animal and clinical studies they home to injured tissue and contribute to tissue regeneration.[29–33,37] MSCs have been observed to differentiate down a fibrochondrogenic line; however, this pathway is not well characterized.[34,35] Co-culture using FCCs and MSCs increases fibrochondrogenic differentiation in MSCs. However, co-culture techniques have yet to be applied to 3D high density collagen scaffolds for developmental implants.

Hypothesis 1: Co-culture of MSCs with FCCs in a 3D collagen scaffold will facilitate increased matrix secretion and mechanical properties.

Specific Aim 1: Evaluate the effects of 3D co-culture on matrix secretion through mechanical and biochemical properties and MSC phenotype as indicated by cell shape.

Specific Aim 2 (Chapter 4)

Rationale 2: Mechanical boundary conditions have a profound effect on cellular behavior and remodeling.[40] In development, even in the absence of a dynamic load, anchoring the meniscus through attachments at the horns will provide critical mechanical signals for tissue organization.[37] We have demonstrated that anchoring

meniscus constructs facilitates FCC reorganization of collagen to form circumferential and radial tie fibers. MSC differentiation is known to be guided by mechanical cues, specifically in meniscus development, anchoring at the attachments provides critical mechanical signals for tissue organization and cartilage development.[40],[26],[37] Co-culture using FCCs and MSCs have yet to be used to produce functionally organized and mechanically robust whole TE meniscal implants. [34,35]

Hypothesis 2: Application of a mechanical boundary condition inducing hoop stress will produce circumferentially aligned and anisotropic tissue with improved mechanical properties when cultured with MSC and FCC co-culture.

Specific Aim 2: Investigate matrix synthesis and fiber formation in a high density collagen tissue engineered meniscus with MSCs and FCCs.

Specific Aim 3 (Chapter 5)

Rationale 3: The meniscal collagen fiber architecture provides essential mechanical infrastructure to support meniscal tissue function. Small leucine-rich proteoglycans (SLRPs) are present in the meniscus and are known to regulate fiber formation and maintenance.[59–63] Increasing the amount of small proteoglycans, decreased collagen fibril diameter *in vitro*.[64] Larger proteoglycans such as aggrecan may sterically hinder the formation of large fibers.[65] The presence of proteoglycans is relatively low during fiber development and increases with age,[66] suggesting a low concentration of proteoglycans are required for large diameter fiber formation in tissue engineered constructs. Glucose is the primary building block for GAG production in the cell.[67]

Hypothesis 3: Reducing the amount of proteoglycans produced in tissue engineered constructs through glucose reduction will increase fiber diameter and fiber alignment in tissue engineered menisci.

Specific Aim 3: Examine the role of small and large proteoglycans in modulating fiber formation in tissue engineered constructs.

Specific Aim 4 (Chapter 6)

Rationale 4: The meniscus is connected to the underlying bone through a soft tissue-to-bone interface, called the enthesis, at the posterior and anterior meniscal horns. The meniscal entheses fix the meniscus in the joint and prevent meniscal extrusion during loading.[68,69] These entheses are highly complex and difficult to regenerate in meniscal replacements. Meniscal allograft transplants that maintain an intact allogenic enthesis and fix the tissue in the knee joint using the underlying bone have shown improved load distribution over those that suture the soft tissue to bone.[46] There is limited information on how to regenerate the soft tissue-to-bone transition zone and a tissue engineered meniscus would require a means for proper fixation *in vivo*.

Hypothesis 4: Injection molding collagen into decellularized bone will create a model enthesis construct containing a bone, interface, and collagenous zone.

Specific Aim 4: Establish an experimental test platform for engineering the soft tissue to bone enthesis. Determine the effect of clamping on the organization of collagen at the soft tissue to bone interface.

REFERENCES

1. E. Makris, P. Hadidi and K. Athanasiou. The knee meniscus: structure-function, pathophysiology, current repair techniques, and prospects for regeneration. *Biomaterials*. **32,** 7411–31 (2011).
2. S. P. Arnoczky and R. F. Warren. Microvasculature of the human meniscus. *Am. J. Sports Med.* **10,** 90–5 (1982).
3. A. Chevrier, M. Nelea, M. B. Hurtig, C. D. Hoemann and M. D. Buschmann. Meniscus structure in human, sheep, and rabbit for animal models of meniscus repair. *J. Orthop. Res.* **27,** 1197–203 (2009).
4. F. N. Ghadially, J. M. Lalonde and J. H. Wedge. Ultrastructure of normal and torn menisci of the human knee joint. *J. Anat.* **136,** 773–91 (1983).
5. T. Kusayama, C. D. Harner, G. J. Carlin, J. W. Xerogeanes and B. a. Smith. Anatomical and biomechanical characteristics of human meniscofemoral ligaments. *Knee Surgery, Sport. Traumatol. Arthrosc.* **2,** 234–237 (1994).
6. R. J. Webber, M. G. Harris and a J. Hough. Cell culture of rabbit meniscal fibrochondrocytes: proliferative and synthetic response to growth factors and ascorbate. *J. Orthop. Res.* **3,** 36–42 (1985).
7. R. J. McDevitt, C.A. and Webber. The ultrastructure and biochemistry of meniscal cartilage. *Clin. Orthop. Relat. Res.* **252,** 8–18 (1990).
8. W. Petersen and B. Tillmann. Collagenous fibril texture of the human knee joint menisci. *Anat. Embryol. (Berl).* **197,** 317–24 (1998).
9. B. E. Baker, A. C. Peckham, F. Pupparo and J. C. Sanborn. Review of meniscal injury and associated sports. *Am. J. Sports Med.* **13,** 1–4

10. I. J. Cox, J.S., Nye, C.E., Schaefer, W.W., and Woodstein. The degenerative effects of partial and total resection of the medial meniscus in dogs' knees. *Clin. Orthop.* **109,** 178–183 (1975).

11. S. Kawamura, K. Lotito and S. A. Rodeo. BIOMECHANICS AND HEALING RESPONSE OF. **11,** 68–76 (2003).

12. T. Shybut and E. J. Strauss. Surgical Management of Meniscal Tears. **69,** 56–62 (2011).

13. E. A. Khetia and B. P. McKeon. Meniscal allografts: biomechanics and techniques. *Sports Med. Arthrosc.* **15,** 114–20 (2007).

14. I. D. Hutchinson, C. J. Moran, H. G. Potter, R. F. Warren and S. a Rodeo. Restoration of the meniscus: form and function. *Am. J. Sports Med.* **42,** 987–98 (2014).

15. Food and Drug Administration. Review of the ReGen Menaflex: Departures from Processes, Procedures, and Practices Leave the basis for a REview Decision in Question. (2009). Available at: Food and Drug.

16. T. G. Tienen, R. G. J. C. Heijkants, J. H. de Groot, A. J. Pennings, A. J. Schouten, R. P. H. Veth and P. Buma. Replacement of the knee meniscus by a porous polymer implant: a study in dogs. *Am. J. Sports Med.* **34,** 64–71 (2006).

17. B. B. Mandal, S.-H. Park, E. S. Gil and D. L. Kaplan. Multilayered silk scaffolds for meniscus tissue engineering. *Biomaterials*. **32,** 639–51 (2011).

18. K. Messner. Meniscal substitution with a Teflon-periosteal composite graft: a rabbit experiment. *Biomaterials*. **15,** 223–30 (1994).

19. D. J. Wood, R. J. Minns and A. Strover. Replacement of the rabbit medial

meniscus with a polyester-carbon fibre bioprosthesis. *Biomaterials*. **11,** 13–16 (1990).

20. K. J. Stabile, D. Odom, T. L. Smith, C. Northam, P. W. Whitlock, B. P. Smith, M. E. Van Dyke and C. M. Ferguson. An acellular, allograft-derived meniscus scaffold in an ovine model. *Arthrosc. J. Arthrosc. Relat. Surg.* **26,** 936–48 (2010).

21. J. H. de Groot, F. M. Zijlstra, H. W. Kuipers, A. J. Pennings, J. Klompmaker, R. P. H. Veth and H. W. B. Jansent. Meniscal tissue regeneration in porous 50/50 copoly (L-lactideh-caprolactone) implants. **18,** 613–622 (1997).

22. S. Kang, S. Son, J. Lee, E. Lee, K. Lee, S. Park, J. Park and B. Kim. Regeneration of whole meniscus using meniscal cells and polymer scaffolds in a rabbit total meniscectomy model. 7–11 (2006). doi:10.1002/jbm.a

23. K. R. Myers, N. a. Sgaglione and P. R. Kurzweil. A Current Update on Meniscal Scaffolds. *Oper. Tech. Sports Med.* **21,** 75–81 (2013).

24. C. H. Lee, S. A. Rodeo, L. A. Fortier, C. Lu, C. Erisken and J. J. Mao. Protein-releasing polymeric scaffolds induce fibrochondrocytic differentiation of endogenous cells for knee meniscus regeneration in sheep. **6,** 1–12 (2014).

25. J. J. Ballyns, J. P. Gleghorn, V. Niebrzydowski, J. J. Rawlinson, H. G. Potter, S. A. Maher, T. M. Wright and L. J. Bonassar. Image-guided tissue engineering of anatomically shaped implants via MRI and micro-CT using injection molding. *Tissue Eng. Part A*. **14,** 1195–202 (2008).

26. J. L. Puetzer, E. Koo and L. J. Bonassar. Induction of fiber alignment and mechanical anisotropy in tissue engineered menisci with mechanical anchoring.

J. Biomech. **48,** 1436–1443 (2015).

27. N. J. Gunja and K. A. Athanasiou. Passage and reversal effects on gene expression of bovine meniscal fibrochondrocytes. *Arthritis Res. Ther.* **9,** R93 (2007).

28. A. I. Caplan and J. E. Dennis. Mesenchymal stem cells as trophic mediators. *J. Cell. Biochem.* **98,** 1076–84 (2006).

29. M. Agung, M. Ochi, S. Yanada, N. Adachi, Y. Izuta, T. Yamasaki and K. Toda. Mobilization of bone marrow-derived mesenchymal stem cells into the injured tissues after intraarticular injection and their contribution to tissue regeneration. *Knee surgery, Sport. Traumatol. Arthrosc. Off. J. ESSKA.* **14,** 1307–14 (2006).

30. J.-D. Kim, G. W. Lee, G. H. Jung, C. K. Kim, T. Kim, J. H. Park, S. S. Cha and Y.-B. You. Clinical outcome of autologous bone marrow aspirates concentrate (BMAC) injection in degenerative arthritis of the knee. *Eur. J. Orthop. Surg. Traumatol.* **24,** 1505–1511 (2014).

31. C. J. Centeno, D. Busse, J. Kisiday, C. Keohan, M. Freeman and D. Karli. Regeneration of meniscus cartilage in a knee treated with percutaneously implanted autologous mesenchymal stem cells. *Med. Hypotheses.* **71,** 900–8 (2008).

32. F. Duygulu, M. Demirel, G. Atalan, F. F. Kaymaz, Y. Kocabey, T. C. Dulgeroglu and H. Candemir. Effects of intra-articular administration of autologous bone marrow aspirate on healing of full-thickness meniscal tear: an experimental study on sheep. *Acta Orthop. Traumatol. Turc.* **46,** 61–67 (2012).

33. M. F. Pittenger, A. M. Mackay, S. C. Beck, R. K. Jaiswal, R. Douglas, J. D.

Msca, M. A. Moorman, D. W. Simonetti, S. Craig and D. R. Marshak. Multilineage Potential of Adult Human Mesenchymal Stem Cells. *Science.* **284,** 143–147 (1999).

34. X. Cui, A. Hasegawa, M. Lotz and D. D'Lima. Structured three-dimensional co-culture of mesenchymal stem cells with meniscus cells promotes meniscal phenotype without hypertrophy. *Biotechnol. Bioeng.* **109,** 2369–80 (2012).

35. D. J. Saliken, A. Mulet-Sierra, N. M. Jomha and A. B. Adesida. Decreased hypertrophic differentiation accompanies enhanced matrix formation in co-cultures of outer meniscus cells with bone marrow mesenchymal stromal cells. *Arthritis Res. Ther.* **14,** R153 (2012).

36. E. Gardner and R. O'Rahilly. The early development of the knee joint in staged human embryos. *J. Anat.* **102,** 289–99 (1968).

37. C. R. Clark and J. A. Ogden. Prenatal and Postnatal Development of Human Knee Joint Mensci. *Iowa Orthop. J.* **1,** 20–27 (1981).

38. M. a Sweigart and K. a Athanasiou. Toward tissue engineering of the knee meniscus. *Tissue Eng.* **7,** 111–29 (2001).

39. P. a Dowdy, a Miniaci, S. P. Arnoczky, P. J. Fowler and D. R. Boughner. The effect of cast immobilization on meniscal healing. An experimental study in the dog. *Am. J. Sports Med.* **23,** 721–8 (1993).

40. K. D. Costa, E. J. Lee and J. W. Holmes. Creating alignment and anisotropy in engineered heart tissue: role of boundary conditions in a model three-dimensional culture system. *Tissue Eng.* **9,** 567–77 (2003).

41. S. S. G. B. V Sc, T. J. B. S. Blanchet and E. A. D. V. M. Morris. The surgical

destabilization of the medial meniscus (DMM) model of osteoarthritis in the 129 / SvEv mouse. 1061–1069 (2007). doi:10.1016/j.joca.2007.03.006

42. J. Gao. Immunolocalization of types I, II, and X collagen in the tibial insertion sites of the medial meniscus. *Knee Surg. Sports Traumatol. Arthrosc.* **8,** 61–65 (2000).

43. P. J. Yang and J. S. Temenoff. Engineering orthopedic tissue interfaces. *Tissue Eng. Part B. Rev.* **15,** 127–41 (2009).

44. J. H. Lubowitz, P. C. M. Verdonk, J. B. Reid and R. Verdonk. Meniscus allograft transplantation: A current concepts review. *Knee Surgery, Sport. Traumatol. Arthrosc.* **15,** 476–492 (2007).

45. W. R. Shelton and A. D. Dukes. Meniscus replacement with bone anchors: a surgical technique. *Arthrosc. J. Arthrosc. Relat. Surg.* **10,** 324–7 (1994).

46. H. Wang, A. O. Gee, I. D. Hutchinson, K. Stoner, R. F. Warren, T. O. Chen and S. A. Maher. Bone Plug Versus Suture-Only Fixation of Meniscal Grafts: Effect on Joint Contact Mechanics During Simulated Gait. *Am. J. Sports Med.* **42,** 1682–1689 (2014).

47. V. Martinek, P. Ueblacker, K. Bräun, S. Nitschke, R. Mannhardt, K. Specht, B. Gansbacher and a B. Imhoff. Second generation of meniscus transplantation: in-vivo study with tissue engineered meniscus replacement. *Arch. Orthop. Trauma Surg.* **126,** 228–34 (2006).

48. C. Chiari, U. Koller, R. Dorotka, C. Eder, R. Plasenzotti, S. Lang, L. Ambrosio, E. Tognana, E. Kon, D. Salter and S. Nehrer. A tissue engineering approach to meniscus regeneration in a sheep model. *Osteoarthr. Cartil.* **14,** 1056–1065

(2006).

49. M. M. Alhalki, S. M. Howell and M. L. Hull. How three methods for fixing a medial meniscal autograft affect tibial contact mechanics. *Am. J. Sports Med.* **27,** 320–328 (1999).

50. J. P. Spalazzi, S. B. Doty, K. L. Moffat, W. N. Levine and H. H. Lu. Development of controlled matrix heterogeneity on a triphasic scaffold for orthopedic interface tissue engineering. *Tissue Eng.* **12,** 3497–508 (2006).

51. J. E. Phillips, K. L. Burns, J. M. Le Doux, R. E. Guldberg and A. J. García. Engineering graded tissue interfaces. *Proc. Natl. Acad. Sci. U. S. A.* **105,** 12170–12175 (2008).

52. K. L. Moffat, I. E. Wang, S. A. Rodeo and H. H. Lu. Orthopaedic Interface Tissue Engineering for the Biological Fixation of Soft Tissue Grafts. **28,** 157–176 (2012).

53. J. J. Ballyns and L. J. Bonassar. Dynamic compressive loading of image-guided tissue engineered meniscal constructs. *J. Biomech.* **44,** 509–16 (2011).

54. J. L. Puetzer, J. J. Ballyns and L. J. Bonassar. The Effect of the Duration of Mechanical Stimulation and Post-Stimulation Culture on the Structure and Properties of Dynamically Compressed Tissue-Engineered Menisci. **18,** (2012).

55. J. J. Ballyns, T. M. Wright and L. J. Bonassar. Effect of media mixing on ECM assembly and mechanical properties of anatomically-shaped tissue engineered meniscus. *Biomaterials*. **31,** 6756–63 (2010).

56. J. L. Puetzer and L. J. Bonassar. High Density Type I Collagen Gels for Tissue Engineering of Whole Menisci. *Acta Biomater.* **9,** 7787–7795 (2013).

57. S. Kang, S. Son, J. Lee, E. Lee, K. Lee, S. Park, J. Park and B. Kim. Regeneration of whole meniscus using meniscal cells and polymer scaffolds in a rabbit total meniscectomy model. *J. Biomed. Mater. Res. Part A*. 7–11 (2006). doi:10.1002/jbm.a

58. D. J. Huey and K. a Athanasiou. Tension-compression loading with chemical stimulation results in additive increases to functional properties of anatomic meniscal constructs. *PLoS One*. **6,** e27857 (2011).

59. E. J. Vanderploeg, C. G. Wilson, S. M. Imler, C. H. Y. Ling and M. E. Levenston. Regional variations in the distribution and colocalization of extracellular matrix proteins in the juvenile bovine meniscus. *J. Anat.* **221,** 174–186 (2012).

60. M. Viola, B. Bartolini, M. Sonaggere, C. Giudici, R. Tenni and M. E. Tira. Fibromodulin interactions with type I and II collagens. *Connect. Tissue Res.* **48,** 141–8 (2007).

61. A. Hildebrand, M. Romarís, L. M. Rasmussen, D. Heinegård, D. R. Twardzik, W. A. Border and E. Ruoslahti. Interaction of the small interstitial proteoglycans biglycan, decorin and fibromodulin with transforming growth factor beta. *Biochem. J.* **302,** 527–34 (1994).

62. K. G. Danielson, H. Baribault, D. F. Holmes, H. Graham, K. E. Kadler and R. V. Iozzo. Targeted disruption of decorin leads to abnormal collagen fibril morphology and skin fragility. *J. Cell Biol.* **136,** 729–743 (1997).

63. R. V Iozzo. The Biology of the Small Leucine-rich Proteoglycans. *Jouranl Biol. Chem.* **274,** 18843–18846 (1999).

64. K. G. Vogel and J. A. Trotter. The Effect of Proteoglycans on the Morphology of Collagen Fibrils Formed In Vitro. *Coll. Relat. Res.* **7,** 105–114 (1987).

65. V. M. Wang, R. M. Bell, R. Thakore, D. R. Eyre, J. O. Galante, J. Li, J. D. Sandy and A. Plaas. Murine tendon function is adversely affected by aggrecan accumulation due to the knockout of ADAMTS5. *J. Orthop. Res.* **30,** 620–6 (2012).

66. C. H. Y. Ling, J. H. Lai, I. J. Wong and M. E. Levenston. Bovine meniscal tissue exhibits age- and interleukin-1 dose-dependent degradation patterns and composition-function relationships. *J. Orthop. Res.* **34,** 801–811 (2016).

67. A. Mobasheri, S. J. Vannucci, C. A. Bondy, S. D. Carter, J. F. Innes, M. F. Arteaga, E. Trujillo, I. Ferraz, M. Shakibaei and P. Mart??n-Vasallo. Glucose transport and metabolism in chondrocytes: A key to understanding chondrogenesis, skeletal development and cartilage degradation in osteoarthritis. *Histol. Histopathol.* **17,** 1239–1267 (2002).

68. A. C. Abraham and T. L. Haut Donahue. From meniscus to bone: A quantitative evaluation of structure and function of the human meniscal attachments. *Acta Biomater.* **9,** 6322–6329 (2013).

69. H. J. Park, S. S. Kim, S. Y. Lee, Y. J. Choi, E. C. Chung, M. H. Rho and H. J. Kwag. Medial meniscal root tears and meniscal extrusion transverse length ratios on MRI. *Br. J. Radiol.* **85,** (2012).

CHAPTER 2

Next Generation Tissue Engineering of Orthopedic Soft Tissue-to-Bone Interfaces[1]

Abstract

Soft tissue-to-bone interfaces are complex structures that consist of gradients of extracellular matrix materials, cell phenotypes, and biochemical signals. These interfaces, called entheses for ligaments, tendons, and the meniscus, are crucial to joint function, transferring mechanical loads and stabilizing orthopedic joints. When injuries occur to connected soft tissue, the enthesis must be re-established to restore function, but due to structural complexity, repair has proven challenging. Tissue engineering offers a promising solution for regenerating these tissues. This prospective review discusses methodologies for tissue engineering the enthesis, outlined in three key design inputs: materials processing methods, cellular contributions, and biochemical factors.

[1]This work has been submitted for publication: M. C. McCorry A.J. Boys, S. Rodeo, L. J. Bonassar, and L.A. Estroff. Next Generation Tissue Egnineering of Orthopedic Soft Tissue-to-Bone Interfaces. Submitted to *MRS Communications.*

Introduction

Soft tissue-to-bone interfaces are present in many tissues, supporting movement in vertebrate animals. These interfaces mediate mechanical transitions between highly dissimilar materials, with a three or more order of magnitude change in stiffness that occurs over only a few hundred microns.[1–3] While these interfaces are robust, undergoing wear and tear over the entire lifespan of humans, they fail in instances of extreme joint loading. Tissue engineered replacements can be constructed outside of the body and implanted as living tissue, offering a promising alternative to current repair options. This review discusses the structure and development of some representative orthopedic interfaces in the body (e.g., ligamentous, tendinous, and meniscal attachments) and how we can use this information to engineer living tissues for the repair and replacement of these mechanically, compositionally, and structurally complex interfaces.

The ligamentous, tendinous, and meniscal attachments, also called entheses, act to anchor soft tissues to bone. Injuries to the enthesis often result in acute disability and may ultimately pre-dispose the affected joint to diseases such as osteoarthritis, a disease estimated to affect over 70% of people aged 55 to 78.[4] Severe injuries of these tissues often require replacement, which is typically accomplished using cadaveric tissue (allograft) or tissue removed from the patient's own body (autograft) (Fig. 2.1). Allograft tissue can effectively replace the damaged tissue in its entirety. For example, in the case of meniscus replacement, an allograft tissue consists of the entire meniscus, including the entheses.[5] Proper fixation of the implant at the entheses is a necessity for surgical success.[6] Including the entheses also obviates the need to reconstruct this

complex interface between soft tissue and bone. Despite the advantages of allografts, limitations relate to cost, tissue sizing, availability, and potential for an adverse immune response. Autograft tissue is also frequently used for ligament and tendon repair, where a portion of the patient's native tendon is used. However, autograft tissue replacement can require multiple surgical sites, and harvest of autografts from ligament sites is not feasible. Tissue engineered implants combine the advantages of both the allograft and autograft options in that they offer a customizable, living implant that can be produced without requiring a donor or donor site.

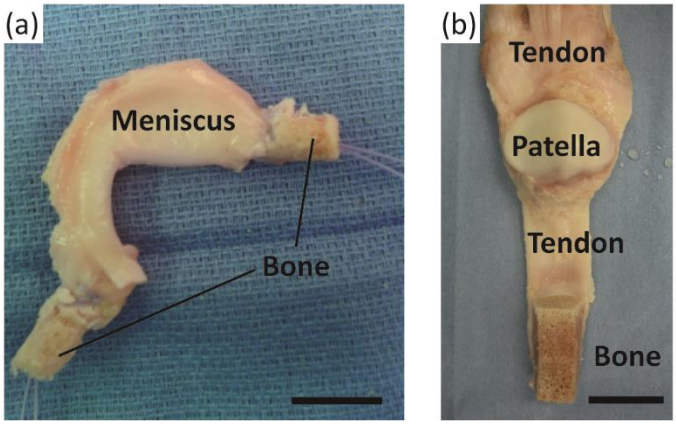

Fig. 2.1. Surgical adult human allograft replacements for (A) meniscus and (B) patellar tendon with full bone insertions intact. Sutures are threaded through the insertion points and pulled into bone tunnels to anchor allograft tissues in place. Leaving the entheses intact obviates the need for enthesis healing, increasing the success rate for patient recovery. Scale bars are 20 mm.

Tissue engineering interfaces requires an interdisciplinary effort among biomedical engineers, materials scientists, and orthopedic surgeons. These tissues are complex in nature, consisting of multi-scale arrangements of multiple tissue types. The mechanical function of these interfaces is derived in part from the hierarchical arrangement of relatively simple building blocks into composite materials. Interfacial tissues are integrated into a continuous gradient populated by a variety of cell types, and

these cell types are accompanied by chemical factors and signaling molecules that influence the maturation of these tissues and maintain homeostasis. Two types of entheses can be found in the body: direct and indirect. Direct entheses have a fibrocartilaginous region between the bone and the highly organized collagen fibers of the ligament, tendon, etc.[7] Conversely, indirect entheses are usually observed on the shafts of long bones and have fibers that connect directly into bone (Sharpey's fibers). This review will focus on direct entheses.

All direct entheses have the same general subdivisions based on tissue type, as observed through histological analysis: subchondral bone, calcified fibrocartilage, uncalcified fibrocartilage, and oriented soft tissue.[8–10] Comparative structures of tendon, ligament, and meniscal entheses are highlighted using a tetrachrome stain of sagittal sections of these interfaces (Fig. 2.2). The extracellular matrix (ECM) of these tissues consists primarily of collagen, proteoglycans, and apatite. The interfacial region, or interphase[11,12], consists of a spatial distribution of cell types, moving from bone cells (osteoblasts, osteoclasts, osteocytes) to hypertrophic fibrochondrocytes in the calcified fibrocartilage to fibrochondrocytes in the uncalcified fibrocartilage to fibroblasts in the oriented collagenous region of the enthesis (Fig. 2.3). These cell types are accompanied by biochemical and biomechanical cues that also vary by region, often with temporal and spatial gradients in concentration. [13–16]

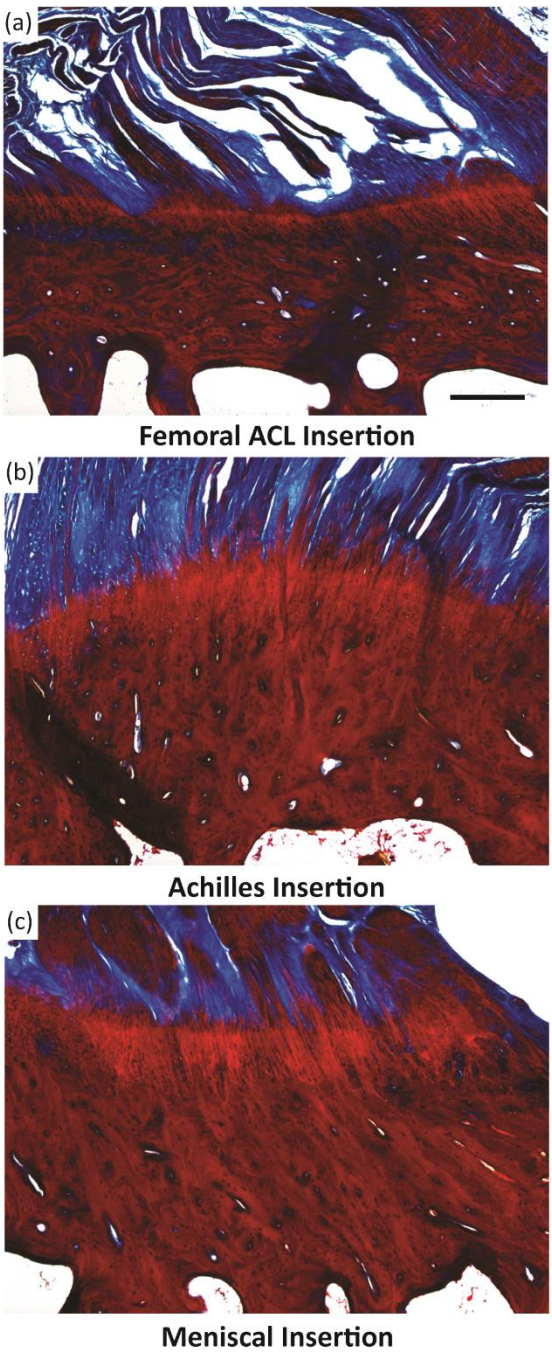

Fig. 2.2. Light microscope images of three different osteochondral interfacial tissues, stained with tetrachrome stain. All images show ovine tissue, cut in the sagittal plane of the enthesis: (A) the femoral anterior cruciate ligament (ACL) insertion, (B) insertion point of gastrocnemius tendon with the calcaneal bone, referred to here as the Achilles insertion, and (C) the meniscal insertion. Trabecular pores are visible on the bottoms of each image, beneath dense calcified bone (deep red). Porous regions transition through to fibers (blue). Note the varying thicknesses of the interfacial regions, and variable morphology of the intermediate bony regions per anatomy. Scale bar is 400 μm.

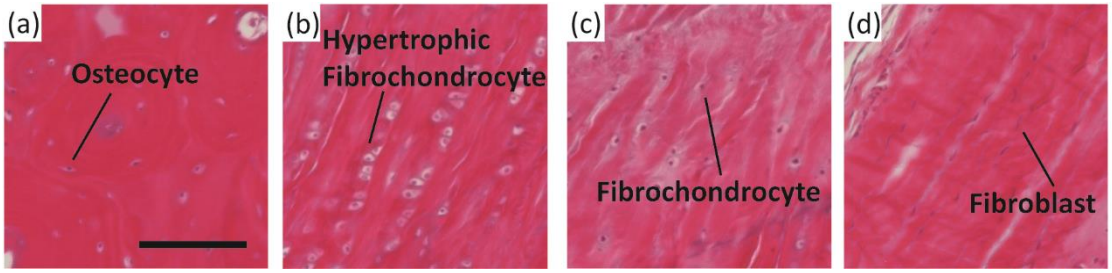

Fig. 2.3. Representative histological images of cellular phenotypes from (A) bone, (B) calcified fibrocartilage, (C) fibrocartilage, and (D) ligament from a mature ovine ACL enthesis (hematoxylin and eosin). (A) Osteocyte embedded between lamellae of an osteon. (B) Enlarged hypertrophic fibrochondrocytes organized in columns indicating rapid proliferation. (C) Fibrochondrocyte in disorganized fiber region. (D) Elongated spindle shaped fibroblast between large organized fibers. Scale bar is 200 μm.

As a prospective review, this paper highlights current methods of designing and fabricating a tissue engineered enthesis construct with a view toward future directions. Enthesis engineering is still at an early stage, even when compared with other tissue engineering efforts. While prior studies have examined methods to engineer bulk tendon, ligament, meniscus, and even other orthopedic interfaces,[17,18] such as the osteochondral interface and the periodontal interface,[19,20] few studies have focused on engineering entheseal tissues.[21–23] This review divides the orthopedic interface engineering process into three main design inputs: materials processing methods, cellular contributions, and biochemical factors. These inputs must be developed in parallel for both the osteogenic and soft tissue-generating portions of a construct, then combined across an interfacial region of the construct to promote continuity and integration. This interphase can be formulated into either continuous but opposing gradients of soft tissue and bone inputs or a graded interface, consisting of multiple regions that reflect the composition of the native tissue. Following tissue assembly, the maturation process is key to promote eventual integration with the local joint tissues

(Fig. 2.4). The following sections discuss these inputs individually and address how these methods can be utilized in parallel to generate soft tissue-to-bone interfaces.

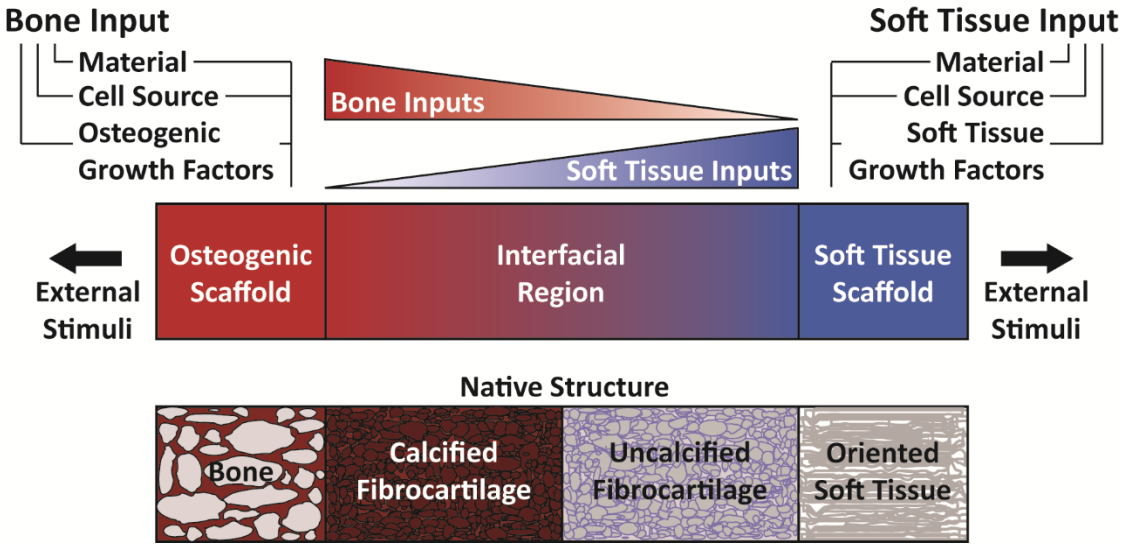

Fig. 2.4. Schematic highlighting the process for constructing a tissue engineered interfacial construct. Materials, cell source, and growth factors are the central input considerations for a tissue engineering study design. The interfacial region requires complementary gradients of bone and soft tissue inputs. Following construct assembly, external stimuli such as mechanical loading can be applied to further aid in tissue development.

Materials Processing Methods

The architecture of the enthesis is complex, consisting of hierarchical arrangements of collagen fibrils, proteoglycans, and apatite [$Ca_{10}(PO_4)_6(OH)_2$] crystals. The molecular composition, spatial distribution, and nano- to micro-scale assembly of these components dictate the properties of each tissue region and are critical for defining the mechanical stability of the entire enthesis. The following sections describe the native enthesis structure and methods for mimicking this structure through tissue engineering.

Native Organization

Collagen is the main component of the enthesis. Three major types of collagen are found across the interface: type I, type II, and type X. Collagens III, V, and VI are

also found in these interfaces at much lower concentrations.[24] Types I and II collagen are fibrillar collagens, meaning they self-assemble into organized nanofibers, ~50 to 500 nm in diameter.[25] Type I collagen is deposited in association with tensile forces and is found in bone and ligamentous tissue. Type II collagen is associated with compressive forces and is found primarily in fibrocartilaginous regions.[13] These fibrillar collagens can further assemble into increasingly large fiber-like structures. This type of organization is found within the oriented soft tissue of the entheseal attachments and is typically associated with type I collagen. Collagen fibrils in this region can bundle together into structures called fascicles, ~50 to 300 μm in diameter, which are in turn bundled into large fibers, ~100 to 500 μm in diameter.[25] Type X collagen is found in calcified fibrocartilage regions and is non-fibrillar,[13] but its exact role as a matrix protein is unknown.

The enthesis contains proteoglycans that bind water, provide compressive strength, and contribute to collagen fiber formation. Proteoglycans consist of a central core protein and at least one covalently attached glycosaminoglycan (GAG) chain. GAGs are linear, highly charged polysaccharides that can contain sulfate and carboxylate groups.[26] Aggrecan is the predominant proteoglycan in cartilage and is the largest of the proteoglycans. The large "bottle brush" structure and negative charge of aggrecan helps to bind and retain water, which contributes to the ability of cartilage to resist compression.[27] Small leucine-rich proteoglycans (SLRPs) such as fibromodulin, decorin, and biglycan are known to bind to collagen and help to regulate collagen fiber formation and maintenance.[28–30] Aggrecan is often found in regions of

soft tissue-to-bone interfaces under compressive loading, while SLRPs are found in regions with large fibers experiencing tensile loads.[31]

Apatitic mineral is found within the subchondral bone and calcified fibrocartilage regions of the interfacial tissues. The mineral phase is primarily non-stoichiometric hydroxyapatite with carbonate substitutions that is arranged into nanocrystalline platelets. In bone, these platelets are contained within collagen fibrils and are oriented with their c-axis parallel to the direction of the fibril. Non-collagenous proteins are thought to organize the apatite platelets into the intrafibrillar spacing of collagen, but the exact mechanism through which this hierarchical structuring occurs is unknown[32]. Thorough reviews of bone structure are available.[33,34] The mineral phase in calcified fibrocartilage is also mainly carbonate-substituted hydroxyapatite, but the organization of the crystals within the matrix is not as well understood.[8,35]

Aggregating the above information, subchondral bone consists of type I collagen fibrils infiltrated with nanocrystalline, carbonated apatite arranged circumferentially around pores, typically on the order of 1 mm in diameter.[36] This structure transitions into non-porous calcified fibrocartilage, consisting of type II and type X collagen, apatitic mineral, and proteoglycans. Uncalcified fibrocartilage consists of splayed fibrils of type II collagen with proteoglycans. These splayed fibrils transition from the uncalcified fibrocartilage region into large type I collagen fibers that make up the oriented fiber region of the enthesis. These large fascicles further organize into large fibers that constitute the remainder of the bulk of the soft tissue.[31,37] Understanding native structure/composition should inform material selection for tissue engineering.

Materials Selection

Appropriate materials for a tissue engineered scaffold must possess adequate mechanical properties, support cellular attachment and differentiation/proliferation, and potentiate cellular remodeling. Since the modulus ranges drastically across soft tissue-to-bone interfaces, a variety of materials have been used for tissue engineered constructs. To match the moduli of the stiff, mineralized regions of the enthesis, various calcium phosphate minerals, such as hydroxyapatite and tricalcium phosphate, and bioglass have been used.[38–44] The compliant portions of the enthesis have been constructed from polymers and copolymers consisting of poly(capralactone) (PCL), poly(lactic acid) (PLA), poly(glycolic acid) (PGA), and/or poly(ethylene glycol) diacrylate (PEGDA),[42,44–49] as well as other biopolymers such as silk, agarose, gelatin, hyaluronic acid, and collagen.[41,50–55] Decellularized or demineralized native matrices have also been used to engineer the enthesis.[42,53,54,56,57]

Materials-Based Design & Fabrication

The complex structure of the enthesis is related to its function, providing continuity and integration between multiple tissues with differing properties. The necessity for this integration and continuity arises from the loading of such interfaces in tension;[58] hence, failure modes like delamination become relevant for poorly integrated constructs. To promote continuity, various materials processing techniques have been used. Many of these techniques revolve around the construction of gradients. Controlled crystal growth on electrospun poly(lactic-*co*-glycolic) acid (PLGA) resulted in a nanofiber scaffold with a mineral gradient.[40] This gradient was formed through syringe pump-mediated injection of a calcium and phosphate salt-containing solution. Upon cell-seeding, the activity of alkaline phosphatase (ALP), an enzyme associated with

mineral deposition, the expression of RUNX2, an osteoblast-related transcription factor, and the expression of osteocalcin, an osteoblast-related protein, were correlated with mineral deposition. Cellular density and cell proliferation were negatively correlated with mineral deposition.[40] These results indicate that proper processing and appropriate arrangement of enthesis-related materials result in spatially localized cellular responses that mimic those found in the body. However, implantation of this scaffold for the repair of the murine supraspinatus tendon resulted in scar formation, indicating that further processing is required for optimal enthesis reconstruction.[59]

Regional integration in scaffolds can also be induced through the production of microstructure gradients. For example, freeze-casting coupled with salt-leaching enabled the formation of a multi-region scaffold composed of silk fibroin (Fig. 2.5A).[51] The processing conditions were designed to form a continuous scaffold with a porous, trabecular bone-like structure that transitions into a fiber-like morphology. The porous region results from salt-leaching, in which a solution of silk fibroin and NaCl is frozen and freeze-dried. The precipitated salt crystals are subsequently dissolved, creating pores within the silk matrix. This region transitions to a fiber-like morphology, created using freeze-casting, a process in which directional freezing is used to grow elongated ice crystals within a polymer solution. During solidification, the polymer, i.e. silk fibroin, is concentrated into the boundaries between the crystals.[60] Upon sublimation of the ice crystals, oriented fiber-like structures composed of silk fibroin remain. These processing methods result in a continuous silk structure that mimics the morphology of collagen in the native enthesis.[51] Similar scaffolds have been produced for the osteochondral interface, demonstrating the customizability of these techniques.[61]

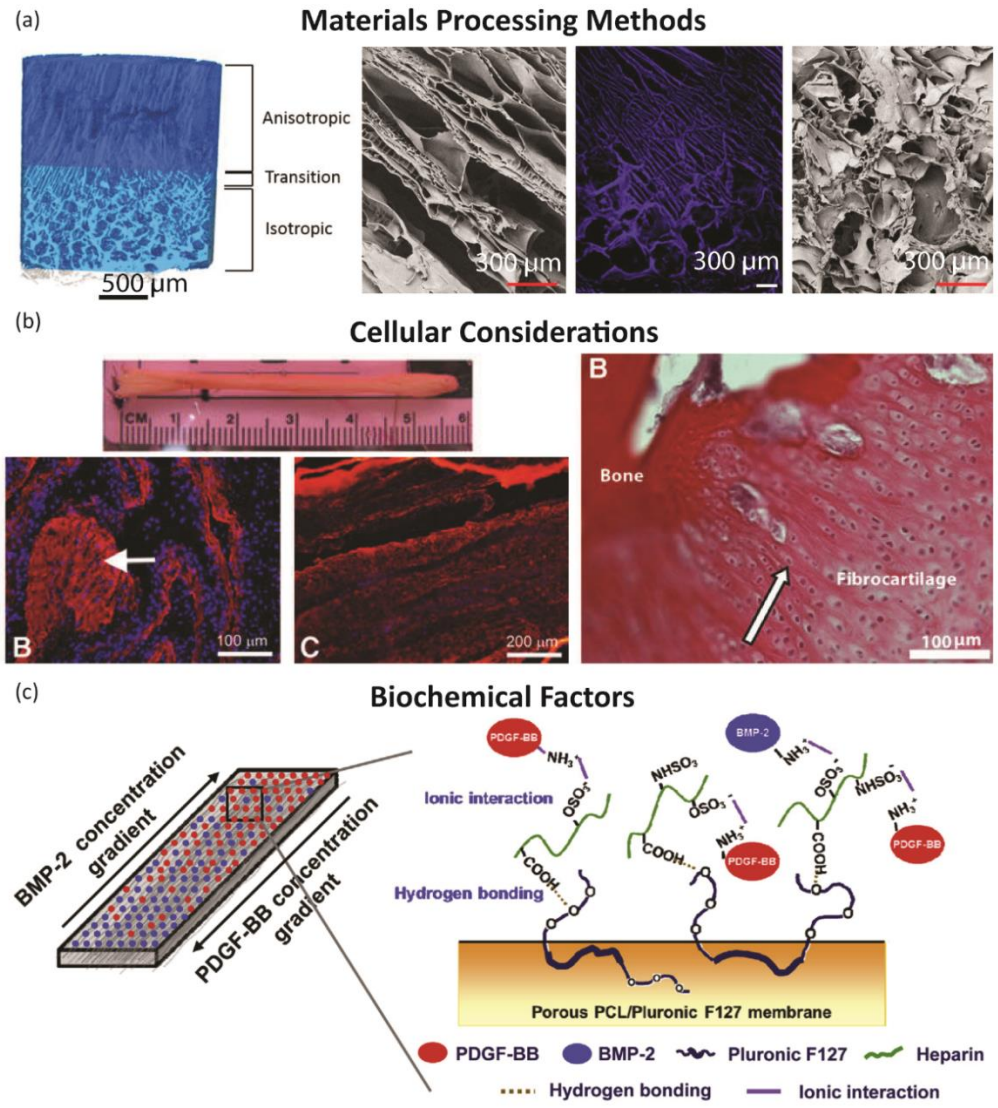

Fig. 2.5. Examples of tissue engineered interface constructs for soft tissue to bone. (A) Biphasic anisotropic silk fibroin scaffold with integrated fiber/bone interface. Images from left-to-right: µCT of full construct, field emission scanning electron microscopy (FESEM) image of, anisotropic (fiber) region, fluorescence microscopy image of transition region, and FESEM image of porous (trabecular) region.[51] (B) Bone-ligament-bone ACL replacement generated using stem cell self-assembly and targeted differentiation. Images from left-to-right: full tissue engineered construct, immunostained for collagen (red) and DAPI stained (nuclear stain) section showing bony region prior to implantation, immunostained for collagen (red) and DAPI stained (nuclear stain) section showing ligament region prior to implantation, image of regenerated fibrocartaliginous region with aligned nuclei (arrow) after 2 months implantation.[97] (C) Porous membrane with inverse gradients of PDGF and BMP-2 for tendon-bone repair.[134]

Structural characteristics are important in that they not only affect the mechanical properties of the scaffold but also drive cellular differentiation. Fiber alignment drives matrix deposition rates in meniscal fibrochondrocytes and mesenchymal stem cells (the progenitor cells for bone, cartilage, etc.).[62] Pore size affects the production of cartilage matrix proteins by cells. For example, smaller pore sizes cause cells to produce more GAGs.[19] In addition to structurally-derived cellular effects, the material composition of scaffolds also has an effect on differentiation. The addition of hydroxyapatite to scaffolds improves osteogenic properties and increases cellular attachment,[38,49] and the presence of GAGs in scaffolds drives cells toward a chondrogenic lineage.[63,64]

The use of materials to control cellular responses can also be achieved through biodegradability and remodeling. For example, a triphasic scaffold, created by sintering polyglactin mesh, PLGA microspheres, and bioglass and PLGA microspheres together, shows varying rates and types of tissue ingrowth into the scaffold following subcutaneous implantation.[44] All regions of the scaffold showed collagen deposition, and the bioglass and PLGA microsphere region allowed for mineral deposition. The polyglactin region degraded entirely, producing a fibrocartilage-like area between the polyglactin and PLGA microsphere region.[44,65] Biodegradation is heavily utilized in many scaffolds to promote tissue infiltration. The mechanism of biodegradation should also be considered for tissue engineering. Biodegradable polymers like PLA and PGA can be degraded through hydrolysis, opening up space for tissue to grow into, whereas biopolymers such as collagen must be enzymatically degraded and rearranged by cells,

providing a template for remodeling. For example, cells rearranged collagen gels into large, oriented fibers during culture of a meniscus construct, indicating the value of incorporating cellular remodeling capability into a scaffold.[66] Implementation of continuity, integration of structure, and support for cellular remodeling in scaffolds allows for control of mechanical properties, strengthening of interfacial regions, and ability of the scaffold to integrate with native tissue upon *in vivo* implantation.

Persistent Challenges

Materials processing techniques and induction of cellular remodeling capabilities provide many of the benefits in these highlighted scaffolds. From a materials structuring standpoint, utilization of processing techniques like freeze casting and electrospinning produce microstructures that mimic portions of the enthesis. In addition to variations in structure at the microscale, the native enthesis also possesses multiple levels of hierarchy that produce many chemical and mechanical benefits, perhaps most well known in bone.[34] In the oriented soft tissue of the enthesis, the hierarchical construction of collagen fibers from fascicles, fibrils, etc. allows for multiple regimes of mechanical properties, most obvious by the presence of a "toe region" during tendon loading.[25] Additionally, hierarchical construction facilitates cellular remodeling, as cells can subsist within the tendon fibers, rather than just being adhered to the outside of the fiber. Despite the prevalence of hierarchical structures in the enthesis, few scaffolds implement similar multi-scale features. Traditionally, tissue engineering approaches have relied on cells to produce an ECM with the desired chemical and structural heterogeneity. However, in forming complex tissue interfaces, such as those in the enthesis, cells benefit from pre-existing hierarchy within the

scaffold. For example, in the construction of bone-like scaffolds, physical mixtures of hydroxyapatite nanoparticles within a collagen gel versus mineralized collagen fibrils, in which the hydroxyapatite crystals are grown *within* the collagen fibrils, display clear differences in properties.[67] Similarly, cells respond very differently to the fibrillar structuring of collagen gels as compared to the poorly organized collagen within gelatin gels. Similarly, seeding of cells onto oriented polymer scaffolds not only induces organization in the synthesized ECM, but leads to the development of chemically and mechanically distinct micro-domains within engineered tissues.[64] When designing tissue scaffolds, the introduction of multi-scale chemical and structural heterogeneity can result in an enhancement of cell-based reorganization. Using these principles for tissue engineering can provide similar benefits to native tissue and can also be used to add further functionality to a construct.

Cellular Contributions

Cells and cellular interactions drive the maturation of scaffolds before and after implantation, therefore cellular content is an essential component to the design of any tissue engineered construct. Biocompatibility, cellular integration, and cellular remodeling are key considerations when creating, culturing, and implanting a construct. Cells function in complex 3D environments and respond to a plethora of inputs including materials interactions, substrate stiffness, mechanical conditioning, biochemical signaling, and cell-cell interactions. Tissue engineering approaches utilize such inputs to drive maturation of a functional construct.

Native Cell Types

Soft tissue-to-bone interfaces span four regions with distinct cellular phenotypes (Fig. 2.2 and 2.3). Each cellular type found in the enthesis has a distinctive behavior, cell shape, matrix production profile, and genetic expression that that defines its phenotype. Osteoblasts, osteoclasts, and osteocytes are the three main cell types that reside in bone. Osteoblasts initiate new bone formation, while osteoclasts resorb and remodel bone. An osteocyte is a terminally differentiated osteoblast that resides in the mineral matrix to maintain bone homeostasis (Fig. 2.3A). Together, these cells regulate bone formation and maintenance. The bone phenotype is typically quantified by expression or accumulation of proteins, such as osteopontin and osteocalcin, type I collagen, markers of mineralization, such as ALP activity, and expression of transcription factors, such as RUNX2.[68] The transition from bone to the calcified fibrocartilage region, is regulated by hypertrophic fibrochondrocytes (Fig. 2.3B). Hypertrophy is the process in which chondrocytes increase in size, and secrete type X collagen in a mineralized cartilaginous matrix.[69] In contrast, chondrocytes are found in cartilage and exhibit a rounded morphology. These cells reside in a proteoglycan-rich (mostly aggrecan) matrix composed of collagens I and II. Chondrocytes, found in the cartilaginous tissue, have upregulated levels of aggrecan, collagen type II, link protein, Sox9, and COMP genes.[70] Fibrochondrocytes that reside in the uncalcified fibrocartilage region of the enthesis are named as such because they exhibit phenotypic markers of both fibroblasts and chondrocytes (Fig. 2.3C). The native cell phenotypes serve as benchmarks for cell behavior and stem cell differentiation in tissue engineered constructs. Ligament cells and tenocytes (tendon cells) are often described as exhibiting

a fibroblastic phenotype due to their spindle shape and production of collagen type I (Fig. 2.3D).[16] While these two cell types belong to distinctly different tissues, they share many common markers. Key positive markers for this phenotype are production of type I collagen, tenascin-C, scleraxis, tenomodulin, and proteoglycans such as decorin, biglycan, versican, lumican, and fibromodulin.[71,72]

Tissue Engineering with Cells

A consistent challenge of producing these soft tissue-to-bone interfaces is incorporating cells into the materials processing methods of the scaffold. Cellularizing these constructs can be accomplished by either encapsulating cells directly into the scaffold or by seeding cells onto the material surface and directing migrating cells into the scaffold. Growth factors or other chemoattractants are useful to encourage cellular migration and infiltration into scaffolds.[57,73,74] Processing cells and materials together restricts the conditions in which a scaffold can be processed. Cells require a specific operational window of temperature, pH, pressure, strain, osmolarity, and ion and solute balance in order to maintain viability. Furthermore, the soft tissue-to-bone interface contains an array of cell types. The number of cell types and the cellular locations in the tissue engineered scaffold play a role in soft tissue-to-bone interface assembly, culture, and development.

Given the gradient of cell types present in the enthesis, co-culture is one method to generate a graded interface. Different cell types are constantly interacting during native development and have intertwined signaling feedback mechanisms that are critical to development.[16,69,75] *Ex vivo* co-culture mediates cell-cell contact and paracrine interactions that have been shown to influence cellular phenotype. Co-

culturing of chondrocytes and osteoblasts in direct contact using a high cell density 3D micromass reduced GAG deposition in chondrocytes and cell-mediated mineralization in osteoblasts.[76] Furthermore, co-culture can be used as a tactic to guide stem cell differentiation.[77–81] One strategy to create an integrated gradient is to co-culture the desired cell types and generate cell gradients that utilize cell-cell interactions to mature the material into a graded interface. For ligament-bone interfaces, 2D co-culture of fibroblasts and osteoblasts modeled using a fibroblast region, interface region, and osteoblast region decreased cell proliferation and increased cell-mediated mineralization by fibroblasts. In addition, production of collagen type II and aggrecan increased, indicating that co-culture interactions can lead to cell trans-differentiation from one cell phenotype to another.[55] Co-culturing of different cell types is a useful technique to integrate the different tissue regions of the soft tissue-to-bone interface.

An alternative to using multiple cell types is using stem cells, which can differentiate into multiple cell types. *In* vivo entheses begin as dense mesenchymal condensates and develop into complex interfaces.[82–84] Since stem cells have the capacity to differentiate into all the cell phenotypes of the enthesis, stem cells are a logical cell source to use for tissue engineering the enthesis [85,86] Mesenchymal stem cells (MSCs) from bone marrow are a popular source for tissue engineering because they are easily obtained and expanded. Adipose-derived stem cells (ASCs) are another common stem cell source. Since ASCs are easily obtained from fat which is considered surgical debris, they are the most readily available stem cell source from human tissue. While ASCs do have multipotent properties, they have been shown to be less effective at differentiating into cartilage and bone.[87] Stem cells seeded into tissue engineered

enthesis constructs rely on mimicking the biomaterial and biochemical inputs that direct differentiation during development. For example, regional changes in pore alignment of a tendon/ligament enthesis silk fibroin scaffold resulted in corresponding ASC differentiation into cartilage and tendon lineages (Fig. 2.5A).[51] These examples emphasize the importance of scaffold material and biochemical design in order to inform cell behavior when generating enthesis constructs.

Construct geometry and chemistry have been shown in multiple systems to affect cellular phenotype through cell-material interactions.[88,89] Cellular phenotypes can be dictated by cell-material interactions. A material such as collagen has cellular adhesion sites, allowing cells to bind and spread, encouraging the cells to develop a fibroblastic morphology. Alternatively, a material lacking in cell adhesion sites, like alginate, prevents cells from binding, encouraging a chondrogenic morphology.[90,91] Cell morphology, such as a fibroblastic or chondrogenic morphology, has been shown to be an indicator for cell behavior and matrix production.[92] Scaffold mechanical properties are known to direct stem cell fate, where materials with stiffer structures promote osteogenic differentiation.[93,94] Lastly, chemical composition dictates cellular response. Cells embedded in a proteoglycan-rich region experience increased strain shielding compared to cells embedded in collagen fibers when a tissue level mechanical deformation is applied to the scaffold.[64] Furthermore, the arrangement and alignment of fibers in a 3D microenvironment affects cellular behavior and the distribution of applied loads. In an aligned poly(ethylene oxide) scaffold, cells attach and elongate in the direction of the fibers. Fiber alignment aided MSC differentiation into a fibrous phenotype compared to the same MSCs in pellet culture which developed a

chondrogenic phenotype.[92] Furthermore, aligned fibers improved ligamentous phenotype, as cells develop characteristic spindle shapes and increase production of collagen when compared to random fiber alignment. The alignment of fibers also affects the cellular response to an applied strain, with longitudinal strains in the fiber direction inducing the largest increase in collagen production.[95,96] These studies emphasize the importance of material mechanical properties and structure when considering cellular interactions and response.

Another approach to tissue engineering soft tissue-to-bone interfaces shifts the focus from materials design to utilizing the cells themselves to create the scaffold. Cells grown in mono-layers have the ability to proliferate to fill the surface area and then self-assemble to form their own matrix. A multi-phasic bone-ligament-bone tissue engineered ACL graft was created using confluent cell monolayers (Fig. 2.5B). MSCs were first pre-differentiated into ligamentous or bone pathways in monolayer and then assembled together into a 3D scaffold. The resulting scaffold showed sufficient properties for ACL replacement and performed well during long term implantation in an ovine model.[97] Gene transfer is another strategy to spatially regulate genetic modification and differentiation of primary dermal fibroblasts. A retrovirus encoding the factors RUNX2 and cbfa1 was used to induce osteoblastic and fibroblastic differentiation respectively.[98] These techniques demonstrate that cells can be used to produce complex gradients for soft tissue-to-bone interfaces.

Persistent Challenges

Cellular phenotype is a constant point of discussion when working with tissue engineered constructs. However, cell phenotype specifically describes cells in a static

system in the native environment. The application of this word to a tissue engineered system is only used for convenience, given that a cell in a tissue engineered environment can only show an osteoblast-like or fibroblast-like phenotype. While this point may seem trivial, the distinction between phenotypes is important when characterizing the cellular differentiation in tissue engineered scaffolds. Previous literature in the field has extensively characterized bone, cartilage, ligament, meniscus, and tendon individually, but little information exists on the cell phenotypes in the enthesis. The enthesis also contains several tissue types over a short distance, which means the tissue contains complex gradients of phenotypic markers such as gene expression, growth factors, and ECM.[75] These gradients make categorizing cell type difficult, given that no one cell experiences the same cellular inputs. Furthermore, the development and maintenance of the enthesis may involve a more complex formulation of matrix components than is currently known. Obtaining a better understanding of the native development and native cell phenotypes will help provide tools to target differentiation gradients for tissue engineering the soft tissue-to-bone interface.

Biochemical Factors

A range of biochemical factors can influence production and remodeling of ECM. Growth factors are proteins that are secreted by a cell and act as signaling molecules to other cells via cell surface receptors. These molecules play active roles in establishing the complex structure of the enthesis, healing the tissue after injury, and maintaining tissue homeostasis. This section highlights relevant biochemical signals in development and their application to enthesis tissue engineering.

Native Biochemical Signaling

Soft tissue-to-bone interfaces have a wide array of growth factors that influence cellular activities such as differentiation, proliferation, apoptosis, and matrix production. Key growth factor contributors to bone growth, repair, and differentiation are BMPs, transforming growth factor-βs (TGF-βs), and insulin-like growth factor (IGF) (Table 2.1).[99–101] The growth plate contains similar regional zones as the enthesis since it is an interface between bone and cartilage. Growth factors secreted in the growth plate are essential to endochondral bone formation and include IGF, Indian hedgehog (Ihh), parathyroid hormone-related peptide (PTHrP), BMPs, Wnts, fibroblast growth factor (FGF), and TGF-β.[69] Key players in bulk tendon and ligament healing and remodeling are IGF, TGF-β, vascular endothelial growth factor (VEGF), platelet-derived growth factor (PDGF), and FGFs.[102,103] IGF, FGFs, TGF-β, and PDGF are the central growth factors that contribute to developing and maintaining organized collagen structures and high levels of proteoglycans in cartilage and meniscus.[104] While many of these growth factors are present in all of these tissues (Table 2.1), the spatial and temporal expression of growth factors are important drivers of tissue development.

Table 2.1. See the following reviews for more on growth factors [101–103,191] ? indicates that no native study on these growth factors has been performed; however, TE applications have been performed using these growth factors and they are believed to play a role

Native Expression							Tissue Engineering Applications	
Growth Plate	Bone	Tendon	Ligament	Cartilage	Meniscus	Growth Factor	Isoform	Effect
X	X			X		Bone Morphogenic Proteins (**BMPs**)	**BMP-2**	Stem cell proliferation and differentiation into osteoblasts [43,47,128,134,185] Stimulate bone formation and mineralization [43,47,120,128,133,185]
							BMP-6	Enhance effect of TGF-β3 [146] Increase collagen production [81]
							BMP-7	Stimulate bone formation and mineralization [129]
X	X	X	X	X	X	Transforming Grown Factor-β (**TGF-β**)	**TGF-β1**	Encourages chondrogenesis [47,186,187] Increased production of collagen and GAGs [47,126,130,188] Increases proliferation [119,125,130] Under certain conditions can be osteogenic and associate with hypertrophy [43,119,150]
							TGF-β3	Encourages chondrogenesis [63,73,81,86,132] Increased production of collagen and GAGs [63,73,81,86,132,146] Enhance hypertrophic chondrocyte phenotype [150]
X	X	X	X	X	?	Insulin-like Growth Factor	**IGF-I**	Stimulates proteoglycan synthesis [123,188,189] Enhance effect of TGF-β3 [146]
X	X	X	X	X	?	Fibroblast Growth Factor (**FGF**)	Basic FGF **bFGF** or **FGF-2**	Enhances proliferation [118,130] Enhance chondrogenesis [130] Increase collagen production [118]
X	X	X	X	X	X	Platelet-derived Growth Factor (**PDGF**)	**PDGF-BB**	Enhances proliferation [118] Enhances tenogenesis [134] Boost ECM deposition for tendon and ligament regeneration [118,134,190]
X	X	X	X		X	Vascular Endothelial Growth factor (**VEGF**)	**VEGF**	Increases vascularization [185] Enhances bone formation [120,185]

TGF-βs, BMPs, and IGFs regulate bone and joint development by influencing stem cell differentiation, matrix synthesis and remodeling, and cellular migration and proliferation. The TGF-β superfamily is a group of structurally related proteins including TGF-βs and BMPs that influence a broad range of activities in musculoskeletal development. Members of the BMP family encourage stem cell proliferation and differentiation into osteoblasts.[105,106] Furthermore, BMPs are osteoinductive, encouraging bone formation and maintenance by recruiting bone-forming cells that result in the formation of mineralized bone. BMPs have successfully navigated the FDA approval process for bone healing applications, notably BMP-2 (Infuse® Medtronic) and BMP-7 (also called OP-1 by Stryker).[107] TGF-βs are prevalent in all of these tissues and are known to play a role in proliferation and stem cell differentiation.[108] In particular, TGF-β is heavily implicated for its role in chondrogenic differentiation and development.[109,110] IGF is a regulator of longitudinal bone growth in that it stimulates osteoblast proliferation and differentiation as well as increasing general cell proliferation and ECM synthesis.[111–114] These growth factors are essential signaling contributors to stem cell differentiation and tissue development in native orthopedic tissues.

Several growth factors prevalent in the inflammatory and healing processes also aid in the production of tissue. Vascularization-related growth factors are important in soft tissue development and healing; common growth factors include PDGF and VEGF.[47,101,103,115–118] Basic fibroblastic growth factor (bFGF-2) is known to contribute to cell proliferation and is expressed in the developmental and healing phases of these tissues.[106,118] Growth factors have been specifically targeted for tissue engineering

applications because they are exogenously secreted factors that can be dosed into a system with relative ease and can drive stem cell differentiation and tissue maintenance.

Biochemical Applications in Tissue Engineering

Since growth factors are known to play influential roles in cell behavior, they have been frequently applied to tissue engineer bone, cartilage, meniscus, tendon, and ligament (Table 2.1). BMPs are popular for tissue engineering applications in bone interfaces and have been shown to induce mineralization as well as to stimulate osteoblast proliferation in scaffolds.[107,119,120] Scaffolds doped with IGF-I increased cartilage regeneration in growth plate injuries *in vivo* and increased the collagen and GAG content in tissue engineered cartilage constructs *in vitro*.[121–123] VEGF was incorporated into a mineralized degradable polymer scaffold to provide osteoconductive signals for bone growth and angiogenesis.[124] TGF-βs increase GAG and collagen production which improve the quality of tissue engineered cartilage and meniscus.[73,125–127] Growth factors provide signaling mechanisms to encourage cellular components to exhibit a specific phenotype.

Prominent growth factors in these developmental processes can also guide stem cell differentiation in tissue engineered constructs. BMP-2 combined with hydroxyapatite in a silk fibroin fiber scaffold supported MSC growth and differentiation towards an osteogenic phenotype, quantified by increased BMP-2 transcription levels and mineral deposition.[128] Delivering BMP-2 and BMP-7 sequentially increased ALP activity while suppressing proliferation of MSCs,[129] highlighting the potential for benefits from temporal application of biochemical factors to cells. Growth factor delivery using a scaffold can increase efficiency of stem cell differentiation into a

desired cell phenotype. Localized delivery of IGF in a PLGA scaffold increased MSC chondrogenesis *in vitro,*[121] while FGF-2 and TGF-β1 increased chondrogenesis of periosteum derived cells.[130] TGF-β3 conjugated with chondroitin sulfate increased MSC chondrogenic differentiation by increasing GAG production and expression of Sox9, COMP, aggrecan, and type II collagen genes.[63] Controlled release of TGF-β3 also promoted chondrogenesis of human infrapatellar fat pad-derived stem cells, measured by increased production of sulfated GAGs and collagen.[131,132]

Growth factors are a useful chemical tools for generating complex materials gradients. Since growth factors can be incorporated into a biomaterial, they can be strategically placed or applied to influence cellular behavior in controlled chemical gradients for soft tissue-to-bone tissue engineering. BMP-2, delivered using microspheres in a poly(propylene fumarate) scaffold, increased bone regeneration and ACL graft fixation.[133] An integrated gradient of BMP-2 and TGF-β1 has been shown to create a continuous material and phenotypic transition between cartilage and bone.[43,47] Application of growth factors is especially favorable when using a single progenitor cell type in the scaffold. Rather than seeding multiple cell types, growth factors can be incorporated to initiate the differentiation of stem cells. ASCs, seeded in a porous PCL/Pluronic F127 membrane with gradients of PDGF, specifically PDGF-BB (tendon) and BMP-2, created a continuous interface between tendon and bone, with PDGF promoting tenogenesis and BMP-2 promoting osteogenesis (Fig. 2.5C).[134] In combination with materials processing methods and cells, growth factor gradients contribute to the development of integrated and graded regions for engineered soft tissue-to-bone interfaces.

In addition to facilitating cell-biochemical interactions, growth factors can be sequestered by ECM proteins. Proteoglycans function as physiologic regulators by sequestering growth factors and controlling release. SLRPS, such as biglycan, decorin, and fibromodulin, are capable of binding to TGF-β and are likely to regulate the availability of TGF-β to cells.[135] While the exact mechanism is not well understood, increased levels of type II collagen in a scaffold enhance the effect of TGF-β on chondrocytes.[136] FGFs bind to heparin proteoglycans in the ECM. For example perlecan, a heparin sulfate proteoglycan, co-localizes with FGF thus regulating FGF availability to cell receptors.[137] Availability of BMP-2 is regulated through sequestering with heparin and type IIA procollagen.[138,139] Biomaterials, such as alginate, have been modified with binding peptides that specifically bind a growth factor in order to sustain growth factor availability over longer culture periods.[123] The ability of ECM proteins to regulate growth factor availability contributes to the highly complex interplay of materials, cells, and biochemical signaling in a tissue engineered construct, but also allows for the engineered regulation of cellular behavior and scaffold maturation.

Other non-growth factor chemical stimulants also influence cell behavior. Dexamethasone is a glucocorticoid that has been shown to increase ALP activity in MSCs.[140] β-glycerophosphate is an organic phosphate donor classically used to induce MSC differentiation towards bone phenotypes.[45,141–143] Application of β-glycerophosphate at the interface of a calcium polyphosphate substrate cultured with chondrocytes formed two zones, a calcified region between a calcium phosphate bony substrate and a hyaline cartilage-like zone.[38] Furthermore, combining β-

glycerophosphate and BMP-2 in the bone region of an osteochondral scaffold directed stem cell osteogenesis.[119] Ascorbic acid or ascorbate-2-phosphate (a format used to stabilize ascorbic acid in solution)[144] has been shown to increase the hydroxylation rate of proline,[145] aiding in collagen production. These chemical stimulants are incorporated into the scaffold design to enhance a desired cell behavior either through direct interaction with cells or complementary mechanisms to other growth factors or ECM materials present in the scaffold.

Persistent Challenges

While the described biochemical factors have influential effects on cell behavior, application of appropriate spatial distribution, temporal release, and concentration ranges for cell culture must be explored further. In biological systems, cells are highly sensitive to chemical signaling during development. An acute high dose of TGF-β during culture increased long term cartilaginous stem cell differentiation in a tissue engineered construct versus maintaining a constant low concentration dose,[132] indicating that temporal effects can be directly observed. Growth factors are also known to have complex synergistic effects, in which dual or sequential application can change cellular behavior and tissue maturation.[81,129,146] In addition to interacting with other growth factors, growth factors also interrelate with ECM molecules that can change their bioavailability to cells. Understanding more about the interactions between growth factors and ECM proteins could enable the use of natural ECM binding mechanisms to control growth factor localization and release. More research needs to be conducted on the interplay of these biochemical factors in order to better apply these components to tissue engineered systems. In the native system a vast amount of variables are involved

in small molecule signaling, warranting the development of more techniques to characterize and quantify stable spatial and temporal gradients.

Construct Maturation

After producing a viable, chemically active, cell-seeded scaffold, the maturation of the scaffold must be driven through external stimuli, either *in vitro* or *in vivo* (Fig. 2.4). In the body, chemical and mechanical signals guide development. Mechanical loading of the tissue helps to direct proper enthesis development, as immobilization during development results in altered enthesis geometry and significantly decreased mechanical properties.[147] As described in the previous section, various biochemical factors affect the differentiation of cells in different regions of the enthesis. These biochemical factors can be engineered into a scaffold with a controlled release over time or can be supplemented into culture media utilizing diffusion to create stimulation gradients. Given these two factors, this section discusses culture methods and bioreactor designs for driving proper maturation using chemical and mechanical stimulation.

Chemically Driven Maturation

Chemical means of driving cell maturation typically occur through media supplementation. In the case of the enthesis, bone media, cartilage media, ligamentous/tendinous media, and meniscal media are typically used individually or in combination. The majority of osteogenic media contains β-glycerophosphate and dexamethasone,[45,48,97,142,148,149] with some including BMP-2[142,149] and TGF-β.[97] Dexamethasone is also included in some chondrogenic media,[148–150] while TGF-β is often used in media for the soft tissue portions of the enthesis.[45,97,142,148–150] Ascorbic acid and L-proline are added to media to promote collagen production.

Many of the relevant published systems have been produced for the osteochondral interface, given its similarity to the soft tissue-to-bone interface. The majority of systems designed to promote interface formation in culture rely on diffusion-based bioreactors; the general principle being that bone phenotype-promoting media and soft tissue phenotype-promoting media will diffuse through the construct, meet in the middle, and facilitate the formation of an interface.[54,148,149,151] Using this concept, a microfluidic bioreactor directed MSC differentiation along osteogenic and chondrogenic pathways in parallel (Fig. 2.6A). The bioreactor consisted of an MSC-seeded agarose gel sandwiched between two other MSC-seeded agarose gels that contained channels. The channel-containing gels are perfused with osteogenic and chondrogenic media, respectively, creating a tri-layered scaffold with an interfacial region. This system produced gradients from the osteogenic to chondrogenic regions: decreasing type I collagen content, increasing type II collagen content, and decreasing Alizarin Red staining, reflecting decreasing matrix-immobilized calcium content. These gradients indicate that interfacial regions can be formed by supplying one cell type with different medias and flow conditions simultaneously (Fig. 2.6A).[149,152] Flow of chondrogenic and osteogenic media through the top and bottom of a singular osteochondral scaffold, while maintaining media separation around the scaffold using an O-ring, produced distinctive corresponding regions (Fig. 2.6B). Osteochondral scaffolds were produced by pipetting a chondrogenic, photo-crosslinked, cell-seeded gel onto an osteogenic, photo-crosslinked, cell-seeded gel. Chondrogenic gels consisted of MSC-seeded methacrylated gelatin with hyaluronic acid and a photo-crosslinker (lithium phenyl-2,4,6-trimethylbenzoylphosphinate). Osteogenic gels had a similar

composition, except with hydroxyapatite rather than hyaluronic acid. After 4 weeks of culture, the corresponding sections of the osteochondral construct showed heightened expression of chondrogenic and osteogenic markers. The construct also contained a junction between the sections of the scaffold, with visible GAG staining in the chondrogenic portion and calcium staining in the osteogenic portion (Fig. 2.6B).[142]

Mechanically Driven Maturation

The native enthesis sustains dynamic tensile, compressive, and shear loading that contributes to the development of the integrated regions. The structural transition from soft tissue-to-bone promotes gradual load transfer across the interface, indicating the importance of the structure-function relationship in the enthesis.[1,153,154] The native enthesis contains a dense network of collagen fibers interdigitated into bone that aid in tensile and compressive load transmission.[155–158] The loading environment of the enthesis provides mechanical cues to cells that instruct matrix production and remodeling. Lack of loading during native development results in impaired mineral deposition and disorganized fiber distribution.[159] In the case of healing after tendon injury, immobilization actually increased structural, compositional, and viscoelastic properties compared to an exercised group.[160] Considering the mechanical influences on tissue development is important when designing methods for tissue engineered enthesis maturation.

During development, anchoring of the meniscus to the tibia produces a static mechanical boundary condition that triggers longitudinal fiber organization in the soft tissue.[82–84,161] Mimicking this static mechanical boundary condition has shown organized fiber remodeling from several cell types including fibroblasts,[162–165]

MSCs,[166–168] cardiomyocytes,[165] annulus fibrosis chondrocytes,[169] and meniscal fibrochondrocytes.[53,66,78] Mechanical anchoring at the bony ends of a soft tissue-to-bone model system directed longitudinal fiber formation as well as formed interdigitated fibers at the collagen-bone interface (Fig. 2.6C).[53] Cell-monolayers mechanically fixed at the end points contracted the cell sheet into a 3D construct. Using this method, the cells organized a highly aligned and integrated enthesis for ACL repair (Fig. 5B).[97] While mechanically-directed fiber remodeling has been shown in several systems, different cell types have also displayed varying levels of remodeling capability. When tendon and meniscal fibrochondrocytes were embedded in a collagen matrix and clamped, fibrochondrocytes formed significantly larger fibers than tendon cells.[170] MSCs in a tissue engineered meniscus also showed decreased fiber alignment and diameter compared to fibrochondrocytes.[78] These studies indicate that the response to mechanical stimuli is highly dependent on cell type.

Active mechanical loading is applied to enthesis tissues *in vivo*, and these active mechanical signals guide differential tissue formation. While active mechanical loading has not been applied to *in vitro* enthesis tissue engineering yet, other systems have utilized active loading. Bioreactors have been designed to apply uniaxial tensile loads in bulk ligament and tendon tissue engineering (constructs excluding an enthesis).[95,96] After tensile loading of an aligned scaffold seeded with MSCs, type I and III collagen expression increased as did expression of fibroblastic markers including tenascin-C, fibronectin, and integrin.[96] Simultaneous tensile and compressive stimulation by compressively loading a self-assembled meniscus ring, resulted in significant increases in mechanical and biochemical properties.[171] This effect was further demonstrated by

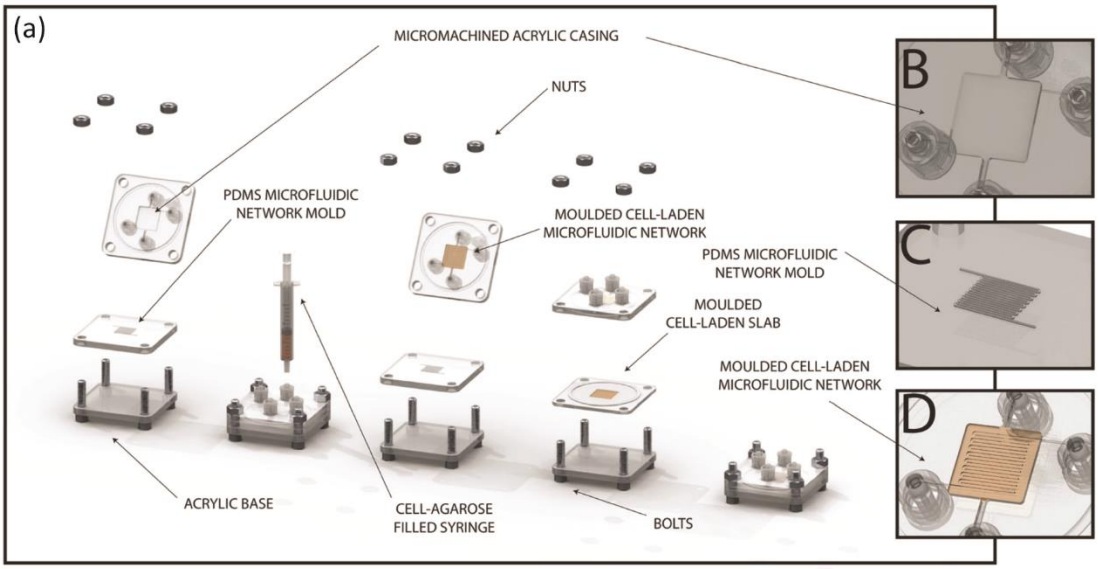
(a)
MICROMACHINED ACRYLIC CASING
NUTS
PDMS MICROFLUIDIC NETWORK MOLD
MOULDED CELL-LADEN MICROFLUIDIC NETWORK
PDMS MICROFLUIDIC NETWORK MOLD
MOULDED CELL-LADEN SLAB
MOULDED CELL-LADEN MICROFLUIDIC NETWORK
ACRYLIC BASE
CELL-AGAROSE FILLED SYRINGE
BOLTS
B
C
D

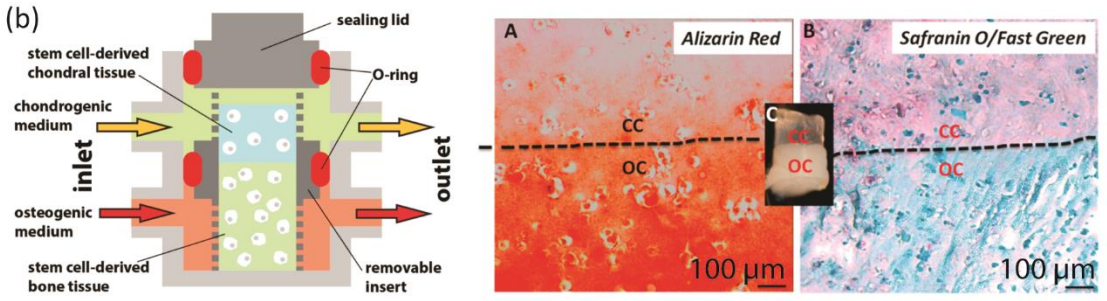
(b)
sealing lid
stem cell-derived chondral tissue
O-ring
chondrogenic medium
inlet
outlet
osteogenic medium
stem cell-derived bone tissue
removable insert
A
Alizarin Red
CC
OC
C
100 µm
B
Safranin O/Fast Green
CC
OC
100 µm

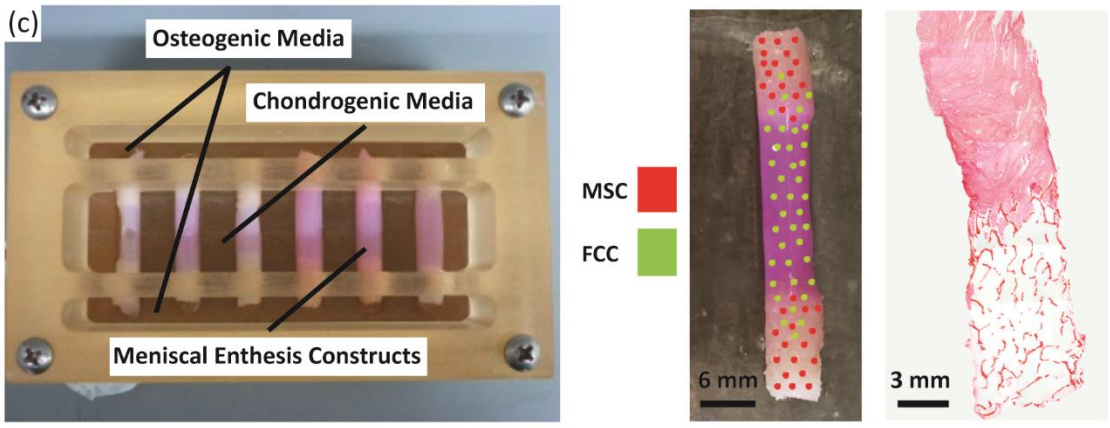
(c)
Osteogenic Media
Chondrogenic Media
Meniscal Enthesis Constructs
MSC
FCC
6 mm
3 mm

Fig. 2.6. Examples of bioreactor designs for maturation of tissue engineering interfacial tissues. (A) Osteochondral microfluidic bioreactor.[184] This bioreactor creates two microchannel arrays in a gel, separated by a non-channel gel slab in the center. Osteogenic and chondrogenic media are flowed through the microchannels allowing for diffusion into surrounding walls and through central slab, creating an interfacial construct. Histology shows interface of scaffold. (B) Osteochondral bioreactor.[142] Chondrogenic and osteogenic media are continuously flowed through a scaffold, while maintaining separation of media baths through use of an O-ring. Histology shows interfacial region for construct: chondral component (CC) and osseous component (OC). Alizarin Red stains for calcium, Safranin-O stains for negatively charged molecules (GAGs), and fast green stains for proteins. (C) Combination mechanical, chemical, and co-culture bioreactor for culturing meniscal enthesis constructs. These constructs consist of two bone plugs seeded with mesenchymal stem cells (MSCs) injected and connected with a high density collagen gel embedded with meniscal fibrochondrocytes (FCCs). The bone plugs are anchored down in the bioreactor using the walls, and then osteogenic media and meniscal media can be applied to different portions of the scaffold. Image shows distribution of co-cultured cells on constructs, and histology shows the morphology of the interfacial region of the construct (images courtesy of Leanne Iannucci).[53]

loading mechanically anchored tissue engineered menisci. Dynamic compressive loading of the meniscus enhanced organized collagen fiber formation, mechanical properties, and GAG accumulation. Mimicking native mechanical loads guided heterogeneous tissue development, where tensile loads in the outer meniscus produced a fiber-containing, collagen-rich tissue and compressive loads on the inner meniscus increased GAG development.[172] The native environment can also serve as a natural load inducer to guide tissue maturation, assuming the construct is robust enough for implantation. A cell self-assembled bone-ligament-bone construct underwent marked increases in collagen content and alignment as well as increased stiffness after implantation, driving biochemical content and mechanical properties towards native ACL.[97] These studies collectively support active mechanical stimulation as a useful tool to the drive structural development of tissue engineered constructs.

Persistent Challenges

Maturation is a necessity for the integration of a tissue engineered construct with surrounding native tissue after implantation.[173] However, implants must be able to survive implantation, and no standards exist for the threshold mechanical properties that must be reached during *in vitro* fabrication. Chemical and mechanical bioreactors provide a means for maturing tissue engineered constructs *in vitro*, but given that different regions of the enthesis experience different chemical and mechanical stimulants, increased bioreactor design complexity is required to mimic maturation in these tissues. For example, maintaining gradients of various molecules and growth factors is hindered by the higher diffusivities of smaller molecules, as compared to larger proteins. Ideally such reactors could create concentration gradients for various

molecules while also providing temporal control. Some reactors create precise control of gradients using microfluidics and similarly small systems, but while these systems provide an excellent platform for studying interfacial tissue *in vitro*, these systems are difficult to scale up. Therefore, design of bioreactors for application to full tissue engineered constructs is necessary.

In vivo enthesis loading is complex, producing multidirectional strains during a loading cycle. Mimicking these states is challenging for tissue engineered constructs, in that constructs must be loaded on multiple axes while maintaining sterility. Application of cyclic strains could benefit the maturation of the enthesis, as cyclic strains are applied to native tissues during a gait cycle. Cyclic loading can also increase nutrient transport into tissues,[174] which in turn allows for production of larger constructs, since nutrient transfer in these constructs occurs through diffusion. Bioreactors are useful for driving this type of *in vitro* maturation but largely have not been applied to engineered entheses. Given that loading plays an important role in enthesis development, and that mechanical, chemical, and biological interfaces exist in enthesis tissue, bioreactors provide a means for inducing similar stimuli during *in vitro* maturation. These devices have also proven useful, in the case of chemical bioreactors, for osteochondral interface development,[142] and, in the case of mechanical bioreactors, for *in vitro* fiber production.[53] These successes demonstrate the promise of these technologies for application in engineering entheses.

Looking Forward

The field of orthopedic interfacial tissue engineering presents a number of exciting opportunities for pushing forward the fields of biomaterials, tissue engineering,

and biomechanics. In the coming years, advances are required in our understanding of both the *in vivo* function and generation of entheses, as well as in our capabilities to engineer constructs to replace these complex tissues. Specifically, we have identified three areas of opportunity to inform the design and development of next-generation tissue engineered entheses: 1) understanding the development and homeostasis of the native enthesis, 2) development of new materials and bioreactors for enthesis engineering, and 3) mechanical and structural verification of tissue engineering and implant success.

1. Understanding the Development and Homeostasis of Native Entheses
    a. Structure-function relationships, specifically at the length scales critical for the function of this hierarchically structured tissue (Fig. 2.2), remain poorly understood in the native enthesis. Improving our understanding of how specific molecular, cellular, and architectural features contribute to the healthy function of entheses, requires correlative compositional and mechanical data collected with micrometer-scale resolution. In addition to high resolution data sets, these measurements need to be performed on hydrated tissue samples under physiologically-relevant conditions. This type of characterization will require the development of creative imaging strategies that correlatively combine multiple techniques capable of providing chemical, structural, and mechanical information on the same piece of tissue.[175]
    b. Various proteins and molecules are present in low concentrations throughout the regions of the enthesis (e.g., non-collagenous proteins in

bone, type X collagen in mineralized cartilage, SLRPs in areas with oriented collagen fiber bundles), but the specific functional roles of these macromolecules are largely unknown. For example, the exact function of non-collagenous proteins in bone is unknown given the redundant roles of these proteins in bone formation. Therefore, the cause of irregularities is hard to characterize using knockout models of non-collagenous proteins.[32] Studies examining the roles of these molecules in the formation of these regional structures, either through knockout models or *in vitro* concentration studies, will allow for tissue engineers to target specific results (fibers with controlled diameters, fibrocartilage formation, etc.) to create integrated, biomimetic constructs.

c. Tendon, ligament, cartilage, and bone cell phenotypes have been well characterized independently (Fig. 2.3), but the enthesis incorporates these phenotypes in overlapping gradients, which make specific phenotypic categorization challenging. Spatial characterization of cell phenotypes within the enthesis are needed to define concrete objectives regarding cell seeding and localized stem cell differentiation. While differentiation into bone and cartilage is well studied, less is known about appropriate inputs for fibrochondrocyte and hypertrophic fibrochondrocyte differentiation.

d. Growth factors play an essential role in the development and maintenance of the enthesis, however limited information exists regarding spatial and temporal expression of growth factors in

developing and mature entheses. Additionally, growth factors have complex interactions with each other and the extracellular matrix that complicate the study of each one's exact role. Further study should focus on characterizing the spatial and temporal frequencies of expression of growth factors *in vivo*, thereby generating a greater understanding of the time- and length-scales over which growth factors must be applied to drive cellular differentiation in tissue engineered constructs.

2. Develop New Materials and Bioreactors for Entheses Engineering
    a. Hierarchical structures within the native tissue give rise to mechanical, cellular, and biochemical cues critical to healthy tissue function. However, generating biomaterials with similar types of hierarchical structuring remains a challenge and requires extensive control over assembly at various length scales. New synthetic approaches need to be developed that can create materials with the critical features of the native tissue (e.g., strategic biomimicry) and that are scalable.[60] This task can only be accomplished by both understanding the native structures and evaluating which features are critical for a given function. Once key hierarchical structures are identified and synthetic methods have been developed, then new biomaterials can be designed to possess many of the same properties that native tissue benefits from *in vivo*.
    b. The range of materials properties (e.g., several orders of magnitude change in stiffness on the order of less than 1 mm) in the enthesis presents unique challenges in creating a graded interface. In order for a

tissue engineered construct to be mechanically robust, differing materials must be fully integrated, utilizing concentration gradients, interpenetrating materials, etc., to avoid stress concentrators at the point of material interface. A specific challenge in this regard is the design of structures with partially mineralized collagen fibers or gradients in alignment and fiber diameter to help anchor soft tissue to bone.

c. Current designs of bioreactors for interfacial tissue constructs have been utilized to apply spatially controlled stimuli (Fig. 2.6). Moving forward, new bioreactor designs that more effectively mimic the native environment are necessary. For example, the simultaneous application of chemical and mechanical stimuli, with temporal control of these stimuli, would provide culture conditions very similar to those experienced by the native enthesis. As such, combining existing approaches that apply chemical gradients to tissues with others that apply controlled mechanical stimulation will be critical for engineering of entheses.

3. Improve Mechanical and Structural Verification of Tissue Engineering and Implant Success

    a. The baseline mechanical properties (e.g., toughness, stiffness, failure strain) required for enthesis construct implantation have not been identified. Baseline properties are largely unknown and likely vary significantly with anatomic location. Such mechanical benchmarks would provide engineers with a more concrete goal to work towards

when developing constructs. Devices for measuring native load distributions exist,[176] and similar devices should be developed and utilized in these systems to inform design criteria.

b. The mechanical behavior of enthesis is non-linear and heterogeneous. As such, properties and test protocols used to describe the mechanics of linear elastic materials do not fully describe the behavior of these tissues. For example, cyclic loading would provide information on viscoelastic properties (e.g. storage modulus, loss modulus, hysteresis), but would also provide information on the fatigue life of such constructs. Tissue are frequently loaded cyclically in vivo, following gait cycles or other repetitive motions, meaning that the properties of these tissue during cyclic loading need to be explored to validate implant viability.

c. In addition to mechanical characterization, analysis of the structure of the enthesis provides a great opportunity for the development of new techniques. The presence of orientation and heterogeneity necessitates the development or adaptation of techniques to highlight these features. Advances in MR imaging of soft tissues includes pulse sequences such as ultrashort T2 echo times that highlight collagen orientation,[177] but these techniques have not been applied to assess the structure or health of entheses. Additionally, while standard histological analyses enable semi-quantitative assessment of spatial patterns of the components of the enthesis, mapping mineral, proteoglycan, and collagen requires different tissue processing methods, distinct stains, and multiple sections.

Vibrational microspectroscopy methods enable detection of multiple chemical species at once through infrared absorption and Raman scattering. These techniques have been more frequently applied to bone, cartilage, tendon, and ligament than the entheses.[8,35,178,179]

As we capitalize on these opportunities and begin to answer these outstanding questions, we will increase our understanding of the native enthesis and, in return, be able to design the next-generation of tissue engineered orthopeadic interfaces. Emerging technologies, such as gene therapy and induced pluripotent stem cells (iPSCs),[98] provide new possibilities for engineering complex tissues. iPSCs are a clinically available cell source; however precise control of cell differentiation remains a challenge.[180] Gene therapy potentially allows for more direct control of cell differentiation, which is highly pertinent in systems containing many cell types. Other similar technologies, like CRISPR,[181] have been unexplored in orthopedic systems and may be of great value for spatially guiding local differentiation to achieve desired phenotypic gradients. Additionally, as tissue engineering is a relatively new field, many of the materials processing methods that have been developed for other materials systems (electronic, structural, etc.) have not been applied to biological systems. For example, the electronics industry has demonstrated nanometer-scale control over semiconductor systems using lithography. Some of these technologies have been translated to biological systems,[182] but the requirement of 3D structuring makes application of these techniques difficult. Other cutting edging processing methods, such as 3D printing[183], have been utilized to develop complex geometries for tissue engineering, but printing resolution needs to be improved in order to gain clinical

viability for these constructs. Utilizing materials design principles external to the biological fields could greatly benefit implant production. In the next ten years, we will be able to demonstrate control over the assembly and culture of hierarchically structured living tissues for the repair of orthopedic soft tissue-to-bone interfaces.

REFERENCES

1. A. C. Abraham and T. L. Haut Donahue. From meniscus to bone: A quantitative evaluation of structure and function of the human meniscal attachments. *Acta Biomater.* **9,** 6322–6329 (2013).
2. L. Mente and J. L. Lewis. Elastic Modulus of Calcified Cartilage is an Order of Magnitude Less Than That of Subchondral Bone. *J. Orthop. Res.* **12,** (1994).
3. R. M. Schinagl, D. Gurskis, A. C. Chen and R. L. Sah. Depth-Dependent Confined Compression Modulus of Full-Thickness Bovine Articular Cartilage. *J. Orthop. Res.* **15,** 499–506 (1997).
4. P. Brooks. Inflammation as an important feature of osteoarthritis. *Bull. World Health Organ.* **81,** 689–690 (2003).
5. W. R. Shelton and A. D. Dukes. Meniscus replacement with bone anchors: a surgical technique. *Arthrosc. J. Arthrosc. Relat. Surg.* **10,** 324–7 (1994).
6. E. A. Khetia and B. P. McKeon. Meniscal allografts: biomechanics and techniques. *Sports Med. Arthrosc.* **15,** 114–20 (2007).
7. T. M. Hammoudi and J. S. Temenoff. in *Biomaterials for Tissue Engineering Applications*. **11,** 307–341 (2011).
8. J. P. Spalazzi, A. L. Boskey, N. Pleshko and H. H. Lu. Quantitative mapping of matrix content and distribution across the ligament-to-bone insertion. *PLoS One*. **8,** e74349 (2013).
9. S. Thomopoulos, G. M. Genin and L. M. Galatz. The development and morphogenesis of the tendon-to-bone insertion - What development can teach us about healing. *J. Musculoskelet. Neuronal Interact.* **10,** 35–45 (2010).

10. K. Messner and J. Gao. The menisci of the knee joint. Anatomical and functional characteristics, and a rationale for clinical treatment. *J. Anat.* **193,** 161–178 (1998).

11. G. R. S. Naveh, N. Lev-Tov Chattah, P. Zaslansky, R. Shahar and S. Weiner. Tooth-PDL-bone complex: Response to compressive loads encountered during mastication - A review. *Arch. Oral Biol.* **57,** 1575–1584 (2012).

12. T. Hayami, M. Pickarski, Y. Zhuo, G. A. Wesolowski, G. A. Rodan and L. T. Duong. Characterization of articular cartilage and subchondral bone changes in the rat anterior cruciate ligament transection and meniscectomized models of osteoarthritis. *Bone*. **38,** 234–243 (2006).

13. J. Gao. Immunolocalization of types I, II, and X collagen in the tibial insertion sites of the medial meniscus. *Knee Surg. Sports Traumatol. Arthrosc.* **8,** 61–65 (2000).

14. W. Petersen and B. Tillmann. Structure and vascularization of the cruciate ligaments of the human knee joint. *Anat. Embryol. (Berl).* **200,** 325–334 (1999).

15. I.-N. E. Wang, S. Mitroo, F. H. Chen, H. H. Lu and S. B. Doty. Age-Dependent Changes in Matrix Composition and Organization at the Ligament-to-Bone Insertion. *J. Orthop. Res.* **24,** 1745–1755 (2006).

16. M. Benjamin and J. R. Ralphs. The cell and developmental biology of tendons and ligaments. *Int. Rev. Cytol.* **196,** 85–130 (2000).

17. P. Buma, N. N. Ramrattan, T. G. van Tienen and R. P. H. Veth. Tissue engineering of the meniscus. *Biomaterials*. **25,** 1523–1532 (2004).

18. M. T. Rodrigues, R. L. Reis and M. E. Gomes. Engineering tendon and ligament tissues: present developments towards successful clinical products. *J. Tissue Eng. Regen. Med.* **7,** 673–686 (2013).

19. A. Di Luca, C. A. Van Blitterswijk and L. Moroni. The osteochondral interface as a gradient tissue: From development to the fabrication of gradient scaffolds for regenerative medicine. *Birth Defects Res. Part C.* **105,** 34–52 (2015).

20. C. Vaquette, W. Fan, Y. Xiao, S. Hamlet, D. W. Hutmacher and S. Ivanovski. A biphasic scaffold design combined with cell sheet technology for simultaneous regeneration of alveolar bone/periodontal ligament complex. *Biomaterials*. **33,** 5560–5573 (2012).

21. P. J. Yang and J. S. Temenoff. Engineering orthopedic tissue interfaces. *Tissue Eng. Part B. Rev.* **15,** 127–41 (2009).

22. H. H. Lu and S. Thomopoulos. Functional attachment of soft tissues to bone: development, healing, and tissue engineering. *Annu. Rev. Biomed. Eng.* **15,** 201–26 (2013).

23. S. Font Tellado, E. R. Balmayor and M. Van Griensven. Strategies to engineer tendon/ligament-to-bone interface: Biomaterials, cells and growth factors. *Adv. Drug Deliv. Rev.* **94,** 126–140 (2015).

24. A. D. Waggett, J. R. Ralphs, A. P. L. Kwan, D. Woodnutt and M. Benjamin. Characterization of collagens and proteoglycans at the insertion of the human Achilles tendon. *Matrix Biol.* **16,** 457–470 (1998).

25. P. Fratzl and R. Weinkamer. Nature's hierarchical materials. *Prog. Mater. Sci.* **52,** 1263–1334 (2007).

26. T. E. Hardingham and A. J. Fosang. Proteoglycans: many forms and many function. *FASEB J.* **6,** 861–870 (1992).

27. H. Tavakoli Nia, L. Han, I. Soltani Bozchalooi, P. Roughley, K. Youcef-Toumi, A. J. Grodzinsky and C. Ortiz. Aggrecan nanoscale solid-fluid interactions are a primary determinant of cartilage dynamic mechanical properties. *ACS Nano*. **9,** 2614–2625 (2015).

28. A. K. Garg, R. A. Berg, F. H. Silver and H. G. Garg. Effect of proteoglycans on type I collagen fibre formation. *Biomaterials*. **10,** 413–419 (1989).

29. K. G. Vogel and J. A. Trotter. The Effect of Proteoglycans on the Morphology of Collagen Fibrils Formed In Vitro. *Coll. Relat. Res.* **7,** 105–114 (1987).

30. K. G. Vogel, M. Paulsson and D. Heinegård. Specific inhibition of type I and type II collagen fibrillogenesis by the small proteoglycan of tendon. *Biochem. J.* **223,** 587–97 (1984).

31. L. Rossetti, L. A. Kuntz, E. Kunold, J. Schock, H. Grabmayr, S. A. Sieber, R. Burgkart and A. R. Bausch. The microstructure and micromechanics of the tendon–bone insertion. *Nat. Mater.* (2017). doi:10.1038/NMAT4863

32. F. Nudelman, A. J. Lausch, N. a J. M. Sommerdijk and E. D. Sone. In vitro models of collagen biomineralization. *J. Struct. Biol.* **183,** 258–69 (2013).

33. S. Weiner and H. D. Wagner. THE MATERIAL BONE: Structure-Mechanical Function Relations. *Annu. Rev. Mater. Sci.* **28,** 271–298 (1998).

34. N. Reznikov, R. Shahar and S. Weiner. Bone hierarchical structure in three dimensions. *Acta Biomater.* **10,** 3815–3826 (2014).

35. A. G. Schwartz, J. D. Pasteris, G. M. Genin, T. L. Daulton and S. Thomopoulos. Mineral Distributions at the Developing Tendon Enthesis. *PLoS One*. **7,** (2012).

36. T. M. Keaveny, E. F. Morgan, G. L. Niebur and O. C. Yeh. Biomechanics of Trabecular Bone. *Annu. Rev. Biomed. Eng.* **3,** 307–333 (2001).

37. A. C. Deymier-Black, J. D. Pasteris, G. M. Genin and S. Thomopoulos. Allometry of the Tendon Enthesis: Mechanisms of Load Transfer Between Tendon and Bone. *J. Biomech. Eng.* **137,** 111005–13 (2015).

38. K. S. Allan, R. M. Pilliar, J. Wang, M. D. Grynpas and R. a Kandel. Formation of biphasic constructs containing cartilage with a calcified zone interface. *Tissue Eng.* **13,** 167–177 (2007).

39. X. Huang, D. Yang, W. Yan, Z. Shi, J. Feng, Y. Gao, W. Weng and S. Yan. Osteochondral repair using the combination of fibroblast growth factor and amorphous calcium phosphate/poly(l-lactic acid) hybrid materials. *Biomaterials*. **28,** 3091–3100 (2007).

40. W. Liu, J. Lipner, J. Xie, C. N. Manning, S. Thomopoulos and Y. Xia. Nanofiber Scaffolds with Gradients in Mineral Content for Spatial Control of Osteogenesis. *ACS Appl. Mater. Interfaces*. **6,** 2842–2849 (2014).

41. B. S. Kim, E. J. Kim, J. S. Choi, J. H. Jeong, C. H. Jo and Y. W. Cho. Human collagen-based multilayer scaffolds for tendon-to-bone interface tissue engineering. *J. Biomed. Mater. Res. - Part A*. **102,** 4044–4054 (2014).

42. E. Nyberg, A. Rindone, A. Dorafshar and W. L. Grayson. Comparison of 3D-Printed Poly-ε-caprolactone Scaffolds Functionalized with Tricalcium

Phosphate, Hydroxyapatite, Bio-Oss, or Decellularized Bone Matrix. *Tissue Eng. Part A.* **0,** ten.TEA.2016.0418 (2016).

43. A. Tevlek, P. Hosseinian, C. Ogutcu, M. Turk and H. M. Aydin. Bi-layered constructs of poly(glycerol-sebacate)-β-tricalcium phosphate for bone-soft tissue interface applications. *Mater. Sci. Eng. C*. **72,** 316–324 (2017).

44. J. P. Spalazzi, S. B. Doty, K. L. Moffat, W. N. Levine and H. H. Lu. Development of controlled matrix heterogeneity on a triphasic scaffold for orthopedic interface tissue engineering. *Tissue Eng.* **12,** 3497–508 (2006).

45. G. Criscenti, A. Longoni, A. Di Luca, C. De Maria, C. A. Van Blitterswijk, G. Vozzi and L. Moroni. Triphasic scaffolds for the regeneration of the bone–ligament interface. *Biofabrication*. **8,** 15009 (2016).

46. J. A. Cooper, H. H. Lu, F. K. Ko, J. W. Freeman and C. T. Laurencin. Fiber-based tissue-engineered scaffold for ligament replacement: Design considerations and in vitro evaluation. *Biomaterials*. **26,** 1523–1532 (2005).

47. N. H. Dormer, M. Singh, L. Zhao, N. Mohan, C. J. Berkland and M. S. Detamore. Osteochondral interface regeneration of the rabbit knee with macroscopic gradients of bioactive signals. *J. Biomed. Mater. Res. - Part A.* **100 A,** 162–170 (2012).

48. Y. Liu, S. Thomopoulos, C. Chen, V. Birman, M. J. Buehler and G. M. Genin. Modelling the mechanics of partially mineralized collagen fibrils, fibres and tissue. *J. R. Soc. Interface*. **11,** 20130835 (2014).

49. J. Z. Paxton, K. Donnelly, R. P. Keatch and K. Baar. Engineering the Bone–Ligament Interface Using Polyethylene Glycol Diacrylate Incorporated with Hydroxyapatite. *Tissue Eng. Part A.* **15,** 1201–1209 (2009).

50. G. H. Altman, R. L. Horan, H. H. Lu, J. Moreau, I. Martin, J. C. Richmond and D. L. Kaplan. Silk matrix for tissue engineered anterior cruciate ligaments. *Biomaterials*. **23,** 4131–4141 (2002).

51. S. Font Tellado, W. Bonani, E. Rosado Balmayor, P. Föhr, A. Motta, C. Migliaresi and M. van Griensven. *Fabrication and characterization of biphasic silk fibroin scaffolds for tendon/ligament-to-bone tissue engineering*. *Tissue Engineering Part A*. (2017). doi:10.1089/ten.TEA.2016.0460

52. Y.-B. Park, C.-W. Ha, C.-H. Lee and Y.-G. Park. Restoration of a large osteochondral defect of the knee using a composite of umbilical cord blood-derived mesenchymal stem cells and hyaluronic acid hydrogel: a case report with a 5-year follow-up. *BMC Musculoskelet. Disord.* **18,** 59 (2017).

53. M. C. McCorry, M. M. Mansfield, X. Sha, D. J. Coppola, J. W. Lee and L. J. Bonassar. A model system for developing a tissue engineered meniscal enthesis. *Acta Biomater.* **56,** 110–117 (2017).

54. C. H. Chang, F. H. Lin, C. C. Lin, C. H. Chou and H. C. Liu. Cartilage tissue engineering on the surface of a novel gelatin-calcium- phosphate biphasic scaffold in a double-chamber bioreactor. *J. Biomed. Mater. Res. - Part B Appl. Biomater.* **71,** 313–321 (2004).

55. I.-N. E. Wang, J. Shan, R. Choi, S. Oh, C. K. Kepler, F. H. Chen and H. H. Lu. Role of osteoblast–fibroblast interactions in the formation of the ligament-to-bone interface. *J. Orthop. Res.* 1609–1620 (2007). doi:10.1002/jor

56. K. Xu, L. A. Kuntz, P. Foehr, K. Kuempel, A. Wagner, J. Tuebel, C. V Deimling and R. H. Burgkart. Efficient decellularization for tissue engineering of the tendon-bone interface with preservation of biomechanics. *PLoS One*. **12,** e0171577 (2017).

57. S. Sundar, C. J. Pendegrass and G. W. Blunn. Tendon bone healing can be enhanced by demineralized bone matrix: A functional and histological study. *J. Biomed. Mater. Res. - Part B Appl. Biomater.* **88,** 115–122 (2009).

58. H. H. Lu and S. Thomopoulos. Functional attachment of soft tissues to bone: development, healing, and tissue engineering. *Annu. Rev. Biomed. Eng.* **15,** 201–26 (2013).

59. J. Lipner, H. Shen, L. Cavinatto, W. Liu, N. Havlioglu, Y. Xia, L. M. Galatz and S. Thomopoulos. In Vivo Evaluation of Adipose-Derived Stromal Cells Delivered with a Nanofiber Scaffold for Tendon-to-Bone Repair. *Tissue Eng. Part A.* **21,** 2766–74 (2015).

60. U. G. K. Wegst, H. Bai, E. Saiz, A. P. Tomsia and R. O. Ritchie. Bioinspired structural materials. *Nat. Mater.* **14,** 23–36 (2014).

61. X. Ding, M. Zhu, B. Xu, J. Zhang, Y. Zhao, S. Ji, L. Wang, L. Wang, X. Li, D. Kong, X. Ma and Q. Yang. Integrated Trilayered Silk Fibroin Sca ff old for Osteochondral Di ff erentiation of Adipose-Derived Stem Cells. *Appl. Mater. Interfaces*. **6,** 16696–705 (2014).

62. B. M. Baker and R. L. Mauck. The effect of nanofiber alignment on the maturation of engineered meniscus constructs. *Biomaterials*. **28,** 1967–1977 (2007).

63. J. S. Park, H. J. Yang, D. G. Woo, H. N. Yang, K. Na and K. H. Park. Chondrogenic differentiation of mesenchymal stem cells embedded in a scaffold by long-term release of TGF-B3 complexed with chondroitin sulfate. *J. Biomed. Mater. Res. - Part A*. **92,** 806–816 (2010).

64. W. M. Han, S.-J. Heo, T. P. Driscoll, J. F. Delucca, C. M. McLeod, L. J. Smith, R. L. Duncan, R. L. Mauck and D. M. Elliott. Microstructural heterogeneity directs micromechanics and mechanobiology in native and engineered fibrocartilage. *Nat. Mater.* **15,** 477–484 (2016).

65. J. P. Spalazzi, E. Dagher, S. B. Doty, X. E. Guo, S. a Rodeo and H. H. Lu. In vivo evaluation of a multiphased scaffold designed for orthopaedic interface tissue engineering and soft tissue-to-bone integration. *J. Biomed. Mater. Res. A.* **86,** 1–12 (2008).

66. J. L. Puetzer, E. Koo and L. J. Bonassar. Induction of fiber alignment and mechanical anisotropy in tissue engineered menisci with mechanical anchoring. *J. Biomech.* **48,** 1436–1443 (2015).

67. D. E. Rodriguez, T. Thula-Mata, E. J. Toro, Y. W. Yeh, C. Holt, L. S. Holliday and L. B. Gower. Multifunctional role of osteopontin in directing intrafibrillar mineralization of collagen and activation of osteoclasts. *Acta Biomater.* **10,** 494–507 (2014).

68. J. B. Lian and G. S. Stein. Concepts of osteoblast growth and differentiation: basis for modulation of bone cell development and tissue formation. *Crit. Rev. Oral Biol. Med.* **3,** 269–305 (1992).

69. E. J. Mackie, Y. A. Ahmed, L. Tatarczuch, K. S. Chen and M. Mirams. Endochondral ossification: How cartilage is converted into bone in the developing skeleton. *Int. J. Biochem. Cell Biol.* **40,** 46–62 (2008).

70. L. J. Sandell and T. Aigner†. Articular cartilage and changes in arthritis. An introduction: Cell biology of osteoarthritis. *Arthritis Res.* **3,** 107–113 (2001).

71. K. Spanoudes, D. Gaspar, A. Pandit and D. I. Zeugolis. The biophysical, biochemical, and biological toolbox for tenogenic phenotype maintenance in vitro. *Trends Biotechnol.* **32,** 474–482 (2014).

72. A. Hasegawa, H. Nakahara, M. Kinoshita, H. Asahara, J. Koziol and M. K. Lotz. Cellular and extracellular matrix changes in anterior cruciate ligaments during human knee aging and osteoarthritis. *Arthritis Res. Ther.* **15,** R29 (2013).

73. C. H. Lee, S. A. Rodeo, L. A. Fortier, C. Lu, C. Erisken and J. J. Mao. Protein-releasing polymeric scaffolds induce fibrochondrocytic differentiation of endogenous cells for knee meniscus regeneration in sheep. **6,** 1–12 (2014).

74. F. A. Monibi and J. L. Cook. Tissue-Derived Extracellular Matrix Bioscaffolds: Emerging Applications in Cartilage and Meniscus Repair. *Tissue Eng. Part B Rev.* (2017). doi:10.1089/ten.TEB.2016.0431

75. E. Zelzer, E. Blitz, M. L. Killian and S. Thomopoulos. Tendon-to-bone attachment: From development to maturity. *Birth Defects Res. Part C - Embryo Today Rev.* **102,** 101–112 (2014).

76. J. Jiang, S. B. Nicoll and H. H. Lu. Co-culture of osteoblasts and chondrocytes modulates cellular differentiation in vitro. *Biochem. Biophys. Res. Commun.* **338,** 762–70 (2005).

77. M. C. McCorry, J. L. Puetzer and L. J. Bonassar. Characterization of mesenchymal stem cells and fibrochondrocytes in three-dimensional co-culture: analysis of cell shape, matrix production, and mechanical performance. *Stem Cell Res. Ther.* **7,** 39 (2016).

78. M. C. McCorry and L. J. Bonassar. Fiber development and matrix production in tissue-engineered menisci using bovine mesenchymal stem cells and fibrochondrocytes. *Connect. Tissue Res.* **58,** 329–341 (2017).

79. G. Im. Coculture in Musculoskeletal Tissue Regeneration. *Tissue Eng. Part B Rev.* **20,** 545–554 (2014).

80. L. Bian, D. Y. Zhai, R. L. Mauck and J. A. Burdick. Coculture of Human Mesenchymal Stem Cells and Enhances Functional Properties of Engineered Cartilage Reverse primer. *Tissue Eng. Part A.* **17,** 1137–1145 (2011).

81. G. M. Hoben, V. P. Willard and K. A. Athanasiou. Fibrochondrogenesis of hESCs: growth factor combinations and cocultures. *Stem Cells Dev.* **18,** 283–92 (2009).

82. E. Gardner and R. O'Rahilly. The early development of the knee joint in staged human embryos. *J. Anat.* **102,** 289–99 (1968).

83. D. J. Gray and E. Gardner. Prenatal development of the human knee and superior tibiofibular joints. *Am. J. Anat.* **86,** 235–287 (1950).

84. J. a Mérida-Velasco, I. Sánchez-Montesinos, J. Espín-Ferra, J. F. Rodríguez-Vázquez, J. R. Mérida-Velasco and J. Jiménez-Collado. Development of the human knee joint. *Anat. Rec.* **248,** 269–78 (1997).

85. A. I. Caplan and J. E. Dennis. Mesenchymal stem cells as trophic mediators. *J. Cell. Biochem.* **98,** 1076–84 (2006).

86. A. M. Mackay, S. C. Beck, J. M. Murphy, F. P. Barry, C. O. Chichester and M. F. Pittenger. Chondrogenic differentiation of cultured human mesenchymal stem cells from marrow. *Tissue Eng.* **4,** 415–28 (1998).

87. G. Il Im, Y. W. Shin and K. B. Lee. Do adipose tissue-derived mesenchymal stem cells have the same osteogenic and chondrogenic potential as bone marrow-derived cells? *Osteoarthr. Cartil.* **13,** 845–853 (2005).

88. J. P. Spalazzi and H. H. Lu. Osteoblast and chondrocyte interactions during cocul- ture on scaffolds. *IEEE Eng. Med. Biol. Mag.* **22,** 27–34 (2003).

89. N. J. Gunja and K. A. Athanasiou. Passage and reversal effects on gene expression of bovine meniscal fibrochondrocytes. *Arthritis Res. Ther.* **9,** R93 (2007).

90. C. Zeltz and D. Gullberg. The integrin-collagen connection - a glue for tissue repair? *J. Cell Sci.* **129,** 653–664 (2016).

91. A. D. Augst, H. J. Kong and D. J. Mooney. Alginate hydrogels as biomaterials. *Macromol. Biosci.* **6,** 623–633 (2006).

92. B. M. Baker, A. S. Nathan, A. O. Gee and R. L. Mauck. The influence of an aligned nanofibrous topography on human mesenchymal stem cell fibrochondrogenesis. *Biomaterials*. **31,** 6190–6200 (2010).

93. J. R. Tse and A. J. Engler. Stiffness gradients mimicking in vivo tissue variation regulate mesenchymal stem cell fate. *PLoS One*. **6,** e15978 (2011).

94. A. J. Engler, S. Sen, H. L. Sweeney and D. E. Discher. Matrix elasticity directs stem cell lineage specification. *Cell*. **126,** 677–89 (2006).

95. C. H. Lee, H. J. Shin, I. H. Cho, Y.-M. Kang, I. A. Kim, K.-D. Park and J.-W. Shin. Nanofiber alignment and direction of mechanical strain affect the ECM production of human ACL fibroblast. *Biomaterials*. **26,** 1261–70 (2005).

96. S. D. Subramony, B. R. Dargis, M. Castillo, E. U. Azeloglu, M. S. Tracey, A. Su and H. H. Lu. The guidance of stem cell differentiation by substrate alignment and mechanical stimulation. *Biomaterials*. **34,** 1942–1953 (2013).

97. J. Ma, M. J. Smietana, T. Y. Kostrominova, E. M. Wojtys, L. M. Larkin and E. M. Arruda. Three-Dimensional Engineered Bone–Ligament–Bone Constructs for Anterior Cruciate Ligament Replacement. *Tissue Eng. Part A*. **18,** 103–116 (2012).

98. J. E. Phillips, K. L. Burns, J. M. Le Doux, R. E. Guldberg and A. J. García. Engineering graded tissue interfaces. *Proc. Natl. Acad. Sci. U. S. A.* **105,** 12170–12175 (2008).

99. M. Urist, R. DeLange and G. Finerman. Bone cell differentiation and growth factors. *Science.* **220,** 680–686 (1983).

100. T. A. Linkhart, S. Mohan and D. J. Baylink. Growth factors for bone growth and repair: IGF, TGF and BMP. *Bone*. **19,** 1S–12S (1996).

101. J. R. Lieberman, A. Daluiski and T. a Einhorn. The Role of Growth Factors in the Repair of Bone. *J. Bone Jt. Surg.* **84,** 1032–1044 (2002).

102. T. Molloy, Y. Wang and G. A. C. Murrell. The Roles of Growth Factors in Tendon and Ligament Healing. *Sport. Med.* **33,** 381–394 (2003).

103. R. James, G. Kesturu, G. Balian and A. B. Chhabra. Tendon: Biology, Biomechanics, Repair, Growth Factors, and Evolving Treatment Options. *J. Hand Surg. Am.* **33,** 102–112 (2008).

104. P. M. Van der Kraan, P. Buma, T. Van Kuppevelt and W. B. Van Den Berg. Interaction of chondrocytes, extracellular matrix and growth factors: Relevance for articular cartilage tissue engineering. *Osteoarthr. Cartil.* **10,** 631–637 (2002).

105. B. S. Yoon, R. Pogue, D. a Ovchinnikov, I. Yoshii, Y. Mishina, R. R. Behringer and K. M. Lyons. BMPs regulate multiple aspects of growth-plate chondrogenesis through opposing actions on FGF pathways. *Development*. **133,** 4667–4678 (2006).

106. E. Minina, C. Kreschel, M. C. Naski, D. M. Ornitz and A. Vortkamp. Interaction of FGF, Ihh/Pthlh, and BMP signaling integrates chondrocyte proliferation and hypertrophic differentiation. *Dev. Cell*. **3,** 439–449 (2002).

107. P. C. Bessa, M. Casal and R. L. Reis. Bone morphogenetic proteins in tissue engineering: the road from laboratory to clinic, part II (BMP delivery). *J. Tissue Eng. Regen. Med.* **2,** 81–96 (2008).

108. U. Heine, E. F. Munoz, K. C. Flanders, L. R. Ellingsworth, H. Y. Lam, N. L. Thompson, A. B. Roberts and M. B. Sporn. Role of transforming growth factor-beta in the development of the mouse embryo. *J. Cell Biol.* **105,** 2861–76 (1987).

109. C. M. Leonard, H. M. Fuld, D. A. Frenz, S. A. Downie, J. Massague and S. A. Newman. Role of transforming growth factor-B in chondrogenic pattern formation in the embryonic limb: Stimulation of mesenchymal condensation and fibronectin gene expression by exogenenous TGF-B and evidence for endogenous TGF-B-like activity. *Dev. Biol.* **145,** 99–109 (1991).

110. W. M. Kulyk, B. J. Rodgers, K. Greer and R. A. Kosher. Promotion of embryonic chick limb cartilage differentiation by transforming growth factor-B. *Dev. Biol.* **135,** 424–430 (1989).

111. O. G. P. Isaksson, J.-O. Jansson and I. A. M. Gause. Growth Hormone Stimulates Longitudinal Bone Growth. *Science.* **216,** 1237–1239 (1982).

112. S. Mohan, Y. Nakao, Y. Honda, E. Landale, U. Leser, C. Dony, K. Lang and D. J. Baylink. Studies on the mechanisms by which insulin-like growth factor (IGF) binding protein-4 (IGFBP-4) and IGFBP-5 modulate IGF actions in bone cells. *Journal of Biological Chemistry*. **270,** 20424–20431 (1995).

113. E. B. Hunziker, J. Wagner and J. Zapf. Differential effects of insulin-like growth factor I and growth hormone on developmental stages of rat growth plate chondrocytes in vivo. *J. Clin. Invest.* **93,** 1078–86 (1994).

114. S. O. Abrahamsson. Similar effects of recombinant human insulin-like growth factor-I and II on cellular activities in flexor tendons of young rabbits: experimental studies in vitro. *J. Orthop. Res.* **15,** 256–262 (1997).

115. V. Midy and J. Plouët. Vasculotropin/vascular endothelial growth factor induces differentiation in cultured osteoblasts. *Biochemical and Biophysical Research Communications*. **199,** 380–386 (1994).

116. D. W. Leung, G. Cachianes, W. J. Kuang, D. V. Goeddel and N. Ferrara. Vascular endothelial growth factor is a secreted angiogenic mitogen. *Science.* **246,** 1306–9 (1989).

117. P. J. Keck, S. D. Hauser, G. Krivi, K. Sanzo, T. Warren, J. Feder and D. T. Connolly. Vascular permeability factor, an endothelial cell mitogen related to PDGF. *Science.* **246,** 1309–1312 (1989).

118. S. Thomopoulos, F. L. Harwood, M. J. Silva, D. Amiel and R. H. Gelberman. Effect of several growth factors on canine flexor tendon fibroblast proliferation and collagen synthesis in vitro. *J. Hand Surg. Am.* **30,** 441–447 (2005).

119. A. Augst, D. Marolt, L. E. Freed, C. Vepari, L. Meinel, M. Farley, R. Fajardo, N. Patel, M. Gray, D. L. Kaplan and G. Vunjak-Novakovic. Effects of chondrogenic and osteogenic regulatory factors on composite constructs grown using human mesenchymal stem cells, silk scaffolds and bioreactors. *J. R. Soc. Interface*. **5,** 929–939 (2008).

120. Z. S. Patel, S. Young, Y. Tabata, J. A. Jansen, M. E. K. Wong and A. G. Mikos. Dual delivery of an angiogenic and an osteogenic growth factor for bone regeneration in a critical size defect model. *Bone*. **43,** 931–940 (2008).

121. S. K. C. Sundararaj, R. D. Cieply, G. Gupta, T. A. Milbrandt and D. A. Puleo. Treatment of growth plate injury using IGF-1 loaded PLGA scaffold. *J. Tissue Eng. Regen. Med.* **9,** E202-209 (2015).

122. K. J. Gooch, T. Blunk, D. L. Courter, A. L. Sieminski, P. M. Bursac, G. Vunjak-Novakovic and L. E. Freed. IGF-I and Mechanical Environment Interact to Modulate Engineered Cartilage Development. *Biochem. Biophys. Res. Commun.* **286,** 909–915 (2001).

123. N. I. Aguilar, S. Trippel, S. Shi and L. J. Bonassar. Customized Biomaterials to Augment Chondrocyte Gene Therapy. *Acta Biomater.* **53,** 260–267 (2017).

124. W. L. Murphy, M. C. Peters, D. H. Kohn and D. J. Mooney. Sustained release of vascular endothelial growth factor from mineralized poly(lactide-co-glycolide) scaffolds for tissue engineering. *Biomaterials*. **21,** 2521–2527 (2000).

125. H. Park, J. S. Temenoff, T. A. Holland, Y. Tabata and A. G. Mikos. Delivery of TGF-1 and chondrocytes via injectable, biodegradable hydrogels for cartilage tissue engineering applications. *Biomaterials*. **26,** 7095–7103 (2005).

126. R. F. Macbarb, E. a Makris, J. C. Hu and K. a Athanasiou. A chondroitinase-ABC and TGF-β1 treatment regimen for enhancing the mechanical properties of tissue-engineered fibrocartilage. *Acta Biomater.* (2012). doi:10.1016/j.actbio.2012.09.037

127. A. F. Steinert, G. D. Palmer, R. Capito, J. G. Hofstaetter, C. Pilapil, S. C. Ghivizzani, M. Spector and C. H. Evans. Genetically enhanced engineering of

meniscus tissue using ex vivo delivery of transforming growth factor-beta 1 complementary deoxyribonucleic acid. *Tissue Eng.* **13,** 2227–37 (2007).

128. C. Li, C. Vepari, H.-J. Jin, H. J. Kim and D. L. Kaplan. Electrospun silk-BMP-2 scaffolds for bone tissue engineering. *Biomaterials*. **27,** 3115–3124 (2006).

129. P. Yilgor, K. Tuzlakoglu, R. L. Reis, N. Hasirci and V. Hasirci. Incorporation of a sequential BMP-2/BMP-7 delivery system into chitosan-based scaffolds for bone tissue engineering. *Biomaterials*. **30,** 3551–3559 (2009).

130. R. P. Marini, I. Martin, M. M. Stevens, R. Langer and V. P. Shastri. FGF-2 enhances TGF-B1 induced periosteal chondrogenesis. *J. Orthop. Res.* **22,** 1114–1119 (2004).

131. H. V. Almeida, Y. Liu, G. M. Cunniffe, K. J. Mulhall, A. Matsiko, C. T. Buckley, F. J. O'Brien and D. J. Kelly. Controlled release of transforming growth factor-β3 from cartilage-extra-cellular-matrix-derived scaffolds to promote chondrogenesis of human-joint-tissue-derived stem cells. *Acta Biomater.* **10,** 4400–4409 (2014).

132. M. Kim, I. E. Erickson, M. Choudhury, N. Pleshko and R. L. Mauck. Transient exposure to TGF-B3 improves the functional chondrogenesis of MSC-laden hyaluronic acid hydrogels. *J. Mech. Behav. Biomed. Mater.* **11,** 92–101 (2012).

133. J. A. Parry, M. G. L. Olthof, K. L. Shogren, M. Dadsetan, A. Van Wijnen, M. Yaszemski and S. Kakar. Three-Dimension-Printed Porous Poly(Propylene Fumarate) Scaffolds with Delayed rhBMP-2 Release for Anterior Cruciate Ligament Graft Fixation. *Tissue Eng. Part A*. (2017). doi:10.1089/ten.tea.2016.0343

134. H. K. Min, S. H. Oh, J. M. Lee, G. Il Im and J. H. Lee. Porous membrane with reverse gradients of PDGF-BB and BMP-2 for tendon-to-bone repair: In vitro evaluation on adipose-derived stem cell differentiation. *Acta Biomater.* **10,** 1272–1279 (2014).

135. A. Hildebrand, M. Romarís, L. M. Rasmussen, D. Heinegård, D. R. Twardzik, W. A. Border and E. Ruoslahti. Interaction of the small interstitial proteoglycans biglycan, decorin and fibromodulin with transforming growth factor beta. *Biochem. J.* **302,** 527–34 (1994).

136. W.-N. Qi and S. P. Scully. Extracellular collagen regulates expression of trasforming growth factor-beta1 gene. *J. Orthop. Res.* **18,** 928–932 (2000).

137. M. Mongiat, J. Otto, R. Oldershaw, F. Ferrer, J. D. Sato and R. V. Iozzo. Fibroblast Growth Factor-binding Protein is a Novel Partner for Perlecan Protein Core. *J. Biol. Chem.* **276,** 10263–10271 (2001).

138. R. Ruppert, E. Hoffmann and W. Sebald. Human bone morphogenetic protein 2 contains a heparin-binding site which modifies its biological activity. *Eur. J. Biochem.* **237,** 295–302 (1996).

139. Y. Zhu, A. Oganesian, D. R. Keene and L. J. Sandell. Type IIA Procollagen Containing the Cysteine-rich Amino Propeptide is Deposited in the Extracellular Matrix of Prechondrogenic Tissue and Binds to TGF-B1 and BMP-2. *J. Cell Biol.* **144,** 1069–1080 (1999).

140. N. Jaiswal, S. E. Haynesworth, A. I. Caplan and S. P. Bruder. Osteogenic differentiation of purified, culture-expanded human mesenchymal stem cells in vitro. *J. Cell. Biochem.* **64,** 295–312 (1997).

141. W. L. Grayson, M. Fröhlich, K. Yeager, S. Bhumiratana, M. E. Chan, C. Cannizzaro, L. Q. Wan, X. S. Liu, X. E. Guo and G. Vunjak-Novakovic. Engineering anatomically shaped human bone grafts. *Proc. Natl. Acad. Sci. U. S. A.* **107,** 3299–3304 (2010).

142. H. Lin, T. P. Lozito, P. G. Alexander, R. Gottardi and R. S. Tuan. Stem Cell-Based Microphysiological Osteochondral System to Model Tissue Response to Interleukin-1 β. *Mol. Pharm.* **11,** 2203–2212 (2014).

143. A. L. Boskey and R. Roy. Cell Culture Systems for Studies of Bone and Tooth Mineralization. *Chem Rev.* **108,** 4716–4733 (2008).

144. R.-I. Hata and H. Senoo. L-ascorbic acid 2-phosphate stimulates collagen accumulation, cell proliferation, and formation of a three-dimensional tissuelike substance by skin fibroblasts. *J. Cell. Physiol.* **138,** 8–16 (1989).

145. R. I. Schwarz, P. Kleinman and N. Owens. Ascorbate Can Act as an Inducer of the Collagen Pathway Because Most Steps Are Tightly Coupled. *Ann. N. Y. Acad. Sci.* **498,** 172–185 (1987).

146. N. Indrawattana, G. Chen, M. Tadokoro, L. H. Shann, H. Ohgushi, T. Tateishi, J. Tanaka and A. Bunyaratvej. Growth factor combination for chondrogenic induction from human mesenchymal stem cell. *Biochem. Biophys. Res. Commun.* **320,** 914–9 (2004).

147. A. G. Schwartz, J. H. Lipner, J. D. Pasteris, G. M. Genin and S. Thomopoulos. Muscle loading is necessary for the formation of a functional tendon enthesis. *Bone*. **55,** 44–51 (2013).

148. W. L. Grayson, S. Bhumiratana, P. H. Grace Chao, C. T. Hung and G. Vunjak-Novakovic. Spatial regulation of human mesenchymal stem cell differentiation in engineered osteochondral constructs: Effects of pre-differentiation, soluble factors and medium perfusion. *Osteoarthr. Cartil.* **18,** 714–723 (2010).

149. S. M. Goldman and G. A. Barabino. Spatial Engineering of Osteochondral Tissue Constructs Through Microfluidically Directed Differentiation of Mesenchymal Stem Cells. *Biores. Open Access*. **5,** 109–117 (2016).

150. M. B. Mueller, M. Fischer, J. Zellner, A. Berner, T. Dienstknecht, L. Prantl, R. Kujat, M. Nerlich, R. S. Tuan and P. Angele. Hypertrophy in mesenchymal stem cell chondrogenesis: Effect of TGF-β isoforms and chondrogenic conditioning. *Cells Tissues Organs*. **192,** 158–166 (2010).

151. Q. Li, F. Qu, B. Han, R. Mauck, L. Han and D. Ph. Micromechanical Heterogeneity and Anisotropy of the Meniscus Extracellular Matrix. *Acta Biomater.* (2017).

152. S. M. Goldman and G. A. Barabino. Cultivation of agarose-based microfluidic hydrogel promotes the development of large, full-thickness, tissue-engineered articular cartilage constructs. *J. Tissue Eng. Regen. Med.* **11,** 572–581 (2017).

153. K. L. Moffat, W.-H. S. Sun, P. E. Pena, N. O. Chahine, S. B. Doty, G. a Ateshian, C. T. Hung and H. H. Lu. Characterization of the structure-function relationship at the ligament-to-bone interface. *Proc. Natl. Acad. Sci. U. S. A.* **105,** 7947–7952 (2008).

154. S. Thomopoulos, J. P. Marquez, B. Weinberger, V. Birman and G. M. Genin. Collagen fiber orientation at the tendon to bone insertion and its influence on stress concentrations. *J. Biomech.* **39,** 1842–1851 (2006).

155. D. F. Villegas, T. a. Hansen, D. F. Liu and T. L. Haut Donahue. A quantitative study of the microstructure and biochemistry of the medial meniscal horn attachments. *Ann. Biomed. Eng.* **36,** 123–131 (2008).

156. D. F. Villegas and T. L. H. Donahue. Collagen morphology in human meniscal attachments: a SEM study. *Connect. Tissue Res.* **51,** 327–336 (2010).

157. D. F. Villegas, J. a. Maes, S. D. Magee and T. L. Haut Donahue. Failure properties and strain distribution analysis of meniscal attachments. *J. Biomech.* **40,** 2655–2662 (2007).

158. Y. Hu, V. Birman, A. Demyier-Black, A. G. Schwartz, S. Thomopoulos and G. M. Genin. Stochastic interdigitation as a toughening mechanism at the interface between tendon and bone. *Biophys. J.* **108,** 431–437 (2015).

159. H. M. Kim, L. M. Galatz, N. Patel, R. Das and S. Thomopoulos. Recovery Potential After Postnatal Shoulder Paralysis. *J. Bone Jt. Surg.* **91,** 879–891 (2009).

160. S. Thomopoulos. Tendon to Bone Healing: Differences in Biomechanical, Structural, and Compositional Properties Due to a Range of Activity Levels. *J. Biomech. Eng.* **125,** 106 (2003).

161. C. R. Clark and J. A. Ogden. Prenatal and Postnatal Development of Human Knee Joint Mensci. *Iowa Orthop. J.* **1,** 20–27 (1981).

162. D. Huang, T. R. Chang, A. Aggarwal, R. C. Lee and H. P. Ehrlich. Mechanisms and dynamics of mechanical strengthening in ligament-equivalent fibroblast-populated collagen matrices. *Ann. Biomed. Eng.* **21,** 289–305 (1993).

163. S. Thomopoulos, G. M. Fomovsky and J. W. Holmes. The development of structural and mechanical anisotropy in fibroblast populated collagen gels. *J. Biomech. Eng.* **127,** 742–750 (2005).

164. F. Grinnell. Fibroblast-collagen-matrix contraction: growth-factor signalling and mechanical loading. *Trends Cell Biol.* **10,** 362–365 (2000).

165. K. D. Costa, E. J. Lee and J. W. Holmes. Creating alignment and anisotropy in engineered heart tissue: role of boundary conditions in a model three-dimensional culture system. *Tissue Eng.* **9,** 567–77 (2003).

166. V. S. Nirmalanandhan, M. S. Levy, A. J. Huth and D. L. Butler. Effects of cell seeding density and collagen concentration on contraction kinetics of mesenchymal stem cell-seeded collagen constructs. *Tissue Eng.* **12,** 1865–72 (2006).

167. R. G. Young, D. L. Butler, W. Weber, a I. Caplan, S. L. Gordon and D. J. Fink. Use of mesenchymal stem cells in a collagen matrix for Achilles tendon repair. *J. Orthop. Res.* **16,** 406–413 (1998).

168. H. A. Awad, D. L. Butler, M. T. Harris, R. E. Ibrahim, Y. Wu, R. G. Young, S. Kadiyala and G. P. Boivin. In vitro characterization of mesenchymal stem cell-seeded collagen scaffolds for tendon repair: Effects of initial seeding density on contraction kinetics. *J. Biomed. Mater. Res.* **51,** 233–240 (2000).

169. R. D. Bowles, R. M. Williams, W. R. Zipfel and L. J. Bonassar. Self-Assembly of Aligned Tissue-Engineered Annulus fibrosus and Intervertebral Disc Composite Via Collagen Gel Contraction. *Tissue Eng. Part A.* **16,** (2010).

170. J. L. Puetzer, I. Sallent, A. Gelmi and M. M. Stevens. Investigating Collagen Fiber Formation for Functional Musculoskeletal Engineering: Going beyond the Fibril. *ORS 2017 Annu. Meet.* (2017).

171. D. J. Huey and K. a Athanasiou. Tension-compression loading with chemical stimulation results in additive increases to functional properties of anatomic meniscal constructs. *PLoS One*. **6,** e27857 (2011).

172. J. L. Puetzer and L. J. Bonassar. Physiologically Distributed Loading Patterns Drive the Formation of Zonally Organized Collagen Structures in Tissue Engineered Meniscus. *Tissue Eng. Part A.* **22,** 907–916 (2016).

173. M. B. Fisher, E. A. Henning, N. B. Soegaard, G. R. Dodge, D. R. Steinberg and R. L. Mauck. Maximizing cartilage formation and integration via a trajectory-based tissue engineering approach. *Biomaterials*. **35,** 2140–2148 (2014).

174. C. D. DiDomenico, Z. X. Wang and L. J. Bonassar. Cyclic Mechanical Loading Enhances Transport of Antibodies into Articular Cartilage. *J. Biomech. Eng.* **139,** 11012-11012–7 (2016).

175. C. T. Hendley, J. Tao, J. A. M. R. Kunitake, J. J. De Yoreo and L. A. Estroff. Microscopy techniques for investigating the control of organic constituents on biomineralization. *MRS Bull.* **40,** 480–489 (2015).

176. H. Wang, A. O. Gee, I. D. Hutchinson, K. Stoner, R. F. Warren, T. O. Chen and S. A. Maher. Bone Plug Versus Suture-Only Fixation of Meniscal Grafts: Effect

on Joint Contact Mechanics During Simulated Gait. *Am. J. Sports Med.* **42,** 1682–1689 (2014).

177. K. A. Ross, R. M. Williams, L. V. Schnabel, H. O. Mohammed, H. G. Potter, G. Bradica, E. Castiglione, S. L. Pownder, P. W. Satchell, R. A. Saska and L. A. Fortier. Comparison of Three Methods to Quantify Repair Cartilage Collagen Orientation. *Cartilage*. **4,** 111–120 (2013).

178. N. T. Khanarian, M. K. Boushell, J. P. Spalazzi, N. Pleshko, A. L. Boskey and H. H. Lu. FTIR-I Compositional Mapping of the Cartilage-to-Bone Interface as a Function of Tissue Region and Age. *J. Bone Miner. Res.* **29,** 1–26 (2014).

179. J. Mansfield, J. Moger, E. Green, C. Moger and C. P. Winlove. Chemically specific imaging and in-situ chemical analysis of articular cartilage with stimulated raman scattering. *J. Biophotonics*. **6,** 803–814 (2013).

180. S. Yamanaka. A Fresh Look at iPS Cells. *Cell*. **137,** 13–17 (2009).

181. E. S. Lander. The Heroes of CRISPR. *Cell*. **164,** 18–28 (2016).

182. N. W. Choi, M. Cabodi, B. Held, J. P. Gleghorn, L. J. Bonassar and A. D. Stroock. Microfluidic scaffolds for tissue engineering. *Nat. Mater.* **6,** 908–915 (2007).

183. R. R. Jose, M. J. Rodriguez, T. A. Dixon, F. Omenetto and D. L. Kaplan. Evolution of Bioinks and Additive Manufacturing Technologies for 3D Bioprinting. *ACS Biomater. Sci. Eng.* **2,** 1662–1678 (2016).

184. S. M. Goldman and G. A. Barabino. Cultivation of agarose-based microfluidic hydrogel promotes the development of large, full-thickness, tissue-engineered

articular cartilage constructs. *J. Tissue Eng. Regen. Med.* (2014). doi:10.1002/term

185. N. Kakudo, K. Kusumoto, Y. B. Wang, Y. Iguchi and Y. Ogawa. Immunolocalization of vascular endothelial growth factor on intramuscular ectopic osteoinduction by bone morphogenetic protein-2. *Life Sci.* **79,** 1847–1855 (2006).

186. J. T. Connelly, C. G. Wilson and M. E. Levenston. Characterization of proteoglycan production and processing by chondrocytes and BMSCs in tissue engineered constructs. *Osteoarthr. Cartil.* **16,** 1092–1100 (2008).

187. B. Johnstone, T. M. Hering, A. I. Caplan, V. M. Goldberg and J. U. Yoo. In vitro chondrogenesis of bone marrow-derived mesenchymal progenitor cells. *Exp Cell Res*. **238,** 265–272 (1998).

188. S. M. Imler, A. N. Doshi and M. E. Levenston. Combined effects of growth factors and static mechanical compression on meniscus explant biosynthesis. *Osteoarthritis Cartilage*. **12,** 736–44 (2004).

189. J. L. Puetzer, B. N. Brown, J. J. Ballyns and L. J. Bonassar. The Effect of IGF-I on Anatomically Shaped Tissue-Engineered Menisci. *Tissue Eng. Part A.* **19,** 1443–1450 (2013).

190. C. K. Hee, J. S. Dines, L. a Solchaga, V. R. Shah and J. O. Hollinger. Regenerative tendon and ligament healing: opportunities with recombinant human platelet-derived growth factor BB-homodimer. *Tissue Eng. Part B. Rev.* **18,** 225–34 (2012).

191. D. J. Baylink, R. D. Finkelman and S. Mohan. Growth factors to stimulate bone formation. *J. Bone Miner. Res.* **8,** S565–S572 (1993).

CHAPTER 3

Characterization of Mesenchymal Stem Cells and Fibrochondrocytes in 3D Co-Culture: Analysis of cell shape, matrix production, and mechanical performance[2]

Abstract

Introduction: Bone marrow mesenchymal stem cells (MSCs) have shown positive therapeutic effects for meniscus regeneration and repair. Preliminary *in vitro* work has indicated positive results for MSC applications for meniscus tissue engineering, however more information is needed on how to direct MSC behavior. The objective of this study was to examine the effect of MSC co-culture with primary meniscal fibrochondrocytes (FCCs) in a 3D collagen scaffold in fibrochondrogenic media. Co-culture of MSCs and FCCs was hypothesized to facilitate the transition of MSCs to a FCC cell phenotype as measured by matrix secretion and morphology.

Methods: MSCs and FCCs were isolated from bovine bone marrow and meniscus respectively. Cells were seeded in a 20 mg/mL high density type I collagen gel at MSC:FCC ratios of 0:100,25:75, 50:50, 75:25, and 100:0. Constructs were cultured for up to two weeks then analyzed for cell morphology, glycosaminoglycan content, collagen content, and production of collagen type I, II, and X.

Results: Cells were homogeneously mixed throughout the scaffold and cells had limited direct cell-cell contact. After two weeks in culture MSCs transitioned from a spindle-like morphology toward a rounded phenotype, while FCCs remained rounded throughout culture. Although MSC shape changed with culture, the overall size was significantly larger than FCCs throughout culture. While 75:25 and 100:0 (MSC mono-culture) culture groups produced significantly more GAG/DNA

(glycosaminoglycan/deoxyribonucleic acid) than FCCs in mono-culture, GAG retention was highest in 50:50 co-cultures. Similarly, the aggregate modulus was highest in 100:0 and 50:50 co-cultures. All samples contained both collagen types I and II after two weeks and collagen type X expression was evident in only MSC mono-culture gels.

Conclusions: MSCs shift to a FCC morphology in both mono- and co-culture. Co-culture reduced hypertrophy by MSCs, indicated by collagen type X. This study shows that MSC phenotype can be influenced by indirect homogeneous cell culture in a 3D gel, demonstrating the applicability of MSCs in meniscus tissue engineering applications.

---

[2]M. C. McCorry, J. L. Puetzer and L. J. Bonassar. Characterization of mesenchymal stem cells and fibrochondrocytes in three-dimensional co-culture: analysis of cell shape, matrix production, and mechanical performance. *Stem Cell Res. Ther.* **7,** 39 (2016).

Introduction

Meniscus damage is one of the most common knee injuries with a reported incidence of 61/100,000 and over 1 million procedures performed annually in the United States [1]. Like most cartilaginous structures, the meniscus has a limited healing capacity because the tissue is primarily avascular. Depending on the severity of the tear, the meniscus is either partially resected or replaced using a meniscus allograft. Meniscal allograft procedures are limited in availability, shape and immunocompatibility [2–4]. Recent studies have demonstrated the applicability of intra-articular stem cell injection for repair of small meniscal tears [5–8]. For more extensive injuries, tissue engineering of the meniscus may offer a promising alternative to meniscus allograft replacement.

Progress toward a tissue engineered meniscus has shown great promise, but has yet to reach clinical application [9–13]. Tissue engineered menisci often lack native biochemical and mechanical properties necessary for successful function *in vivo*. The addition of cells to engineered menisci provide an essential mediator for development and modification of the construct, often resulting in a better match to native properties. Previously, we have shown that fibrochondrocytes (FCCs) seeded in a collagen tissue engineered meniscus under static mechanical boundary conditions are able to mimic anisotropic fiber formation seen in native menisci as well as improve mechanical properties [14]. However, obtaining the sufficient number of cells for an engineered meniscus is challenging. FCCs derived from surgical debri have been shown as a viable cell source for tissue engineering [15], but they remain a challenge since cell number is limited, as FCCs proliferate slowly and often lose their phenotype in two-dimensional

(2D) culture [16]. As tissue engineered constructs approach clinical application there is an increasing need for a cell source that is easy to obtain and expand in culture.

Mesenchymal stem cells (MSCs) have shown great potential as treatment option for meniscus repair and regeneration. Intraarticular injection of bone marrow MSCs in human and animal studies have demonstrated that MSCs mobilize to the site of injury and contribute to tissue regeneration [5–8]. MSCs from the bone marrow are easily obtained and expanded in culture and are well established as multipotent stem cells that can differentiate down chondrogenic lineage [17, 18]. However, differentiation of MSCs down the fibrochondrogenic lineage is not well understood [19]. MSC co-culture with either meniscus or articular cartilage cells has been shown to direct differentiation and increase matrix secretion [20–24]. Pellet culture of MSCs co-cultured with meniscus FCCs increased expression of fibrochondrogenic genes, reduced hypertrophy, and increased matrix production [20, 21]. However, studies using FCC co-culture with stem cells have been limited to 2D culture and 3D cell pellets. Little is known about how cell proximity, exogenous signaling, and cell-matrix interactions will affect cellular phenotype in 3D scaffold culture.

The goal of this study was to evaluate the effects of 3D co-culture of MSCs and FCCs on cell phenotype indicated by cell shape, matrix secretion, and mechanical properties of constructs. We hypothesize that co-culture of MSCs with FCCs in a 3D collagen scaffold will facilitate increased matrix secretion and mechanical properties.

Methods

Cell Isolation

Methods for cell isolation were based on those previously described, in which all cells were isolated from 1-3 day old bovids postmortem [25, 26]. Briefly, MSCs were extracted by washing the trabecular region of the femoral head with heparin supplemented media [26]. The extract solution was centrifuged at 300 x *g* and the pellet was suspended and plated on tissue culture plastic. Plates were washed after 48 hours to remove the unattached cell population. Trilineage differentiation assays were performed to confirm multipotency of MSCs for ostegenic, adipogenic, and chondrogenic (Supp. 3.1) [18, 27]. MSCs were plated at 2,000 cells/cm^2 and expanded in 2D culture until passage 4 with a growth medium containing low glucose Dulbecco's modified Eagle's medium (DMEM) supplemented with 10% fetal bovine serum (FBS), 100 I.U./mL penicillin, 100 μg/mL streptomycin, 0.25 μg/mL amphotericin B, 2mM L-glutamine, and 1 ng/mL basic fibroblast growth factor. FCCs were digested from menisci in 0.3% collagenase (Worthington Biochemical Corporation, Lakewood, NJ) in DMEM with 100 μg/mL penicillin and 100 μg/mL streptomycin, followed by filtering through a 100 μm cell strainer [25, 28]. Following cell isolation, FCCs were prepared for direction seeding into collagen gels with passaged MSCs. Prior to mixing cells into 3D constructs, MSCs were labeled using CellTrace Green CFSE (Invitrogen, Grand Island, NY, C34554) and FCCs were labeled with CellTrace FarRed DDAO-SE (Invitrogen, C34553). Cell media cocktails were mixed at MSC:FCC ratios of 0:100, 25:75, 50:50, 75:25, and 100:0. Since no live animals were used in this study, no IACUC approval was required.

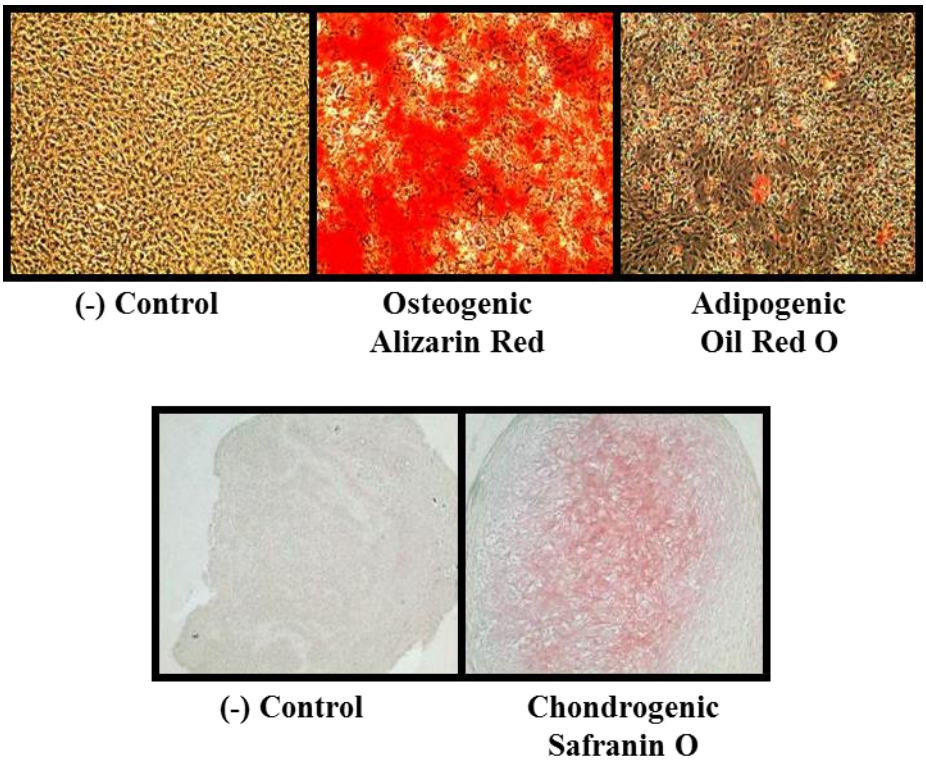

Supplemental 3.1: Trilineage differentiation of bone marrow derived MSCs. Control samples cultured in growth medium and stained with Alizarin Red S, Oil Red O or Safranin O. Samples cultured in osteogenic media stained with Alizarin Red, samples cultured in adpogenic media stained with Oil Red O and samples cultured in chondrogenic media stained with Safranin O.

Construct Generation

Collagen type I was extracted from Sprague-Dawley rat tails (Pel-Freez Biologicals, Rogers, AZ) and reconstituted in 0.1% acetic acid at 30 mg/mL concentration as previously described [25, 29, 30]. Briefly, the stock collagen solution was mixed with working solutions of 1N NaOH, 10x phosphate-buffered saline (PBS), and 1x PBS to return the collagen to a neutral 7.0 pH and 300mOsm and begin the gelation process [30]. Cell-media cocktails were homogeneously mixed at a final concentration of $25x10^6$ cells/mL to form a collagen solution at 20 mg/mL [25]. Collagen solution was gelled between two glass plates to create a sheet gel 2 mm thick,

and molds were allowed to gel for 30 minutes at 37˚C. From each 2 mm thick gel, 30 8mm diameter samples were obtained using biopsy punches. Ten samples were used per time point at 1, 8, and 15 days (2 to confocal/histology, 4 to mechanical, 4 to biochemical analysis). Samples were cultured in media containing DMEM, 10% FBS, 100 μg/mL penicillin, 100 μg/mL streptomycin, 0.1 mM non-essential amino acids, 50 μg/mL ascorbate, and 0.4 mM L-proline [25]. Culture media was collected and replenished every 3-4 days. Images of each sample were obtained at each media change. Images were imported into ImageJ to calculate the area of each construct. Cells and constructs were cultured at 37°C and 5% CO_2.

Cell Shape Analysis

At the desired time points, two samples from each experimental group were fixed in 10% buffered formalin for 48 hours and stored in 70% ethanol. Fluorescence imaging was performed on a Zeiss 710 confocal microscope with a Zeiss Axio Observer Z1 inverted stand using a 40x /1.2 C-Apochromat water immersion objective. Images of MSCs labeled with CellTrace Green CFSE and FCCs labeled with CellTrace FarRed DDAO-SE were obtained separately for analysis. Four images and two z-stacks per sample were taken, with at least ten cells per image. Z-stacks were converted into a 2D projected image. Aspect ratio (AR) and cell area were calculated using “area” and “centroid fit” (AR=major axis/minor axis) in ImageJ software (National Institute of Health) [31].

Biochemical Content

Samples were collected and weighed to obtain a wet weight (WW) then frozen, lyophilized, and weighed again to obtain dry weight (DW). As previously described

DNA, glycosaminoglycan (GAG), and collagen content were measured via the Hoechst DNA assay [32], a modified 1,9-dimethylmethylene blue (DMMB) assay at pH 1.5 [33], and a hydroxyproline (hypro) assay respectively [34]. Biochemical contents were normalized to DNA to account for construct contraction and cell proliferation. Biochemical tests were analyzed on both construct samples and media samples collected throughout culture. Total content was calculated as a sum biochemical content in media added to total biochemical content in the construct. Retention was calculated as a percentage of content in construct relative to total content.

Histology

Following fluorescent imaging, samples were dehydrated, embedded into paraffin blocks, sectioned, and stained. Picrosirious red staining was imaged using brightfield microscopy and collagen fiber organization was visualized under polarized light [25]. Immunohistochemistry was conducted as previously described to further investigate collagen content using antibodies for collagen type I (Abcam, Cambridge, MA. 34710), collagen type II (Chondrex, Redmond, WA, 7005), and collagen type X (Abcam, 58632) [35]. Primary and secondary antibody controls were run in parallel with samples for immunohistochemistry stains (Supp. 3.3). Control samples and experimental samples were stained in the same batch process and exposed to the same duration and concentration of reagents. Images were obtained with a SPOT RT camera (Diagnostic Instruments, Steriling Heights, MI) attached to a Nikon Eclipse TE2000-S microscope (Nikon Instruments, Melville, NY).

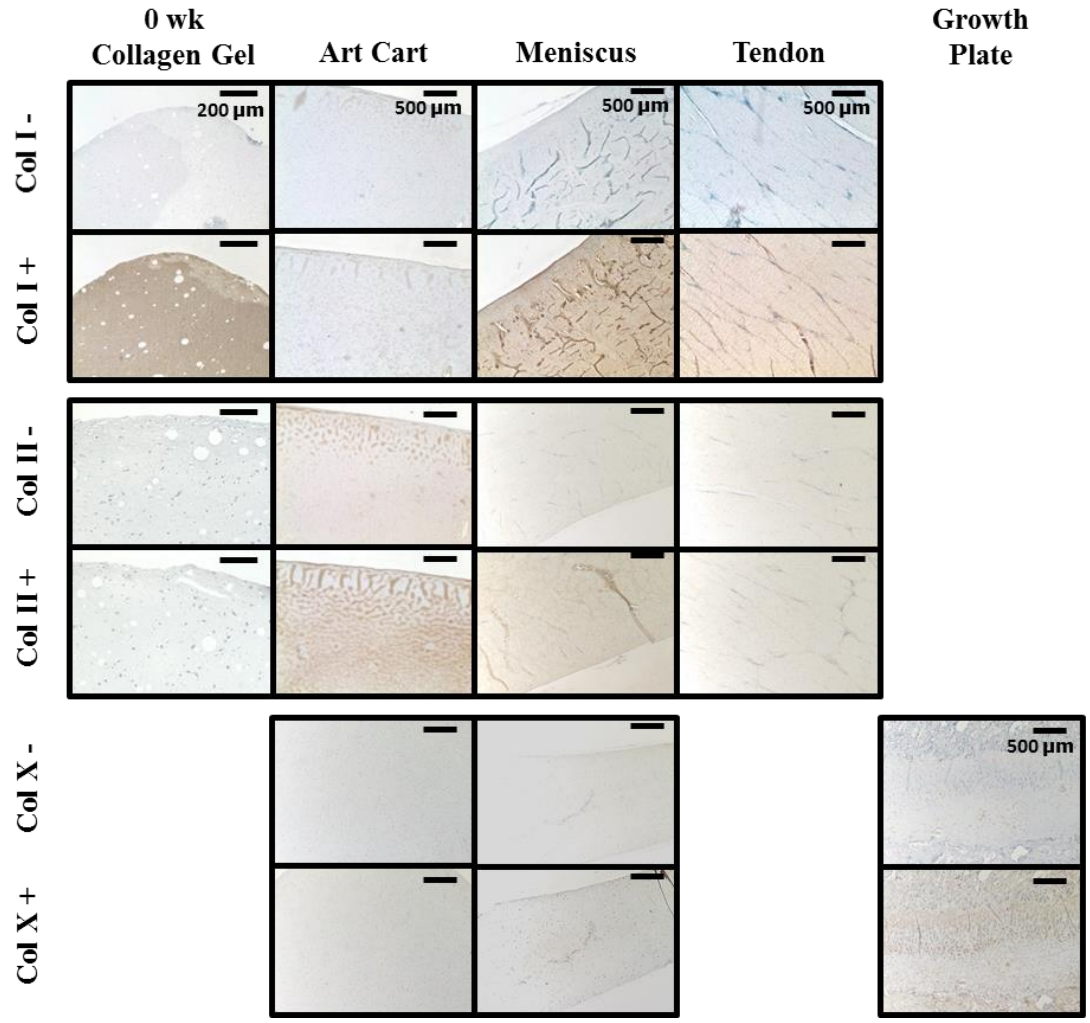

Supplemental 3.3: Immunohistochemicial staining controls for Collagen type I, II, X. Primary antibody controls run for all groups represented by (-). Extensor tendon section from bovine knee as positive control for collagen type I. Articular cartilage transverse section from bovine distal femur as positive control for collagen type II. Growth plate from bovine distal femur as positive control for collagen type X. (counterstained with hematoxylin, 0 wk collagen gel bar= 200 µm on 100x objective, all others bar=500 µm on 40x objective)

Mechanical Properties

Four samples per experimental group were cut into 4 mm diameter plugs and tested for compressive properties [36–38]. 2 mm thick samples were tested in confined compression via a stress relaxation test performed by imposing 10x100 μm steps (relaxation=12 min., strain=5-45%, steps=5%, n=4). The resulting load was then fit to a poroelastic model using a custom MATLAB program to determine aggregate modulus (HA) and hydraulic permeability (k). Mechanical testing was performed on an Enduratec ElectroForce 3200 System (Bose, Eden Prairie, MN) using a 1 kg load cell.

Statistics

Biochemical data were analyzed by 2-way-ANOVA using Tukey's t-test for post hoc analysis (SigmaPlot, San Jose, California). An equal probability averaging method was used for GAG retention calculations to pair media samples with a construct samples [39]. All data are expressed as mean ±SD and significance was determined with $p<0.05$.

Results

Characterization of Cell Morphology

Cells embedded in collagen gels visualized using fluorescent probes showed that cells were homogeneously distributed in each construct with limited direct cell-cell contact. Within each construct, cells were homogenously mixed between two cell types with FCCs and MSCs distributed throughout the construct (Figure 3.1A).

MSCs had an increased projected area relative to FCCs, with MSCs (mono-culture Area=169+/-119 μm^2) ~2 times the size of FCCs (mono-culture Area=75+/-40

μm^2) at day 1. FCCs became smaller in area after 8 days (mono-culture Area=42+/-13μm^2) but maintained size between 8 and 15 days (mono-culture Area=45+/-18 μm^2). After 15 days in culture MSCs had reduced in size (mono-culture Area=162+/-90 μm^2); however, were still significantly larger than FCC cell population (Figure 3.1B).

MSCs and FCCs exhibited distinct cell morphologies at day 1 that became more homogeneous after 15 days of culture (Figure 3.1). FCCs appeared more rounded (mono-culture AR=1.4+/-0.3) and MSCs appeared more elongated (mono-culture AR=2.0+/-1.2) at day 1 (Figure 3.1C). MSC cell shape at day 1 was a mixture of circular and elongated cell morphologies. After 15 days in culture both FCCs (mono-culture 1.5+/-0.4) and MSCs (mono-culture AR=1.7+/-0.6) displayed a circular morphology (Figure 3.1A). FCC AR remained consistent between experimental groups in co-culture and throughout the duration of co-culture with no statistical differences. MSCs showed variable morphologies at 1 and 8 days and appeared to converge on the circular phenotype after 15 days (Figure 3.1A&C).

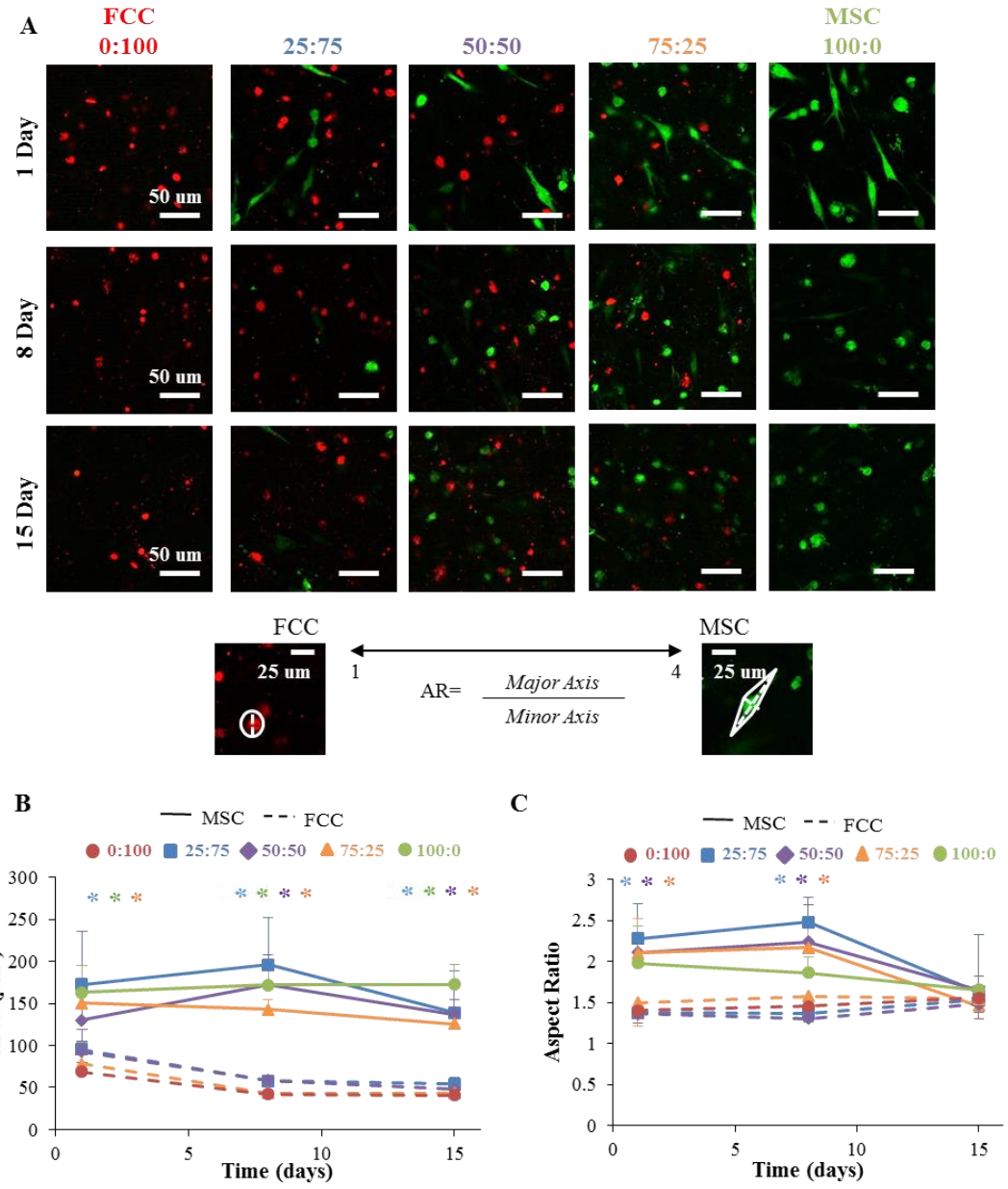

Figure 3.1: Cell shape and size images with analysis with all ratios presented as MSC:FCC. (A) Fluorescent images of biopsy constructs (red=FCC, green=MSC) (bar=50μm, n=2). (B) Cell area calculations and (C) aspect ratio calculations (dotted line represents FCC population in co-culture and solid line represents MSC cell population in co-culture) (* significantly different than 100% FCC, $p<0.05$) (n=4).

Matrix Synthesis

Phenotypic changes were observed in MSC laden gels as measured through changes in matrix content over time. Gels contained essentially no GAG at the beginning of culture. After fifteen days GAG normalized to DNA content increased to 1.08 +/- 0.3 μg/μg in FCC mono-culture and to 1.91 +/- 0.16 μg/μg in MSC mono-culture. GAG/DNA content increased linearly with MSC content at fifteen days (R^2 =0.94) and all groups had a significant increase in GAG/DNA content with time (Figure 3.2A, $p< 0.001$). GAG content in media was recorded in order to observe if cells were producing GAGs that were being lost into the cell media. The increasing GAG/DNA content increasing with MSC content remains consistent when GAG in media is combined with GAG in the construct (Figure 3.2B). Interestingly, 50:50 co-culture retained the greatest amount of GAG within the construct (73% +/- 3%), significantly higher than both FCC and MSC mono-culture. 50:50, 75:25, and 100:0 MSC gels all retained significantly higher amounts of GAG (73% +/- 3%, 70% +/- 2%, 63% +/- 2% respectively) compared to FCC mono-culture (52% +/-7%) (Figure 3.2C). Hydroxyproline was measured as an indication of collagen content. All gels contained collagen at 1 day since the gels were comprised of collagen type I, however over time the cells breakdown their collagen matrix. FCCs displayed a more catabolic response than the MSCs as MSC mono-culture group had no significant changes in hypro/DNA (Figure 3.2D). Hydroxyproline content measured in the media and construct together indicate that the total collagen in the system is not changing with time (Figure 3.2E). Similar to GAG retention, hydroxyproline retention in the constructs was greatest in the 50:50 co-culture group (77% +/- 3%) (Figure 3.2F). Collagen constructs contracted over

time, but maintained cylindrical shape (Supp. 3.2A).MSC containing constructs contracted between 40-60% of their original size by day 15 while FCC mono-culture gels contracted only 82% (Supp. 3.2B). There was no significant difference between gels, therefore contraction does not play a role in biochemical differences between these groups. Cells in constructs proliferated between days 1, 8, and 15 indicating a healthy cell population. DNA content between groups at day 1 showed no significant differences however co-culture and MSC mono-culture groups had greater proliferation than FCC mono-culture over time (Supp. 3.2C). GAG and hydroxyproline content were normalized to DNA to account for cellular proliferation with time.

Histological staining and immunochemistry revealed matrix presence and localization. All experimental groups showed the presence of collagen with small disorganized fibers forming in the body of the constructs. Small clumps of fibers form throughout the construct with some increased alignment occurring near the edges (Figure 3.3 rows 1&2). Immunohistochemistry was used to probe for specific types of collagen in the constructs. All groups stained positive for collagen type I and II after 15 days (Figure 3.3 rows 2&3). No staining for collagen type II was observed in 1 day samples, thus positive staining for collagen type II at 15 days was produced during culture (Supp. 3.4). After two weeks of culture, MSC mono-culture gels showing positive staining for collagen type X compared to other culture groups (Figure 3.3 row 5).

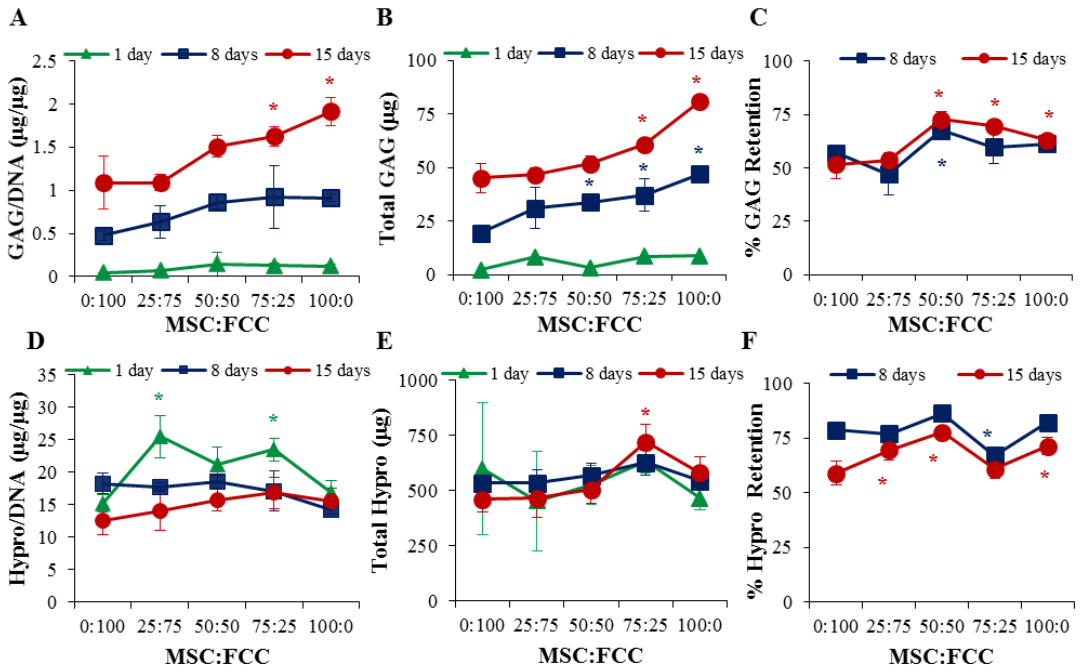

Figure 3.2: Biochemical analysis with all ratios presented as MSC:FCC.(A) GAG content in construct normalized to DNA content. (B) Total GAG produced by sample calculated as a sum of GAG in the media and GAG in the construct. (C) GAG retained within construct calculated as a percentage of content in samples to total content in samples and media over time. (D) Hydroxyproline (hypro) content in construct normalized to DNA content. (E) Total Hypro produced by sample calculated as a sum of GAG in the media and GAG in the construct. (F) Hypro retained within construct calculated as a percentage of content in samples to total content in samples and media over time. (* significantly different than 100% (0:100) FCC within time pt, $p<0.05$, n=4)

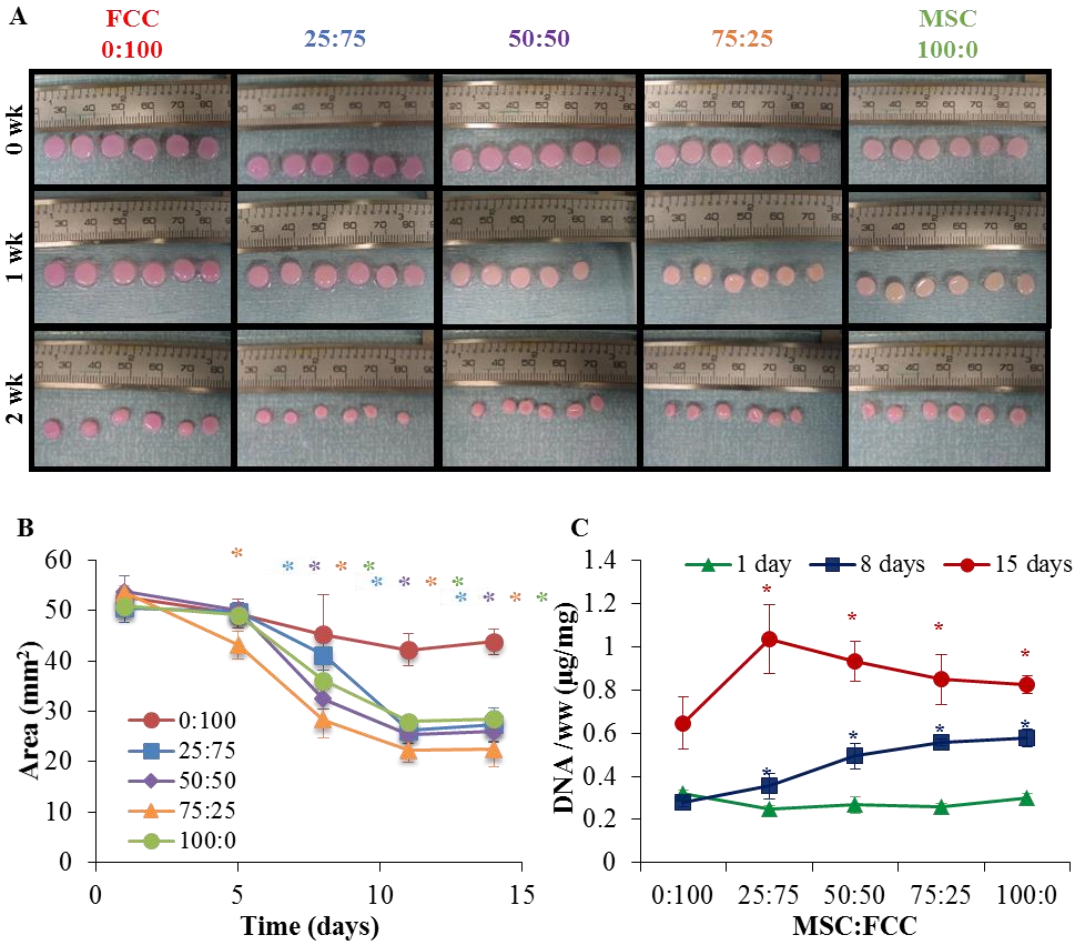

Supplemental 3.2: (A) Macroscopic images of constructs taken at each time point and condition. (B) Projected area calculations of samples over time. (C) DNA content normalized to wet weight of samples. (* significantly different than 100% FCC, $p<0.05$, n=4).

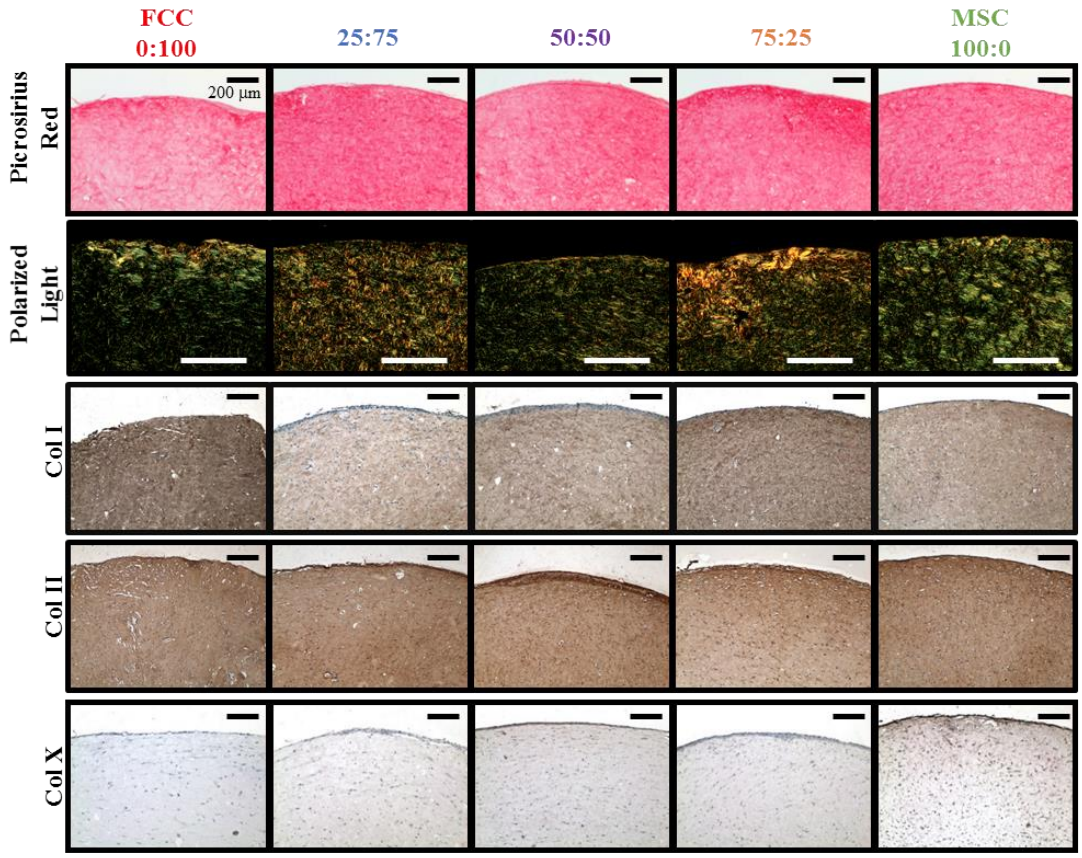

Figure 3.3: Histological staining of samples after 15 days of culture, all ratios presented as MSC:FCC. Picrosirius red staining imaged with brightfield microscopy (row 1) and polarized light (row 2). Immunohistochemical staining of collagen type I (row 3), collagen type II (row 4), and collagen type X (row 5). (Counterstained with hematoxylin, Bar= 200 µm)

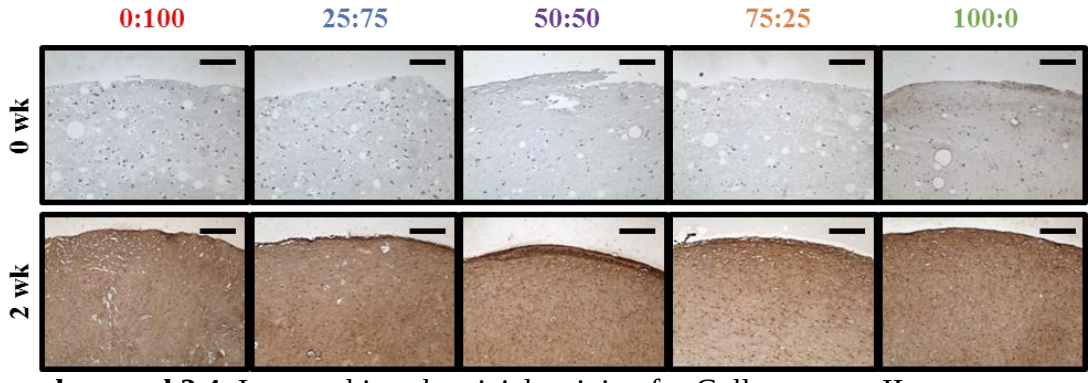

Supplemental 3.4: Immunohistochemicial staining for Collagen type II (Counterstained with hematoxylin, Bar= 200 µm)

Mechanical Characterization

Mechanical properties of samples improved with MSCs cellular content and time in culture (HA values p<.05). The aggregate modulus of 50:50 co-culture (31 +/- 2 kPa) was significantly higher that FCC mono-culture after 15 days. FCCs had the lowest aggregate modulus after 15 days in culture (21 +/- 1 kPa) (Figure 3.4). Permeability reflected a similar trend to aggregate modulus with permeability decreasing from day 1 in culture, however there was no statistical difference between sample groups at 15 days (Figure 3.4B).

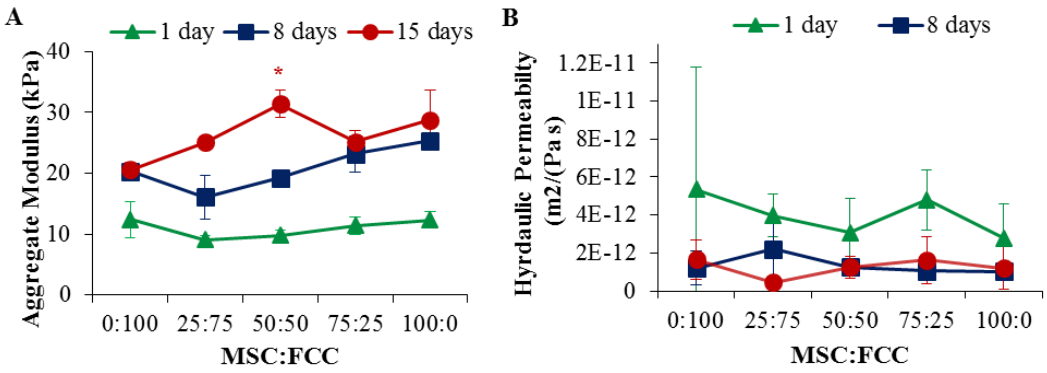

Figure 3.4: Mechanical analysis with all ratios presented as MSC:FCC. (A) Aggregate modulus and (B) permeability of constructs (* significantly different than 100% FCC, p<0.05, n=3-4).

Discussion

The objective of this study was to examine MSC phenotype when co-cultured with FCCs with the overarching goal to examine regenerative potential of MSCs for meniscus repair. We hypothesized that co-culture of MSCs with FCCs in a 3D collagen scaffold would facilitate increased matrix accumulation and mechanical properties. In this study, MSCs mono-cultured and co-cultured with FCCs displayed a phenotypic change related to cell morphology and matrix production. MSCs transition to a

chondrogenic morphology and outperform FCCs in GAG production after 15 days of culture. Despite MSCs advantageous matrix synthesis, MSCs had a hypertrophic tendency that was mitigated by co-culture. These data show that MSCs in co-culture with meniscal FCCs present specific advantages for meniscus tissue engineering; specifically increasing GAG retention in the construct, decreasing MSC hypertrophy, and improved mechanical properties.

Cell aspect ratio is well established as a measure of cell morphology and cell phenotype, however, this is the first study to examine changes in MSC morphology in co-culture with FCCs. In this study, MSCs underwent a distinct change in cell morphology between 1, 8, and 15 days. FCCs exhibited a consistent circular morphology while MSCs started with an elongated morphology that transitioned to a circular morphology over time. Cell shape is directly linked to cell phenotype and has been shown to be dictated by the surrounding mechanical and chemical environment [40–42]. Reduction in cell spreading and/or transition to circular phenotype is associated with mesenchymal chondrogenesis. Previous work has shown that prevention of cell spreading, through disruption of the cytoskeleton using cytochalasin, increased chondrogenesis [43]. Pellet cultures are hypothesized to aid in MSC chondrogenesis by providing a 3D environment that forces cells into a compacted shape, reducing cell spreading [18]. In this study, cultured MSCs, even in a material that supports adhesion and spreading, moved to a rounded phenotype and produced proteoglycans.

Consistent with other studies, we found that MSCs increased collagen type X expression in mono-culture and that this response was mitigated in co-culture. These

MSCs originate from bone marrow and are known to have similar functional behavior to growth plate chondrocytes which express the hypertrophic phenotype [44]. Co-culture has been shown in multiple studies to mitigate hypertrophic effects both with chondrocytes [22, 24, 26] and fewer times with fibrochondrocytes [20, 21]. Previous studies focused on evaluating collagen type X gene expression as a marker of hypertrophy whereas we measured collagen type X presence in constructs using immunohistochemistry. Hypertrophy is also characterized by an enlargement of cell area and volume. In this study we measure cell area and observed that MSCs were nearly 2x the size of FCCs, but there was no significant enlargement of cells with time in culture. Although not significant, the MSC fraction of cells in co-culture groups showed a reduction in area after 15 days, while MSCs in mono-culture showed a slight increase in area, indicated a more hypertrophic cell population in MSCs mono-culture [45]. This study supports the body of work that suggests that co-culture of MSCs with chondrocytes or FCCs is a mechanism for functional inhibition of MSC hypertrophy.

Cell-material interactions are known to influence changes in cellular behavior and phenotype. Collagen was the primary scaffold material in our gels which is known to influence cell phenotype through both chemical and mechanical pathways. Similar to previous pellet culture studies of MSC and FCC mono- and co-culture [20, 21], GAG and collagen type II were increased in all culture groups in meniscal media. The FCC mono-culture gel in this study appeared to have an increased collagen type I expression compared to gels with MSCs. The meniscus is composed primarily of collagen type I, with collagen type II being the second most prominent collagen especially in the cartilaginous inner region [46, 47]. The MSC containing groups did produce more GAG

in constructs which is consistent with a more chondrogenic behavior and less collagen type I production seen in the inner zone of the meniscus [48]. In this study the MSC mono-culture group produced the most GAG, in contrast to other studies in which MSC mono-cultures usually contain the lowest GAG concentration [20, 21, 26, 49]. This discrepancy is likely due to cell-material interactions which provides a physical diffusion barrier that is lacking in pellet culture. Previous studies using alginate showed that MSCs produced more GAG in mono-culture than FCCs, but were unable to retain GAG within the construct [50]. Another study showed that MSCs cultured on a collagen scaffold had increased expression of collagen type II, sox9, and aggrecan expression compared to alginate [51]. Further, a study investigating the effect of articular chondrocytes co-cultured with MSCs in pellet culture vs within a collagen type I scaffold demonstrated that GAG/WW content was lowest in FCC mono-culture group in collagen, whereas in pellet culture the FCC group contained the greatest amount on GAG/DNA [52]. This study is the first to examine MSC and FCC co-culture in a collagen gel and supports that the matrix used to culture MSCs is an important contributor to guiding MSC phenotype.

Previous studies attribute phenotypic changes to close cellular proximity in pellet cultures, however, our study demonstrated that direct cell-cell contact is not necessary for phenotypic changes in MSC behavior. Studies in pellet culture have noted increased matrix expression in co-cultures compared to mono-culture controls, which could be attributed to direct cell-cell contact resulting in an interaction effect [20, 21]. Furthermore, pellet culture may promote chondrogenesis because cells are forced into a circular phenotype in a compact rather than allowing them to spread on a surface [18].

Previous studies have shown that stem cell differentiation can be controlled by soluble signaling factors [53]. Specifically, conditioned media from chondrocytes directed chondrogenic differentiation of MSCs and enhanced matrix production [54, 55]. A modeling study concluded that a single cell can effectively communicate within a domain of 250 μm [56]. Another study demonstrated that soluble effects require close proximity because increased matrix and mechanical properties were only seen in co-cultured MSC and chondrocyte hydrogels as opposed to two distinct hydrogels cultured in the same well [24]. In this study, there was increased matrix expression of GAG and collagen type I in constructs. Of particular interest was that the 50:50 culture group had the highest GAG retention. Previously, we have shown that MSCs in mono-culture are deficient in link protein compared to chondrocyte cells which resulted in a loss of GAG into media in MSC constructs [50]. Our co-cultured groups likely had the advantage of FCC production of link protein to retain the increased production of GAG from MSCs. This study supports that MSC phenotypic changes do not require direct cell-cell contact suggesting that soluble signaling factors play a key role in directing phenotypic changes.

This study was the first to show mechanical evaluation of constructs using FCC and MSC co-culture. Conducting these studies in a 3D scaffold enabled the measurement of mechanical properties to quantify effects that cellular remodeling and matrix production had on mechanical properties. MSCs and FCCs cultured in collagen gels stiffened with time in all groups. 50:50 co-culture showed the greatest increase in compressive properties with 100:0 MSC mono-cultures showing a similar increase. 100:0 MSC mono-culture had the greatest GAG/DNA production; however 50:50 co-culture had the greatest GAG retention. Previously we have shown that compressive

mechanical properties are not exclusively correlated with GAG content and that collagen content is particularly important for the compressive properties of meniscal constructs [25, 28]. Furthermore, the mechanical properties of a substrate are a key factor that contribute to MSC fate [40, 57]. Increasing construct stiffness in a 3D gel likely contributed to phenotypic changes in gels toward chondrogenic morphology and matrix expression.

This study has some limitations. The stem cells used in this study were not tested and sorted for cell surface antigens and are therefore a heterogeneous population. However, MSCs used in this study were characterized and validated by two well established defining criteria; plastic adherence and trilineage differentiation. The protocol used in this study has been well established in previous literature to yield viable stem cells [26]. Bovine MSCs and FCCs were used for the purposes of these experiments. The use of bovine as a cell source could affect clinical translatability of experiments. 50:50 co-culture showed best mechanical properties and GAG retention; however obtaining 50% FCCs may not be clinically feasible.

Conclusion

This study shows that MSC phenotype can be influenced by co-culture in a 3D dimensional construct. MSCs demonstrated a transition to chondrogenic phenotype supported by changes in cell shape, matrix production, and mechanical properties. Maximal mechanical performance and GAG retention was observed in the 50:50 co-culture group. Additionally, co-culture groups showed reduced hypertrophy to MSCs in mono-culture. While the specific cause of MSC differentiation remains unknown, this study validates that MSCs in 3D scaffold co-culture transition to FCC phenotype,

demonstrating their applicability for 3D tissue engineered menisci as well as other TE applications.

REFERENCES

[1] Baker BE, Peckham AC, Pupparo F, and Sanborn JC. Review of meniscal injury and associated sports. Am. J. Sports Med. 13:1: 1–4.

[2] Shybut T and Strauss EJ. Surgical Management of Meniscal Tears. 2011; 69:1: 56–62.

[3] Lubowitz JH, Verdonk PCM, Reid JB, and Verdonk R. Meniscus allograft transplantation: A current concepts review. Knee Surgery, Sport. Traumatol. Arthrosc. 2007; 15:5: 476–492.

[4] Khetia EA and McKeon BP. Meniscal allografts: biomechanics and techniques. Sports Med. Arthrosc. 2007; 15:3: 114–20.

[5] Agung M, Ochi M, Yanada S, Adachi N, Izuta Y, Yamasaki T, and Toda K. Mobilization of bone marrow-derived mesenchymal stem cells into the injured tissues after intraarticular injection and their contribution to tissue regeneration. Knee surgery, Sport. Traumatol. Arthrosc. Off. J. ESSKA. 2006; 14:12: 1307–14.

[6] Kim J-D, Lee GW, Jung GH, Kim CK, Kim T, Park JH, Cha SS, and You Y-B. Clinical outcome of autologous bone marrow aspirates concentrate (BMAC) injection in degenerative arthritis of the knee. Eur. J. Orthop. Surg. Traumatol. 2014; 24: 1505–1511.

[7] Centeno CJ, Busse D, Kisiday J, Keohan C, Freeman M, and Karli D. Regeneration of meniscus cartilage in a knee treated with percutaneously implanted autologous mesenchymal stem cells. Med. Hypotheses. 2008; 71:6: 900–8.

[8] Duygulu F, Demirel M, Atalan G, Kaymaz FF, Kocabey Y, Dulgeroglu TC, and Candemir H. Effects of intra-articular administration of autologous bone marrow aspirate on healing of full-thickness meniscal tear: an experimental study on sheep. Acta Orthop. Traumatol. Turc. 2012; 46:1: 61–67.

[9] Mandal BB, Park S-H, Gil ES, and Kaplan DL. Multilayered silk scaffolds for meniscus tissue engineering. Biomaterials. 2011; 32:2: 639–51.

[10] Messner K. Meniscal substitution with a Teflon-periosteal composite graft: a rabbit experiment. Biomaterials. 1994; 15:3: 223–30.

[11] Wood DJ, Minns RJ, and Strover A. Replacement of the rabbit medial meniscus with a polyester-carbon fibre bioprosthesis. Biomaterials. 1990; 11:1: 13–16.

[12] Stabile KJ, Odom D, Smith TL, Northam C, Whitlock PW, Smith BP, Van Dyke ME, and Ferguson CM. An acellular, allograft-derived meniscus scaffold in an ovine model. Arthrosc. J. Arthrosc. Relat. Surg. 2010; 26:7: 936–48.

[13] de Groot JH, Zijlstra FM, Kuipers HW, Pennings AJ, Klompmaker J, Veth RPH, and Jansent HWB. Meniscal tissue regeneration in porous 50/50 copoly (L-lactideh-caprolactone) implants. 1997; 18:8: 613–622.

[14] Puetzer JL, Koo E, and Bonassar LJ. Induction of fiber alignment and mechanical anisotropy in tissue engineered menisci with mechanical anchoring. J. Biomech. 2015; 48:8: 1436–1443.

[15] Baker BM, Nathan a. S, Huffman GR, and Mauck RL. Tissue engineering with meniscus cells derived from surgical debris. Osteoarthr. Cartil. 2009; 17:3: 336–345.

[16] Gunja NJ and Athanasiou KA. Passage and reversal effects on gene expression of bovine meniscal fibrochondrocytes. Arthritis Res. Ther. 2007; 9:5: R93.

[17] Caplan AI and Dennis JE. Mesenchymal stem cells as trophic mediators. J. Cell. Biochem. 2006; 98:5: 1076–84.

[18] Mackay AM, Beck SC, Murphy JM, Barry FP, Chichester CO, and Pittenger MF. Chondrogenic differentiation of cultured human mesenchymal stem cells from marrow. Tissue Eng. 1998; 4:4: 415–28.

[19] Pittenger MF, Mackay AM, Beck SC, Jaiswal RK, Douglas R, Msca JD, Moorman MA, Simonetti DW, Craig S, and Marshak DR. Multilineage Potential of Adult Human Mesenchymal Stem Cells. Science (80-.). 1999; 284:5411: 143–147.

[20] Cui X, Hasegawa A, Lotz M, and D'Lima D. Structured three-dimensional co-culture of mesenchymal stem cells with meniscus cells promotes meniscal phenotype without hypertrophy. Biotechnol. Bioeng. 2012; 109:9: 2369–80.

[21] Saliken DJ, Mulet-Sierra A, Jomha NM, and Adesida AB. Decreased hypertrophic differentiation accompanies enhanced matrix formation in co-cultures of outer meniscus cells with bone marrow mesenchymal stromal cells. Arthritis Res. Ther. 2012; 14:3: R153.

[22] Cooke ME, Allon AA, Cheng T, Kuo AC, Kim HT, Vail TP, Marcucio RS, Schneider RA, Lotz JC, and Alliston T. Structured three-dimensional co-culture of mesenchymal stem cells with chondrocytes promotes chondrogenic differentiation without hypertrophy. Osteoarthr. Cartil. 2011; 19:10: 1210–8.

[23] Hoben GM, Willard VP, and Athanasiou KA. Fibrochondrogenesis of hESCs: growth factor combinations and cocultures. Stem Cells Dev. 2009; 18:2: 283–92.

[24] Bian L, Zhai DY, Mauck RL, and Burdick JA. Coculture of Human Mesenchymal Stem Cells and Enhances Functional Properties of Engineered Cartilage Reverse primer. Tissue Eng. Part A. 2011; 17:7 and 8: 1137–1145.

[25] Puetzer JL and Bonassar LJ. High Density Type I Collagen Gels for Tissue Engineering of Whole Menisci. Acta Biomater. 2013; 9:8: 7787–7795.

[26] Mauck RL, Yuan X, and Tuan RS. Chondrogenic differentiation and functional maturation of bovine mesenchymal stem cells in long-term agarose culture. Osteoarthr. Cartil. 2006; 14:2: 179–89.

[27] Bernacki SH, Wall ME, and Loboa EG. Isolation of human mesenchymal stem cells from bone and adipose tissue. Methods Cell Biol. 2008; 86:08: 257–78.

[28] Ballyns JJ, Wright TM, and Bonassar LJ. Effect of media mixing on ECM assembly and mechanical properties of anatomically-shaped tissue engineered meniscus. Biomaterials. 2010; 31:26: 6756–63.

[29] Bowles RD, Williams RM, Zipfel WR, and Bonassar LJ. Self-Assembly of Aligned Tissue-Engineered Annulus Fibrosis and Intervertebral Disc Composite Via Collagen Gel Contraction. Tissue Eng. Part A. 2010; 16:4: 1339–1348.

[30] Cross VL, Zheng Y, Won Choi N, Verbridge SS, Sutermaster B a., Bonassar LJ, Fischbach C, and Stroock AD. Dense type I collagen matrices that support cellular remodeling and microfabrication for studies of tumor angiogenesis and vasculogenesis in vitro. Biomaterials. 2010; 31:33: 8596–8607.

[31] Abràmoff MD, Magalhães PJ, and Ram SJ. Image processing with imageJ. Biophotonics Int. 2004; 11:7: 36–41.

[32] Kim YJ, Sah RL, Doong JY, and Grodzinsky AJ. Fluorometric assay of DNA in cartilage explants using Hoechst 33258. Anal. Biochem. 1988; 174:1: 168–176.

[33] Enobakhare BO, Bader DL, and Lee DA. Quantification of sulfated glycosaminoglycans in chondrocyte/alginate cultures, by use of 1,9-dimethylmethylene blue. Anal. Biochem. 1996; 243:1: 189–191.

[34] Neuman R and Logan M. The determination of hydroxyproline. J. Biol. Chem. 1949; 184:1: 299–306.

[35] Puetzer JL, Brown BN, Ballyns JJ, and Bonassar LJ. The Effect of IGF-I on Anatomically Shaped. Tissue Eng. Part A. 2013; 19:11 and 12: 1443–1450.

[36] Ballyns JJ, Gleghorn JP, Niebrzydowski V, Rawlinson JJ, Potter HG, Maher SA, Wright TM, and Bonassar LJ. Image-guided tissue engineering of anatomically shaped implants via MRI and micro-CT using injection molding. Tissue Eng. Part A. 2008; 14:7: 1195–202.

[37] Frank EH and Grodzinsky AJ. Cartilage electromechanics--II. A continuum model of cartilage electrokinetics and correlation with experiments. J. Biomech. 1987; 20:6: 629–639.

[38] Kim YJ, Bonassar LJ, and Grodzinsky AJ. The role of cartilage streaming potential, fluid flow and pressure in the stimulation of chondrocyte biosynthesis during dynamic compression. J. Biomech. 1995; 28:9: 1055–1066.

[39] Taylor JR. An Introduction to Error Analysis: The Study of Uncertainties in Physical Measurements, 2nd Editio. Sausalito, CA: University Science Books, 1997.

[40] Engler AJ, Sen S, Sweeney HL, and Discher DE. Matrix elasticity directs stem cell lineage specification. Cell. 2006; 126:4: 677–89.

[41] Kim J Bin, Stein R, and O'Hare MJ. Three-dimensional in vitro tissue culture models of breast cancer-- a review. Breast Cancer Res. Treat. 2004; 85:3: 281–91.

[42] Yeung T, Georges PC, Flanagan LA, Marg B, Ortiz M, Funaki M, Zahir N, Ming W, Weaver V, and Janmey PA. Effects of substrate stiffness on cell morphology, cytoskeletal structure, and adhesion. Cell Motil. Cytoskeleton. 2005; 60:1: 24–34.

[43] Zanetti NC and Solursh M. Induction of chondrogenesis in limb mesenchymal cultures by disruption of the actin cytoskeleton. J. Cell Biol. 1984; 99:1 I: 115–123.

[44] Mueller MB and Tuan RS. Functional characterization of hypertrophy in chondrogenesis of human mesenchymal stem cells. Arthritis Rheum. 2008; 58:5: 1377–1388.

[45] Buckwalter J a, Mower D, Ungar R, Schaeffer J, and Ginsberg B. Morphometric analysis of chondrocyte hypertrophy. J. Bone Joint Surg. Am. 1986; 68:2: 243–55.

[46] McDevitt, C.A. and Webber RJ. The ultrastructure and biochemistry of meniscal cartilage. Clin. Orthop. Relat. Res. 1990; 252: 8–18.

[47] Cheung HS. Distribution of type I, II, III and V in the pepsin solubilized collagens in bovine menisci. Connect. Tissue Res. 1987; 16:4: 343–356.

[48] Johnstone B, Hering TM, Caplan a I, Goldberg VM, and Yoo JU. In vitro chondrogenesis of bone marrow-derived mesenchymal progenitor cells. Exp. Cell Res. 1998; 238:1: 265–72.

[49] Meretoja V V, Dahlin RL, Kasper FK, and Mikos AG. Enhanced chondrogenesis in co-cultures with articular chondrocytes and mesenchymal stem cells. Biomaterials. 2012; 33:27: 6362–9.

[50] Babalola OM and Bonassar LJ. Effects of Seeding Density on Proteoglycan Assembly of Passaged Mesenchymal Stem Cells. Cell. Mol. Bioeng. 2010; 3:3: 197–206.

[51] Bosnakovski D, Mizuno M, Kim G, Takagi S, Okumura M, and Fujinaga T. Chondrogenic Differentiation of Bovine Bone Marrow Mesenchymal Stem Cells (MSCs) in Different Hydrogels : Influence of Collagen Type II Extracellular Matrix on MSC Chondrogenesis. Biotechnol. Bioeng. 2006; 93:6: 1152–63.

[52] Sabatino MA, Santoro R, Gueven S, Jaquiery C, Wendt DJ, Martin I, Moretti M, and Barbero A. Cartilage graft engineering by co-culturing primary human articular chondrocytes with human bone marrow stromal cells. J. Tissue Eng. Regen. Med. 2012;

[53] Mackay a M, Beck SC, Murphy JM, Barry FP, Chichester CO, and Pittenger MF. Chondrogenic differentiation of cultured human mesenchymal stem cells from marrow. Tissue Eng. 1998; 4:4: 415–28.

[54] Ahmed N, Dreier R, Göpferich A, Grifka J, and Grässel S. Soluble Signalling Factors Derived from Differentiated Cartilage Tissue Affect Chondrogenic Differentiation of Rat Adult Marrow Stromal Cells. Cell. Physiol. Biochem. 2007; 20: 665–678.

[55] Levorson EJ, Santoro M, Kasper FK, and Mikos AG. Direct and indirect co-culture of chondrocytes and mesenchymal stem cells for the generation of polymer/extracellular matrix hybrid constructs. Acta Biomater. 2014; 10:5: 1824–35.

[56] Francis K and Palsson BO. Effective intercellular communication distances are determined by the relative time constants for cyto/chemokine secretion and diffusion. Proc. Natl. Acad. Sci. U. S. A. 1997; 94:23: 12258–12262.

[57] Tse JR and Engler AJ. Stiffness gradients mimicking in vivo tissue variation regulate mesenchymal stem cell fate. PLoS One. 2011; 6:1: e15978.

CHAPTER 4

Fiber Development and Matrix Production in Tissue Engineered Menisci using Bovine Mesenchymal Stem Cells and Fibrochondrocytes[3]

Abstract

Mesenchymal stem cells (MSCs) have been investigated with promising results for meniscus healing and tissue engineering. While MSCs are known to contribute to ECM production, less is known about how MSCs produce and align large organized fibers for application to tissue engineering the meniscus. The goal of this study was to investigate the capability of MSCs to produce and organize extracellular matrix molecules compared to meniscal fibrochondrocytes (FCCs). Bovine FCCs and MSCs were encapsulated in an anatomically accurate collagen meniscus using mono-culture and co-culture of each cell type. Each meniscus was mechanically anchored at the horns to mimic the physiological fixation by the meniscal entheses. Mechanical fixation generates a static mechanical boundary condition previously shown to induce formation of oriented fiber by FCCs. Samples were cultured for 4 weeks and then evaluated for biochemical composition and fiber development. MSCs increased the GAG and collagen production in both co-culture and mono-culture groups compared to FCC mono-culture. Collagen organization was greatest in the FCC mono-culture group. While MSCs had increased matrix production they lacked the fiber organization capabilities of FCCs. This study suggests that GAG production and fiber formation are linked. Co-culture can be used as a means of balancing the synthetic properties of MSCs and the matrix remodeling capabilities of FCCs for tissue engineering applications.

[3] M. C. McCorry and L. J. Bonassar. Fiber development and matrix production in tissue-engineered menisci using bovine mesenchymal stem cells and fibrochondrocytes. *Connect. Tissue Res.* **58,** 329–341 (2017).

Introduction

The meniscus is a fibrocartilaginous tissue comprised of a complex network of fibers with distributed glycosaminoglycans (GAGs) that collectively contribute to its ability to support loads in the knee (1). The meniscus is connected to the underlying bone through a meniscal enthesis located at each of the meniscal horns (2,3). The meniscal entheses provide an anchor point for the meniscus to support tensile loads and prevent meniscal extrusion during the gait cycle (4). A majority of the fibers in the meniscus are arranged in the circumferential direction (5,6). A smaller portion of radial tie fibers help to anchor the circumferential fibers and contribute to the anisotropic properties of the meniscus (5,7,8). GAGs make up a smaller fraction of the meniscus and contribute its compressive properties (1,9,10).

Damage to the meniscus disrupts this organization, increasing contact pressure in the joint resulting in pain, swelling, and loss of motion (11,12). Since the meniscus is primarily avascular, surgical intervention is the primary treatment option. There are over 1 million meniscus related surgeries in the United States per year (13). In severe cases of injury or degeneration, a meniscal allograft is used to replace the damaged meniscus. While meniscal allografts relieve patient pain and restore mechanical stability to the knee, allograft transplant is limited by material availability, cost, immune competency, and ability to correctly match anatomic size and shape (14,15). Size matching must be within a tolerance of 5%, the donor must have less than mild pre-existing arthrosis, and be immunocompatible with recipient (14,15). Synthetic scaffold such as Menaflex and Actifit are used for partial meniscal replacement, however results are inconclusive as to their efficacy with specific challenges in tissue fixation, integration, material properties,

and surface characteristics (16–18). An anatomically accurate tissue engineered (TE) meniscus could address many of these limitations by using imaging techniques to recapitulate size and shape, as well as natural materials, and autologous cells with the ability to modify and integrate with native tissue (19,20).

Previous efforts to TE the whole meniscus utilize synthetic polymers, hydrogels, and tissue-derived scaffolds (21–25). However, none of these are currently in clinical practice because they lack the anatomical, mechanical or biochemical properties necessary for native function (19). Previously, we developed an anatomically accurate tissue engineered meniscus using fibrochondrocytes (FCCs) in a high density collagen gel (26). FCCs, embedded in the meniscal construct, developed large fibers under static mechanical boundary conditions with mechanical properties approaching native values (27).

These studies show great promise, however, FCCs used for tissue engineered menisci have limited clinical availability and are difficult to expand in 2D culture (28). Obtaining the sufficient number of cells for a tissue engineered meniscus is challenging because FCCs proliferate slowly and often lose their phenotype in two-dimensional (2D) culture (28). Mesenchymal stem cells (MSCs) have been shown to contribute to meniscal regeneration *in vivo*, however, there is limited knowledge on MSC performance in the context of whole tissue engineered menisci (29–31). *In vivo* studies in both animals and humans have shown that MSCs delivered through intraarticular injection localize to the site of injury and contribute to tissue regeneration (30–33). However directing fibrochondrogenic differentiation of stem cells has proven to be challenging (34–36). Co-culture of FCCs and MSCs has been particularly successful

with increased expression of fibrochondrogenic genes, reduced hypertrophy, and increased matrix production (35,36). We have shown that MSCs transition to a fibrochondrogenic phenotype in 3D collagen gel, with maximal mechanical performance and GAG retention observed in the 50:50 co-culture group (37). Furthermore, MSCs have been shown to increase the lubrication properties of a engineered menisci (38). These studies suggest the potential advantages and feasibility of MSCs as an alternative or supplemental cell source for meniscus tissue engineering.

A successful tissue engineered meniscus must have organized fibers, which are essential to the mechanical stability of the meniscus in the knee (7). MSC differentiation is known to be guided by mechanical cues, specifically in meniscal development the meniscus begins as a dense mesenchymal condensate. In meniscus tissue engineering, MSCs have been shown to produce collagen and GAG that perform similar mechanical functions to native when seeded in an aligned matrix (39). The meniscus develops from a dense disorganized mesenchymal condensate (40). However, there is little data on MSCs produce a functionally organized fibers from a disorganized matrix. Anchoring at the attachments provides critical mechanical signals for collagen organization and matrix secretion (27,40,41). However there is little data on how mechanical anchoring affects MSCs in the context of producing a functionally organized meniscus.

The goal of this study was to characterize matrix synthesis and fiber formation in MSC and FCC co-culture in collagen gels. Specifically, we evaluated GAG accumulation and fiber formation in mono- and co-cultured menisci anchored at the horns. MSCs and FCCs differ in their ability to synthesize GAGs, however little is known about MSCs ability to form large organized fibers. We hypothesize that MSCs

will have similar fiber organization and matrix producing capabilities as FCCs for the production of a tissue engineered meniscus.

Methods

Cell Isolation

As previously described, MSCs were isolated from 1-3 day old bovids (26,42). Briefly, the bone marrow from the trabeculae of the distal femoral head was washed with a heparin supplemented media to obtain the MSCs (37,42). Heparin solution containing bone marrow was centrifuged at 300 x *g*. The adherent cell population after 48 hours was expanded and tested to confirm multipotency using trilineage differentiation assays for osteogenesis, adipogenesis, and chondrogenesis (Supp. 1) (43,44). MSCs were plated at 2,000 cells/cm^2 and expanded in 2D culture until passage 4 with a growth medium containing low glucose Dulbecco's modified Eagle's medium (DMEM) supplemented with 10% fetal bovine serum (FBS), 100 μg/mL penicillin, 100 μg/mL streptomycin, 0.25 μg/mL amphotericin B, 2mM L-glutamine, and 1 ng/mL basic fibroblast growth factor.

FCCs were isolated from juvenile bovine menisci digested using collagenase as previously described (26,45). FCCs were digested from menisci in 0.3% collagenase (Worthington Biochemical Corporation, Lakewood, NJ) in DMEM with 100 μg/mL penicillin and 100 μg/mL streptomycin, followed by filtering through a 100 μm cell strainer (26,45). FCCs were directly encapsulated in collagen gels with passaged MSCs as described in construct generation. Prior to injecting cells into meniscal molds, MSCs were labeled using CellTrace Green CFSE (Invitrogen, Grand Island, NY, C34554) and FCCs were labeled with CellTrace FarRed DDAO-SE (Invitrogen, C34553). Cell types

were mixed with media to generate FCC mono-culture, 50/50 co-culture, and MSC mono-culture groups.

Construct Generation

Collagen type I was extracted from Sprague-Dawley rat tails (Pel-Freez Biologicals, Rogers, AZ) and reconstituted in 0.1% acetic acid at 30 mg/mL concentration as previously described (26,46,47). To initiate gelation, a syringe stop cock was used to mix the stock collagen solution with a working solution comprised of 1N NaOH, 10x phosphate-buffered saline (PBS), and 1x PBS to return the collagen to a neutral 7.0 pH and 300mOsm (47). Previously prepared cell groups suspended in media were mixed to a final concentration of $25x10^6$ cells/mL in a collagen gel at 20 mg/mL (26). The collagen solution was injected into an anatomically accurate meniscal mold and incubated for 1 hour at 37˚C (27). Anatomically accurate molds were 3D printed from negative molds rendered using magnetic resonance imaging and microcomputed tomography images of ovine menisci (27,48). As described previously, injection molding into anatomically accurate meniscal molds yields a construct with high geometric fidelity to native tissue, within ±10% error of key geometric features (49,50). Anatomical molds included extension tabs at the horns for clamping (27,48).

Eight menisci per group, with four tested at day 1 and the remaining four tested after 4 weeks. Each meniscus was clamped at the extensions to a 3D printed culture dish as previously described (27). Clamping at the extensions mimics the static mechanical boundary conditions of the native meniscus. Samples were cultured in media containing DMEM, 10% FBS, 100 μg/mL penicillin, 100 μg/mL streptomycin, 0.1 mM non-essential amino acids, 50 μg/mL ascorbate, and 0.4 mM L-proline at 37°C and 5% CO_2

(26). Culture media was collected and replenished three times a week. Images were taken at each media change and imported into ImageJ to calculate the area of each construct. At the conclusion of culture, each meniscus was sectioned to obtain samples for biochemical, histological, and SEM analysis (Figure 4.1).

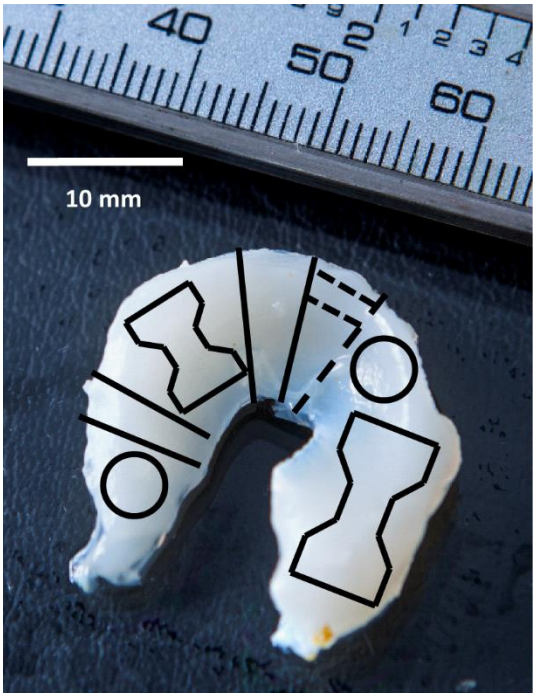

Figure 4.1: Sample delegation from constructs at the conclusion of culture. Dogbone shapes were allocated for tensile testing. Circular shapes indicate 4 mm punch biopsies used for compression testing. Solid lines depict cut lines for confocal slices that were also used for histology. Dotted line indicates freeze fracture lines performed on dried SEM samples prior to mounting on SEM stubs. Remaining material was divided into four parts and analyzed for biochemical analysis. Scale bar = 10mm.

Biochemical Content

Biochemical samples were collected from four different regions on each meniscus. Each sample was weighed to obtain a wet weight (WW) then frozen, lyophilized, and weighed again to obtain dry weight (DW). As previously described, biochemical content of constructs was measured using a Hoechst DNA assay for DNA

content (51), a modified 1,9-dimethylmethylene blue (DMMB) assay at pH 1.5 for GAG content (52) and a hydroxyproline (hypro) assay for collagen content (53). The same assays were performed on both constructs and media samples. The sum of biochemical content in media added to biochemical content in the construct was the total content. Retention was calculated as a percentage of content in each construct relative to total content.

Confocal Microscopy

At the conclusion of each culture period, menisci were sectioned with two slices taken from each meniscus, one each for radial and circumferential imaging (Figure 4.1). Samples were placed in 10% buffered formalin for 48 hours followed by storage in 70% ethanol. Confocal reflectance, autofluorescence, and fluorescence imaging was performed on a Zeiss 710 confocal microscope with a Zeiss Axio Observer Z1 inverted stand using a 40x/1.2 C-Apochromat water immersion objective. Collagen fiber reflectance was captured between 475-510 nm, while cell autofluorescence was captured between 500-580 nm (26).

Images were analyzed for fiber diameter and alignment index (AI) by a custom MATLAB code as previously described (27,48,54). A circumferential cross-section was obtained from each meniscus in which 5-7 images from different regions of the cross-section were taken for analysis. Images were analyzed using a series of fast Fourier transforms (FFT) to determine alignment index followed by a radon transform to determine mean fiber diameter. A 2D FFT determines the maximum angle of alignment. An average cycle count along the x-axis perpendicular to the maximum angle of alignment was converted to pixels and then microns to determine the average diameter.

The AI is a ratio of the number of fibers ±20° from the maximum angle of alignment divided by the predicted number of fibers in a 40° span (54). A sample with no alignment would have an AI of 1 and a sample with perfect alignment would have an AI of 4.5. Native menisci have an average AI of 1.8 in the circumferential direction.

Scanning Electron Microscopy

A 2-4 mm thick slice was obtained from each sample and prepared for scanning electron microscopy (SEM) (55). Samples were fixed overnight in 2.5% glutaraldehyde and then washed with a 0.05 M cacodylate buffer. Samples were then incubated with 2% osmium tetroxide for 1 hour as a secondary fixative. Following fixation, samples were dehydrated in a graded ethanol series over several days. Samples were dried using a critical point dryer and freeze fractured at the imaging face. Samples were coated with gold palladium prior to SEM imaging. Samples were imaged using a Tescan Mira3 FESEM.

Histology

Following confocal imaging, samples were dehydrated in a graded ethanol series, embedded into paraffin blocks, sectioned, and stained. For each sample, one section was embedded to examine the radial direction, with the second section embedded to examine the circumferential direction. Collagen was characterized using a picrosirious red staining, first imaged using brightfield microscopy and then visualized under polarized light to view collagen fiber organization (26). Immunohistochemistry (IHC) was conducted as previously described to further investigate collagen content using antibodies for collagen type I (Abcam, Cambridge, MA, 34710), collagen type II (Chondrex, Redmond, WA, 7005), and collagen type X (Abcam, 58632) (37). Specific

proteoglycans including biglycan (courtesy of Dr. Larry Fischer, NIDCR, LF-96), decorin (courtesy of Dr. Larry Fischer, NIDCR, LF-94), and fibromodulin (Abcam, 81443). Primary and secondary antibody controls were run in parallel with samples for immunohistochemistry stains (Supplemental 4.1 and 4.6). All slide were counterstained with hematoxylin. Images were obtained with a SPOT RT camera (Diagnostic Instruments, Sterling Heights, MI) attached to a Nikon Eclipse TE2000-S microscope (Nikon Instruments, Melville, NY).

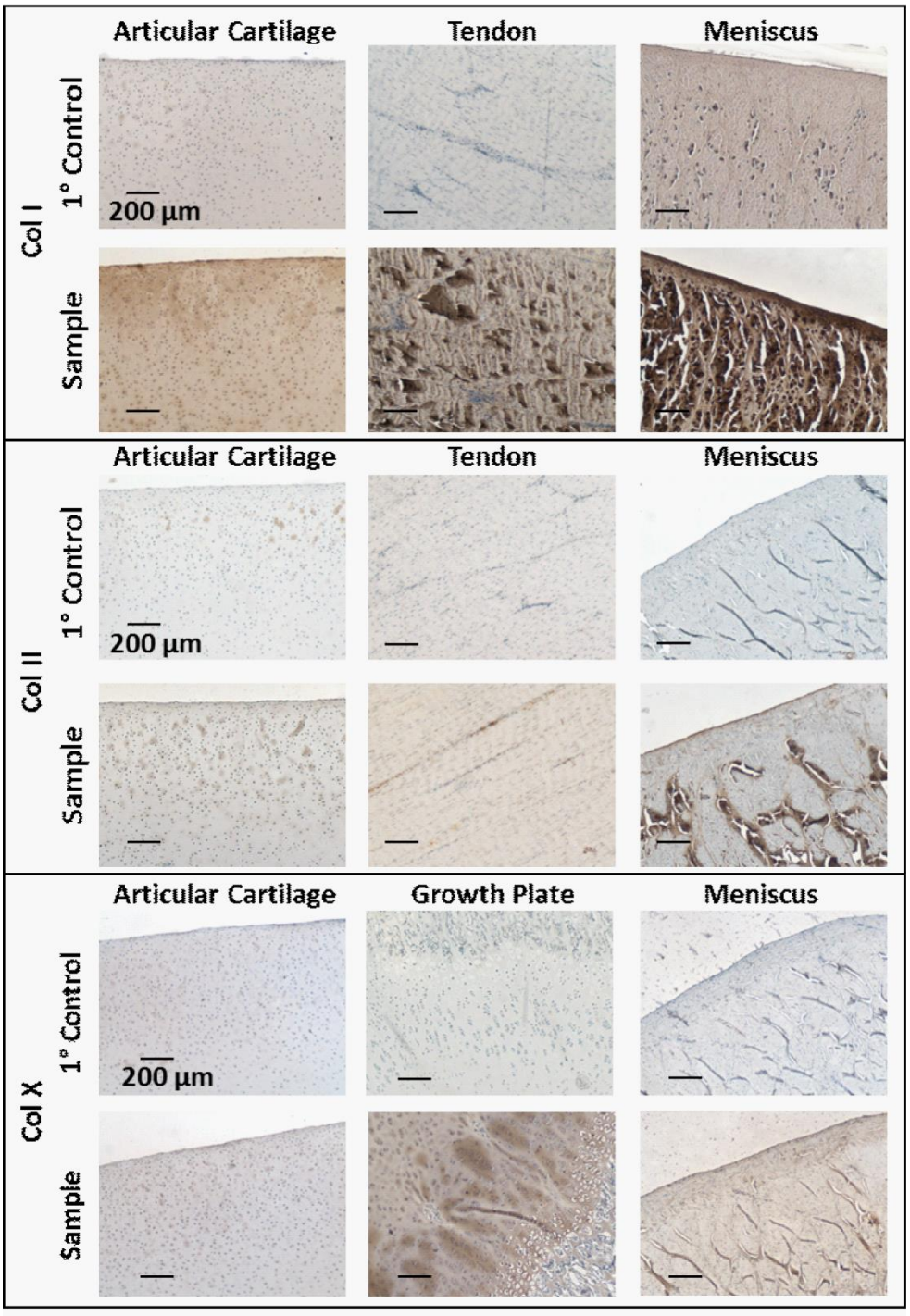

Supplemental 4.1: Immunohistochemical staining controls for collagen type I, II, and X using bovine articular cartilage, tendon, meniscus, and growth plate. The absence of primary was run as a primary control (scale bar=200 µm).

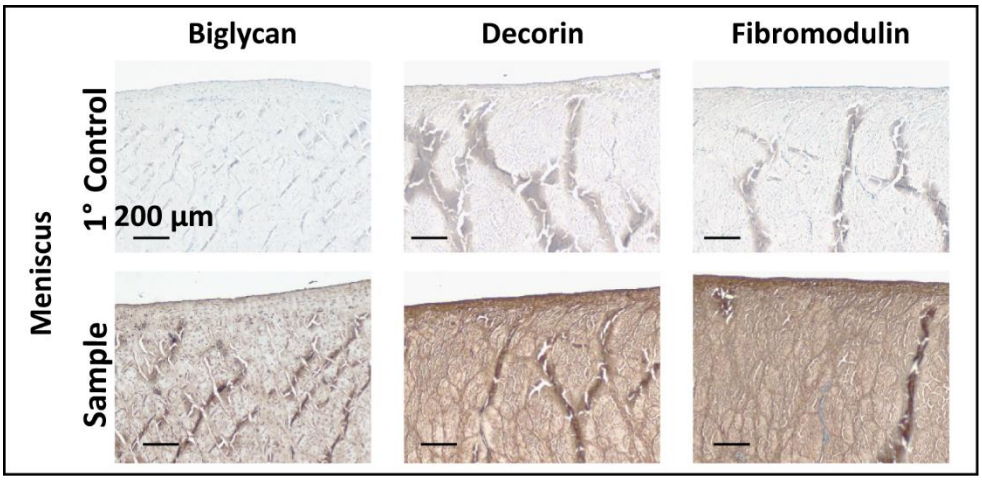

Supplemental 4.6: Immunohistochemical staining controls for biglycan, decorin, fibromodulin on native medial meniscus. All samples counterstained with hematoxylin. The absence of primary was run as a primary control (scale bar=200 µm).

Enzyme-Linked Immunosorbent Assay (ELISA)

Small tissue specimens were obtained from each samples and assayed for collagen type I and II using ELISA. Tissue was lyophilized, pulverized, and weighed for dry weight. ~2 mg of tissue was extracted using a series of 4ºC incubations with guanidine, acetic acid, pepsin and elastase. Prior to assaying, the level of solubilization was evaluated via a 6% SDS-gel stained using Coomassie Blue with collagen II as a standard. A three day solubilization period with pepsin was used to digest tissue. Levels of collagen was detected using a bovine type I and multispecies type II collagen detection kits (Chondrex, Redmond, WA).

Mechanical Properties

Two 4 mm diameter plugs from each sample were tested for compressive properties (49,56,57). Each sample was tested in confined compression via a stress relaxation test performed by imposing 10x100 µm steps (relaxation=12 min., strain=5-45%, steps=5%, n=4). The measured loads were fit to a poroelastic model using a

custom MATLAB program to determine aggregate modulus (HA). A dog bone punch in the radial and circumferential direction was obtained from each samples and tensile tested (Figure 4.1). A 0.75%/sec strain rate was applied to mimic quasistatic loading and the elastic modulus was measured as the slope of the linear region of the stress vs strain curve. Mechanical testing was performed on an Enduratec ElectroForce 3200 System (Bose, Eden Prairie, MN) using a 250 g or 1 kg load cell.

Statistics

Contraction data was analyzed using a 2-way-ANOVA with Tukey's t-test for post hoc analysis. Biochemical and ELISA data were analyzed by 1-way-ANOVA using Tukey's t-test for post hoc analysis. A mixed model with random effect of sample number was used for fiber diameter and fiber alignment data. Fiber diameter had an inter class correlation coefficient (ICC) of 13% and fiber alignment had an ICC of 4%. Biochemical content was compared to fiber formation measures using a least square fit and significance was determined using a Pearson correlation. All data are written as mean ±SD and significance was determined with $p<0.05$. Data analysis was conducted using JMP software (SAS Institute Inc, Cary, NC).

Results

Cell type does not influence contraction

Throughout culture, constructs maintained anatomical size and shape. Constructs had minimal contraction, contracting uniformly to maintain shape with a loss of ~25% projected area (Figure 4.2). All three culture groups contracted gradually over time with no significant differences in contraction between groups at each time point

(p>0.05) (Figure 4.2A). Constructs maintained anatomical definition throughout the 4 weeks of culture (Figure 4. 2B).

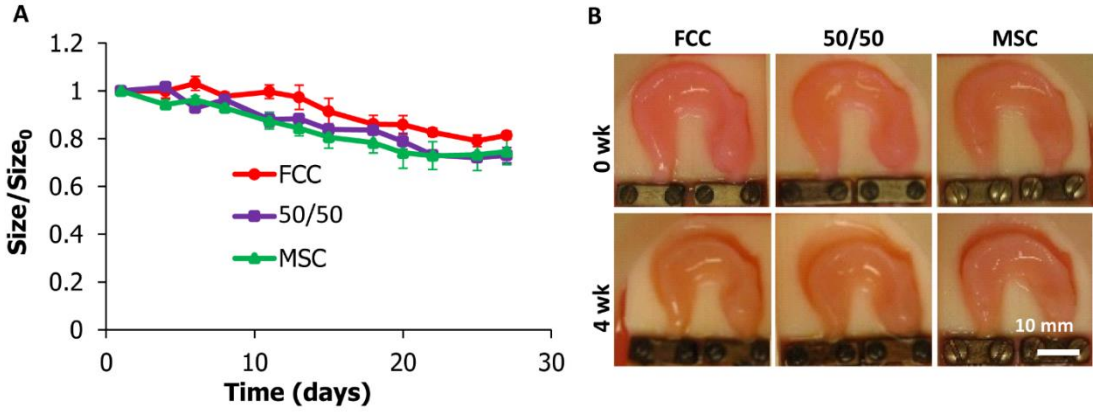

Figure 4.2: Tissue engineered meniscal contraction. (A) Ratio of projected area over initial projected area calculations at day 1. (B) Representative images of menisci at 0-, 4- weeks. No statistical difference was observed between culture groups (mean ±SD, n=4, p<0.05). scale bar = 10mm.

MSC, 50/50, and FCC culture groups organized oriented fibers

At the beginning of culture, menisci had small disorganized fibers (~8.5 µm in diameter and 1.35 AI) with a homogenous cell distribution (Figure 4.4). After 4 weeks in culture, fibers become more organized with regions of directionally oriented fibers. Fiber alignment was directionally dependent, circumferential and radial faces were imaged from different locations from each sample (Figure 4.3). In the circumferential direction collagen fibers were oriented in the circumferential direction running from horn to horn where each sample was clamped at an extension. FCC mono-culture menisci had visible striations analogous to fiber fascicles seen in native meniscal fibers (Figure 4.3). A thin, aligned outer edge with radial fibers extending into the bulk of the tissue was apparent in radially sliced samples. MSC mono-culture group showed early

signs of fiber development and alignment, however, fibers appeared smaller than those in FCC mono-culture and 50/50 co-culture groups.

FCC mono-culture have the greatest fiber diameter

Image analysis of circumferential images quantified the fiber diameter and alignment index in samples groups. Consistent with qualitative image observations, FCC mono-cultured menisci produced significantly larger diameter fibers and more aligned fibers than 50/50 and MSC cultured menisci ($p<0.05$). FCC mono-culture had the highest fiber diameter at ~17 μm and MSC mono-culture had the lowest fiber diameter at ~9 μm (Figure 4.4). The 50/50 co-culture had a diameter in between FCC and MSC mono-culture at ~12 μm. After 4 weeks in culture FCC fiber diameter approached native values averaging at ~35 μm. A similar trend was observed in the alignment index, where FCCs had increased fiber diameter and alignment approaching native values at ~1.75 (27,48).

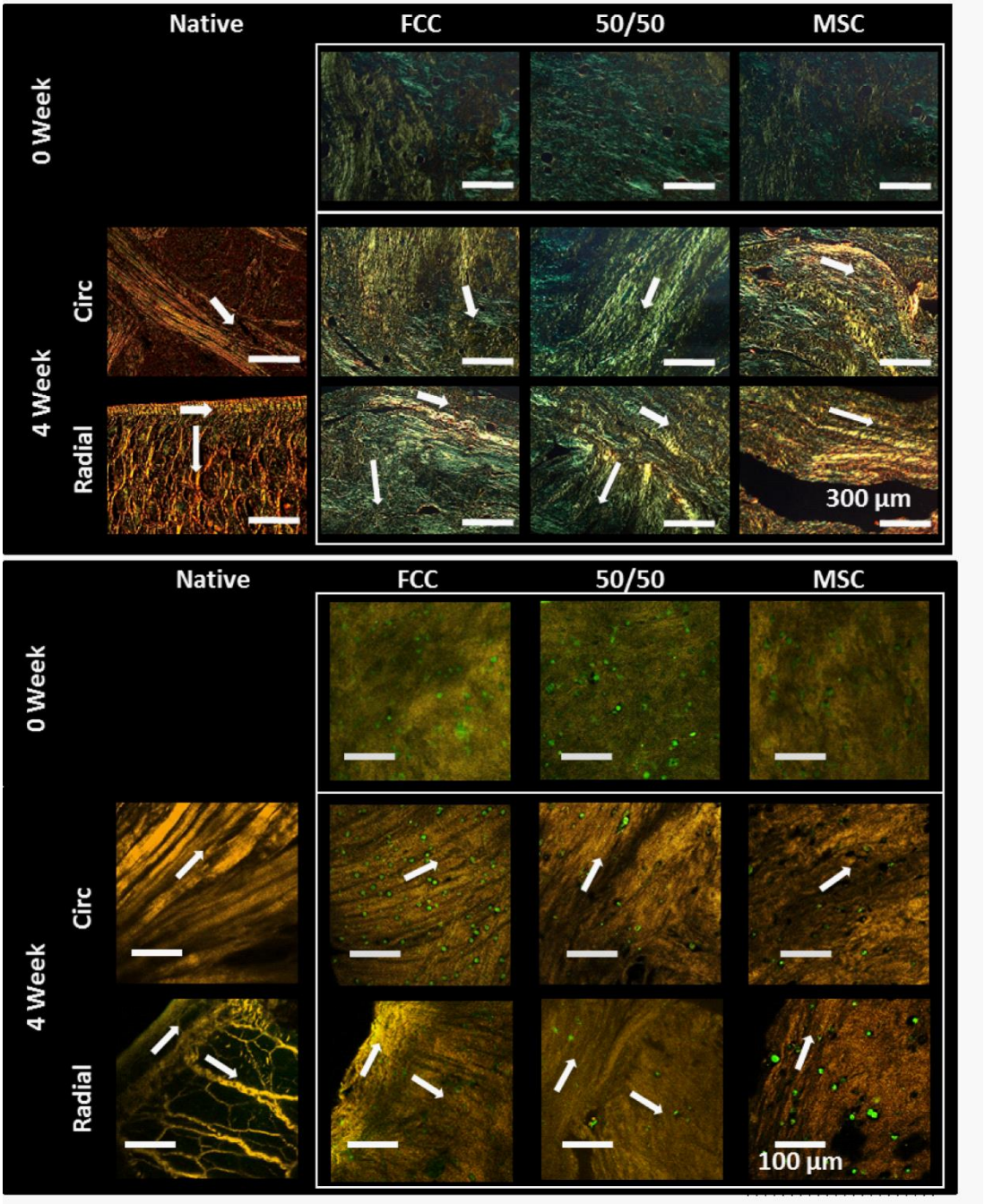

Figure 4.3: MSCs and FCCs form fibers in both the circumferential and radial direction (↑ indicates fiber direction). 0 week menisci have mostly small disorganized fibers. After 4 weeks all culture groups have organized fibers with directionality. Circumferential fibers have formed running from horn to horn of menisci. Aligned fibers around the outer edge and extending into the center of the meniscus are visible in the radial direction. (top) Polarized light, scale bar = 300 µm (bottom) SHG with FCCs labeled red and MSCs labeled green, scale bar = 100 µm.

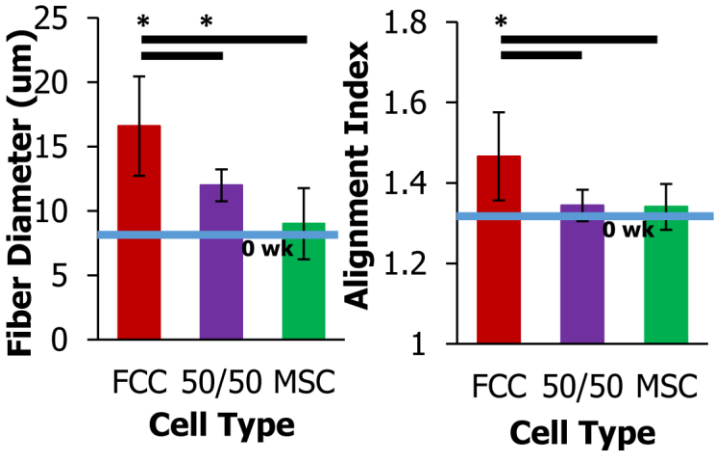

Figure 4.4: Fiber diameter and alignment index of circumferential sections at four weeks measured using SHG images analyzed using custom MATLAB code (----- significantly different between groups, * significantly different with time, $p<0.05$, n=6-8, 7 images per samples).

MSCs transition to chondrogenic morphology while FCCs integrate into collagen fibers

FCCs and MSCs labeled with cell tracker dyes were imaged at the beginning of culture and after 4 weeks of culture. FCCs and MSCs were evenly distributed throughout the depth of the meniscus construct. The FCCs and MSCs in the 50/50 co-culture group were homogenously mixed and distributed throughout the gel at the beginning of culture (Figure 4.5 row 1). At 0 weeks FCCs appeared small and rounded, while MSCs were slightly larger in size and appeared elongated on the collagen gel (Figure 4.5 row 2). After 4 weeks of culture in a fibrochondrogenic media, cells remained evenly distributed throughout the collagen. While the FCCs remained in a circular phenotype, MSCs transitioned from an elongated morphology consistent with a fibroblastic phenotype to a circular morphology consistent with a chondrogenic morphology (Figure 4.5 row 3). Collagen gels have small disorganized fibers at 0 weeks

that develop into larger more organized fibers after 4 weeks. The FCC mono-culture group formed well defined fibers where FCCs integrated into the collagen fibers. The MSC mono-culture group had less developed fibers and MSCs settled into pores between collagen fibers (Figure 4.5 row 4).

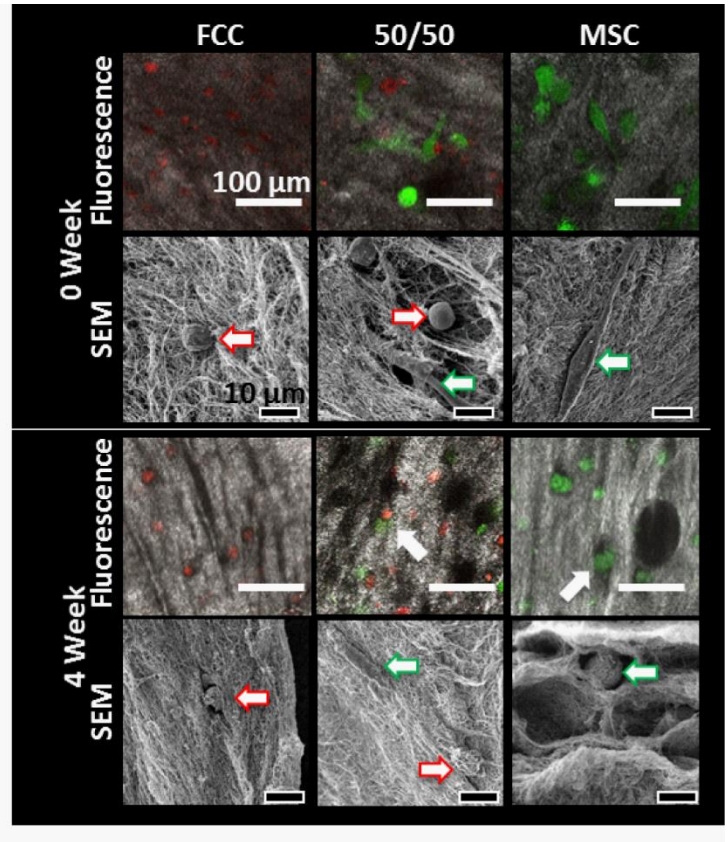

Figure 4.5: Fluorescence and scanning electron microscopy (SEM) of cells in collagen gels. Fluorescence images show FCCs in red and MSCs in green with collagen visualized using second harmonic generation (SHG), scale bar = 100 µm. High magnification cell images are taken using SEM, scale bar = 10 µm. MSCs (→) shifted to a circular phenotype. FCCs (→) integrated into collagen fibers while MSCs (→) settled into collagen pores.

MSCs increased matrix production compared to FCCs

The presence of MSCs in tissue engineered meniscal constructs increased GAG and collagen accumulation. After 4 weeks in culture, the MSC mono-culture menisci had

~350% more GAG/meniscus and the 50/50 co-culture had ~250% more GAG/meniscus than the FCC mono-culture group (Figure 4.6A). Similar trends were noted when GAG content was normalized to DNA (Figure 4.6B). GAG content measured in the media was added to GAG content in the menisci to calculate retention of GAG in the constructs relative to total GAG produced. 50/50 co-culture retained a significantly higher amount of GAG in each meniscus sample (Figure 4.6C). 50/50 co-culture and MSC mono-culture showed an increase in production of hydroxyproline compared to FCC mono-culture, however this increase was not significant (Figure 4.6D, $p>0.05$). Tissue engineered menisci when seeded with MSCs have ~30 % of the GAG (µg)/ww(mg) and 40% hypro(µg)/ww(mg) content of human native menisci, while tissue engineered constructs seeded with FCCs have ~12% and 31% respectively (wet weights presented in Supplemental Figure 4.2)(58). Seeding constructs with MSCs improved the biochemical content to better resemble native values.

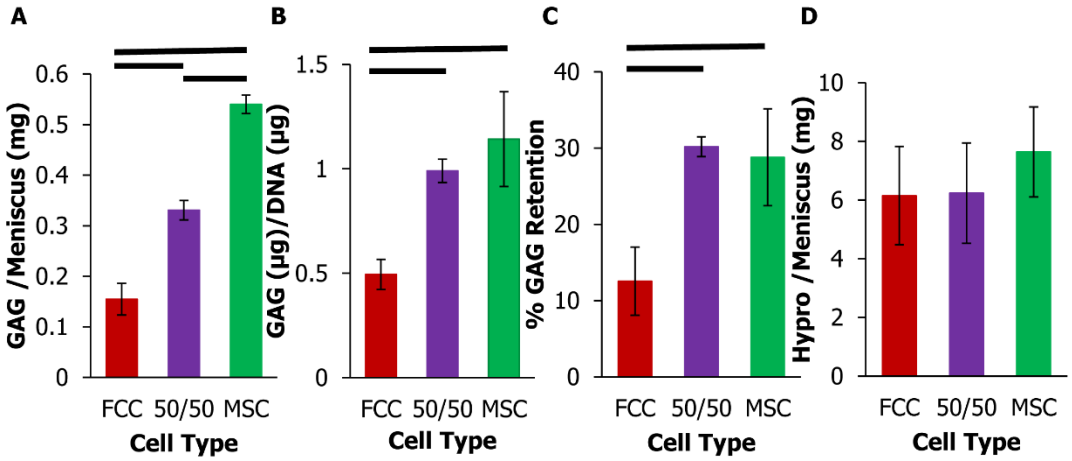

Figure 4.6: Biochemical analysis of meniscal constructs at four weeks. (A) Total GAG content per meniscus. (B) GAG normalized to DNA content. (C) % GAG retained in meniscal construct relative to GAG released in media. (D) Hydroxyproline content per meniscus. ----- significantly different between groups ($p<0.05$, $n=4$).

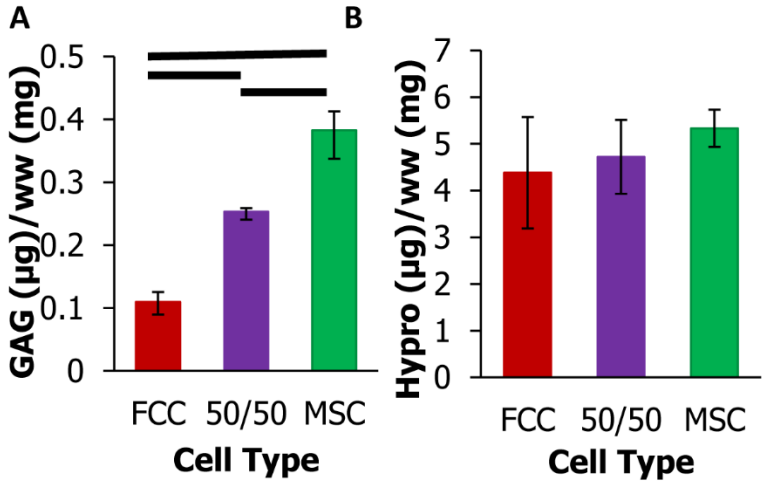

Supplemental 4.2: Biochemical analysis of meniscal constructs at four weeks. (A) Total GAG content normalized to wet weight. (B) Hydroxyproline content normalized to wet weight. ----- significantly different ($p<0.05$, $n=4$)

Collagen and proteoglycans were probed in meniscus scaffolds using immunohistochemistry and ELISA (Figure 4.7 and Supplemental 4.5). MSC mono-cultured constructs had increased levels of staining for biglycan and decorin with heavy staining at the surface of the construct. FCC mono-cultured constructs had increased staining of fibromodulin throughout the depth of the construct (Supplemental 4.5). Meniscus scaffolds were initially cast using collagen type I. Positive staining for collagen type I was consistent between 0 and 4 weeks. After 4 weeks in culture FCC mono-culture stained darker for collagen type II compared to the other culture groups (Figure 4.7). ELISA analysis supports that FCC and 50/50 groups produce more collagen type II than MSC seeded menisci. Conversely, MSC seeded menisci produced significantly more collagen type I than FCC and 50/50 groups (Supplemental 4.3). Minimal staining for collagen type X was seen in culture groups (Figure 4.7).

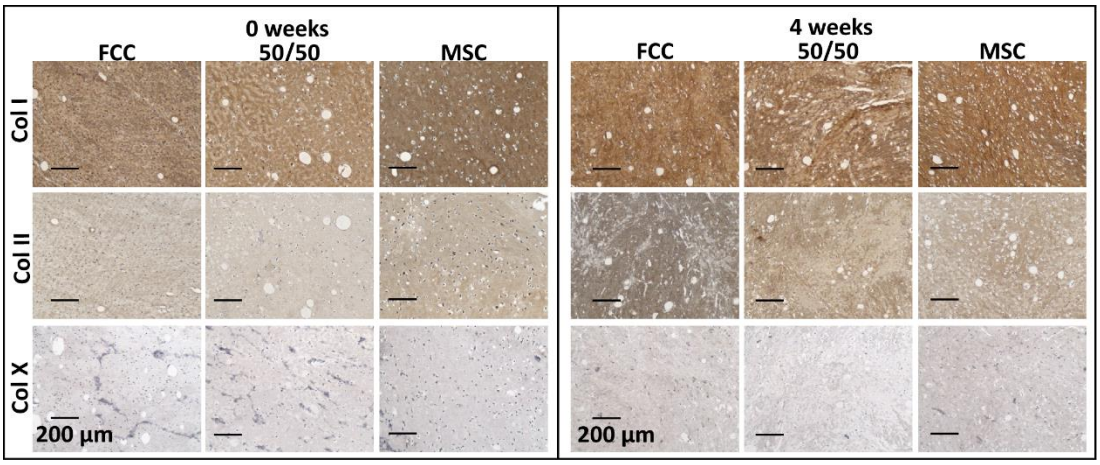

Figure 4.7: Immunohistochemical staining for collagen type I, II, and X after 0 and 4 weeks in culture (scale bar=200 µm).

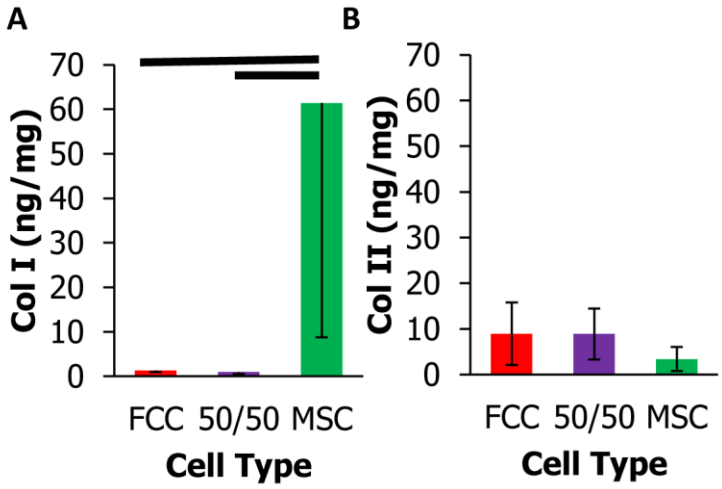

Supplemental 4.3: ELISA analysis of collagen (A) type I and (B) type II. ----- significantly different ($p<0.05$, $n=4$)

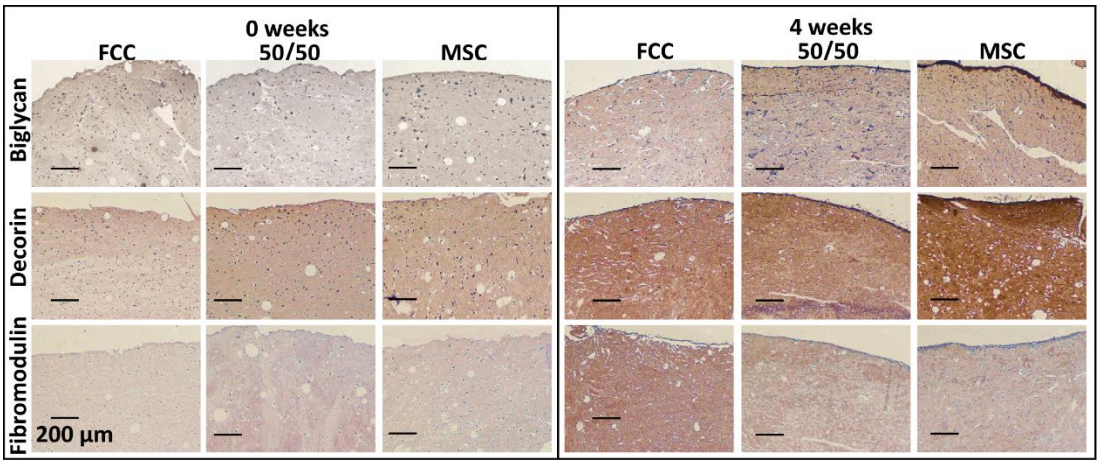

Supplemental 4.5: Immunohistochemical staining for decorin, biglycan, and fibromodulin after 0 and 4 weeks in culture (scale bar=200 µm). All samples counterstained with hematoxylin (scale bar=200 µm).

Fiber diameter was inversely correlated with GAG content

While MSCs have an increased ability to generate GAG and hydroxyproline, constructs seeded with MSCs have smaller collagen fibers. Fiber diameter and alignment index were compared with GAG and hydroxyproline content per construct using a linear regression and Pearson correlation (Figure 4.8). Hydroxyproline content was not correlated with fiber diameter and alignment index. Alignment index had a statistical tend of decreasing as GAG content increased (R^2=0.38, $p<0.056$). Fiber diameter and GAG content per meniscus were negatively correlated with fiber diameter decreasing with increasing GAG content (R^2=0.85, $p<0.05$).

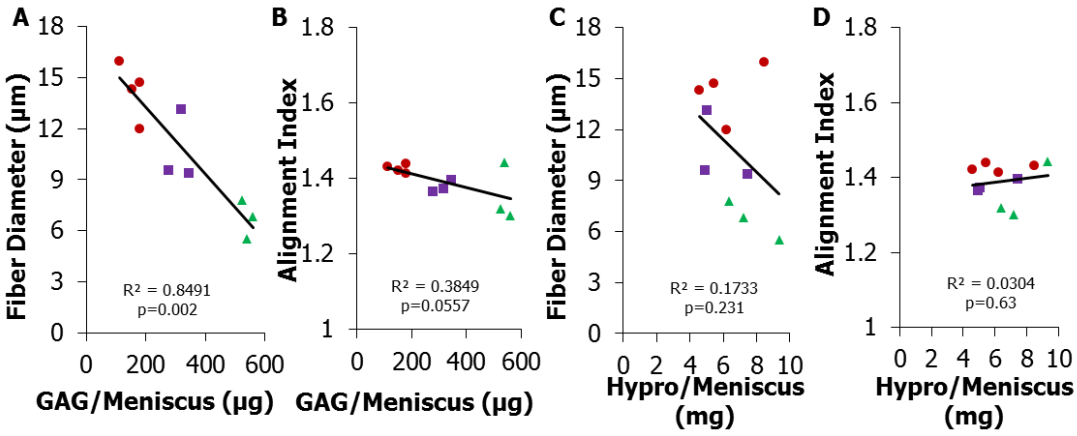

Figure 4.8: Fiber formation and biochemical content relationship in tissue engineered menisci (A-B) Total GAG content per meniscus compared to fiber diameter and alignment index. (C-D) Total Hypro content per meniscus compared to fiber diameter and alignment index. Fiber diameter is strongly correlated to GAG/Meniscus ($p<0.05$, $R^2>0.80$). ● FCC, □ 50/50, Δ MSC.

Mechanical properties improve with time in culture

Meniscal constructs increased in both tensile and compressive modulus after 4 weeks in culture (Supplemental 4.4). Samples from the circumferential and radial direction were not statistically different and were therefore pooled. Tensile properties were highest in the MSC group (60 kPa) and compressive properties were highest in the FCC group (59 kPa). Tissue engineered menisci are at about 15% of native bovine aggregate modulus, however tensile value are still far below native values (59,60). While construct properties increased with time, there was no significant difference between culture groups after 4 weeks.

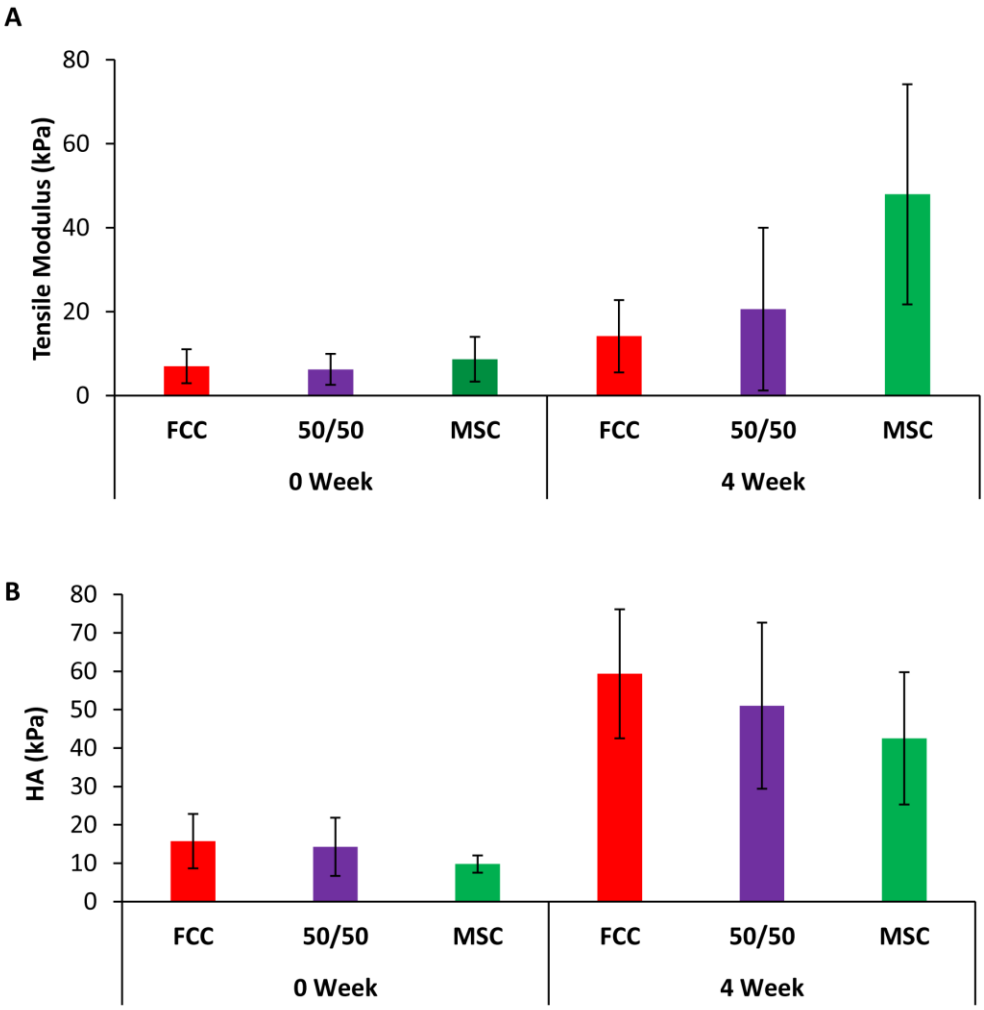

Supplemental 4.4: (A) Tensile testing (.75% strain/sec) testing to evaluate elastic. (B) Aggregate modulus calculated from confined compression testing.

Discussion

The objective of this study was to evaluate GAG production and fiber formation of MSCs in mono- and co-culture with FCCs. This study showed that MSCs incorporated in a 3D tissue engineered meniscus had increased matrix production, but decreased fiber reorganization compared to FCCs. This study demonstrated that while MSCs in this system are highly metabolically active, producing collagen and GAG, the types of collagen and the organization of the collagen network are different between MSCs and FCCs.

Maintenance of size and shape is a critical factor in engineering anatomical meniscus implants. We have previously shown that anchoring a FCC seeded implant at the horns reduced collagen contraction (27). MSCs are known to be a highly proliferative and contractile cell type (44,61–65). The proliferative properties of stem cells are desirable for obtaining sufficient cell numbers for construct generation, however precise control over contraction is important for matching the size and shape of tissue engineered menisci for clinical application. MSCs are known to rapidly contract low density collagen matrixes along a mechanically fixed axis (61,63,64). High concentration collagen with a mechanical boundary condition is known to reduce collagen contraction (26,27,47,66). Given MSCs highly contractile nature, monitoring of anatomical size and shape throughout culture is important for determining if MSCs are an appropriate cell type for use in meniscus tissue engineering. In this study, MSCs were embedded in tissue engineered menisci both in co-culture with FCC and in mono-culture. Changing the cell type had no significant influence on meniscal contraction.

This study showed that the use of MSCs in tissue engineered meniscus has minimal impact on the overall size and shape of the meniscus.

In addition to maintaining anatomical shape, a key challenge in meniscus tissue engineering is generating appropriate microstructure and fiber organization. Mechanical constraints are a well-established method used to direct cellular remodeling and guide the alignment of fibers in collagen gels. This has been shown across many systems and cell types including collagen seeded with MSCs (61,64,65), fibroblasts (41,67–69), and annulus fibrosis chondrocytes (46). The mechanical fixation used in this study mimics native fixation at the meniscal enthesis (70). Application of a mechanical constraint at the meniscal horns has been shown to create native like orientation of fibers in a tissue engineered meniscus seeded with FCCs (27). However, there is limited research on MSCs ability to form fibers in the context of meniscus. In other systems for tendon and ligament tissue engineering, MSCs are able to exert tractional forces and align fibers in the direction of axial fixation (61,62,65,67). Contraction was often coupled with fiber formation, however contraction and fiber formation are dependent on the mechanical load, collagen concentration, and cell concentration (61,63,64). Furthermore, contraction does not directly correlate to fiber formation. Previously we have seen that groups with increased contraction had decreased fiber size and alignment, where mechanical fixation had a greater effect on fiber formation (27). Another study saw found that MSCs seeded on an aligned matrix had limited GAG and collagen production compared to FCCs seed on the same matrix (71). In the study, MSCs developed and formed fibers, however MSC fiber diameter and alignment were inferior to FCCs. Native fiber diameters are ~35 μm and with an alignment index of ~1.75 (27,48). Of the

three culture groups, the FCC mono-culture menisci were closest to native values at a diameter of ~17 μm and an alignment index of ~1.47. Both FCC mono-culture and co-culture have significant increases in fiber diameter, however, MSC mono-cultured menisci do not significantly increase fiber diameter after 4 weeks of culture. These findings emphasize that FCCs and MSCs have different responses to the mechanical boundary conditions and the structural microenvironment they are cultured in.

Proteoglycans are another factor known to influence the nature of fiber formation. The data from this study showed that increasing GAG content was inversely correlated with decreasing fiber diameter. Notably, the production of GAG was significantly higher in the MSC mono-cultured gels which had the lowest fiber diameter. In this study, MSC mono-cultured gels had ~350% and co-cultured gels had ~250% the amount of GAG/meniscus compared to FCC mono-culture. While GAG production is typically considered a positive marker for a meniscal phenotype, the concentration of GAG in the meniscus is significantly lower than cartilage, with proteoglycans only comprising 1-2% of the dry weight (1,72,73). Furthermore the GAG content of the meniscus increases with age until skeletal maturity (72). The type of GAG can influence the way in which fibers form. Small leucine rich proteoglycans (SLRPs) are present in fibrocartilage and play a key role in matrix assembly (10,74,75). The presence of certain small proteoglycans may actually lead to decreased fiber forming capabilities by inhibiting assembly of collagen fibrils (76–78). The constructs in this study produced SLRPs decorin, biglycan, and fibromodulin. The increased production of GAG in the MSC cultures was correlated with the reduced ability to form large fibers. Over accumulation of SLRPs has been linked with reduced fibrillogenesis, however more research into the

interaction and concentration of these molecules in the meniscus is necessary to better understand how to influence fiber formation for tissue engineering (78,79). While MSCs are the native cell precursor to FCCs in development this system does not adequately differentiate MSCs into FCCs with the same fiber forming capabilities. Fine tuning the amount and types of proteoglycans produced by FCCs and MSCs will provide insight into their role in controlling fiber formation.

The meniscus is known to be largely comprised of water, collagen, and proteoglycans (10,80). Collagen type I is highly prevalent in the outer red-red zone and collagen type II is the predominant collagen type in the inner white-white zone (81). Tissue engineered menisci in this study contained both collagen I and collagen II. MSC seeded constructs produced significantly higher amounts of collagen type I, whereas FCC and co-cultured constructs showed increased levels of collagen type II. At 4 weeks, there were no spatial differences in the expression between collagen type I and II. Collagen type I is found in a region of the meniscus typically under tensile stresses, while collagen type II is prevalent in the inner meniscus typically under more compressive loads (20). The menisci in this study are constrained at the horns providing a static mechanical boundary condition. A dynamic loading regime mimicking native mechanical loading would likely increase regional expression of collagen types resembling native meniscus (48).

The specific use of MSCs in a tissue engineered model of meniscus formation could lend key insight into the development of native meniscus. During the development of the knee, the meniscus begins as a dense mesenchymal condensate (40,82). Throughout embryonic development cellular concentration decreases as collagen content increases

(40,83) Collagen fibers begin as small and disorganized and gradually begin to form larger organized fibers after establishment of the meniscal insertions. Early fiber alignment is established in embryonic development, however meniscal maturity is not reached until after years of normal load bearing in a child (40,84). GAG content is low in early development when fibers form, with age, GAGs are deposited in distinct domains separate from collagen (72,74,85) Mechanical load bearing is essential to the maturation of the meniscus both pre- and post-natally (86). Similar to early stages of meniscal development, our system begins culture with MSCs seeded into a disorganized collagen gel. Similar to enthesis fixation during development, mechanical fixation at the horns helps to direct fiber formation. Tissue engineered menisci seeded with MSCs mimic the developmental process which will help to inform chemical and mechanical signals that may play a role in meniscal development. The system established in this study can be used to ask specific questions about how mechanical and biochemical signals can influence MSC differentiation and meniscal development.

This study compared the ability of MSCs and FCCs to form a large organized meniscal implant. MSCs produced an anatomically accurate TE meniscus with high levels of GAG, however the tissue had inferior fiber microstructure. High levels of GAG are typically considered positive markers for fibrochondrogenic differentiation, however this study indicates that high levels of GAG production is correlated with reduced fiber diameter. MSCs remain a promising cell source for tissue engineering, however achieving targets for fiber size and organization will likely require manipulating the amount and types of GAGs produced by MSCs. In this study, co-cultures achieved intermediate levels fiber formation and GAG production. Co-culture

can be used as a technique to utilize the fiber formation capabilities of FCC and the matrix production properties of MSCs while reducing the clinical dependence on high volumes of FCCs for tissue engineering the meniscus.

REFERENCES

1. McDevitt, C.A. and Webber RJ. The ultrastructure and biochemistry of meniscal cartilage. Clin Orthop Relat Res. 1990;252:8–18.
2. Kohn D, Moreno B. Meniscus insertion anatomy as a basis for meniscus replacement: a morphological cadaveric study. Arthroscopy. 1995;11(1):96–103.
3. Messner K, Gao J. The menisci of the knee joint. Anatomical and functional characteristics, and a rationale for clinical treatment. J Anat. 1998;193 (Pt 2:161–78.
4. Pagnani MJ, Cooper DE, Warren RF. Extrusion of the medial meniscus. Arthrosc J Arthrosc Relat Surg. 1991;7(3):297–300.
5. Petersen W, Tillmann B. Collagenous fibril texture of the human knee joint menisci. Anat Embryol (Berl). 1998;197(4):317–24.
6. Kambic HE, McDevitt CA. Spatial organization of types I and II collagen in the canine meniscus. J Orthop Res. 2005;23(1):142–9.
7. Skaggs DL, Warden WH, Mow VC. Radial tie fibers influence the tensile properties of the bovine medial meniscus. J Orthop Res. 1994;12(2):176–85.
8. Andrews SHJ, Rattner JB, Abusara Z, Adesida A, Shrive NG, Ronsky JL. Tie-fibre structure and organization in the knee menisci. J Anat. 2014 May;224(5):531–7.
9. Melrose J, Smith S, Cake M, Read R, Whitelock J. Comparative spatial and temporal localisation of perlecan, aggrecan and type I, II and IV collagen in the ovine meniscus: An ageing study. Histochem Cell Biol. 2005;124(3–4):225–35.

10. Nakano T, Dodd CM, Scott PG. Glycosaminoglycans and proteoglycans from different zones of the porcine knee meniscus. J Orthop Res. 1997;15(2):213–20.
11. Greis PE, Bardana DD, Holmstrom MC, Burks RT. Meniscal injury: I. Basic science and evaluation. J Am Acad Orthop Surg. 2002;10(3):168–76.
12. Bedi A, Kelly NH, Baad M, Fox AJS, Brophy RH, Warren RF, et al. Dynamic contact mechanics of the medial meniscus as a function of radial tear, repair, and partial meniscectomy. J Bone Joint Surg Am. 2010;92(6):1398–408.
13. Khetia EA, McKeon BP. Meniscal allografts: biomechanics and techniques. Sports Med Arthrosc. 2007 Sep;15(3):114–20.
14. Brophy RH, Matava MJ. Surgical Options for Meniscal Replacement. J Am Acad Orthop Surg. 2012;20(5):265–72.
15. Verdonk R, Volpi P, Verdonk P, Bracht H Van Der, Laer M Van, Almqvist KF, et al. Indications and limits of meniscal allografts. Injury. Elsevier Ltd; 2013;44(SUPPL.1):S21–7.
16. Food and Drug Administration. Review of the ReGen Menaflex: Departures from Processes, Procedures, and Practices Leave the basis for a REview Decision in Question [Internet]. 2009. Available from: Food and Drug
17. Maher S a, Rodeo S a, Doty SB, Brophy R, Potter H, Foo L-F, et al. Evaluation of a porous polyurethane scaffold in a partial meniscal defect ovine model. Arthroscopy. Elsevier Inc.; 2010 Nov;26(11):1510–9.
18. Fox AJS, Wanivenhaus F, Burge AJ, Warren RF, Rodeo S a. The human meniscus: A review of anatomy, function, injury, and advances in treatment. Clin Anat. 2015;28(2):269–87.

19. Makris E, Hadidi P, Athanasiou K. The knee meniscus: structure-function, pathophysiology, current repair techniques, and prospects for regeneration. Biomaterials. Elsevier Ltd; 2011 Oct;32(30):7411–31.

20. Sweigart M a, Athanasiou K a. Toward tissue engineering of the knee meniscus. Tissue Eng. 2001 Apr;7(2):111–29.

21. Mandal BB, Park S-H, Gil ES, Kaplan DL. Multilayered silk scaffolds for meniscus tissue engineering. Biomaterials. Elsevier Ltd; 2011 Jan;32(2):639–51.

22. Messner K. Meniscal substitution with a Teflon-periosteal composite graft: a rabbit experiment. Biomaterials. 1994 Mar;15(3):223–30.

23. Wood DJ, Minns RJ, Strover A. Replacement of the rabbit medial meniscus with a polyester-carbon fibre bioprosthesis. Biomaterials. 1990 Jan;11(1):13–6.

24. Stabile KJ, Odom D, Smith TL, Northam C, Whitlock PW, Smith BP, et al. An acellular, allograft-derived meniscus scaffold in an ovine model. Arthrosc J Arthrosc Relat Surg. Elsevier Inc.; 2010 Jul;26(7):936–48.

25. de Groot JH, Zijlstra FM, Kuipers HW, Pennings AJ, Klompmaker J, Veth RPH, et al. Meniscal tissue regeneration in porous 50/50 copoly (L-lactideh-caprolactone) implants. 1997;18(8):613–22.

26. Puetzer JL, Bonassar LJ. High Density Type I Collagen Gels for Tissue Engineering of Whole Menisci. Acta Biomater. Acta Materialia Inc.; 2013 May 10;9(8):7787–95.

27. Puetzer JL, Koo E, Bonassar LJ. Induction of fiber alignment and mechanical anisotropy in tissue engineered menisci with mechanical anchoring. J Biomech. Elsevier; 2015;48(8):1436–43.

28. Gunja NJ, Athanasiou KA. Passage and reversal effects on gene expression of bovine meniscal fibrochondrocytes. Arthritis Res Ther. 2007 Jan;9(5):R93.

29. Pittenger MF, Mackay AM, Beck SC, Jaiswal RK, Douglas R, Msca JD, et al. Multilineage Potential of Adult Human Mesenchymal Stem Cells. Science (80-). 1999 Apr 2;284(5411):143–7.

30. Centeno CJ, Busse D, Kisiday J, Keohan C, Freeman M, Karli D. Regeneration of meniscus cartilage in a knee treated with percutaneously implanted autologous mesenchymal stem cells. Med Hypotheses. Elsevier Ltd; 2008 Dec;71(6):900–8.

31. Duygulu F, Demirel M, Atalan G, Kaymaz FF, Kocabey Y, Dulgeroglu TC, et al. Effects of intra-articular administration of autologous bone marrow aspirate on healing of full-thickness meniscal tear: an experimental study on sheep. Acta Orthop Traumatol Turc. 2012;46(1):61–7.

32. Agung M, Ochi M, Yanada S, Adachi N, Izuta Y, Yamasaki T, et al. Mobilization of bone marrow-derived mesenchymal stem cells into the injured tissues after intraarticular injection and their contribution to tissue regeneration. Knee surgery, Sport Traumatol Arthrosc Off J ESSKA. 2006 Dec;14(12):1307–14.

33. Kim J-D, Lee GW, Jung GH, Kim CK, Kim T, Park JH, et al. Clinical outcome of autologous bone marrow aspirates concentrate (BMAC) injection in

degenerative arthritis of the knee. Eur J Orthop Surg Traumatol. 2014 Jan 8;24:1505–11.

34. Hoben GM, Willard VP, Athanasiou KA. Fibrochondrogenesis of hESCs: growth factor combinations and cocultures. Stem Cells Dev. 2009 Mar;18(2):283–92.

35. Saliken DJ, Mulet-Sierra A, Jomha NM, Adesida AB. Decreased hypertrophic differentiation accompanies enhanced matrix formation in co-cultures of outer meniscus cells with bone marrow mesenchymal stromal cells. Arthritis Res Ther. BioMed Central Ltd; 2012 Jan;14(3):R153.

36. Cui X, Hasegawa A, Lotz M, D'Lima D. Structured three-dimensional co-culture of mesenchymal stem cells with meniscus cells promotes meniscal phenotype without hypertrophy. Biotechnol Bioeng. 2012 Sep;109(9):2369–80.

37. McCorry MC, Puetzer JL, Bonassar LJ. Characterization of mesenchymal stem cells and fibrochondrocytes in three-dimensional co-culture: analysis of cell shape, matrix production, and mechanical performance. Stem Cell Res Ther. Stem Cell Research & Therapy; 2016;7(1):39.

38. Bonnevie ED, McCorry MC, Bonassar LJ. Mesenchymal Stem Cells Enhance Lubrication of Engineered Meniscus Through Lubricin Localization in Collagen Gels. Biotribology. Elsevier B.V.; 2016;

39. Nerurkar NL, Han W, Mauck RL, Elliott DM. Homologous structure-function relationships between native fibrocartilage and tissue engineered from MSC-seeded nanofibrous scaffolds. Biomaterials. Elsevier Ltd; 2011;32(2):461–8.

40. Clark CR, Ogden JA. Prenatal and Postnatal Development of Human Knee Joint Mensci. Iowa Orthop J. 1981;1(1):20–7.

41. Costa KD, Lee EJ, Holmes JW. Creating alignment and anisotropy in engineered heart tissue: role of boundary conditions in a model three-dimensional culture system. Tissue Eng. 2003 Aug;9(4):567–77.

42. Mauck RL, Yuan X, Tuan RS. Chondrogenic differentiation and functional maturation of bovine mesenchymal stem cells in long-term agarose culture. Osteoarthr Cartil. 2006 Feb;14(2):179–89.

43. Bernacki SH, Wall ME, Loboa EG. Isolation of human mesenchymal stem cells from bone and adipose tissue. Methods Cell Biol. 2008 Jan;86(8):257–78.

44. Mackay AM, Beck SC, Murphy JM, Barry FP, Chichester CO, Pittenger MF. Chondrogenic differentiation of cultured human mesenchymal stem cells from marrow. Tissue Eng. 1998 Jan;4(4):415–28.

45. Ballyns JJ, Wright TM, Bonassar LJ. Effect of media mixing on ECM assembly and mechanical properties of anatomically-shaped tissue engineered meniscus. Biomaterials. Elsevier Ltd; 2010 Sep;31(26):6756–63.

46. Bowles RD, Williams RM, Zipfel WR, Bonassar LJ. Self-Assembly of Aligned Tissue-Engineered Annulus fibrosus and Intervertebral Disc Composite Via Collagen Gel Contraction. Tissue Eng Part A. 2010;16(4).

47. Cross VL, Zheng Y, Won Choi N, Verbridge SS, Sutermaster B a., Bonassar LJ, et al. Dense type I collagen matrices that support cellular remodeling and microfabrication for studies of tumor angiogenesis and vasculogenesis in vitro. Biomaterials. Elsevier Ltd; 2010;31(33):8596–607.

48. Puetzer JL, Bonassar LJ. Physiologically Distributed Loading Patterns Drive the Formation of Zonally Organized Collagen Structures in Tissue Engineered Meniscus. Tissue Eng Part A. 2016;(607):1–40.

49. Ballyns JJ, Gleghorn JP, Niebrzydowski V, Rawlinson JJ, Potter HG, Maher SA, et al. Image-guided tissue engineering of anatomically shaped implants via MRI and micro-CT using injection molding. Tissue Eng Part A. 2008 Jul;14(7):1195–202.

50. Ballyns JJ, Cohen DL, Malone E, Maher S a, Potter HG, Wright T, et al. An optical method for evaluation of geometric fidelity for anatomically shaped tissue-engineered constructs. Tissue Eng Part C Methods. 2010 Aug;16(4):693–703.

51. Kim YJ, Sah RL, Doong JY, Grodzinsky AJ. Fluorometric assay of DNA in cartilage explants using Hoechst 33258. Anal Biochem. 1988;174(1):168–76.

52. Enobakhare BO, Bader DL, Lee DA. Quantification of sulfated glycosaminoglycans in chondrocyte/alginate cultures, by use of 1,9-dimethylmethylene blue. Anal Biochem. 1996;243(1):189–91.

53. Neuman R, Logan M. The determination of hydroxyproline. J Biol Chem. 1949;184(1):299–306.

54. Bowles RD, Williams RM, Zipfel WR, Bonassar LJ. Self-assembly of aligned tissue-engineered annulus fibrosus and intervertebral disc composite via collagen gel contraction. Tissue Eng Part A. 2010;16(4):1339–48.

55. Moran JM, Pazzano D, Bonassar LJ. Characterization of polylactic acid-polyglycolic acid composites for cartilage tissue engineering. Tissue Eng. 2003;9(1):63–70.

56. Frank EH, Grodzinsky AJ. Cartilage electromechanics--II. A continuum model of cartilage electrokinetics and correlation with experiments. J Biomech. 1987;20(6):629–39.

57. Kim YJ, Bonassar LJ, Grodzinsky AJ. The role of cartilage streaming potential, fluid flow and pressure in the stimulation of chondrocyte biosynthesis during dynamic compression. J Biomech. 1995;28(9):1055–66.

58. Ala-Myllymäki J, Honkanen JTJ, Töyräs J, Afara IO. Optical spectroscopic determination of human meniscus composition. J Orthop Res. 2016;34(2):270–8.

59. Proctor CS, Schmidt MB, Whipple RR, Kelly M a, Mow VC. Material properties of the normal medial bovine meniscus. J Orthop Res. 1989;7(6):771–82.

60. Peloquin JM, Santare MH, Elliott DM. Advances in quantification of meniscus tensile mechanics including nonlinearity , yield , and failure. J Biomech Eng. 2016;138(2):021002 (13 pages).

61. Awad HA, Butler DL, Harris MT, Ibrahim RE, Wu Y, Young RG, et al. In vitro characterization of mesenchymal stem cell-seeded collagen scaffolds for tendon repair: Effects of initial seeding density on contraction kinetics. J Biomed Mater Res. 2000;51(2):233–40.

62. Cai D, Marty-Roix R, Hsu H, Spector M. Lapine and Canine Bone Marrow Stromal cElls Contain Smooth Muscle Actin and Contract a Collagen-Glycosaminoglycan Matrix. Tissue Eng Part A. 2001;7(6):829–41.

63. Juncosa-Melvin N, Boivin GP, Galloway MT, Gooch C, West JR, Sklenka AM, et al. Effects of cell-to-collagen ratio in mesenchymal stem cell-seeded implants on tendon repair biomechanics and histology. Tissue Eng. 2005;11(3–4):448–57.

64. Nirmalanandhan VS, Levy MS, Huth AJ, Butler DL. Effects of cell seeding density and collagen concentration on contraction kinetics of mesenchymal stem cell-seeded collagen constructs. Tissue Eng. 2006;12(7):1865–72.

65. Young RG, Butler DL, Weber W, Caplan a I, Gordon SL, Fink DJ. Use of mesenchymal stem cells in a collagen matrix for Achilles tendon repair. J Orthop Res. 1998;16(4):406–13.

66. Bell E, Ivarsson B, Merrill C. Production of a tissue-like structure by contraction of collagen lattices by human fibroblasts of different proliferative potential in vitro. Proc Natl Acad Sci U S A. 1979;76(3):1274–8.

67. Huang D, Chang TR, Aggarwal A, Lee RC, Ehrlich HP. Mechanisms and dynamics of mechanical strengthening in ligament-equivalent fibroblast-populated collagen matrices. Ann Biomed Eng. 1993;21(3):289–305.

68. Thomopoulos S, Fomovsky GM, Holmes JW. The development of structural and mechanical anisotropy in fibroblast populated collagen gels. J Biomech Eng. 2005;127(5):742–50.

69. Grinnell F. Fibroblast-collagen-matrix contraction: growth-factor signalling and mechanical loading. Trends Cell Biol. 2000;10(9):362–5.

70. Abraham AC, Haut Donahue TL. From meniscus to bone: A quantitative evaluation of structure and function of the human meniscal attachments. Acta Biomater. Acta Materialia Inc.; 2013;9(5):6322–9.

71. Baker BM, Nathan AS, Gee AO, Mauck RL. The influence of an aligned nanofibrous topography on human mesenchymal stem cell fibrochondrogenesis. Biomaterials. 2010;31(24):6190–200.

72. McNicol D, Roughley PJ. Extraction and characterization of proteoglycan from human meniscus. Biochem J. 1980;185(3):705–13.

73. Kawamura S, Lotito K, Rodeo SA. BIOMECHANICS AND HEALING RESPONSE OF. 2003;11(2):68–76.

74. Vanderploeg EJ, Wilson CG, Imler SM, Ling CHY, Levenston ME. Regional variations in the distribution and colocalization of extracellular matrix proteins in the juvenile bovine meniscus. J Anat. 2012;221(2):174–86.

75. Hayes AJ, Isaacs MD, Hughes C, Caterson B, Ralphs JR. Collagen fibrillogenesis in the development of the annulus fibrosus of the intervertebral disc. Eur Cells Mater. 2011;22(0):226–41.

76. Vogel KG, Paulsson M, Heinegård D. Specific inhibition of type I and type II collagen fibrillogenesis by the small proteoglycan of tendon. Biochem J. 1984;223(3):587–97.

77. Vogel KG, Trotter JA. The Effect of Proteoglycans on the Morphology of Collagen Fibrils Formed In Vitro. Coll Relat Res. Gustav Fischer Verlag · Stuttgart · New York; 1987;7(2):105–14.

78. Viola M, Bartolini B, Sonaggere M, Giudici C, Tenni R, Tira ME. Fibromodulin interactions with type I and II collagens. Connect Tissue Res. 2007;48(3):141–8.

79. Wang VM, Bell RM, Thakore R, Eyre DR, Galante JO, Li J, et al. Murine tendon function is adversely affected by aggrecan accumulation due to the knockout of ADAMTS5. J Orthop Res. 2012;30(4):620–6.

80. Eyre DR, Koob TJ, Chun LE. Biochemistry of the meniscus: unique profile of collagen types and site-dependent variations in composition. Orthop Trans. 1983;8(53).

81. Cheung HS. Distribution of type I, II, III and V in the pepsin solubilized collagens in bovine menisci. Connect Tissue Res. 1987;16(4):343–56.

82. Gray DJ, Gardner E. Prenatal development of the human knee and superior tibiofibular joints. Am J Anat. 1950;86(2):235–87.

83. Mérida-Velasco J a, Sánchez-Montesinos I, Espín-Ferra J, Rodríguez-Vázquez JF, Mérida-Velasco JR, Jiménez-Collado J. Development of the human knee joint. Anat Rec. 1997 Jun;248(2):269–78.

84. Arnoczky SP, Warren RF. Microvasculature of the human meniscus. Am J Sports Med. 1936;10(2):90–5.

85. Han WM, Heo S-J, Driscoll TP, Delucca JF, McLeod CM, Smith LJ, et al. Microstructural heterogeneity directs micromechanics and mechanobiology in native and engineered fibrocartilage. Nat Mater. 2016;(January).

86. Mikic B, Johnson TL, Chhabra a B, Schalet BJ, Wong M, Hunziker EB. Differential effects of embryonic immobilization on the development of fibrocartilaginous skeletal elements. J Rehabil Res Dev. 2000;37(2):127–33.

CHAPTER 5

Controlling Fiber Formation in Tissue Engineered Menisci by Regulating Proteoglycan Production[4]

Abstract

Collagen is highly prevalent in the extracellular matrix and therefore commonly used as a biomaterial in tissue engineering applications. In the native environment, collagen is arranged in a complex hierarchical structure that is often difficult to recreate in a tissue engineered construct. Proteoglycans, specifically small leucine rich proteoglycans, have been implicated as influential in directing fiber formation. In this study, we controlled proteoglycan production and evaluated its effect on the development of collagen fibers inside tissue engineered meniscal constructs. Glucose concentrations of 4500, 1000, 500, 250, and 125 mg/L in culture media were applied to meniscal constructs. Reduction of glucose resulted in a dose dependent decrease in glycosaminoglycan (GAG) production and minimal decreases of decorin and biglycan. However, fibromodulin doubled in production between 125 and 4500 mg/L glucose concentration. A peak in fiber formation was observed at 500 mg/L glucose concentration and corresponded with reductions in GAG production. Fiber formation reduction at 125 and 250 mg/L glucose concentrations are likely due to glucose starvation and changes in metabolic activity. These results point to proteoglycan production as a means to manipulate fiber architecture in tissue engineered constructs.

---

[4]Chapter in Preperation for Publication: M. C. McCorry, J. Kim, N. Springer, Anna Plaas, John Sandy, and L. J. Bonassar. Controlling Fiber Formation in Tissue Engineered Menisci by Regulating Proteoglycan Production. *In Preparation for Submission to Biomaterials.*

Introduction

Collagen is the most prevalent structural protein in the mammalian extracellular matrix. For this reason collagen is a popular biomaterial of choice as a scaffold for medical biomaterials and tissue engineering applications. In highly fibrous tissues, such as meniscus, tendon, ligament, and cartilage, the structure and orientation of collagen into organized fibers is crucial to the mechanical integrity of the tissue. Mimicking the development of a complex fiber architecture seen in the native tissue has been particularly challenging for tissue engineers due to the complex interplay between collagen, cells, and other proteins present in smaller amounts. The relative amount of each component can have profound effects on the fiber architecture that is generated during development both *in vivo* and *in vitro*.

The meniscus is a highly fibrous tissue primarily composed of collagen (60-70% of the dry weight). The meniscus relies on an organized collagen fiber network with interspersed proteoglycans (PGs) to provide its robust mechanical properties that can withstand high loads within the knee and protect the surrounding articular cartilage [1, 2]. The meniscus is primarily composed of 72% water, 22% collagen, 0.8% proteoglycan, and 0.12% DNA of the hydrated tissue weight [3]. The meniscus contains large diameter (~20-50 μm) circumferential fibers that run from horn to horn and fix the meniscus to the underlying tibial plateau through interdigitating fibers at the meniscal enthesis insertion [4, 5]. These large diameter circumferential fibers are interconnected by radial tie fibers that extend from outer edge of the meniscus [2, 6]. The meniscal fiber structure is established early in joint development from a dense mesenchymal condensate [7, 8]. Glycosaminoglycans (GAGs) are distributed throughout the

meniscus, however GAGs tend to be more prevalent in the inner portion of the meniscus [9]. GAG content lags behind fiber formation in meniscal development, with GAG content being low during fiber formation and increasing with age [10, 11]. Together the collagen fiber network and the GAG content in the meniscus work to support both tensile and compressive loads within the knee in order to maintain healthy knee function.

Given the essential role of fiber architecture in supporting meniscal function, meniscus tissue engineering efforts have heavily focused on mimicking the structure and orientation of the native collagen fibers. Several techniques have been utilized to recreate the fiber architecture in tissue engineered menisci using synthetic polymer fibers. A weaving technique of single filament polymer fiber composed of poly(desaminotyrosyl-tyrosine dodecyl ester dodecanoate) (p(DTD DD) was used to mimic native fiber architecture and achieve native mechanical properties [12–14]. An anatomically accurate meniscus was generated using a 3D printing technique that printed poly-ε-caprolactone (PCL) in a structure that mimicked native collagen orientation [15]. Creating scaffolds with an organized structure, can not only serve as a mechanical support structure, but can also guide cell production and organization of extracellular matrix molecules to improve mechanical properties [16].

An alternative approach is to utilize cellular production and remodeling of collagen to generate organized meniscal constructs either from a disorganized collagen matrix or matrix self-assembly. Static mechanical constraints help direct cellular remodeling to produce fiber alignment and establish anisotropic properties of tissue engineered scaffolds [17–20]. Mechanical anisotropy and directional fiber alignment

via cellular remodeling were further enhanced by mechanical loading that mimicked native compressive and tensile loading [21, 22]. The success of these scaffolds is highly dependent on recapitulating the native collagen fiber structure. Directing cellular remodeling to reproduce the complex fiber architecture of the meniscus is not fully understood at this time.

The collagen fiber structure is surrounded by a matrix of hydrophillic GAGs that are known to help support compressive loads in the meniscus [23, 24]; therefore high GAG content is typically viewed as a positive marker for meniscus tissue engineering. However, while GAGs are the second most prevalent structural component of meniscus, it is important to note the total make up of GAG content is still relatively small compared to a tissue such as cartilage [3, 25]. Previously, we found that increasing concentrations of GAG were negatively correlated with fiber diameter in tissue engineered constructs [20]. Furthermore, studies that applied chondoitinase ABC during construct development had a corresponding increase in tensile properties and improved fiber production, indicating that removing chondroitin and dermatan sulfate GAG chains during construct maturation improves collagen production [17, 26]. In meniscal development GAG content is minimal during early stages of fiber development and increases substantially with aging after fiber architecture has been established [10, 11, 27]. While GAGs have an important role to play in meniscus structure and function, it is not clear how to utilize GAGs in order to control fiber development for tissue engineering applications.

Proteoglycans, proteins containing GAGs, are primarily known for their role in supporting mechanical loading in the meniscus; however, proteoglycans also have an

influential role in fiber development and organization. Aggrecan is known to be prevalent throughout the inner and outer meniscus [27]. The large bottle-brush structure of aggrecan helps to retain water within the tissue and resist compressive loads in healthy tissue [28]. In tendinopathies, increasing aggrecan accumulation disturbs normal collagen organization, indicating that aggrecan may sterically hinder normal cell matrix binding that is needed for collagen remodeling (Figure 5.1C) [29]. Small leucine-rich proteoglycans (SLRPs) such fibromodulin, decorin, and biglycan are known to regulate fiber formation and maintenance through interactions with collagen fibers (Figure 5.1B) [30–32]. Knockout models of each of these SLRPs resulted in adverse fiber formation [33, 34]; however, over accumulation of SLRPs resulted in smaller diameter fibers [35–37]. It is clear that proteoglycans both small and large have complex interactions with collagen that influence how collagen fiber architecture is developed and maintained and that there is delicate balance between helping and inhibiting fiber development. The formation of large organized fibers in meniscus tissue engineering will require a better understanding of the specific roles and amounts of a proteoglycan that will optimize fiber formation.

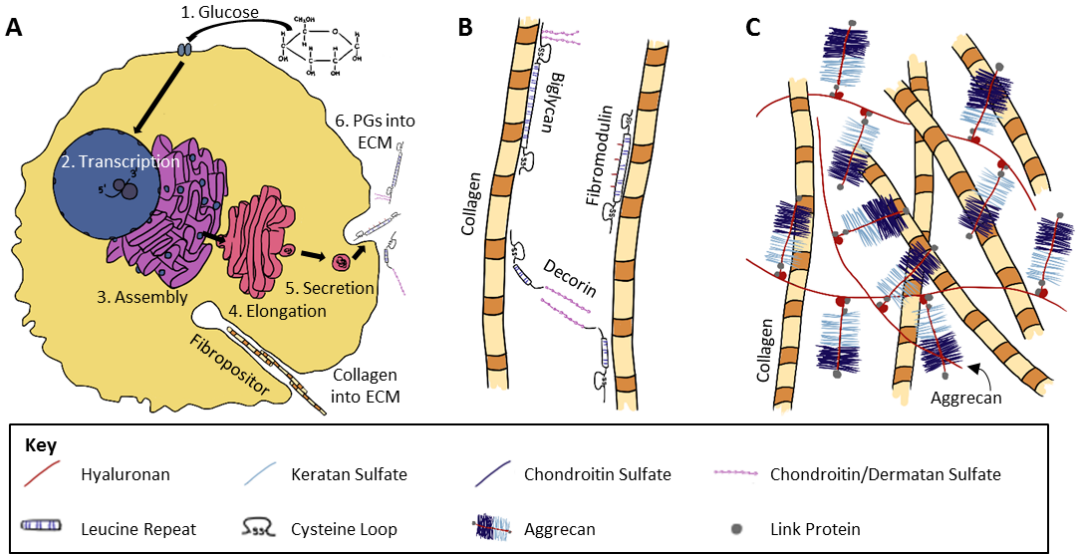

Figure 5.1: The relationship between glucose, proteoglycans, and collagen fibers. (A) Glucose is transported into the cell. Transcription initiates the assembly of proteoglycans with glucose sugars as building blocks. Proteoglycans are elongated and glycosylated through the ER-Golgi pathway. Following elongation, proteoglycans are secreted into the extracellular matrix. (B) SLRP interaction with collagen fibers. (C) Aggrecan molecules intertwined between fibers, preventing fibers from aligning and forming larger fibers.

Production of GAG depends directly on glucose metabolism in the cell. When glucose enters a cell, glucose is used for metabolic production or protein synthesis of ECM macromolecules such as proteoglycans (Figure 5.1A) [38, 39]. Traditionally, meniscus tissue engineered constructs are cultured in a high glucose media (4500 mg/L or 25 mM) [5, 16, 17]. However, a low glucose media (1000 mg/L or 5.5 mM) is considered to be physiologic [40, 41] . Chondrocyte and nucleus pulposus cells have been shown to be highly sensitive to changes in glucose concentration and that reducing glucose results in a corresponding reduction of GAGs [42, 43]. Little is known about the effect of glucose on fibrochondrocytes (FCC) and the corresponding implications for tissue engineering. Mesenchymal stem cells (MSCs) are common source for tissue engineering. MSCs have already demonstrated variable matrix forming abilities

compared to FCCs [20, 44, 45], therefore, how MSCs process glucose to form ECM needs to be investigated for tissue engineering applications. It is possible that high glucose media formulations result in excessive production of GAGs that retard the ability of cells in a tissue engineered scaffold to organize large fibers.

We hypothesize that reducing the glucose concentration in the culture media of tissue engineered menisci would reduce the proteoglycan concentration, which would in turn facilitate improved collagen fiber assembly and organization. In this study, we applied several concentrations of glucose to tissue engineered menisci and measured total GAG output, SLRP production, glucose metabolism, quantified the fiber organization and diameter at each glucose concentration, and explored the relationship between GAGs and fiber formation.

Methods

Cell Isolation

As previously described, FCCs were isolated from the menisci of 1-3 day old bovids using a 0.3% collagenase digestion (Worthington Biochemical Corporation, Lakewood, NJ) [46, 47]. Cells were filtered through a 100 μm cell strainer and rinsed with PBS to remove collagenase before embedding in scaffolds. Mesenchymal stem cells (MSCs) were obtained from the trabecular bone marrow of 1-3 day old bovid distal femur as previously described [20, 48]. The adherent population of cells after 48 hours was tested using a trilineage differentiation assay (Supp. 5.1) [49, 50]. Cells were expanded in 2D culture until passage 4 with a growth medium containing low glucose Dulbecco's modified Eagle's medium (DMEM) supplemented with 10% fetal bovine

serum (FBS), 100 μg/mL penicillin, 100 μg/mL streptomycin, 0.25 μg/mL amphotericin B, 2mM L-glutamine, and 1 ng/mL basic fibroblast growth factor.

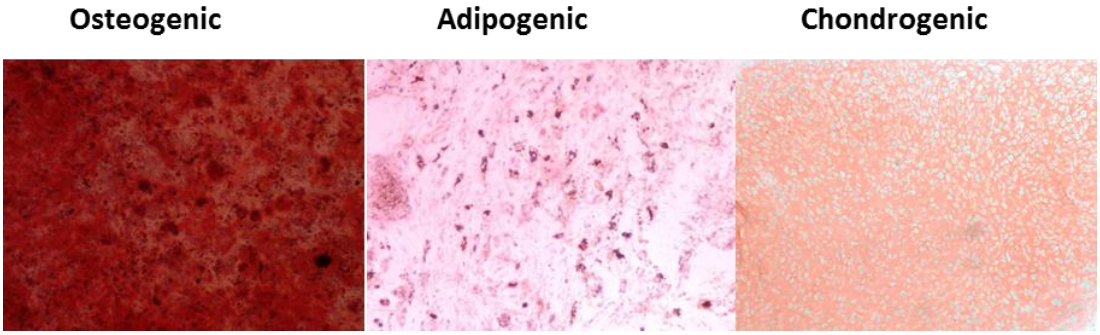

Supplemental 5.1: MSC multipotency validation using Alizarin red on osteogenic wells, oil red-o on adipogenic wells and safranin-o on histologic sections of a chondrogenic cell pellet.

Construct Generation

Meniscus molds were generated by CNC machining a negative mold of a semilunar structure with a wedge shaped cross-section into polysulfone. The scaffold material was generated by extracting collagen type I from Sprague-Dawley rat tails (Pel-Freeze Biologicals, Rogers, AZ). Collagen was solubilized, lyophilized, and reconstituted in 0.1% acetic acid at 30 mg/mL concentration as previously described [47, 51, 52]. To initiate gelation, the stock collagen solution was mixed with a working solution comprised of 1N NaOH, 10x phosphate-buffered saline (PBS), and 1x PBS [52]. Either MSCs or FCCs were suspended in media and mixed to a final concentration of $25x10^6$ cells/mL and 20 mg/mL collagen gel [47]. The collagen and cell mixture was injected into meniscal molds and incubated for 30 minutes at 37˚C [19].

Each meniscus was clamped into a polysulfone disk by stacking a stainless steel mesh with a stainless steel bar to increase construct grip and provide a static mechanical boundary condition to direct collagen orientation (Figure 5.2) [19, 20]. Samples were

cultured in media containing DMEM, 10% FBS, 100 μg/mL penicillin, 100 μg/mL streptomycin, 0.1 mM non-essential amino acids, 50 μg/mL ascorbate, and 0.4 mM L-proline at 37°C and 5% CO_2 [47]. Each construct (0.75 mL of collagen with $25x10^6$ cell/mL) was cultured in a 6-well plate with 5 mL of medium at 5 different concentrations of glucose: 4500, 1000, 500, 250, 125 mg/L. Culture media was collected and replenished two times a week. At the conclusion of 2 and 4 weeks of culture, each meniscus was weighed and sectioned to obtain samples for biochemical, histological, western blot, and multiphoton analysis.

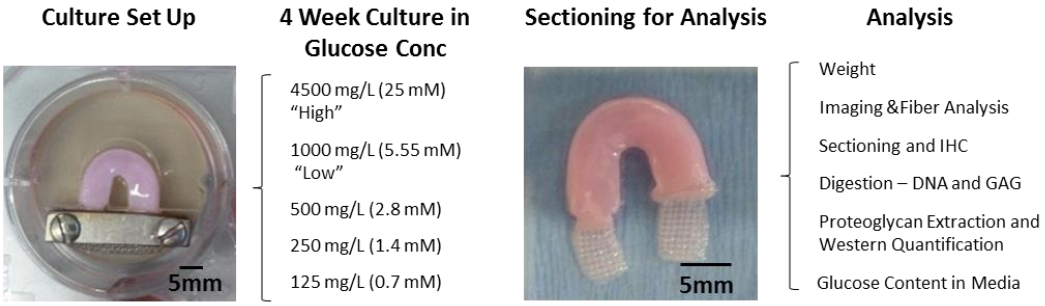

Figure 5.2: Experimental processing methods. A 20 mg/mL collagen tissue engineered meniscus construct seeded with 25 x 10^6 cell/mL is clamped in a polysulfone disk using a stainless steel bar and placed into a 6 well plate. Samples are cultured in one of five different glucose concentrations in the media. Following culture, the tissue engineered meniscus is weighted and then sectioned for analysis.

Cell Metabolism and Health

The protocol outlined in the previous section for cell isolation and collagen gel preparation was followed. 1 mm thick collagen sheet gels were generated and 8 mm diameter cylinders were punched out from the sheet gels. Each punch was cultured in a 24 well plate at a comparable cell/media ratio to the meniscal constructs. Cell metabolic activity was measured using the Alamar blue assay after 3 days, 1-, 2-, 3-, and 4-weeks at the 5 different glucose concentrations.

Glucose Consumption Assay

The medium samples from each group were harvested at the conclusion of a 3 day incubation period after 4 weeks of culture. The glucose concentrations were measured using Amplex Red glucose assay kit (Invitrogen, Eugene, OR) according to the manufacturer's instructions. The glucose consumption was calculated by subtracting the amount of glucose remaining after three days from the uncultured media control. Percent of glucose consumed in the media after three days in culture is a ratio of glucose consumed over total available glucose in each condition.

Biochemical Content

DNA, GAG, and hydroxyproline content were measured from each meniscus samples as previously described [20, 48, 53, 54]. Biochemical samples were measured for wet weight (ww) and measured again after lypholizing for dry weight. (dw). Samples were digested overnight using a papain digest. As previously described, biochemical content of constructs was measured using a Hoechst DNA assay for DNA content [55], a modified 1,9-dimethylmethylene blue (DMMB) assay at pH 1.5 for GAG content [56] and a hydroxyproline (hypro) assay for collagen content [57].

Multiphoton Microscopy

At the conclusion of each culture period, two sections from each meniscus were placed in 10% buffered formalin for 48 hours followed by storage in 70% ethanol. Each section was imaged into the bottom surface to visualize circumferential fibers. A Zeiss LSM 880 confocal/multiphoton inverted microscope using a 40x/1.2 C-Apochromat water immersion objective was used to image circumferential fibers using second harmonic generation and cell autofluorescence. Collagen fiber reflectance was captured

between 437-464 nm, while cell autofluorescence was captured between 495-580 nm. Fiber diameter (FD) and alignment index (AI) were calculated using a custom MATLAB code as previously described [19, 20, 22, 58]. Fiber patterns in images were analyzed using a series of fast Fourier transforms (FFT). After determining the maximum degree of alignment the AI is calculated as a ratio of the number of fibers ±20° from the maximum angle of alignment divided by the predicted number of fibers in a 40° span [58]. The average fiber diameter is calculated by converting the average cycle count along the x-axis of the maximum angle of alignment into microns. 5 images were taken from each slice, 2 slices per sample with a total of 10 images per sample (n=4-6).

Immunohistochemistry

Following multiphoton imaging, samples were dehydrated, embedded in paraffin, and sectioned for histological processing. Sections were staining for immunohistochemistry using primary antibodies for collagen type II (Chondrex, Redmond, WA, 7005), biglycan (courtesy of Dr. Larry Fischer, NIDCR, LF-96), decorin (courtesy of Dr. Larry Fischer, NIDCR, LF-94), and fibromodulin (Abcam, 81443), as previously described [20]. Staining was visualized using DAB peroxidase (Vector, Burlingame, CA) Images were collected using a 10x objective on a SPOT RT camera (Diagnostic Instruments, Sterling Heights, MI) attached to a Nikon Eclipse TE2000-S microscope (Nikon Instruments, Melville, NY). Biglycan, decorin, and fibromodulin were also visualized using a fluorescent secondary antibody (Alexa Fluor 546, Thermo Fisher). Collagen confocal reflectance and fluorescence imaging was performed on a Zeiss 710 confocal microscope with a Zeiss Axio Observer Z1 inverted

stand using a 40x/1.2 C-Apochromat water immersion objective. Collagen fiber reflectance was captured between 480-500 nm and Alexa Fluor 546 was captured between 570-700 nm.

Western Blot

GAGs from each sample were extracted with 3M guanidine hydrochloride, followed by dialysis. To verify banding due to glycosylation, a portion of each sample was incubated with chase ABC (chondoitinase ABC, Sigma-Aldrich, St. Louis, MO). The samples were mixed with an equal amount and volume of 4x Laemmli sample buffer (Bio-Rad, Richmond, CA) and β-mercaptoethanol (Thermo Scientific, Scotland, UK), heated at 95 C° for 10 min, loaded onto a 7.5% polyacrylamide gel (Bio-Rad, Richmond, CA), electrophoresed, and transferred to a polyvinylidene difluoride (PVDF) membrane (Bio-Rad, Richmond, CA). The membranes were blocked with 5% dry milk, 0.1% Tween-20 in TBS for 2 hours at room temperature, followed by incubation with diluted primary antibodies at 4 C° overnight. Primary antibodies were rabbit polyclonal anti-biglycan and decorin (1:1,000, courtesy of Dr. Larry Fischer, NIDCR, antibodies LF-94 and LF-96), rabbit polyclonal anti-fibromodulin (1:1,000, Abcam, Cambridge, MA). After washing the membranes three times in TBS/Tween-20, the membranes were incubated with an Elite secondary/HRP-conjugated anti-rabbit antibody (1:500, Vector Laboratories, Burlingame, CA) for probing. The membranes were detected with Pierce ECL Western Blotting Substrate (Thermo Scientific, Rockford, lL) and read by using a ChemiDoc Touch Imaging System (Bio-Rad, Richmond, CA). The intensities of each band were quantified using Image Lab software

(Bio-Rad, Richmond, CA). The quantified data were normalized to an intensity of a native meniscus.

Statistics

Cellular activity and metabolism data was analyzed using a 2-way-ANOVA with Tukey's t-test for post hoc analysis. GAG content measured by the DMMB assay was fit to a 4P sigmoid dose response curve. Logarithmic linear fits were applied to SLRP western blot quantification. A mixed model with random effect of sample number and location was used for fiber diameter and fiber alignment data. A Gaussian model was fit to fiber formation and GAG/ww data to assess GAG content predictability for fiber formation. All data are written as mean ±SD and significance was determined with $p<0.05$. Data analysis was conducted using JMP software (SAS Institute Inc, Cary, NC).

Results

Bioenergetics

Glucose is a critical sugar required for cell health and metabolism. After 4 weeks in culture, only 63% of FCC and 21% of MSC glucose in the 4500 mg/L glucose concentration group was consumed over three days of incubation (Figure 5.3A). However, at concentrations below 1000 mg/L glucose, a majority of the glucose was consumed in the media over the 3 day incubation period. Meniscus samples cultured in high glucose concentration media haed an excess availability of glucose throughout the four week duration of culture in contrast to lower glucose concentrations where there was likely some degree of glucose starvation occurring in the lowest glucose concentration groups. Glucose consumption was also measured at two weeks on 3 day incubated media (data not shown). A similar trend was found, but with slightly lower

consumption, with MSC menisci consuming 18% and FCC menisci consuming 33% of the glucose in high glucose media. 95% of glucose was consumed in both groups in low glucose media (1000 mg/L).

To assess if glucose starvation at a lower concentration had a negative effect on cell viability we assessed the DNA content in samples. After four weeks of culture, while there was a small reduction in DNA content at lower glucose concentrations, these differences were not statistically significant in both MSC and FCC cultured menisci (Figure 5.3B, $p<0.05$). Therefore glucose starvation that may be occurring at below physiologic glucose concentrations (1000 mg/mL) is not causing significant changes in cell viability.

Since cell viability was not significantly affected by glucose concentration, cell metabolism and activity was evaluated using an Alamar blue assay. The Alamar blue assay uses an indicator that fluoresces when oxidation reduction occurs in the medium. The Alamar blue was added to medium for 2 hours and then recorded after 3 days and 4 weeks of construct exposure to glucose concentrations. No significant differences were found between glucose groups at both the beginning (3 days) and end of culture (4 weeks) (Figure 5.3C, $p<0.05$).

Meniscal constructs are primarily composed of collagen and water. As cells contract and remodel the collagen matrix, water is displaced and therefore measurements of weight can serve as an indicator for collagen contraction. Collagen contraction occurred in both MSC and FCC constructs and increased with time after both 2 and 4 weeks of culture in all glucose concentrations (Figure 5.3D, $p<0.05$). After 4 weeks in culture, MSCs in 4500 mg/L contracted more than MSC constructs cultured

in 250 and 125 mg/L glucose ($p<0.05$). In FCC constructs, the 500mg/L glucose constructs contracted more than the 4500 mg/L glucose constructs ($p<0.05$). Cellular contractility occurred throughout the duration of culture in all groups, indicating the presence of an active and healthy cell population within the collagen meniscal constructs.

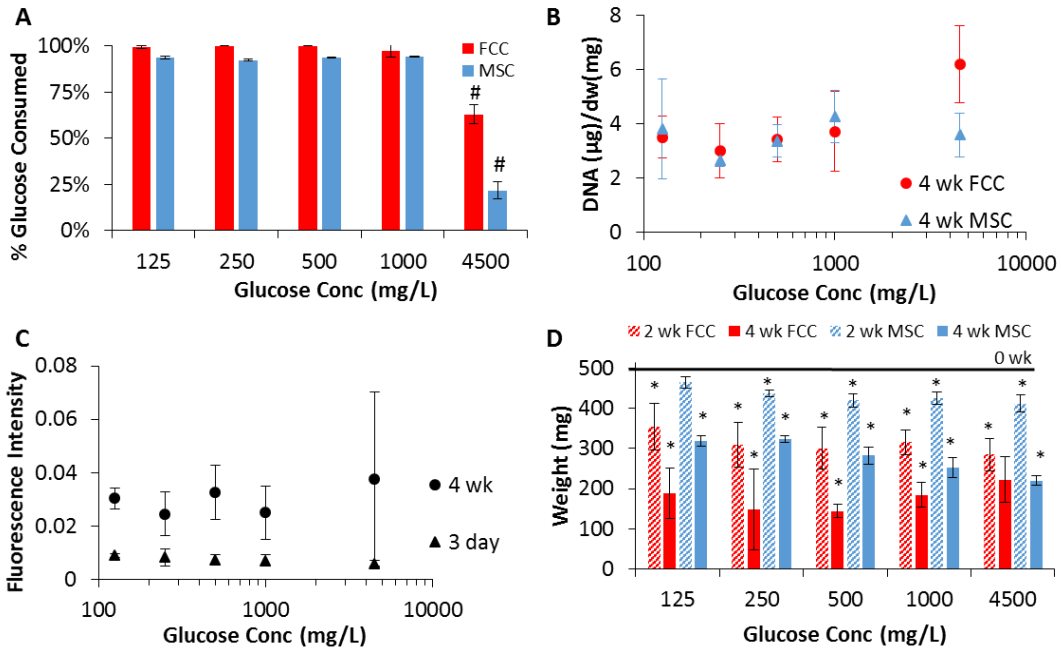

Figure 5.3: Cellular activity and metabolism. (A) Glucose consumption measured using the Amplex Red glucose assay. Glucose was measured in media after 3 days of incubation with meniscus constructs at the 4 week time point. (# significantly lower than other glucose concentrations, $p<0.05$, n=4-6) (B) DNA content normalized to meniscus dry weight (dw) (no statistical difference detected between glucose concentration, $p<0.05$, n=4-6) (C) Fluorescence intensity of Alamar blue after 2 hours of incubation with FCCs seeded in collagen punch biopsy. Molecule fluoresces after undergoing oxidative-reduction indicating cell metabolic activity. (no statistical difference detected between glucose conc, $p<0.05$, n=4) (D) Meniscus weight (mg) at 0-, 2-, 4-wk culture time points (*significantly lower than previous time pt, $p<0.05$, n=4-6).

Proteoglycan Production

Total GAG content in meniscal constructs had a corresponding decrease with reduction in glucose concentration in the media (Figure 5.4). Reduction of GAG content showed a dose dependent response with a FCC EC_{50} at ~380 mg/L (R^2=0..68) and a

MSC EC_{50} at ~370 mg/L (R^2=0.52). The maximum GAG/ww was in the 4500 mg/L group at 0.48 µg/mg and 0.41 µg/mg in FCC and MSC menisci respectively. The minimum GAG/ww was in the 125 mg/L group at 0.25 µg/mg and 0.28 µg/mg in FCC and MSC menisci respectively. The FCC group showed a greater sensitivity to changes in glucose with higher GAG levels at 4500 mg/L and lower GAG levels at 125 mg/L. Interestingly, the MSC and FCC group also had an EC_{50} between 250-500 mg/L glucose concentration culture group.

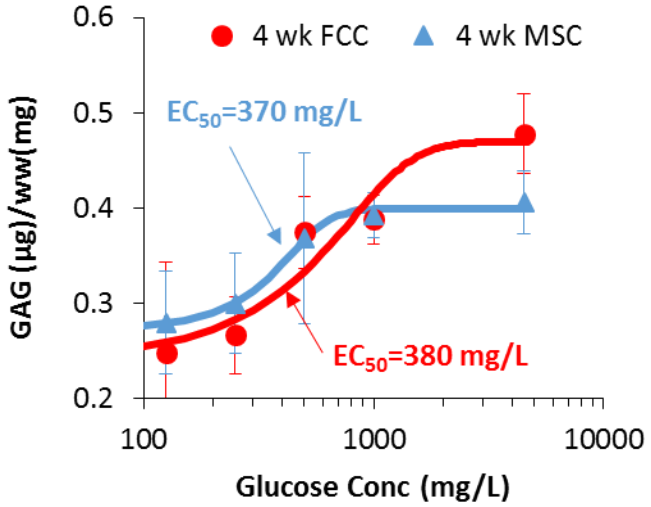

Figure 5.4: GAG content in 4 wk meniscus constructs measured using the DMMB assay. Lines indicate logistic 4P Sigmoid, n=4.

SLRP expression was quantified using western blot analysis and localization was visualized using IHC techniques. Biglycan increased after four weeks in cultures and had a strong intracellular expression (Figure 5.5A). Western blot quantification revealed no statistically significant trends, however FCC showed a slight logarithmic linear increase in biglycan expression with increasing glucose concentration (Figure 5.5B and 5.5C) (MSC R^2=0.38 and FCC R^2=0.66). Similar to biglycan, decorin expression also increased over the duration of four week culture. In contrast to biglycan,

decorin was heavily expressed throughout the matrix (Figure 5.6A). Decorin expression peaked at 500 mg/L with no significant trends (Figure 5.6B and 5.6C) (MSC R^2=0.0015 and FCC R^2=0.48). Fibromodulin expression increased to nearly two times between 125 mg/L and 4500 mg/L glucose cultured menisci seeded with FCCs after four weeks (Figure 5.7). Expression of fibromodulin had a log linear increase with increasing levels of glucose present in the media (Figure 5.7C) (MSC R^2=0.87 and FCC R^2=0.99). SLRP expression in relation to nuclei staining and collagen reflectance channels was measured using immunofluorescence (Supp. 5.3). Multiple banding in western blots for biglycan, decorin, and fibromodulin was knocked down from application of chase ABC (Supp. 5.2).

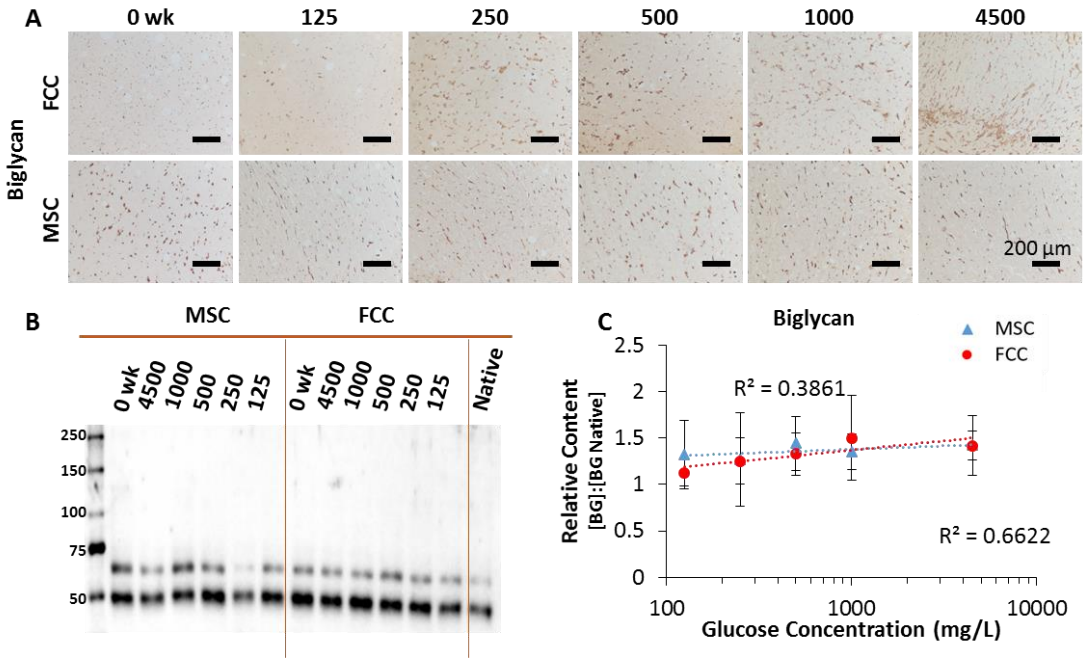

Figure 5.5: Biglycan expression in tissue engineered constructs after 4 weeks. (A) IHC staining of LF-96 biglycan antibody (B) Representative western blot of LF-96 Biglycan antibody (C) Densitometry analysis of western blots (n=4). Relative expression compared to native meniscus tissue. Bar=200µm

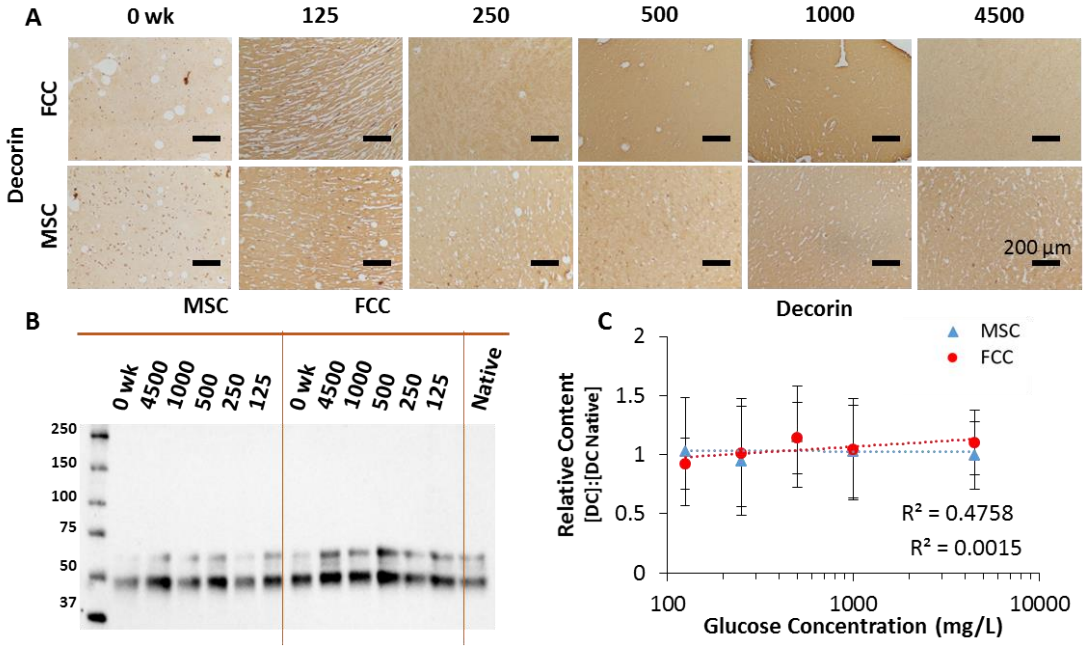

Figure 5.6: Decorin expression in tissue engineered constructs after 4 weeks. (A) IHC staining of LF-94 decorin antibody (B) Representative western blot of LF-94 decorin antibody (C) Densitometry analysis of western blots (n=4). Relative expression compared to native meniscus tissue.

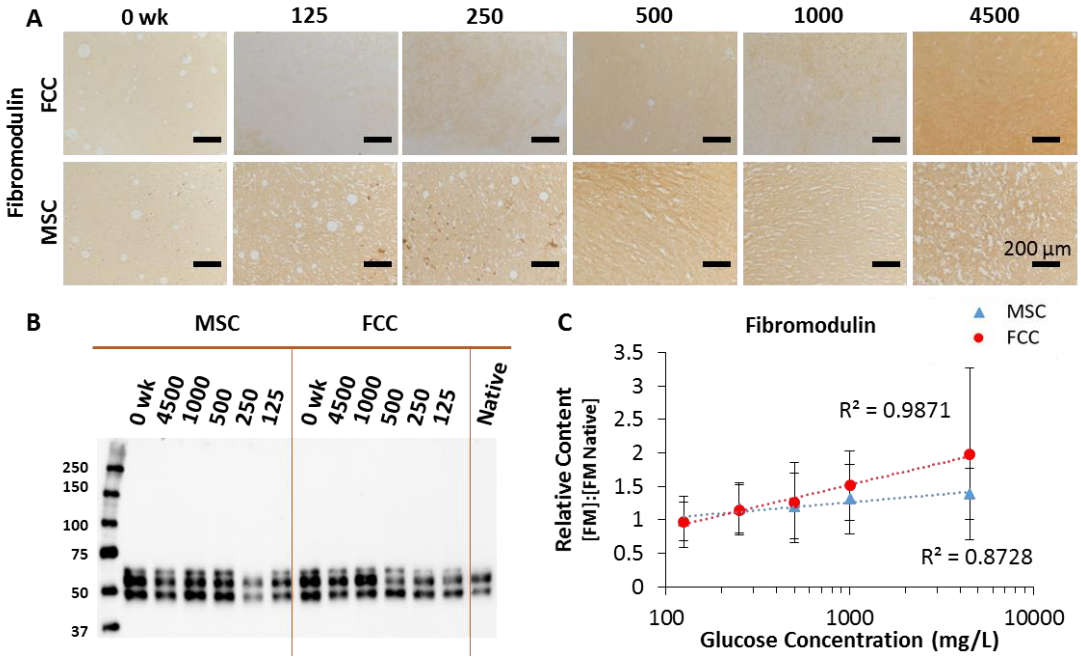

Figure 5.7: Fibromodulin expression in tissue engineered constructs after 4 weeks. (A) IHC staining of fibromodulin antibody (B) Representative western blot of fibromodulin antibody (C) Densitometry analysis of western blots (n=4). Relative expression compared to native meniscus tissue.

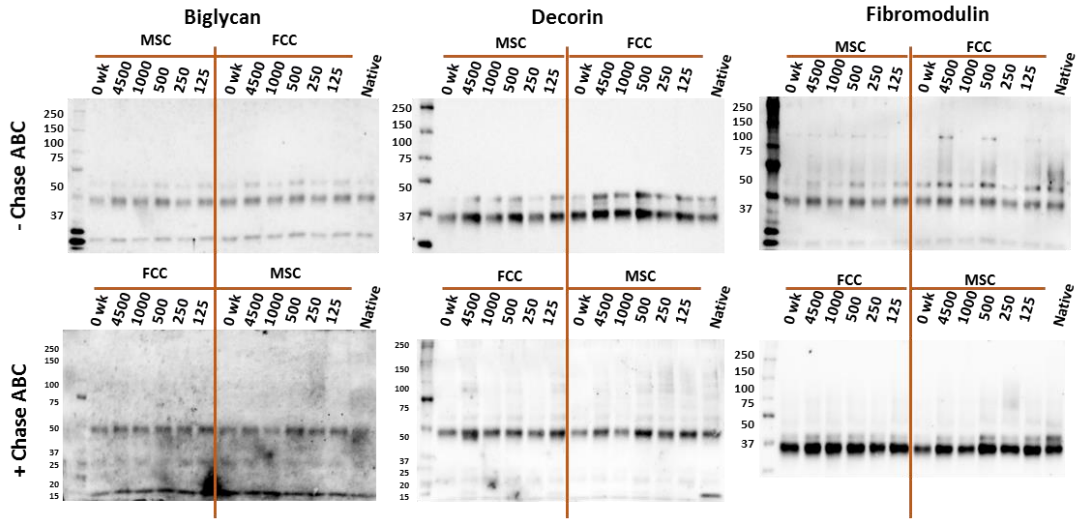

Supplemental 5.2: Western blots with and without chondoitinase ABC (Chase ABC). Banding is reduced after application of chondoitinase ABC to biglycan, decorin, and fibromodulin western blots.

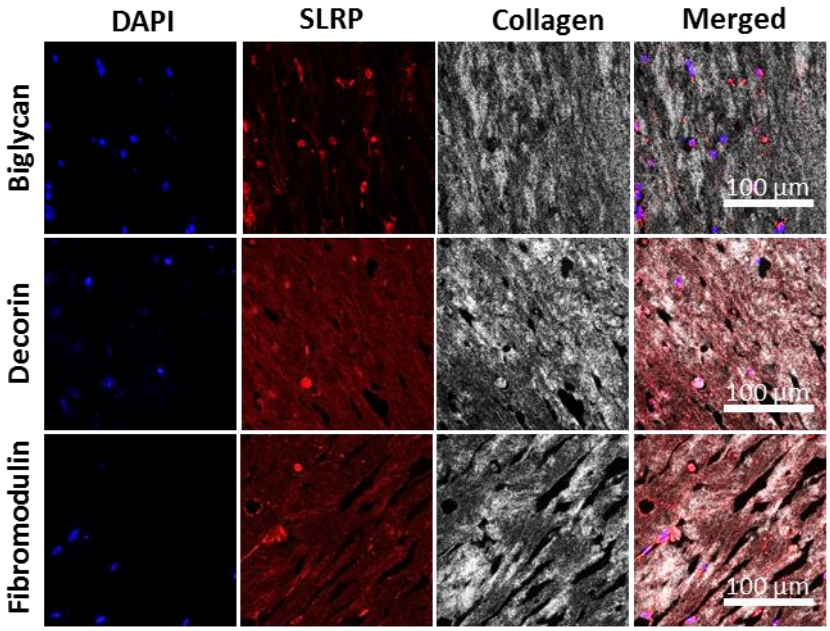

Supplemental 5.3: Immunofluorescent staining of SLRP antibodies biglycan, decorin, and fibromodulin. DAPI staining was used to label cell nuclei and confocal reflectance was used to visualize collagen fibers.

Collagen Fiber Formation

Collagen fibers were visualized using multiphoton microscopy (Figure 5.8A). At 0 weeks meniscus constructs appeared amorphous with no clear fiber definition and fiber directionality. Following 4 weeks of culture, fiber formation was evident in all culture groups. A striated appearance in collagen signal indicates the formation of fibers. Fibers showed greater definition and fiber directionality at 500 mg/L with definition and directionality decreasing at higher and lower glucose concentration. Fiber analysis quantified a peak in fiber alignment and fiber diameter at 500 mg/L glucose concentration (Figure 5.8B and 5.8C). Paired measurements between GAG/ww and fiber formation quantification fit to a Gaussian model indicated peak alignment and fiber diameter at 0.38 and 0.39 µg GAG/ww respectively (alignment index R^2=0.04 and FCC R^2=0.21) (Figure 5.8D and 5.8E).

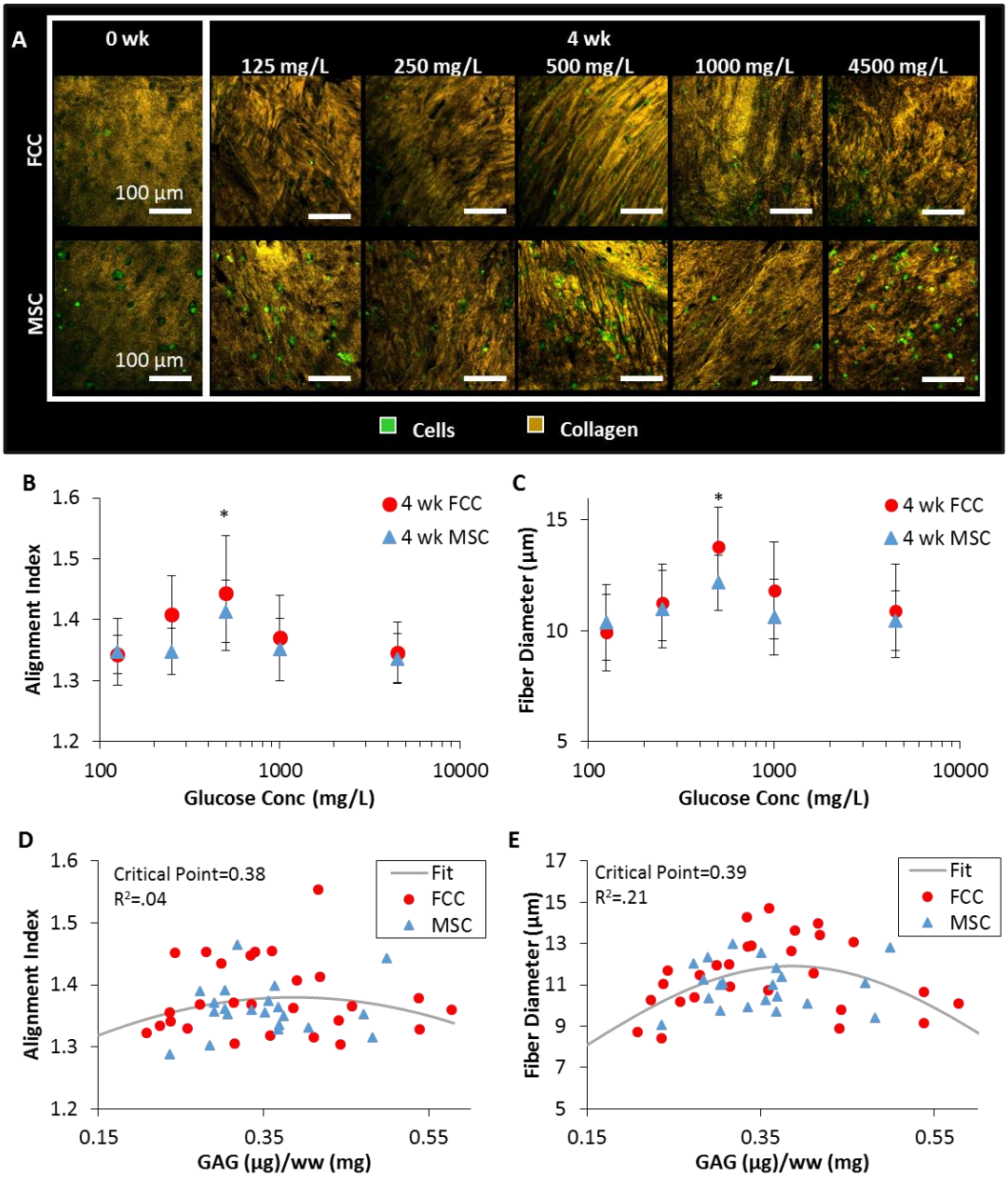

Figure 5.8: Fiber formation analysis in tissue engineered menisci after 4 weeks at different glucose concentrations. (A) Representative multiphoton microscopy images showing fiber formation in 0 and 4 week meniscus constructs. Fiber analysis of multiphoton microscopy images. (B) Degree of alignment measured as the alignment index. (C) Average collagen fiber diameter. (* significantly different than other glucose concentrations, $p<0.05$, n=4-6). (D) GAG/ww as a predictor for fiber formation measured by alignment index or (E) fiber diameter (Gaussian fit model applied to paired measurements in all glucose concentration groups, n=21-27).

Discussion

The goal of this study was to further explore the relationship between proteoglycans and fiber organization in tissue engineered constructs. We hypothesized that reducing downstream production of proteoglycans through decreased glucose availability in the media would result in increased fiber formation in tissue engineered constructs. Reduction in glucose availability to cells did result in small reductions in DNA and oxidative reduction, however cell contractility actively occurred throughout the duration of the 4 week culture. GAG production in the construct had a dose dependent response to glucose concentration in the media with average EC_{50} at ~375 mg/L glucose. The SLRP with the highest sensitivity to changes in glucose was fibromodulin. Alignment index and fiber diameter were highest in the 500 mg/L group, which is significantly lower than traditional media. Model fit analysis indicates that fiber formation is maximal at 0.39 µg GAG/ww in constructs.

Cells are known to be highly sensitive to changes in glucose availability. When glucose is removed from chondrocytes, glycolysis is inhibited, which reduces ATP production from the Krebs cycle and oxidative phosphorylation/electron transport chain increases as a mechanism known as the crabtree effect [59]. These studies identified the threshold of glucose deprivation is 2.7 mM where cellular oxygen consumption begin to be upregulated [59]. In this study, we worked with concentrations above and below this threshold: 4500 mg/L or 25 mM, 1000 mg/L or 5.5 mM, 500 mg/L or 2.75 mM, 250 mg/L or 1.4 mM, and 125 mg/L or 0.69 mM. Glucose consumption analysis indicated that glucose starvation is likely occurring at lower glucose concentration groups. Glucose starvation reduced the level of oxidative reduction and likely the level

of cell proliferation, indicated by DNA and Alamar blue assays. However, cells in meniscal constructs are still actively contracting throughout the duration of culture. Glucose reduction does result in a corresponding decrease in GAG production, consistent with previous literature [42]. However, fiber formation increases temporarily with glucose reduction, peaking at 500 mg/L. Changes in glucose concentration can also affect collagen biosynthesis, with reduced collagen production in low glucose compared to high glucose [42]. There is a delicate balance in glucose concentration between cellular metabolism and matrix production. The peak in collagen formation just above the threshold for glucose deprivation is likely attributed to the delicate balance.

SLRPs have been implicated as major players in fiber formation in many tissues including the meniscus. IHC analysis showed that fibromodulin and decorin are distributed throughout the collagen matrix whereas biglycan was mostly localized to the intracellular and pericellular space. These findings are consistent with native meniscus, where decorin co-localized heavily with collagen type I and biglycan was largely co-localized with the intracellular and pericellular space [9]. In the western blot analysis, SLRP staining does show multiple banding pattern that were knocked down by chase ABC application, which indicates different levels of glycosylation. Both decorin and biglycan have heavier staining on the core protein band whereas fibromodulin has several bands which may represent keratin sulfate additions during SLRP production. The reduction of fibromodulin maturity with glucose concentration may explain it's more prevalent role in fiber formation. In this study, we found that fibromodulin was the most sensitive to changes in glucose with a 200% increase in FCC menisci between 125 and 4500 mg/mL. Fibromodulin has been heavily implicated in its role in fiber

development in the intervertebral disk [60]. Biglycan and decorin had weak increases in expression in response to changes in glucose. Previous research has shown that while biglycan has a high affinity to fibers, it has little impact on fibrillogenesis, whereas increasing amounts of decorin reduced fibril diameter [35]. Several knockout models of decorin heavily implicate decorin's important role in fiber formation [21, 22]. This study demonstrates that glucose can be used to control production of fibromodulin, however has an insignificant impact on biglycan and decorin. A different model will need to be used to further probe the role of decorin in guiding fiber formation in tissue engineered constructs.

Large scale proteoglycans can sterically hinder fiber formation through the aggregation of ions and physically reducing the proximity of fibrils to block fibril aggregation into fibers. SLRPs are known for their role in modulating fiber formation whereas larger molecules such as versican and aggrecan influence fiber formation through their physical presence rather than their interaction with fibers (Figure 5.1). SLRPs only account for a very small portion of the total GAG in the meniscus, with chondroitin sulfate from aggrecan accounting for most of what's measured by the DMMB assay [61, 62]. Decorin has 1 chondroitin sulfate chain, biglycan has 2 chondroitin or dermatan sulfate chain, and fibromodulin has 3-5 keratin sulfate side chains compared to aggrecan with >100 chondroitin sulfate chains [39] . The changes in SLRP concentration measured by western blot account for a small portion of the GAG reduction measured by the DMMB assay. Therefore the changes in GAG production measured by the DMMB assay are likely attributed to aggrecan. A peak in fiber formation at reduced GAG concentration supports the hypothesis that excessive GAG

production, specifically large proteoglycans, is inhibiting fiber formation. This hypothesis is further supported in other work using chondoitinase ABC to remove chondoitinase side chains on aggrecan molecules. Previous work in chondrocytes showed increases in tensile modulus and collagen concentration with treatments of chondoitinase ABC [63]. This has also been shown with FCCs in tissue engineered menisci in which chondoitinase ABC increased mechanical properties, collagen accumulation and fiber diameter [17, 26]. In this study we show that glucose is another tool to decrease the prevalence of GAGs in tissue engineered constructs.

The amount of glucose used in most meniscus media is 4.5x the concentration of blood and synovial fluid glucose concentrations. After surveying publications from the meniscus tissue engineering field, of those that reported glucose concentration, 100% of those groups used high glucose media formulation throughout culture, some examples [5, 16, 17]. It is important to note that tendon tissue engineering, another highly fibrous tissue, typically uses low glucose media formulations, some examples [64, 65]. In this study, the EC_{50} for GAG production in this study was less than 10% of the 4500 mg/L glucose concentration. High glucose formulations originated from cartilage tissue engineering research which was trying to achieve high levels of GAG. While the meniscus does contain GAGs, the concentration of GAGs when compared to articular cartilage is 8-fold less [61]. GAGs only make up 0.2-0.8% of wet weight and 1-2% of the dry weight, compared to articular cartilage with is about 10-15% of the wet weight [3, 25, 66, 67]. While increasing levels of GAGs are typically considered positive markers in meniscus tissue engineering, GAG levels increase throughout meniscus development [10]. In development the increasing levels of GAG content occur

after initial fiber architecture is established [8, 10, 68, 69]. The high glucose formulation of media was initially targeted for articular cartilage where high levels of GAG are desirable and large organized fibers are not essential. In order to better guide cellular organization of large diameter fibers, lower glucose formulations could be used to aid in fiber development before increasing GAG content in tissue engineered menisci.

In conclusion, we found that glucose can be used as a tool to reduce total GAG production and specifically reduces fibromodulin production. Changes in GAG production resulted in corresponding increase in fiber alignment and fiber diameter. Increases in fiber formation declined at concentrations below 500 mg/L likely due to decreased cellular metabolic activity. Menisci seeded with MSCs and FCCs both showed similar trends, demonstrating that these effects apply to multiple cell types and can be applied as a technique to guide stem cell behavior.

REFERENCES

[1] Skaggs DL, Warden WH, and Mow VC. Radial tie fibers influence the tensile properties of the bovine medial meniscus. J. Orthop. Res. 1994; 12:2: 176–185.

[2] Andrews SHJ, Rattner JB, Abusara Z, Adesida A, Shrive NG, and Ronsky JL. Tie-fibre structure and organization in the knee menisci. J. Anat. 2014; 224:5: 531–7.

[3] Herwig J, Egner E, and Buddecke E. Chemical changes of human knee joint menisci in various stages of degeneration. Ann. Rheum. Dis. 1984; 43:4: 635–40.

[4] Messner K and Gao J. The menisci of the knee joint. Anatomical and functional characteristics, and a rationale for clinical treatment. J. Anat. 1998; 193 (Pt 2: 161–178.

[5] Puetzer JL and Bonassar LJ. Physiologically Distributed Loading Patterns Drive the Formation of Zonally Organized Collagen Structures in Tissue Engineered Meniscus. Tissue Eng. Part A. 2016; 22:607: 1–40.

[6] Petersen W and Tillmann B. Collagenous fibril texture of the human knee joint menisci. Anat. Embryol. (Berl). 1998; 197:4: 317–24.

[7] Arnoczky SP and Warren RF. Microvasculature of the human meniscus. Am. J. Sports Med. 1982; 10:2: 90–5.

[8] Clark CR and Ogden JA. Prenatal and Postnatal Development of Human Knee Joint Mensci. Iowa Orthop. J. 1981; 1:1: 20–27.

[9] Vanderploeg EJ, Wilson CG, Imler SM, Ling CHY, and Levenston ME. Regional variations in the distribution and colocalization of extracellular matrix proteins in the juvenile bovine meniscus. J. Anat. 2012; 221:2: 174–186.

[10] Ling CHY, Lai JH, Wong IJ, and Levenston ME. Bovine meniscal tissue exhibits age- and interleukin-1 dose-dependent degradation patterns and composition-function relationships. J. Orthop. Res. 2016; 34:5: 801–811.

[11] Han WM, Heo S-J, Driscoll TP, Delucca JF, McLeod CM, Smith LJ, Duncan RL, Mauck RL, and Elliott DM. Microstructural heterogeneity directs micromechanics and mechanobiology in native and engineered fibrocartilage. Nat. Mater. 2016; 15: 477–484.

[12] Balint E, Gatt CJ, and Dunn MG. Design and mechanical evaluation of a novel fiber-reinforced scaffold for meniscus replacement. J. Biomed. Mater. Res. - Part A. 2012; 100 A:1: 195–202.

[13] Patel JM, Merriam AR, Culp BM, Gatt CJ, and Dunn MG. One-Year Outcomes of Total Meniscus Reconstruction Using a Novel Fiber-Reinforced Scaffold in an Ovine Model. Am. J. Sports Med. 2016; 44:4: 898–907.

[14] Merriam a. R, Patel JM, Culp BM, Gatt CJ, and Dunn MG. Successful Total Meniscus Reconstruction Using a Novel Fiber-Reinforced Scaffold: A 16- and 32-Week Study in an Ovine Model. Am. J. Sports Med. 2015;

[15] Lee CH, Rodeo SA, Fortier LA, Lu C, Erisken C, and Mao JJ. Protein-releasing polymeric scaffolds induce fibrochondrocytic differentiation of endogenous cells for knee meniscus regeneration in sheep. 2014; 6:266: 1–12.

[16] Baker BM and Macuk RL. The effect of nanofiber alignment on the maturation of engineering meniscus constructs. Biomaterials. 2007; 28:11: 1967–1977.

[17] Huey DJ and Athanasiou KA. Maturational growth of self-assembled, functional menisci as a result of TGF-B1 and enzymatic chondroitinase-ABC stimulation. Biomaterials. 2011; 32:8: 2052–2058.

[18] Higashioka MM, Chen J a, Hu JC, and Athanasiou K a. Building an anisotropic meniscus with zonal variations. Tissue Eng. Part A. 2014; 20:1–2: 294–302.

[19] Puetzer JL, Koo E, and Bonassar LJ. Induction of fiber alignment and mechanical anisotropy in tissue engineered menisci with mechanical anchoring. J. Biomech. 2015; 48: 1436–1443.

[20] McCorry MC and Bonassar LJ. Fiber development and matrix production in tissue-engineered menisci using bovine mesenchymal stem cells and fibrochondrocytes. Connect. Tissue Res. 2017; 58:3–4: 329–341.

[21] Huey DJ and Athanasiou K a. Tension-compression loading with chemical stimulation results in additive increases to functional properties of anatomic meniscal constructs. PLoS One. 2011; 6:11: e27857.

[22] Puetzer JL and Bonassar LJ. Physiologically Distributed Loading Patterns Drive the Formation of Zonally Organized Collagen Structures in Tissue Engineered Meniscus. Tissue Eng. Part A. 2016; 22:13 and 14: 907–916.

[23] Moyer JT, Priest R, Bouman T, Abraham AC, and Haut Donahue TL. Indentation properties and glycosaminoglycan content of human menisci in the deep zone. Acta Biomater. 2013; 9:5: 6624–6629.

[24] Nakano T, Dodd CM, and Scott PG. Glycosaminoglycans and proteoglycans from different zones of the porcine knee meniscus. J. Orthop. Res. 1997; 15:2: 213–220.

[25] Wilson CG, Nishimuta JF, and Levenston ME. Chondrocytes and Meniscal Fibrochondrocytes Differentially Process Aggrecan During De Novo Extracellular Matrix Assembly. Tissue Eng. Part A. 2009; 15:7: 1513–1522.

[26] Macbarb RF, Makris E a, Hu JC, and Athanasiou K a. A chondroitinase-ABC and TGF-β1 treatment regimen for enhancing the mechanical properties of tissue-engineered fibrocartilage. Acta Biomater. 2012; October:

[27] Melrose J, Smith S, Cake M, Read R, and Whitelock J. Comparative spatial and temporal localisation of perlecan, aggrecan and type I, II and IV collagen in the ovine meniscus: An ageing study. Histochem. Cell Biol. 2005; 124:3–4: 225–235.

[28] Tavakoli Nia H, Han L, Soltani Bozchalooi I, Roughley P, Youcef-Toumi K, Grodzinsky AJ, and Ortiz C. Aggrecan nanoscale solid-fluid interactions are a primary determinant of cartilage dynamic mechanical properties. ACS Nano. 2015; 9:3: 2614–2625.

[29] Wang VM, Bell RM, Thakore R, Eyre DR, Galante JO, Li J, Sandy JD, and Plaas A. Murine tendon function is adversely affected by aggrecan accumulation due to the knockout of ADAMTS5. J. Orthop. Res. 2012; 30:4: 620–6.

[30] Garg AK, Berg RA, Silver FH, and Garg HG. Effect of proteoglycans on type I collagen fibre formation. Biomaterials. 1989; 10:6: 413–419.

[31] Viola M, Bartolini B, Sonaggere M, Giudici C, Tenni R, and Tira ME. Fibromodulin interactions with type I and II collagens. Connect. Tissue Res. 2007; 48:3: 141–8.

[32] Wiberg C, Hedbom E, Khairullina A, Lamandé SR, Oldberg Å, Timpl R, Mörgelin M, and Heinegård D. Biglycan and Decorin Bind Close to the N-terminal Region of the Collagen VI Triple Helix. J. Biol. Chem. 2001; 276:22: 18947–18952.

[33] Zhang G, Ezura Y, Chervoneva I, Robinson PS, Beason DP, Carine ET, Soslowsky LJ, Iozzo R V., and Birk DE. Decorin regulates assembly of collagen fibrils and acquisition of biomechanical properties during tendon development. J. Cell. Biochem. 2006; 98:6: 1436–1449.

[34] Danielson KG, Baribault H, Holmes DF, Graham H, Kadler KE, and Iozzo R V. Targeted disruption of decorin leads to abnormal collagen fibril morphology and skin fragility. J. Cell Biol. 1997; 136:3: 729–743.

[35] Douglas T, Heinemann S, Bierbaum S, Scharnweber D, and Worch H. Fibrillogenesis of collagen types I, II, and III with small leucine-rich proteoglycans decorin and biglycan. Biomacromolecules. 2006; 7:8: 2388–2393.

[36] Vogel KG, Paulsson M, and Heinegård D. Specific inhibition of type I and type II collagen fibrillogenesis by the small proteoglycan of tendon. Biochem. J. 1984; 223:3: 587–97.

[37] Vogel KG and Trotter JA. The Effect of Proteoglycans on the Morphology of Collagen Fibrils Formed In Vitro. Coll. Relat. Res. 1987; 7:2: 105–114.

[38] Mobasheri A, Vannucci SJ, Bondy CA, Carter SD, Innes JF, Arteaga MF, Trujillo E, Ferraz I, Shakibaei M, and Mart??n-Vasallo P. Glucose transport and metabolism in chondrocytes: A key to understanding chondrogenesis, skeletal development and cartilage degradation in osteoarthritis. Histol. Histopathol. 2002; 17:4: 1239–1267.

[39] Varki A, Cummings R, Esko J, Freeze H, Stanley P, Bertozzi C, Hart G, and Etzler M. Essentials of Glycobiology, 2nd Editio. Cold Spring Harbor, NY: Cold Spring Harbor Laboratory Press, 2009.

[40] Otte P. basic metablism of articular cartilage. Z. Rheumatol. 1991; 50:5: 304–312.

[41] Silver IA. Measurement of pH and ionic compostion of pericellular sites.pdf. Philos. Trans. Biol. Sci. 1975; 271:912: 261–272.

[42] Chawla S, Chameettachal S, and Ghosh S. Probing the role of scaffold dimensionality and media composition on matrix production and phenotype of fibroblasts. Mater. Sci. Eng. C. 2015; 49: 588–596.

[43] Rinkler C, Heuer F, Pedro MT, Mauer UM, Ignatius A, and Neidlinger-Wilke C. Influence of low glucose supply on the regulation of gene expression by nucleus pulposus cells and their responsiveness to mechanical loading. J. Neurosurg. Spine. 2010; 13:4: 535–42.

[44] Baker BM, Nathan AS, Gee AO, and Mauck RL. The influence of an aligned nanofibrous topography on human mesenchymal stem cell fibrochondrogenesis. Biomaterials. 2010; 31:24: 6190–6200.

[45] Bonnevie ED, McCorry MC, and Bonassar LJ. Mesenchymal Stem Cells Enhance Lubrication of Engineered Meniscus Through Lubricin Localization in Collagen Gels. Biotribology. 2016;

[46] Ballyns JJ, Wright TM, and Bonassar LJ. Effect of media mixing on ECM assembly and mechanical properties of anatomically-shaped tissue engineered meniscus. Biomaterials. 2010; 31:26: 6756–63.

[47] Puetzer JL and Bonassar LJ. High Density Type I Collagen Gels for Tissue Engineering of Whole Menisci. Acta Biomater. 2013; 9:8: 7787–7795.

[48] McCorry MC, Puetzer JL, and Bonassar LJ. Characterization of mesenchymal stem cells and fibrochondrocytes in three-dimensional co-culture: analysis of cell shape, matrix production, and mechanical performance. Stem Cell Res. Ther. 2016; 7:1: 39.

[49] Bernacki SH, Wall ME, and Loboa EG. Isolation of human mesenchymal stem cells from bone and adipose tissue. Methods Cell Biol. 2008; 86:8: 257–78.

[50] Mackay AM, Beck SC, Murphy JM, Barry FP, Chichester CO, and Pittenger MF. Chondrogenic differentiation of cultured human mesenchymal stem cells from marrow. Tissue Eng. 1998; 4:4: 415–28.

[51] Bowles RD, Williams RM, Zipfel WR, and Bonassar LJ. Self-Assembly of Aligned Tissue-Engineered Annulus fibrosus and Intervertebral Disc Composite Via Collagen Gel Contraction. Tissue Eng. Part A. 2010; 16:4:.

[52] Cross VL, Zheng Y, Won Choi N, Verbridge SS, Sutermaster B a., Bonassar LJ, Fischbach C, and Stroock AD. Dense type I collagen matrices that support

cellular remodeling and microfabrication for studies of tumor angiogenesis and vasculogenesis in vitro. Biomaterials. 2010; 31:33: 8596–8607.

[53] Puetzer JL and Bonassar LJ. Acta Biomaterialia High density type I collagen gels for tissue engineering of whole menisci. 2013; 9: 7787–7795.

[54] McCorry MC, Mansfield MM, Sha X, Coppola DJ, Lee JW, and Bonassar LJ. A model system for developing a tissue engineered meniscal enthesis. Acta Biomater. 2017; 56: 110–117.

[55] Kim YJ, Sah RL, Doong JY, and Grodzinsky AJ. Fluorometric assay of DNA in cartilage explants using Hoechst 33258. Anal. Biochem. 1988; 174:1: 168–176.

[56] Enobakhare BO, Bader DL, and Lee DA. Quantification of sulfated glycosaminoglycans in chondrocyte/alginate cultures, by use of 1,9-dimethylmethylene blue. Anal. Biochem. 1996; 243:1: 189–191.

[57] Neuman R and Logan M. The determination of hydroxyproline. J. Biol. Chem. 1949; 184:1: 299–306.

[58] Bowles RD, Williams RM, Zipfel WR, and Bonassar LJ. Self-assembly of aligned tissue-engineered annulus fibrosus and intervertebral disc composite via collagen gel contraction. Tissue Eng. Part A. 2010; 16:4: 1339–1348.

[59] Heywood HK, Bader DL, and Lee DA. Rate of oxygen consumption by isolated articular chondrocytes is sensitive to medium glucose concentration. J. Cell. Physiol. 2006; 206:2: 402–410.

[60] Hayes AJ, Isaacs MD, Hughes C, Caterson B, and Ralphs JR. Collagen fibrillogenesis in the development of the annulus fibrosus of the intervertebral disc. Eur. Cells Mater. 2011; 22:0: 226–241.

[61] Adams ME and Muir H. The glycosaminoglycans of canine menisci. Biochem. J. 1981; 197:2: 385–389.

[62] Farndale RW, Sayers CA, and Barrett AJ. A Direct Spectrophotometric Microassay for Sulfated Glycosaminoglycans in Cartilage Cultures. Connect. Tissue Res. 1982; 9:4: 247–248.

[63] Bian L, Crivello KM, Ng KW, Xu D, Williams DY, Ateshian GA, and Hung CT. Influence of Temporary Chondroitinase ABC-Induced Glycosaminoglycan Suppression on Maturation of Tissue-Engineered Cartilage. Tissue Eng. Part A. 2009; 15:8: 2065–2072.

[64] Awad HA, Butler DL, Harris MT, Ibrahim RE, Wu Y, Young RG, Kadiyala S, and Boivin GP. In vitro characterization of mesenchymal stem cell-seeded collagen scaffolds for tendon repair: Effects of initial seeding density on contraction kinetics. J. Biomed. Mater. Res. 2000; 51:2: 233–240.

[65] Nirmalanandhan VS, Levy MS, Huth AJ, and Butler DL. Effects of cell seeding density and collagen concentration on contraction kinetics of mesenchymal stem cell-seeded collagen constructs. Tissue Eng. 2006; 12:7: 1865–72.

[66] Chen S, Fu P, Wu H, and Pei M. Meniscus, articular cartilage and nucleus pulposus: a comparative review of cartilage-like tissues in anatomy, development and function. Cell Tissue Res. 2017;

[67] Heinegård D and Oldberg A. Structure and biology of cartilage and bone matrix noncollagenous macromolecules. FASEB J. 1989; 3:9: 2042–2051.

[68] Gardner E and O'Rahilly R. The early development of the knee joint in staged human embryos. J. Anat. 1968; 102:Pt 2: 289–99.

[69] Gray DJ and Gardner E. Prenatal development of the human knee and superior tibiofibular joints. Am. J. Anat. 1950; 86:2: 235–287.

CHAPTER 6

A Model System for Developing a Tissue Engineered Meniscal Enthesis[5]

Abstract

The meniscus acts as a stabilizer, lubricator, and load distributer in the knee joint. The mechanical stability of the meniscus depends on its connection to the underlying bone by a fibrocartilage to bone transition zone called the meniscal enthesis. Tissue engineered menisci hold great promise as a treatment alternative however lack a means of integrated fixation to the underlying bone needed in order for a tissue engineered meniscal replacement to be successful. Tissue engineering the meniscal enthesis is a difficult task given the complex gradients of cell type, mineral, and extracellular matrix molecules. Therefore there is a need for a simplified and high throughput enthesis model to test experimental parameters. The goal of this study was to develop a simplified enthesis model to test collagen integration with decellularized bone. We found that injection molding collagen into tubing loaded with decellularized bone plugs results in a scaffold with three regions: bone, bone-collagen, and collagen. Furthermore, collagen formation was directed in the axial direction using mechanical fixation at the bony ends. The results of this study show that this technique can be used to mimic the native enthesis morphology and serves as ideal test platform to generate a model tissue engineered enthesis.

---

[5]M. C. McCorry, M. M. Mansfield, X. Sha, D. J. Coppola, J. W. Lee and L. J. Bonassar. A model system for developing a tissue engineered meniscal enthesis. *Acta Biomater*. **56,** 110–117 (2017).

Introduction

The meniscus is a fibrocartilaginous structure in the knee that plays an essential role in the biomechanics and lubrication of the knee [1]. Loss or damage of the meniscus increases contact pressures within the knee and is known to lead to osteoarthritis [2,3]. Since natural healing of the meniscus is limited, current treatment options are partial meniscectomy, surgical repair, or meniscal allograft [4]. Other promising treatment options include artificial replacements, such as Actifit® and Menaflex™ collagen meniscus implant, and tissue engineered menisci [5,6].

A significant amount of work has been done on meniscus tissue engineering. Multiple reported approaches include using poly($^{\varepsilon}$-caprolactone) fibers seeded with encapsulated growth factors [7], biodegradable polyglycolic acid scaffold [8], and scaffold free self-assembly [9] to tissue engineer the meniscus. We have developed a cellular collagen based construct that is anatomically accurate including ligamentous extensions from the horns [10,11]. Additionally, we used mechanical fixation to anchor the tissue engineered meniscus at the horns to guide anisotropic fiber formation which improved mechanical and biochemical properties of the tissue engineered menisci [12]. Tissue engineered approaches have focused on the main body of the meniscus or simply aimed at a partial replacement. Proper fixation and restoration of the meniscal enthesis is necessary for long term success of a replacement. Tissue engineered menisci have shown great promise, however these methods are limited to partial meniscal replacement since they lack a soft tissue to bone enthesis for meniscal horn fixation.

The meniscus is attached to underlying bone at the meniscal horns by the meniscal entheses. The meniscal enthesis is a highly complex structure that consists of

a gradient from fibrocartilage to bone tissue and provides mechanical fixation from a tensile loading environment to a compressive loading environment [13]. The meniscus to bone enthesis has four distinct regions: the ligamentious zone, uncalcified fibrocartilage, calcified fibrocartilage, and bone [14,15]. The ligamentous zone contains primarily fibroblasts and highly aligned collagen type I. The uncalcified fibrocartilage zone consists of fibrochondrocytes (FCCs), chondrocytes, unaligned collagen type II, and proteoglycans. The calcified fibrocartilage contains hypertrophic chondrocytes and collagen types II and X. The bone region contains osteoblast, osteoclasts, osteocytes and collagen type I. These structures in combination are crucial to the mechanical performance of the meniscus [13,16]. Studies comparing allograft fixation methods have shown preserving the native enthesis and anchoring bone to bone is more successful over soft tissue to bone [17]. These methods provide a template for successful integration of tissue engineered menisci, however, methods for producing a tissue engineered meniscal enthesis have not been established.

The meniscal enthesis is a complex structure that is difficult to replicate *in vitro*. There are no published works on tissue engineering the meniscus to bone enthesis, however several groups have done work on tissue engineering the tendon- and ligament-to bone enthesis. Tendon, ligament, cartilage, and meniscal transitions to bone have similar complexities in structure since all three entheses transition from soft tissue to bone with complex gradients of extracellular matrix and cells [18]. Multiphasic scaffolds that use cell type, material, and chemical gradients are a common approach to tissue engineering the soft tissue to bone transition. Efforts to tissue engineer the ligamentous enthesis have used synthetic materials that are then seeded with co-culture

cell gradients [19–21], while other approaches utilize cellular matrix production to generate constructs from cell monolayers [22–24]. Osteochondral studies have developed bioreactor models that utilize diffusion systems to establish mineralization gradients in hydrogels [25,26]. While the meniscal enthesis has structural similarities to bone transition zones of ligament, tendon, and cartilage, there are distinct aspects to the meniscal attachment that necessitate a unique design approach for this interface.

Notably the fibers extend at an angle from the meniscus into underlying bone, unlike ligament and tendon where the fiber direction is consistent across the interface. Fibers from the meniscus interdigitated into the underlying bone are essential to the biomechanical performance of the meniscus [13,27]. However, little focus has been directed at replicating the integration of collagen fibers at the interface. Furthermore the meniscus has a unique cell type, fibrochondrocytes, whose behavior at such interfaces has not yet been characterized. Collagen type I gels are a common scaffold material used in tissue engineering and local fiber organization can be guided by static mechanical boundary condition such as clamping [28]. We hypothesize that integrated fiber formation can be guided by applying a mechanical boundary condition to a multiphasic scaffold using decellularized bone plugs and collagen.

The meniscal enthesis is a complex tissue and methods to generate an integrated tissue construct with a soft to hard transition is not well understood. The overarching goal of this project is to develop an experimental platform to study integration of meniscus tissue with bone. Such a platform would enable targeted experiments on the effect chemical and mechanical signals that affect cellular behavior in the meniscal enthesis. The specific goal of this study was to examine the integration of FCC seeded

collagen gels to decellularized bone and determine the effect of clamping on the organization of collagen at the soft tissue to bone interface.

Methods

Bone Plug Extraction

Trabecular bone plugs were extracted from the distal femur of 1-3 day old bovids using a 6 mm diameter coring bit. Bone cores were sectioned into 10 mm long cylinders that were then decellularized in order to remove cellular debris while maintaining trabecular scaffold material and shape (Figure 6.6.2A). Bone plugs were rinsed of all marrow and debris using a stream of high velocity deionized water. Plugs were then washed in a solution of phosphate buffered saline (PBS) with 0.1% ethylenediaminetetraacetic acid (EDTA) (wt/vol%) and placed on shaker at room temperature. Following the washes, bone plugs were put in a hypotonic buffer (10mM Trizma base, 0.1% EDTA (wt/vol%) and soaked for at least 24 hours at 4°C. Bone plugs were soaked in a detergent comprised of 10mM Trizma base and 0.5% sodium dodecyl sulfate (SDS) (wt/vol%) for 24 hours at room temperature on a shaker to remove cellular debris. Decellularization of samples was confirmed by staining histological samples with hematoxylin (Supplemental 6.2). Bone plugs demineralized using a similar protocol have been shown to be viable scaffold for tissue engineering bone [29,30]. Following washes with PBS, samples were frozen for later use. Prior to experimental use, bone plugs were lyophilized and soaked in ethanol for 2 hours, rinsed with PBS, and then soaked in Dulbecco's modified Eagle's medium (DMEM).

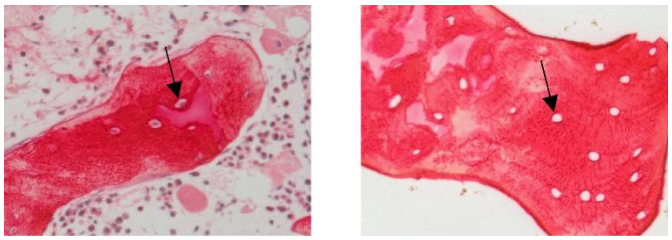

Supplemental 6.2: Bone plug samples stained with Picrosirius red and counterstained with hematoxylin. Trabecular bone untreated control (left). Trabecular bone after decellularization process (right). Arrows indicate cell lacuna, lacuna lack osteocytes in the decellularized trabecular bone.

Construct Generation

Constructs were comprised of decellularized bone plugs, high density collagen type I, and FCCs (Supplementary Video 6.1). Collagen was extracted from Sprague-Dawley rat tails (Pel-Freez Biologicals, Rogers, AZ) as previously described [10,31]. Briefly, rat tail tendons were purified and dissolved in 0.1% acetic acid at a stock concentration of 30 mg/mL stored at 4ºC. FCCs were obtained from the menisci of 1-3 day old bovids as previously described [10,32]. Menisci were digested in 0.3% collagenase (Worthington Biochemical Corporation, Lakewood, NJ) dissolved in DMEM for 16-18 hours. The collagenase solution was then filtered through a 100 µm strainer and cells were centrifuged and washed with PBS and suspended in DMEM.

Anatomically accurate tissue engineered menisci terminating in bone where generated by modifying previously designed meniscus molds. Previously designed anatomically accurate meniscus molds were modified to contain the trabecular bone plugs (Figure 6.1) [11,12]. Molds were 3D printed with injection molding ports. Bone plugs were preloaded into the molds and high density collagen was injected into molds resulting in a tissue engineered construct with bony inserts. These constructs contained a large amount of material far from the bone to soft tissue interface that would require

a significant amount of collagen and FCCs to generate. Therefore, a simplified linear design was used to streamline testing to optimize the collagen to bone interface (Figure 6.2).

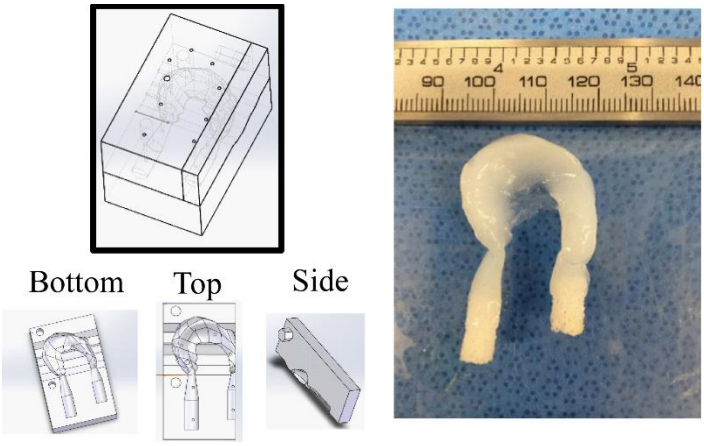

Figure 6.1: Full tissue engineered meniscus with bone plug attachments. Injection mold design for full scale tissue engineered meniscus with enthesis attachments (left). Injection molded anatomically accurate tissue engineered meniscus with integrated bone plug entheses (left).

Enthesis constructs were produced by inserting decellularized bone plugs 20 mm apart into Tygon® tubing (Figure 6.2B). Bone plugs were prevented from moving backwards during injection molding by adding binder clips to either end (Figure 6.2B). Small holes were placed at both ends of the tube to direct air flow and in the center for the injection needle. To start the collagen gelation process the stock collagen was returned to a neutral 7.0 pH and 300mOsm by mixing with a working solution of 1N NaOH, 10x PBS, and 1x PBS. This solution immediately mixed with a cellular media of FCCs for a final concentration of 20 mg/mL collagen and $25x10^6$ cells/mL. The collagen and cells mixture was then injection molded into the center hole in the Tygon® tubing (Figure 6.2C). Constructs were then placed in an incubator at 37ºC for 45 minutes to complete gelation process. Following incubation, constructs were removed from the

Tygon® molding and placed either in a custom machined polysulphone mold for clamping or in a 55 mm^2 petri dish (Figure 6.3A). Constructs placed in the polysulphone mold were clamped into culture troughs 12 hours after construct formation using stainless steel clamps at the bony portion of the constructs. Samples were cultured for 0, 2, and 4 weeks in media containing DMEM, 10% FBS, 100 μg/mL penicillin, 100 μg/mL streptomycin, 0.1 mM non-essential amino acids, 50 μg/mL ascorbate, and 0.4 mM L-proline [10,11]. A total of 10 samples were processed per group with 8 samples tracked for contraction, 6 tensile tested, and 4 embedded in paraffin for histological analysis.

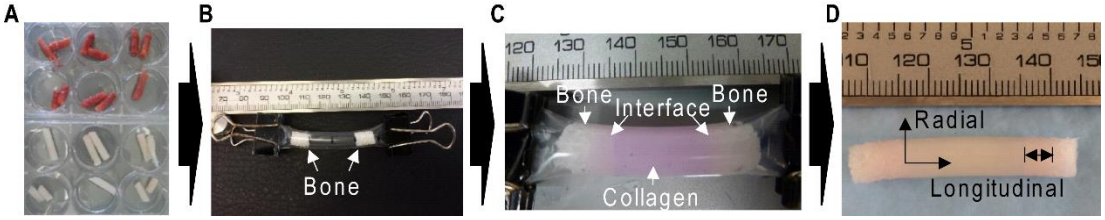

Figure 6.2: (A) Top: 6 mm diameter bone cores from trabecular bone of bovine distal femur. Bottom: Deculluarlized bone cores using a hypotonic and detergent. (B) Bone plugs placed in to Tygon® tubing and clamped at each end (C) Collagen injection molded into Tygon® tubing. (D) Final construct with fiber direction axis labels. Fibers formed along the x-axis in the longitudinal direction or along the y-axis in the radial direction. Double sided arrows on the right indicate interface region where collagen penetrated into the trabecular bone.

Histology

At the conclusion of each culture period, constructs were fixed in 10% buffered formalin for 24-48 hours, demineralized, dehydrated, and embedded in paraffin. Sections of enthesis constructs were cut longitudinally and stained with Masson's trichrome and Picrosirius red. Picrosirius red staining was imaged using both brightfield microscopy and polarized light to illuminate collagen fibers. Histological stains were viewed using a Nikon Eclipse TE2000-S microscope (Nikon Instruments, Melville, NY)

and images taken using a SPOT RT camera (Diagnostic Instruments, Steriling Heights, MI) attached to the microscope.

Tensile Testing

Constructs underwent tensile testing using an Enduratec ElectroForce 3200 System (Bose, Eden Prairie, MN) using a 250 g load cell [11]. A 0.75%/sec strain rate was applied to mimic quasistatic loading. Samples were clamped at bone attachments and length was calculated as the distance between the bone to collagen interfaces. The elastic modulus and ultimate tensile strength (UTS) of the constructs were calculated from the measured stress and strain curves (Supplemental 6.3). The elastic modulus was measured as the slope of the linear elastic region of the stress vs strain curve ($E_{Elastic}$). The UTS was the maximum stress value that the constructs withstood before failure. A second modulus was calculated from the linear portion in the toe region (E_{Toe}). A transition strain (ε_{Trans}) was calculated at the intersection of the linear fits for $E_{Elastic}$ and E_{Toe}.

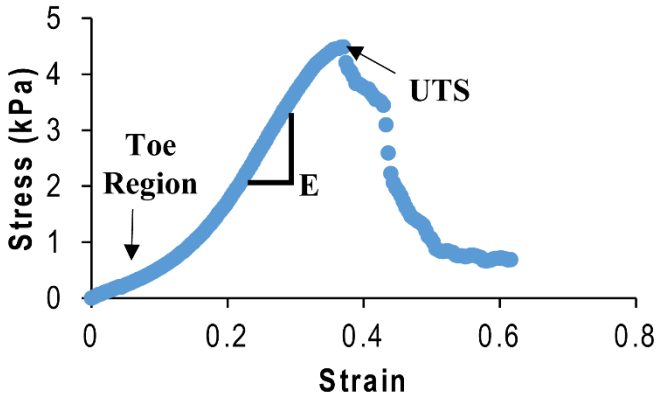

Supplemental 6.3: (A) Sample stress strain curve of tissue engineered meniscal entheses. Samples exhibited non-linear stress-strain behavior with a clear toe region, a linear elastic region, and a failure region. Moduli were calculated from the linear portion of the toe (E_{Toe}) and elastic ($E_{Elastic}$) region of the stress-strain curve. The transition strain (ε_{trans}) was calculated as the intersection of the linear fits to the toe and elastic regions.

Contraction Analysis

Images of the constructs were taken every 3-4 days during media changes. The length, width and area of the constructs were measured using ImageJ [33] and then compared to the length, width and area measured at day 0, to calculate the percent contraction at each day. Length was measured as the distance between the inner edges of bone plugs. Width was measured as the diameter at the center of the construct. Since width varied across the length of the construct, the area of the collagen portion of the construct was measured by outlining the area by hand.

Statistics

All data were analyzed using a 2-way ANOVA with Tukey's post hoc analysis (SigmaPlot, San Jose, California). Data points were graphed with mean ±SD and significance was determined with $p<0.05$.

Results

Construct Generation

Tissue engineered enthesis constructs were assembled in a simple manner that created regions of bone and collagen with a distinct interface (Figure 6.2C). Bone was decellularized, while regions containing collagen were seeded with FCCs throughout the collagen material. Following injection and gelation of collagen, constructs were robust enough for physical handling and manipulation. Collagen penetrated ~3-5mm into the bone plugs on either end, creating an interface region between the bone region and collagen region (Figure 6.2D). Constructs were easily removed from the Tygon® tubing mold and placed in clamping plates to be cultured for up to 4 weeks (Figure

6.3A). Distinct changes in collagen contraction occurred as a result of clamping condition. Clamping greatly affected construct morphology with unclamped samples significantly contracting in length, width, and projected area over 4 weeks ($p<0.05$ for all measurements) (Figure 6.3B-E). In contrast, clamped samples maintained 65-75% of initial dimensions over four weeks (Figure 6.3C-E).

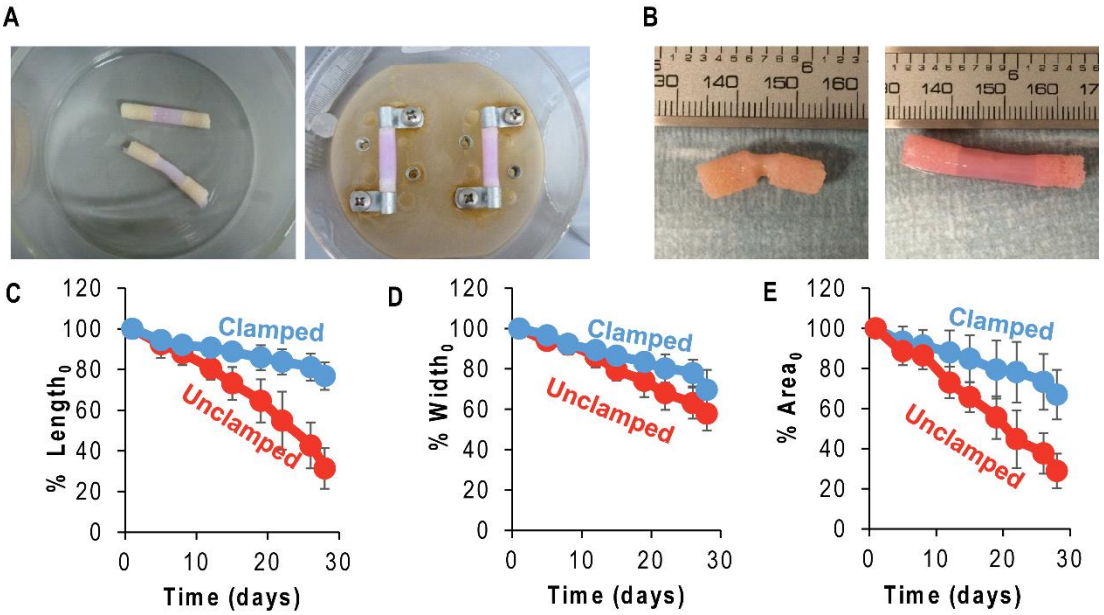

Figure 6.3: (A) Unclamped (left) and clamped (right) enthesis culture set up. (B) Unclamped (left) and clamped (right) construct appearance after 4 week in culture. Projected length (C), width (D), and area (E) over time compared to initial measurements (significantly different with time and condition after 4 weeks or 28 days, $p<0.05$, n=7-8).

Histological Morphology

Apparent morphological similarities between native enthesis and the tissue engineered meniscal enthesis were apparent in Picrosirius red histology (Figure 6.4). The structure of individual trabeculae obtained from decellularized bone have the same morphological organization seen in the native enthesis bone region. Collagen penetrated into the pores between trabeculae at the start of culture, and remained throughout the 4 weeks of culture in both unclamped and clamped samples (Figure 6.4).

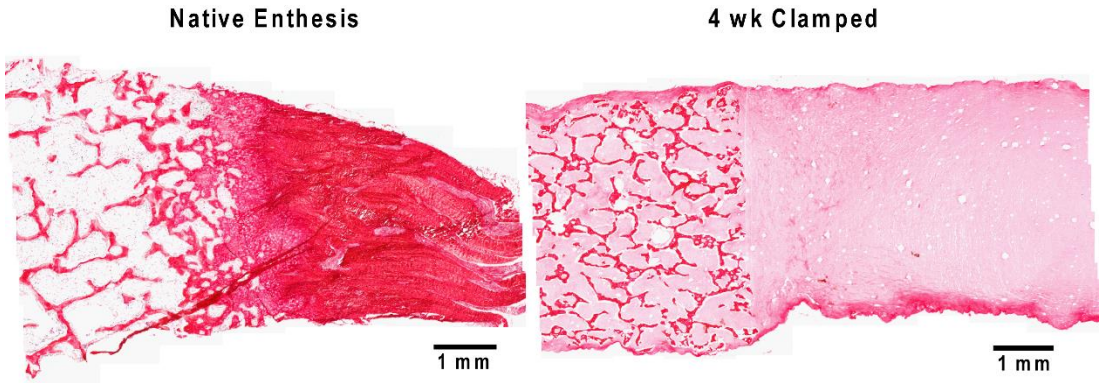

Figure 6.4: Picrosirius red staining of soft tissue to bone interface of native left caudal meniscal enthesis (left) and 4 week clamped tissue engineered meniscal enthesis (right).

Clamping samples during culture induced the formation of large longitudinally oriented fiber bundles (Figure 6.5). At 0 weeks constructs had small disorganized fibers. Unclamped samples developed radially aligned fibers that were parallel to the bone edge interface. In the body and at the radial edge of the collagen region, fibers were smaller and less prominent, but generally still organized parallel to the bone interface. Clamped samples formed fibers mainly along the longitudinal axis of the collagen cylinder. Longitudinal fibers were consistently seen along the outer edge of the collagen cylinder, however fibers were less organized near the center.

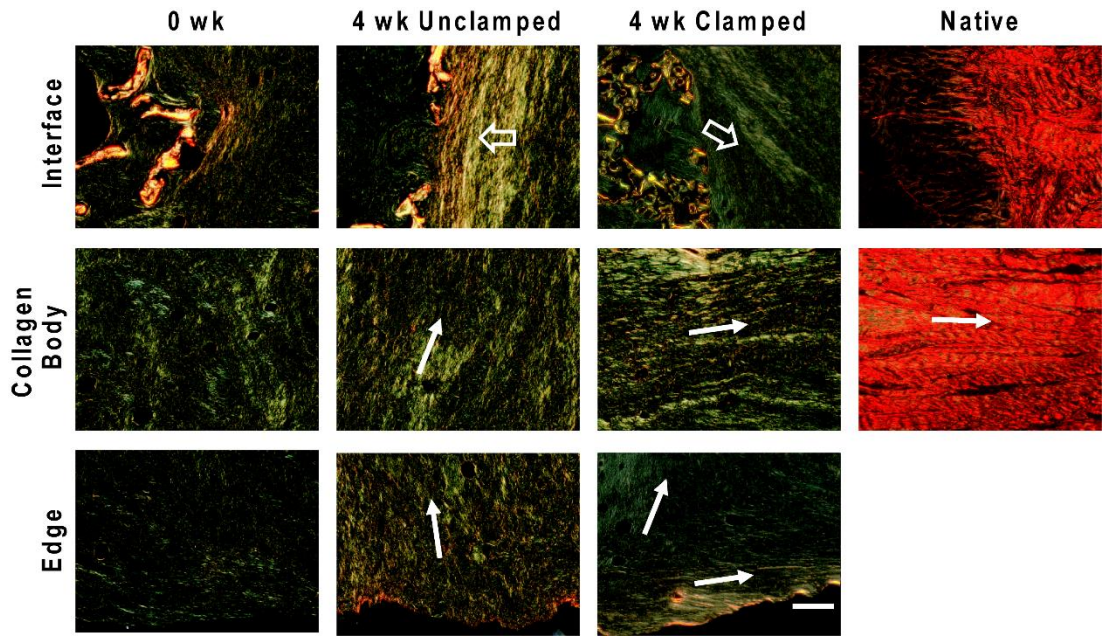

Figure 6.5: Picrosirius red staining imaged using polarized light. 0 week generally disorganized collagen. Accordion compaction in 4 week unclamped versus integrated fibers at 4 week clamped interface (⟹). Fiber direction of collagen indicated by →.

In regions of organized fiber bundles, cells were elongated in the direction of fibers while in regions of less organized collagen, cells were more rounded (Figure 6.6). Cells in the 0 week constructs were uniformly distributed throughout the collagen. Cells in all three regions appeared rounded within the collagen scaffold. After four weeks of culture, cells remained embedded within the collagen and did not migrate onto the bone matrix scaffold. Cells in the bony region appear rounded, whereas cells in the interface and collagen body are a mix of elongated and rounded cells. Cells elongate in the direction of collagen fibers. In the unclamped samples the cells elongated in the radial direction, whereas the cells in the clamped samples elongate more in the longitudinal direction.

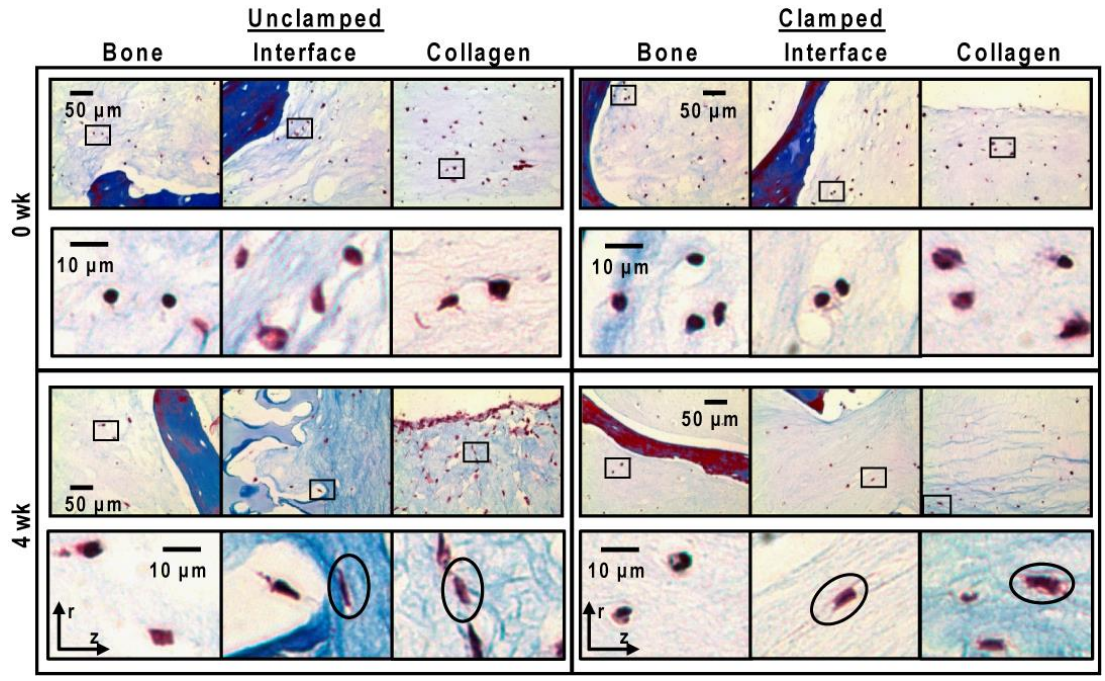

Figure 6.6: Masson's Trichrome staining of cultured samples. Images taken from three areas of constructs: bone, interface, and collagen. Boxes indicate location of high magnification images in the row below. Circles indicate direction of cell elongation. Orientation of images relative to radial (r) and longitudinal (z) axis is shown by axis markers. Cell in bone region remain rounded while cells in the interface and collagen regions have a mix of rounded and elongated cells. Ovals in unclamped samples are aligned in the radial direction, while cells in clamped samples are aligned in the longitudinal direction.

Mechanical Properties

Clamping condition increased mechanical properties of constructs over 4 weeks in culture (Figure 6.7). The elastic modulus significantly increased after 2 and 4 weeks of culture, increasing 500% after 4 weeks under clamped condition compared to the 0 week start point (Figure 6.7A, $p<0.05$). Unclamped samples only increased by 150% after 4 weeks (Figure 6.7A, $p<0.05$). UTS followed a similar trend with significant increases after 4 weeks in culture, increasing 400% with the clamped condition and 250% with the unclamped condition over the 4 week culture period (Figure 6.7B, $p<0.05$). The modulus in the toe region similarly increased with time in culture with

clamped samples transitioning out of the toe region into the elastic region at a lower transition strain (Supplemental 6.4). While the midsubstance of collagen was strengthened over time and condition, ultimate failure location changed accordingly. The 0 week and 2 week unclamped samples' predominant failure location was in the midsubstance of the collagen. The 2 week clamped and both 4 week clamped and unclamped conditions resulted in failure primarily at the collagen to bone interface.

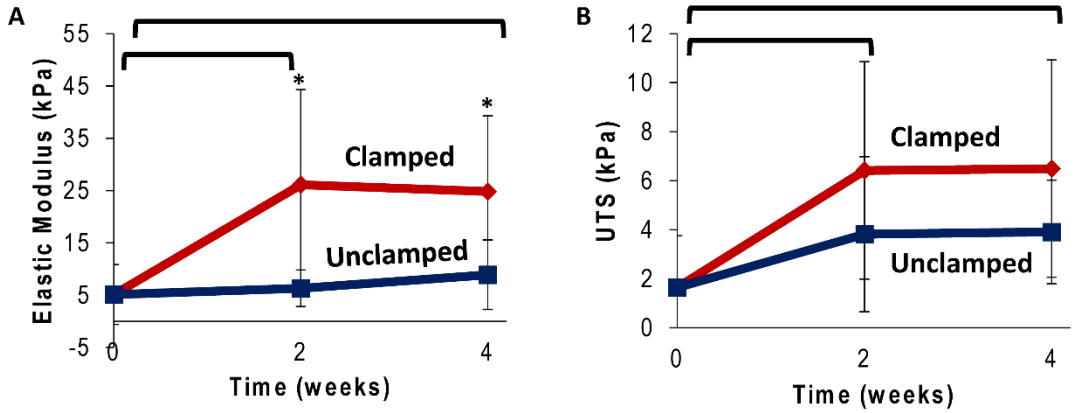

Figure 6.7: Tensile testing (.75% strain/sec) pull to failure testing to evaluate elastic modulus ($E_{Elastic}$) (A) and ultimate tensile strength (B) (* significantly different between conditions, ⌐¬ significantly different over time, $p<0.05$, n=4-6).

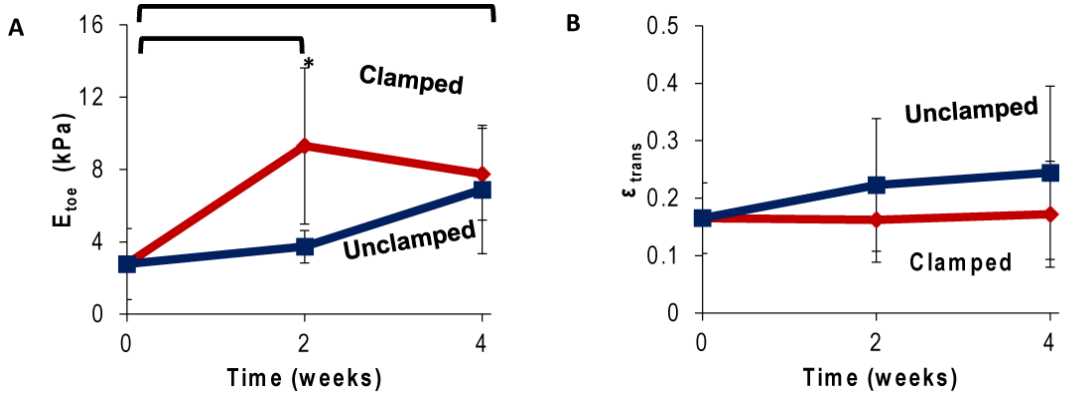

Supplemental 6.4: (A) Modulus from the linear portion of the toe region in cultured constructs. (B) The transition strain ($Ɛ_{trans}$) of constructs at 0-, 2-, 4- weeks of culture. (* significantly different between conditions, ⌐¬ significantly different over time, $p<0.05$, n=4-6).

Discussion

The objective of this study was to develop an experimental test platform for tissue engineering the meniscal enthesis. A major challenge in attaching tissue engineered menisci *in vivo* is anchoring soft tissue to bone, which points to developing soft constructs seeded with FCCs that interface with bone. Here we demonstrated that FCC seeded collagen integrates into decellularized bone plugs producing a mechanically robust interface that can be cultured. Anchoring at the bone (clamping) enhances the formation of tissue with regards to fiber formation and cellular organization. Anchored samples formed fibers in the longitudinal direction which maintained construct morphology and improved mechanical properties.

A collagen injection molding technique established three distinct regions that further developed throughout culture: 1) bone, 2) bone-collagen interface, and 3) collagen. Each region had a distinct material composition and structure. The bony region contained the decellularized bone matrix material which is an excellent template for mineral formation and matrix development [34]. Decellularized bone matrix maintains the native architecture and mechanical properties of bone [35]. Additionally, bone matrix is known to contain critical biological factors and microtopography that increase the osteoinductive properties of the scaffold and in turn improves bone formation [36]. Furthermore, the decellularization process used in this study has been proven amenable to cellular reseeding and new bone development in pre-clinical studies[29,30]. Attaching the meniscus through a bone plug will likely improve implant integration with native bone [17]. Collagen type I was chosen for the soft tissue portion of constructs because it is the major structural protein in the meniscus and ligament and has been used

as a scaffold for regeneration of these tissues in many studies [18,37–39]. Further, collagen type I is unique in that the matrix can be remodeled to form large mature fiber networks [28]. The bone-collagen interface region was formed by infiltrating the pores of decellularized bone with FCC seeded collagen. This infiltration enabled directed mechanical anchoring of the soft collagen to bone as well as cell-mediated reorganization of this region (Figures 3 and 4). The infiltration of large fibers extending from the meniscal horns into the uncalcified cartilage region of the native meniscal enthesis is essential the mechanical integrity of the construct [13,40]. Therefore, the integration of collagen with bone at the interface will be important for transitioning mechanical strains in the tissue engineered enthesis.

Mechanical fixation guided cellular behavior to drive organized fiber formation. After four weeks of culture, the matrix which was disorganized at 0 weeks contained larger and more organized fibers. The specific organization of fibers depended on the absence or presence of mechanical fixation. Unclamped samples contracted along the longitudinal axis bringing the bony ends closer together and forming fibers in the radial direction. In contrast, clamped samples maintained original length and formed fibers in the longitudinal direction between bony ends. Furthermore, clamped samples had continuous fibers that spanned the collagen and bone regions. As the construct contracted in unclamped samples, radial fibers compacted at the bony interface rather than longitudinally integrating like the anchored samples. Stacking of radial fibers at the interface was analogous to the folding of an accordion. The native enthesis contains a dense network of collagen fibrils primarily in the longitudinal direction [14,40]. The

longitudinal fibers in the clamped samples are more representative of the native collagen orientation.

The reorganization of fibers based on mechanical boundary conditions is consistent with several studies of cell based remodeling with collagen [12,28,41,42]. This phenomenon has been noted across several cell types including dermal fibroblasts [41], cardiomyocytes [28], annulus fibrosis chondrocytes [42], and meniscal fibrochondrocytes [12]. Previous studies in whole meniscus tissue engineering showed that FCCs can remodel collagen into organized fibers guided by mechanical fixation [12]. Furthermore, guided collagen reorganization in this study resembles that seen in native meniscus during development. The meniscus begins as a dense mesenchymal condensate and the development of organized fibers is not observed until after meniscal attachments to the tibia are established [43–46]. Similarly in this study, we begin with a high density of cells embedded in a collagen matrix that is then mechanically anchored to induce organized fiber development over time. Further mechanical and chemical stimulation will be required to further develop this tissue, however the system used in this study will serve as a useful model for meniscal enthesis development.

Integration between scaffold regions is paramount to the mechanical performance of hard to soft tissue interfaces. *In vivo* the meniscal enthesis assists in the transition from the tensile loading environment of the meniscus into the underlying compressive loading environment of bone [47,48]. The meniscal enthesis must be able to withstand high tensile loads [49,50]. Native stiffness and UTS range from approximately 125-300 MPa and 5-75MPa respectively [50,51]. Although we have yet to achieve native UTS and stiffness, this study shows that we are able use mechanical fixation to improve

mechanical performance under tensile loads provided by cellular traction forces. The increase in mechanical properties is likely do to local matrix reorganization of fibers in the direction of load as well as increased integration at the bony interface. Since most mechanical failures occurred at the interface, the measurements reported are not a true measure of the bulk collagen properties. The lack of mechanical property accrual between 2 and 4 weeks of culture is likely due to a lack of increased mechanical integration at the interface. While the constructs do not meet the criteria for a fully functional bone-meniscus interface, constructs do develop a bone-soft tissue interface with a continuous collagen matrix that spans the interface with interconnecting fibers. In vivo studies in a tissue engineered ligament have shown the development of integrated fibers to bone that performed well under tensile load after 6 months in vivo [24]. However, development of interconnecting fibers in vitro at the interface has yet to be demonstrated in enthesis tissue engineering. This simplified in vitro system provides a platform for screening methods to enhance the structure and properties of this interface that contribute to mechanical performance.

The simplicity of this model is easily transferable to address several different experimental questions. Previously we designed a tissue engineered meniscus [11,12,52], this meniscus can be combined with the linear model design used in this study to translate into a full scale tissue engineered meniscus (Figure 6.1). We have shown in this the study the application of mechanical constraint to influence fiber formation, however this system can easily be utilized as a model system to test experimental parameters for tissue engineering the meniscus to bone enthesis. The culture set up was further optimized for high throughput testing. Polysulphone molds

were redesigned and expanded to clamp a capacity of six constructs with a media wall for future experiments (Supplemental 6.1). Other efforts to engineer hard to soft interfaces as a model system involve creating media gradients using multi-media chamber bioreactors. The Tuan group recently developed a dual-chamber bioreactor for tissue specific media culture of an osteochondral junction [53], while a different group used a double diffusion system to create a target zone of calcification [25]. The diffusion systems focus on creating chemical gradients, while our system uses boundary conditions to direct fiber formation into the porous bone. Our design has been simplified to serve as a test model to investigate a host of experimental parameters such as the application of different cell types in co-culture, biochemical gradients, and demineralization gradients. Using a streamlined culture system for optimization will improve the ultimate application to a tissue engineered meniscus design.

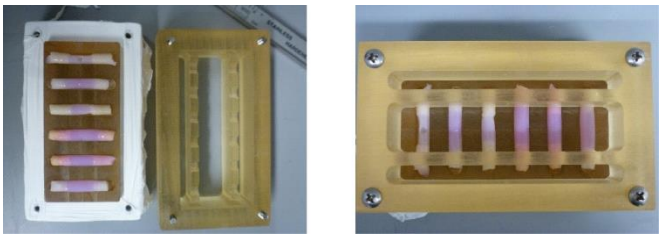

Supplemental 6.1: Culture set up was further optimized for high throughput testing. Polysulphone molds were redesigned and expanded to clamp a capacity of 6 constructs with media wall for future experiments. Chamber opened to place constructs (left). Assembled chamber with constructs clamped down by media divider (right).

The construct designed in this study was primarily engineered to serve as a simplified model for testing tissue engineering considerations when creating the meniscal enthesis *in vitro.* Given that this is a simplified model, the setup has some limitations, notably in the mechanical properties and in the lack of a calcified cartilage layer. Further studies on fabrication and culture technique may enable development of

more functionally organized tissues. Additionally, our construct is a linear structure where the bones on each end are linear and level with each other. Native entheses fibrocartilage to bone transitions are at an angle to the ligamentous fiber direction, additionally this angle will vary depending on the specific enthesis. Meniscal entheses have been shown to each have their own unique mechanical properties and anatomy, which presents a challenge to a one-size-fits-all tissue engineering approach [54,55]. Although the constructs generated in this study showed improvement in mechanical properties, the constructs were still well below native properties. This study only investigated clamping as an approach to improve mechanical properties. Other approaches such as collagen crosslinking, growth factors, and mineral gradients have shown success in other studies and could easily be applied to our experimental set up to improve mechanical properties [25,56–58]. Future studies could benefit from the addition of enthesis specific cells in tissue engineered enthesis region. These constructs did not see the development of a tidemark, likely due to the lack of FCC motility and short culture duration. Future work will focus on the addition of cells directly to bone constructs and increase culture duration. Ideally a tissue engineered meniscal enthesis could continue to remodel once implanted *in vivo* to better suit the unique mechanical loads in that specific location.

Conclusion

This study demonstrated that collagen and bone can be integrated together into a simplified test model for meniscus-to-bone tissue engineering. Furthermore, we showed that collagen alignment can be directed to integrate with bone using mechanical clamping. Collagen infiltration into bone pores at the collagen-bone interface facilitates

the directed integration of fibers at the interface. This experimental model of the bone-fibrocartilage interface serves as a platform to better understand the interaction between these two very different tissues and to provide a platform for screening methods to enhance the structure and properties of this interface.

REFERENCES

[1] E. Makris, P. Hadidi, K. Athanasiou, The knee meniscus: structure-function, pathophysiology, current repair techniques, and prospects for regeneration., Biomaterials. 32 (2011) 7411–31.

[2] A. Bedi, N.H. Kelly, M. Baad, A.J.S. Fox, R.H. Brophy, R.F. S.A. Maher, Dynamic contact mechanics of the medial meniscus as a function of radial tear, repair, and partial meniscectomy., J. Bone Joint Surg. Am. 92 (2010) 1398–1408.

[3] I.D. McDermott, A.A. Amis, The consequences of meniscectomy., J. Bone Joint Surg. Br. 88 (2006) 1549–1556.

[4] I.D. Hutchinson, C.J. Moran, H.G. Potter, R.F. Warren, S.A. Rodeo, Restoration of the meniscus: form and function., Am. J. Sports Med. 42 (2014) 987–98.

[5] V. Martinek, P. Ueblacker, K. Bräun, S. Nitschke, R. Mannhardt, K. Specht, B. Gansbacher, A.B. Imhoff, Second generation of meniscus transplantation: in-vivo study with tissue engineered meniscus replacement., Arch. Orthop. Trauma Surg. 126 (2006) 228–34.

[6] C.J. Moran, F. Orth, D.P. Withers, F. Orth, P.R. Kurzweil, P.C. Verdonk, Clinical Application of Scaffolds for Partial Meniscus Replacement, 23 (2015) 156–161.

[7] C.H. Lee, S.A. Rodeo, L.A. Fortier, C. Lu, C. Erisken, J.J. Mao, Protein-releasing polymeric scaffolds induce fibrochondrocytic differentiation of endogenous cells for knee meniscus regeneration in sheep, 6 (2014) 1–12.

[8] S. Kang, S. Son, J. Lee, E. Lee, K. Lee, S. Park, J. Park, B. Kim, Regeneration of whole meniscus using meniscal cells and polymer scaffolds in a rabbit total meniscectomy model, (2006) 7–11.

[9] A.C. Aufderheide, K. a Athanasiou, Assessment of a bovine co-culture, scaffold-free method for growing meniscus-shaped constructs., Tissue Eng. 13 (2007) 2195–205.

[10] J.L. Puetzer, L.J. Bonassar, High Density Type I Collagen Gels for Tissue Engineering of Whole Menisci., Acta Biomater. 9 (2013) 7787–7795.

[11] J.J. Ballyns, J.P. Gleghorn, V. Niebrzydowski, J.J. Rawlinson, H.G. Potter, S.A. Maher, T.M. Wright, L.J. Bonassar, Image-guided tissue engineering of anatomically shaped implants via MRI and micro-CT using injection molding., Tissue Eng. Part A. 14 (2008) 1195–202.

[12] J.L. Puetzer, E. Koo, L.J. Bonassar, Induction of fiber alignment and mechanical anisotropy in tissue engineered menisci with mechanical anchoring, J. Biomech. 48 (2015) 1436–1443.

[13] A.C. Abraham, T.L. Haut Donahue, From meniscus to bone: A quantitative evaluation of structure and function of the human meniscal attachments, Acta Biomater. 9 (2013) 6322–6329.

[14] D.F. Villegas, T. a. Hansen, D.F. Liu, T.L. Haut Donahue, A quantitative study of the microstructure and biochemistry of the medial meniscal horn attachments, Ann. Biomed. Eng. 36 (2008) 123–131.

[15] J. Gao, Immunolocalization of types I, II, and X collagen in the tibial insertion sites of the medial meniscus., Knee Surg. Sports Traumatol. Arthrosc. 8 (2000) 61–65.

[16] T.L. Haut Donahue, M.L. Hull, M.M. Rashid, C.R. Jacobs, How the stiffness of meniscal attachments and meniscal material properties affect tibio-femoral contact pressure computed using a validated finite element model of the human knee joint, J. Biomech. 36 (2003) 19–34.

[17] H. Wang, A.O. Gee, I.D. Hutchinson, K. Stoner, R.F. Warren, T.O. Chen, S.A. Maher, Bone Plug Versus Suture-Only Fixation of Meniscal Grafts: Effect on Joint Contact Mechanics During Simulated Gait., Am. J. Sports Med. (2014).

[18] P.J. Yang, J.S. Temenoff, Engineering orthopedic tissue interfaces., Tissue Eng. Part B. Rev. 15 (2009) 127–41.

[19] J.P. Spalazzi, S.B. Doty, K.L. Moffat, W.N. Levine, H.H. Lu, Development of controlled matrix heterogeneity on a triphasic scaffold for orthopedic interface tissue engineering., Tissue Eng. 12 (2006) 3497–508.

[20] J.P. Spalazzi, E. Dagher, S.B. Doty, X.E. Guo, S. a Rodeo, H.H. Lu, In vivo evaluation of a multiphased scaffold designed for orthopaedic interface tissue engineering and soft tissue-to-bone integration., J. Biomed. Mater. Res. A. 86 (2008) 1–12.

[21] G. Criscenti, A. Longoni, A. Di Luca, C. De Maria, C.A. Van Blitterswijk, G. Vozzi, L. Moroni, Triphasic scaffolds for the regeneration of the bone–ligament interface, Biofabrication. 8 (2016) 15009.

[22] V.D. Mahalingam, N. Behbahani-Nejad, E.A. Ronan, T.J. Olsen, M.J. Smietana, E.M. Wojtys, D.M. Wellik, E.M. Arruda, L.M. Larkin, Fresh versus frozen engineered bone-ligament-bone grafts for sheep anterior cruciate ligament repair., Tissue Eng. Part C. Methods. 21 (2015) 548–56.

[23] V.D. Mahalingam, N. Behbahani-Nejad, S. V Horine, T.J. Olsen, M.J. Smietana, E.M. Wojtys, D.M. Wellik, E.M. Arruda, L.M. Larkin, Allogeneic versus autologous derived cell sources for use in engineered bone-ligament-bone grafts in sheep anterior cruciate ligament repair., Tissue Eng. Part A Part A. 21 (2015) 1047–54.

[24] J. Ma, M.J. Smietana, T.Y. Kostrominova, E.M. Wojtys, L.M. Larkin, E.M. Arruda, Three-Dimensional Engineered Bone–Ligament–Bone Constructs for Anterior Cruciate Ligament Replacement, Tissue Eng. Part A. 18 (2012) 103–116.

[25] J. Hollenstein, A. Terrier, E. Cory, A.C. Chen, R.L. Sah, D.P. Pioletti, Mechanical evaluation of a tissue-engineered zone of calcification in a bone-hydrogel osteochondral construct., Comput. Methods Biomech. Biomed. Engin. 18 (2013) 37–41.

[26] T.P. Lozito, P.G. Alexander, H. Lin, R. Gottardi, A.W.-M. Cheng, R.S. Tuan, Three-dimensional osteochondral microtissue to model pathogenesis of osteoarthritis., Stem Cell Res. Ther. 4 Suppl 1 (2013) S6.

[27] M.I. Chen, T.P. Branch, W.C. Hutton, Is it important to secure the horns during lateral meniscal transplantation? A cadaveric study., Arthroscopy. 12 (1996) 174–181.

[28] K.D. Costa, E.J. Lee, J.W. Holmes, Creating alignment and anisotropy in engineered heart tissue: role of boundary conditions in a model three-dimensional culture system., Tissue Eng. 9 (2003) 567–77.

[29] W.L. Grayson, M. Fröhlich, K. Yeager, S. Bhumiratana, M.E. Chan, C. Cannizzaro, L.Q. Wan, X.S. Liu, X.E. Guo, G. Vunjak-Novakovic, Engineering anatomically shaped human bone grafts., Proc. Natl. Acad. Sci. U. S. A. 107 (2010) 3299–3304.

[30] W.L. Grayson, S. Bhumiratana, C. Cannizzaro, P.-H.G. Chao, D.P. Lennon, A.I. Caplan, G. Vunjak-Novakovic, Effects of initial seeding density and fluid perfusion rate on formation of tissue-engineered bone., Tissue Eng. Part A. 14 (2008) 1809–20.

[31] V.L. Cross, Y. Zheng, N. Won Choi, S.S. Verbridge, B. a. Sutermaster, L.J. Bonassar, C. Fischbach, A.D. Stroock, Dense type I collagen matrices that support cellular remodeling and microfabrication for studies of tumor angiogenesis and vasculogenesis in vitro, Biomaterials. 31 (2010) 8596–8607.

[32] R.L. Mauck, X. Yuan, R.S. Tuan, Chondrogenic differentiation and functional maturation of bovine mesenchymal stem cells in long-term agarose culture., Osteoarthr. Cartil. 14 (2006) 179–89.

[33] M.D. Abràmoff, P.J. Magalhães, S.J. Ram, Image processing with imageJ, Biophotonics Int. 11 (2004) 36–41.

[34] A.H. Reddi, Morphogenetic messages are in the extracellular matrix: biotechnology from bench to bedside, Biochem. Soc. Trans. 28 (2000) 345–349.

[35] T.W. Gilbert, T.L. Sellaro, S.F. Badylak, Decellularization of tissues and organs, Biomaterials. 27 (2006) 3675–3683.

[36] A. Papadimitropoulos, C. Scotti, P. Bourgine, A. Scherberich, I. Martin, Engineered decellularized matrices to instruct bone regeneration processes, Bone. 70 (2015) 66–72.

[37] S. Oda, S. Otsuki, Y. Kurokawa, Y. Hoshiyama, M. Nakajima, M. Neo, A new method for meniscus repair using type I collagen scaffold and infrapatellar fat pad, J. Biomater. Appl. 0 (2015) 1–10.

[38] M.B. Pabbruwe, W. Kafienah, J.F. Tarlton, S. Mistry, D.J. Fox, A.P. Hollander, Repair of meniscal cartilage white zone tears using a stem cell/collagen-scaffold implant., Biomaterials. 31 (2010) 2583–91.

[39] R. Hansen, E. Bryk, V. Vigorita, Collagen scaffold meniscus implant integration in a canine model: a histological analysis., J. Orthop. Res. 31 (2013) 1914–9.

[40] D.F. Villegas, T.L.H. Donahue, Collagen morphology in human meniscal attachments: a SEM study., Connect. Tissue Res. 51 (2010) 327–336.

[41] F. Grinnell, Fibroblast-collagen-matrix contraction: growth-factor signalling and mechanical loading, Trends Cell Biol. 10 (2000) 362–365.

[42] R.D. Bowles, R.M. Williams, W.R. Zipfel, L.J. Bonassar, Self-Assembly of Aligned Tissue-Engineered Annulus fibrosus and Intervertebral Disc Composite Via Collagen Gel Contraction, Tissue Eng. Part A. 16 (2010).

[43] C.R. Clark, J.A. Ogden, Prenatal and Postnatal Development of Human Knee Joint Mensci, Iowa Orthop. J. 1 (1981) 20–27.

[44] J. a Mérida-Velasco, I. Sánchez-Montesinos, J. Espín-Ferra, J.F. Rodríguez-Vázquez, J.R. Mérida-Velasco, J. Jiménez-Collado, Development of the human knee joint., Anat. Rec. 248 (1997) 269–78.

[45] D.J. Gray, E. Gardner, Prenatal development of the human knee and superior tibiofibular joints, Am. J. Anat. 86 (1950) 235–287.

[46] E. Gardner, R. O'Rahilly, The early development of the knee joint in staged human embryos., J. Anat. 102 (1968) 289–99.

[47] A. Seitz, R. Kasisari, L. Claes, A. Ignatius, L. Dürselen, Forces acting on the anterior meniscotibial ligaments, Knee Surgery, Sport. Traumatol. Arthrosc. 20 (2012) 1488–1495.

[48] C. Stärke, S. Kopf, K.H. Gröbel, R. Becker, Tensile forces at the porcine anterior meniscal horn attachment, J. Orthop. Res. 27 (2009) 1619–1624.

[49] S.D. Masouros, I.D. McDermott, A.A. Amis, a. M.J. Bull, Biomechanics of the meniscus-meniscal ligament construct of the knee, Knee Surgery, Sport. Traumatol. Arthrosc. 16 (2008) 1121–1132.

[50] M.B. Ellman, C.M. Laprade, S.D. Smith, M.T. Rasmussen, L. Engebretsen, C.A. Wijdicks, R.F. LaPrade, Structural Properties of the Meniscal Roots., Am. J. Sports Med. (2014) 1–7.

[51] D.F. Villegas, J. a. Maes, S.D. Magee, T.L. Haut Donahue, Failure properties and strain distribution analysis of meniscal attachments, J. Biomech. 40 (2007) 2655–2662.

[52] J.L. Puetzer, L.J. Bonassar, Physiologically Distributed Loading Patterns Drive the Formation of Zonally Organized Collagen Structures in Tissue Engineered Meniscus, Tissue Eng. Part A. (2016) 1–40.

[53] P.G. Alexander, R. Gottardi, H. Lin, T.P. Lozito, R.S. Tuan, Three-dimensional osteogenic and chondrogenic systems to model osteochondral physiology and degenerative joint diseases., Exp. Biol. Med. (Maywood). (2014) 1–16.

[54] K.N. Hauch, M.L. Oyen, G.M. Odegard, T.L. Haut Donahue, Nanoindentation of the insertional zones of human meniscal attachments into underlying bone, J. Mech. Behav. Biomed. Mater. 2 (2009) 339–347.

[55] Y.J. Wang, J.K. Yu, H. Luo, C.L. Yu, Y.F. Ao, X. Xie, D. Jiang, J.Y. Zhang, An anatomical and histological study of human meniscal horn bony insertions and peri-meniscal attachments as a basis for meniscal transplantation, Chin. Med. J. (Engl). 122 (2009) 536–540.

[56] C.A. Pangborn, K.A. Athanasiou, Effects of growth factors on meniscal fibrochondrocytes., Tissue Eng. 11 (2005) 1141–8.

[57] E.A.. Makris, D.J. Responte, N.K. Paschos, J.C. Hu, K.A.. Athanasiou, Developing functional musculoskeletal tissues through hypoxia and lysyl oxidase-induced collagen cross-linking, Proc. Natl. Acad. Sci. 111 (2014) E4832–E4841.

[58] R. Roy, A.L. Boskey, L.J. Bonassar, Non-enzymatic glycation of chondrocyte-seeded collagen gels for cartilage tissue engineering, J. Orthop. Res. 26 (2008) 1434–1439.

CHAPTER 7

CONCLUSIONS AND FUTURE DIRECTIONS

The goal of this dissertation was to investigate engineering design alternatives and improvements in order to address key pre-clinical challenges for tissue engineering the meniscus. The long term goal of this work is to create a functional replacement for injured meniscal tissue that (1) is relatively easy to implant, (2) will integrate with the native tissue, and (3) will serve as a living tissue replacement made with autologous cells. Tissue engineered menisci in the field hold a lot of great promise as a treatment alternative, however there are several pre-clinical challenges the field needs to overcome to move tissue engineered menisci into the clinic. Many tissue engineered approaches use fibrochondrocytes (FCCs) in their engineered menisci, however FCCs as a singular cell source are not feasible for clinical translation. Stem cells are highly promising as a supplemental cell source, but there is not much known about how to guide fibrochondrogenic differentiation. Mesenchymal stem cells (MSCs) need to be able to produce appropriate matrix such as organized collagen fibers and glycosaminoglycans (GAGs). The meniscus also contains meniscal enthesis insertions into bone, which are critical for mechanical stability. Tissue engineering the meniscal enthesis has not yet been studied. This work explored the applicability of MSCs as a cell source alternative to FCCs in a 3D matrix, investigated co-culture as a technique to guide MSC cellular behavior, applied glucose as a method to manipulate fiber formation, and developed a model system for meniscal enthesis development.

Stem Cells and Meniscus Tissue Engineering

Over the last few decades the scientific community has evolved from the discovery of hematopoietic stem cells (HSCs)[1] and their treatment potential for bone marrow transplants to the targeted reprogramming of induced pluripotent stem cells (iPS)[2,3]. With the unveiling of a vast array of stem cells in the human body, the scientific community is a buzz with dreams of the potential that stem cells have for solving some of the great medical challenges, specifically tissue engineering applications.[4] While these dreams of perfectly engineered organ replacements using stem cells are plausible, arriving at the end point is rather complex. Early work with MSCs demonstrated their multipotent behavior and their potential in orthopedic applications.[5] From an early stage, MSCs chondrogenic potential has been investigated for developmental and therapeutic applications.[6,7] Since 1998 there have been ~19,000 publications related to MSCs and cartilage/chondrocytes, however only 285 publications have been published that pertain to MSCs and meniscus/fibrochondrocytes. Since much of the focus of stem cell applications has been in the field of cartilage research, there is a clear knowledge gap in the potential treatment applications for MSCs in meniscus tissue engineering.

This work mainly focuses on applicability of MSCs to meniscus tissue engineering. MSCs increased healing of small meniscal tears in clinical studies using intra-articular injection.[8–11] Little is known about the repair of larger meniscal injuries using MSCs. Furthermore, fibrochondrogenic differentiation of MSCs is widely unknown. Preliminary studies have looked at using co-culture with native cells, with the idea that native cells will provide extracellular signals to help guide MSC

differentiation toward the native phenotype. [12,13] This work was limited to pellet cultures and further study must be done in a 3D environment that would be beneficial in tissue engineering the meniscus. In Chapter 3, MSC and FCC 3D co-culture was studied in a high density collagen gel. This study showed that MSC phenotype can be influenced by co-culture with FCCs. Co-culture reduced the prevalence of hypertrophy typically seen in MSC mono-culture. Furthermore, co-culture increased GAG retention in collagen constructs and also increased mechanical properties. This work demonstrated that co-culture of MSCs is a useful method for influencing MSC differentiation and that MSCs could be a useful cell source for tissue engineering the meniscus.

Since the meniscus is a highly complex structure that is subject to an array of loading inputs, the work in Chapter 3 was expanded to an anatomically accurate meniscus construct. The establishment of an organized fiber matrix is of utmost importance to the stability of a tissue engineered replacement. In order for stem cells to be a viable replacement, they need to be able to produce large diameter and functionally organized fibers. In Chapter 4, a static mechanical boundary condition fixed the tissue engineered extensions at the meniscal horns to mimic the boundary conditions imposed by the native meniscal enthesis. Similar to the findings in Chapter 3, MSCs had enhanced production of GAGs in the meniscal constructs. However, FCC seeded menisci had increased fiber diameter and alignment. Co-culture of 1:1 ratios of FCCs and MSCs had an averaged value between the two mono-culture groups. MSCs in mono-culture have a significant increase in collagen type I production over type II. Correlative analysis of these data indicate the GAG production and fiber formation are

inversely correlated. Follow up studies in Chapter 5 explored this relationship between GAG and fiber formation.

These studies move forward the understanding of stem cell behavior and methods to influence stem cell phenotype. Furthermore, reliance on FCCs for a full scale meniscus tissue engineered replacement is simply not feasible for clinical application, as the sufficient number of cells for tissue engineered menisci is not possible. In order for the field to progress, there needs to be a greater understanding of how these cells behave in an appropriate environment for tissue engineering. Through this work we know that MSCs can produce the types of matrix molecules required for meniscus tissue engineering. We also know that co-culture is a useful technique to provide intracellular signaling to MSCs, in order to reduce hypertrophy, balance collagen type I and II production, as well as GAG verse fiber formation. While MSCs do create organized fibers in response to static mechanical boundary conditions, their ability to remodel and build large scale fibers is not equivalent to FCCs. Future work should further explore tools to influence MSC's ability to organize and produce large scale collagen fibers.

Future Directions

The work in Chapter 3 largely focused on guiding MSC behavior using co-culture which utilized intracellular signaling to influence cell behavior. There are also potent exogenous small molecules such as growth factors that are known to have a profound role in guiding stem cell differentiation.[14–18] Many growth factors have been explored in meniscus tissue engineering including transforming growth factor (TGF-β), insulin-like growth factor (IGF-1), basic fibroblastic growth factor (bFGF), and platelet-derived growth factor (PDGF). These have each been used to aid in the development

of improved engineered tissue quality.[19–22] Another approach utilized a meniscus scaffold with controlled release of connective tissue growth factor (CTGF) and TGF-β3. This acellular scaffold was implanted as a partial meniscus replacement where endogenous cells repopulated the scaffold and produced an appropriate matrix in accordance with growth factor release.[23] Growth factor studies are highly complex in that there is a complex interplay between concentration, timing, and interplay with other growth factors and matrix molecules. For stem cell differentiation, researchers often look to developmental studies to inform *in vitro* experimental design. Unfortunately at this time, we know very little about how the meniscus develops, especially in relation to growth factor expression during development. Future work could look at the spatial or temporal application of growth factors to stem cell seeded scaffolds. Additionally, further work on the spatial and temporal expression of growth factors in meniscus development would help inform tissue engineering studies. Growth factor work both *in vivo* and *in vitro* will enhance our understanding of stem cell differentiation for meniscus tissue engineering applications.

The work presented in Chapter 4, characterized MSC ability to generate organized fibers as a result of a static mechanical boundary condition. The mechanical boundary condition imposed by the native meniscal enthesis is only one component of the mechanical loading experienced by the meniscus. Previous work in our lab looked at mimicking physiologic dynamic loads in the knee. Loading significantly improved the formation of large organized fibers in the meniscus as well as heterogeneous production of matrix molecules such as GAG production localized to areas of compressive loading. [24] The loading environment in the knee provides critical inputs

that guide meniscal development from a dense mesenchymal condensate to a highly organized tissue. Loading of MSCs in a tissue engineered meniscus would likely lead to improved differentiation and tissue development. Future experiments using dynamic loading of MSCs would elucidate the role that loading plays in MSC differentiation and behavior.

Relationship between Proteoglycans and Fiber Development

In Chapter 3 and Chapter 4, we quantified GAG production and fiber formation. In Chapter 4, there was an inverse correlation between GAG content and fiber formation. Both GAGs and collagen fibers have complex roles in the development of the meniscus and are the most prevalent matrix molecules that contribute to meniscal structure and function. We know from developmental studies that the meniscal fiber architecture is established first, followed by increasing levels of GAG during post-natal development.[25–28] In order for a tissue engineered implant to be mechanically successful *in vivo*, the implant should mimic the native fiber architecture. Proteoglycans are known to play prominent roles in directing, assisting, and inhibiting fiber formation. Small leucine-rich proteoglycans (SLRPs) including decorin, biglycan, and fibromodulin are known to be present in the meniscus and have been shown to assist in the development of organized fibers in multiple tissues. [29,30]

Given the prominent role of proteoglycans in meniscal development *in vivo*, they likely have an important role to play in the in vitro development of tissue engineered menisci. We know from Chapter 4 that MSCs produced large amounts of GAGs, but underperformed in the formation of large fibers. In Chapter 5, we further explored the role of proteoglycans in fiber development *in vitro*. Glucose is the essential building

block for the production of proteoglycans. In Chapter 5, we verified that glucose can be used as a tool to regulate GAG production in the tissue engineered constructs. A peak in fiber alignment and fiber diameter occurred at 500 mg/L glucose concentration which is 1/9 the concentration of standard high glucose media typically used in meniscus tissue engineering. A peak fit showed that fiber formation is optimal at 0.38 µg GAG/wet weight (ww) which corresponded with ~625 mg/mL and ~800 mg/L glucose concentration on the MSC and FCC dose response curve fit for GAG/ww respectively. The decline after the peaks at lower glucose concentrations is likely due to a reduction in cellular metabolism at concentrations where the cells are undergoing glucose starvation.

Most of meniscus tissue engineering protocols are borrowed from cartilage literature, including the glucose media formulation. Meniscus is considered a fibrocartilage and shares many common qualities with tendon. Since cartilage has much higher concentrations of GAG, the culture media contains high glucose media (4500 mg/L) to boost GAG production. However in tendon literature, they typically use low glucose media (1000 mg/L) since fiber production is the main priority in tendon engineering. Since many meniscus protocols are based on cartilage, all meniscus tissue engineering research to date has used a high glucose media formulation. The findings in Chapter 5, support that a lower glucose media formulation should be used to enable large diameter fiber development for tissue engineering the meniscus.

Future Directions

Proteoglycans play a powerful role in matrix assembly for tissue engineering applications. There is still more we need to learn about how these molecule interact with

collagen fibers and how to leverage them to guide tissue maturation in tissue engineered constructs. Chapter 5 demonstrated that lowering GAG production supported improved fiber development. Fiber development in lower concentrations is compromised by a competing effect with glucose starvation. Future studies could evaluate fiber development at different engineered GAG concentrations. Also, this study did not see large changes in decorin, a SLRP heavily implicated for its role in fiber development.[31] Engineering scaffolds with different levels of decorin could provide useful insight on how to better facilitate fiber formation in tissue engineered constructs.

Collagen type I was the scaffold of choice used throughout the studies in this dissertation. This gives cells an existing disorganized fiber structure to remodel throughout culture. The temporal presence of different proteoglycans during remodeling versus during initial assembly could make a difference in fiber formation outcomes. A study such as this would be informative to tissue engineering approaches that use a scaffold as opposed to a self-assembly approach, which solely relies on cellular matrix production for construct generation. The collagen used in these studies was acid solubilized from rat tail tendon, in which some of these SLRPs remain attached to collagen fibrils throughout the collagen processing. Collagen is also sold in purified forms in which a purified versus a digested collagen scaffold may cause variable results for tissue engineering. With collagen as the initial scaffold, quantification of collagen production becomes difficult. Future work could use CP-II and C2C assays to quantify degradation and newly synthesized collagen. Further study should be conducted on when proteoglycans are present in scaffolds and at varied concentrations.

Meniscus Fixation and Enthesis Engineering

Currently the gold standard for meniscus replacement is meniscal allograft. Meniscal allografts are cut with intact boney insertions that are sutured into bone tunnels in the patient recipient. These insertion sites are kept intact because suturing the soft tissue directly into the bone does not adequately regenerate the insertion site and results in inferior restoration of native load distribution in the knee.[32] Meniscal entheses serve to anchor the body of the meniscus into the underlying bone and prevent extrusion of the menisci during loading. Tissue engineered menisci are approaching clinical translation, however no research has been conducted on tissue engineering the meniscal enthesis for surgical fixation.

Ligament, tendon, and osteochondral entheses are analogous soft tissue-to-bone insertions to the meniscal enthesis. While no one has published on tissue engineering the meniscal enthesis, there is a larger body of work on tissue engineering for ligament, tendon, and osteochondral transitions into bone. When designing a tissue engineered enthesis, three main components should be considered: (1) materials processing methods, (2) cellular contributions, and (3) biochemical factors. Once a scaffold has been produced, providing chemical and mechanical cues throughout culture using a bioreactor is a useful technique to guide cellular driven development of the engineered construct. Chapter 2 reviewed these topics in depth.

The end goal of engineering the meniscal enthesis would be to have it fully integrated with a tissue engineered construct. At this time, experimenting with a full scale meniscus attached would be too onerous on materials. There are still many questions to be answered in how to generate the bone to soft tissue transition. These can

be answered using a simplified testing system focused just on the transition zone. A simplified meniscal enthesis model was designed in Chapter 6. A meniscal enthesis was generated by injection molding high density collagen into porous trabecular bone. This model system enables the ability to test a host of experimental conditions in a high throughput manner. Using this system, mechanical anchoring at the bones was found to direct axial fiber formation that interdigitated with the bone. Anchoring also increased mechanical properties and reduced collagen contraction. This is the first study to investigate tissue engineering the meniscal enthesis and one of the few tissue engineered entheses to show interdigitated fibers with the bone.

The system designed in Chapter 6, has been expanded to other studies investigating co-culture at the interface and chemical diffusion of differentiation media. MSCs were seeded onto the trabecular bone and differentiated using osteogenic media before being injected with FCC seeded collagen. This generated a MSC/FCC co-culture region at the interface of collagen gel and bone. These constructs were tested in a single media, clamped culture dish, and in a diffusion bioreactor with osteogenic and fibrochondrogenic media. The addition of the MSC osteogenic portion facilitated the development of new bone, indicated by increased incorporation of calcium. Bioreactor culture saw increased fiber density and organization in the collagen body. While both conditions increased the mechanical properties compared to the mono-cultures tested in Chapter 6, bioreactor samples saw consistently higher values with decreased variability. These studies show that the model presented in Chapter 6 is translatable to a variety of study designs and that the addition of co-culturing and chemical gradients improved the quality of designed tissues.

Future Directions

Since the field on enthesis engineering is relatively young, there is much we still need to learn about the native tissue and how to appropriately engineer this complex tissue. In Chapter 2, three main areas where future work should be focused were outlined: 1) understanding the development and homeostasis of the native enthesis, 2) development of new materials and bioreactors for enthesis engineering, and 3) mechanical and structural verification of tissue engineering and implant success. In order to mimic the developmental processes in tissue engineering, the field needs a better understanding of how specific molecules such as SLRPs or non-collagenous proteins influence tissue development. Furthermore, the enthesis contains complex structure-function relationships that are not fully characterized that could inform engineering designs of tissue engineered constructs. Development of an enthesis *in vitro* involves providing loading stimulation, chemical gradients, and material gradients. Bioreactors that can control loading and chemical stimulation during culture will be essential to generating tissue engineered entheses. We also need to develop standardized techniques to measure "success". For more details on future directions please refer to Chapter 2.

Technical Hurdles Ahead

Throughout this dissertation, the goal of each aim was to design experiments targeted at answering important questions related to clinical translation. While this work contributes to the field's knowledge of stem cell applications and tissue engineering the meniscus, the field still has open questions to address in regards to clinical translation. Establishing a set of quality standards for a tissue engineered meniscus is an ever present

challenge in the field. We do not have a complete understanding of what is needed in a set of guidelines that could serve as a set of benchmarks for meniscus tissue engineering. Quality control measures as well as methods for producing consistent and reliable results will be crucial to the scale up and translation of a tissue engineered meniscus.

In the work presented in this dissertation, measurable outcomes included collagen fiber formation, GAG production, cell shape, mechanical properties, collagen fiber architecture, type of collagen production, and type of proteoglycan production. All of these serve as important measurements, however we do not know what concentrations or values are required for a successful implant. In Chapter 5, GAG concentration was a key contributor to fiber formation. Low concentrations of GAG are likely necessary for fiber formation however higher concentrations of GAG may be necessary in the final product to support compressive loads. How to control these and what exact concentrations are needed for a desired effect is still unknown. In Chapter 4, tensile and compressive testing was conducted, however large standard deviations were observed. While these testing methods seem relatively straightforward, the complex anatomical dimensions of the meniscus make these types of tests more challenging. The meniscus is not only non-uniform in shape, but the fiber architecture that makes up the tissue is highly non-uniform in its organization. Cutting the material into a traditional dog-bone shape with flat top and bottom is nearly impossible if you want to preserve the tissue structure in its entirety. Following the publication of these studies, Dawn Elliot's group published a paper on how to conduct optimal mechanical tests on the meniscus.[33] This work should be informative to future testing done on tissue engineered samples, as well as serve as a potential guideline for mechanical testing.

Once there is standards mechanical testing method, a minimum mechanical value still needs to be established. Potentially mechanical models could be helpful in determining what minimum mechanical properties are required for an implant to withstand low impact loading following surgical implantation. Many tissue engineered approaches rely on further development of the tissue *in vivo*. Furthermore, initial tests are often conducted in animals where post-surgery loading is difficult to control. Therefore a minimum value must be determined.

Stem cells are a blessing and a curse to tissue engineering. They hold seemingly infinite possibilities, however present unique challenges when it comes to reproducibility and quality control. The concept of using an autologous source for tissue engineering solves many issues in terms of immunocompatibility and reduced risk of disease transmission. However, humans are as diverse as snowflakes and so are the cells that make up humans. In Chapters 3, 4, and 5, multipotency differentiation results for the cell line used in the study was presented in the supplemental material. The cell line picked for these studies was chosen from a host of tested cell lines. Even within the same species of the same age, cells from different animals showed varying degrees of multipotency. This protocol has been applied across different species, however in running these tests we did find that human and sheep cells required a higher density of cells to form pellets for chondrogenic testing. While cells do follow a general set of rules, there is a degree of diversity that makes getting predictable results from different autologous sources challenging. Further investigation needs to be conducted into what causes this variability, particularly in the context of aging and disease state. Furthermore, cells with multipotent behaviors are continually being discovered from

different tissue sources. However, each cell line is unique in its differentiation potential and would need to be explored further for any give application. Given enough time and increased chemical concentrations, even a fibroblast can produce GAGs or deposit calcium.[34] This idea feeds into the ongoing debate of whether a cell is truly differentiating or if the cell is just serving a therapeutic role to mediate tissue regeneration.[35] While the end result of tissue regeneration may be the end result, the underlying mechanistic cause is not fully understood at this time.

Significance

Meniscus damage is one of the most common intra-articular knee injuries and currently the gold standard for treatment is meniscus allograft or partial meniscectomy. Meniscus allografts are in short supply due to donor scarcity, shape mismatches, and immune incompatibility. Creating a functional TE meniscus would provide a viable alternative to allograft replacement. The work presented in this dissertation helps move the field of tissue engineered menisci closer to clinical application by (1) investigating co-culture as a techniques to influence MSC differentiation in tissue engineered menisci, (2) evaluating the ability of MSCs to form large diameter fibers, (3) improving the understanding of the relationship between proteoglycans and collagen to form large diameter fibers, and (4) developing a model system to investigate approaches for tissue engineering the meniscal insertion. The work presented in Chapters 3 and 4 was one of the first studies to explore the effect of MSC:FCC co-culture in a 3D scaffold, which provided insight on cellular behavior and interactions within the extracellular environment. A successful co-culture system will provide a pathway for autologous cell therapy through bone marrow aspirate and preliminary meniscus revision. If MSC co-

culture is successful in fibrocartilage replacement, it is a possible approach for driving MSC differentiation into other cell lineages. In Chapter 5, glucose concentration was presented as a tool to control GAG production as well as demonstrated that high levels of GAG production in tissue engineered menisci actually decrease fiber formation. This work has greater implications for any tissue engineering applications that require the formation of large diameter fibers. Also a better understanding of the role of proteoglycans in fiber development will inform applications of stem cells and appropriate matrix expression during development. Results from Chapter 6 provide a method for testing a variety of variables such as mechanical boundary conditions, chemical gradients, and cell type gradients. In this work, application of mechanical boundary conditions directed the formation of integrated fibers at the bone interface, which is a non-trivial challenge in the field of enthesis engineering. Furthermore, the experimental set up in this study has enabled future work studying co-culture experiments and chemical diffusion generated gradients. This dissertation furthers our understanding of MSCs and the development of organized fibers in tissue engineered menisci, as well as facilitates working towards addressing two key preclinical challenges (1) identifying a clinically viable cell source that produces and appropriately organizes matrix molecules and (2) developing a method for surgical fixation.

REFERENCES

1. A. P. Ng and W. S. Alexander. Haematopoietic stem cells: past, present and future. *Cell Death Discov.* **3,** 17002 (2017).
2. K. Takahashi, K. Tanabe, M. Ohnuki, M. Narita, T. Ichisaka, K. Tomoda and S. Yamanaka. Induction of Pluripotent Stem Cells from Adult Human Fibroblasts by Defined Factors. *Cell*. **131,** 861–872 (2007).
3. K. Takahashi and S. Yamanaka. Induction of Pluripotent Stem Cells from Mouse Embryonic and Adult Fibroblast Cultures by Defined Factors. *Cell*. **126,** 663–676 (2006).
4. Committee on the Biological and Biomedical Applications of Stem Cell Research, National Research Council and Institute of Medicine. *Stem Cells and the Future of Regenerative Medicine*. (National Academies Press, 2002).
5. M. F. Pittenger, A. M. Mackay, S. C. Beck, R. K. Jaiswal, R. Douglas, J. D. Msca, M. A. Moorman, D. W. Simonetti, S. Craig and D. R. Marshak. Multilineage Potential of Adult Human Mesenchymal Stem Cells. *Science.* **284,** 143–147 (1999).
6. B. Johnstone, T. M. Hering, A. I. Caplan, V. M. Goldberg and J. U. Yoo. In vitro chondrogenesis of bone marrow-derived mesenchymal progenitor cells. *Exp Cell Res*. **238,** 265–272 (1998).
7. A. M. Mackay, S. C. Beck, J. M. Murphy, F. P. Barry, C. O. Chichester and M. F. Pittenger. Chondrogenic differentiation of cultured human mesenchymal stem cells from marrow. *Tissue Eng.* **4,** 415–28 (1998).
8. M. Agung, M. Ochi, S. Yanada, N. Adachi, Y. Izuta, T. Yamasaki and K. Toda.

Mobilization of bone marrow-derived mesenchymal stem cells into the injured tissues after intraarticular injection and their contribution to tissue regeneration. *Knee surgery, Sport. Traumatol. Arthrosc. Off. J. ESSKA*. **14,** 1307–14 (2006).

9. J.-D. Kim, G. W. Lee, G. H. Jung, C. K. Kim, T. Kim, J. H. Park, S. S. Cha and Y.-B. You. Clinical outcome of autologous bone marrow aspirates concentrate (BMAC) injection in degenerative arthritis of the knee. *Eur. J. Orthop. Surg. Traumatol.* **24,** 1505–1511 (2014).
10. C. J. Centeno, D. Busse, J. Kisiday, C. Keohan, M. Freeman and D. Karli. Regeneration of meniscus cartilage in a knee treated with percutaneously implanted autologous mesenchymal stem cells. *Med. Hypotheses*. **71,** 900–8 (2008).
11. F. Duygulu, M. Demirel, G. Atalan, F. F. Kaymaz, Y. Kocabey, T. C. Dulgeroglu and H. Candemir. Effects of intra-articular administration of autologous bone marrow aspirate on healing of full-thickness meniscal tear: an experimental study on sheep. *Acta Orthop. Traumatol. Turc.* **46,** 61–67 (2012).
12. X. Cui, A. Hasegawa, M. Lotz and D. D'Lima. Structured three-dimensional co-culture of mesenchymal stem cells with meniscus cells promotes meniscal phenotype without hypertrophy. *Biotechnol. Bioeng.* **109,** 2369–80 (2012).
13. D. J. Saliken, A. Mulet-Sierra, N. M. Jomha and A. B. Adesida. Decreased hypertrophic differentiation accompanies enhanced matrix formation in co-cultures of outer meniscus cells with bone marrow mesenchymal stromal cells. *Arthritis Res. Ther.* **14,** R153 (2012).
14. S. K. C. Sundararaj, R. D. Cieply, G. Gupta, T. A. Milbrandt and D. A. Puleo.

Treatment of growth plate injury using IGF-1 loaded PLGA scaffold. *J. Tissue Eng. Regen. Med.* **9,** E202-209 (2015).

15. R. P. Marini, I. Martin, M. M. Stevens, R. Langer and V. P. Shastri. FGF-2 enhances TGF-B1 induced periosteal chondrogenesis. *J. Orthop. Res.* **22,** 1114–1119 (2004).

16. J. S. Park, H. J. Yang, D. G. Woo, H. N. Yang, K. Na and K. H. Park. Chondrogenic differentiation of mesenchymal stem cells embedded in a scaffold by long-term release of TGF-B3 complexed with chondroitin sulfate. *J. Biomed. Mater. Res. - Part A.* **92,** 806–816 (2010).

17. H. V. Almeida, Y. Liu, G. M. Cunniffe, K. J. Mulhall, A. Matsiko, C. T. Buckley, F. J. O'Brien and D. J. Kelly. Controlled release of transforming growth factor-β3 from cartilage-extra-cellular-matrix-derived scaffolds to promote chondrogenesis of human-joint-tissue-derived stem cells. *Acta Biomater.* **10,** 4400–4409 (2014).

18. M. Kim, I. E. Erickson, M. Choudhury, N. Pleshko and R. L. Mauck. Transient exposure to TGF-B3 improves the functional chondrogenesis of MSC-laden hyaluronic acid hydrogels. *J. Mech. Behav. Biomed. Mater.* **11,** 92–101 (2012).

19. J. L. Puetzer, B. N. Brown, J. J. Ballyns and L. J. Bonassar. The Effect of IGF-I on Anatomically Shaped Tissue-Engineered Menisci. *Tissue Eng. Part A.* **19,** 1443–1450 (2013).

20. C. a Pangborn and K. a Athanasiou. Effects of growth factors on meniscal fibrochondrocytes. *Tissue Eng.* **11,** 1141–8 (2005).

21. D. J. Huey and K. A. Athanasiou. Maturational growth of self-assembled,

functional menisci as a result of TGF-B1 and enzymatic chondroitinase-ABC stimulation. *Biomaterials.* **32,** 2052–2058 (2011).

22. N. J. Gunja, R. K. Uthamanthil and K. A. Athanasiou. Effects of TGF-B3 and hydrostatic pressure on meniscus cell-seeded scaffolds. *Biomaterials*. **30,** 565–573 (2010).

23. C. H. Lee, S. A. Rodeo, L. A. Fortier, C. Lu, C. Erisken and J. J. Mao. Protein-releasing polymeric scaffolds induce fibrochondrocytic differentiation of endogenous cells for knee meniscus regeneration in sheep. **6,** 1–12 (2014).

24. J. L. Puetzer and L. J. Bonassar. Physiologically Distributed Loading Patterns Drive the Formation of Zonally Organized Collagen Structures in Tissue Engineered Meniscus. *Tissue Eng. Part A.* **22,** 907–916 (2016).

25. C. H. Y. Ling, J. H. Lai, I. J. Wong and M. E. Levenston. Bovine meniscal tissue exhibits age- and interleukin-1 dose-dependent degradation patterns and composition-function relationships. *J. Orthop. Res.* **34,** 801–811 (2016).

26. C. R. Clark and J. A. Ogden. Prenatal and Postnatal Development of Human Knee Joint Mensci. *Iowa Orthop. J.* **1,** 20–27 (1981).

27. D. J. Gray and E. Gardner. Prenatal development of the human knee and superior tibiofibular joints. *Am. J. Anat.* **86,** 235–287 (1950).

28. E. Gardner and R. O'Rahilly. The early development of the knee joint in staged human embryos. *J. Anat.* **102,** 289–99 (1968).

29. G. Zhang, Y. Ezura, I. Chervoneva, P. S. Robinson, D. P. Beason, E. T. Carine, L. J. Soslowsky, R. V. Iozzo and D. E. Birk. Decorin regulates assembly of collagen fibrils and acquisition of biomechanical properties during tendon

development. *J. Cell. Biochem.* **98,** 1436–1449 (2006).

30. K. G. Danielson, H. Baribault, D. F. Holmes, H. Graham, K. E. Kadler and R. V. Iozzo. Targeted disruption of decorin leads to abnormal collagen fibril morphology and skin fragility. *J. Cell Biol.* **136,** 729–743 (1997).

31. T. Douglas, S. Heinemann, S. Bierbaum, D. Scharnweber and H. Worch. Fibrillogenesis of collagen types I, II, and III with small leucine-rich proteoglycans decorin and biglycan. *Biomacromolecules*. **7,** 2388–2393 (2006).

32. H. Wang, A. O. Gee, I. D. Hutchinson, K. Stoner, R. F. Warren, T. O. Chen and S. A. Maher. Bone Plug Versus Suture-Only Fixation of Meniscal Grafts: Effect on Joint Contact Mechanics During Simulated Gait. *Am. J. Sports Med.* **42,** 1682–1689 (2014).

33. J. M. Peloquin, M. H. Santare and D. M. Elliott. Advances in quantification of meniscus tensile mechanics including nonlinearity , yield , and failure. *J. Biomech. Eng.* **138,** 021002 (13 pages) (2016).

34. S. Giovannini, W. Brehm, P. M.- Varlet and D. Nesic. Multilineage differentiation potential of equine blood-derived fibroblast-like cells. *Differentiation*. **76,** 118–129 (2008).

35. A. I. Caplan. Mesenchymal Stem Cells : Time to Change the Name ! *Stem Cells Transl. Med.* (2017). doi:10.1002/sctm.17-0051